CHAPTER 3: STRUCTURAL EVALUATION[†]

3.0 OVERVIEW

In this chapter, the structural components of the HI-STORM FW system subject to certification by the USNRC are identified and described. The objective of the structural analyses is to ensure that the integrity of the HI-STORM FW system is maintained under all credible loadings under normal, off-normal and extreme environmental conditions as well all credible accident events. The results of the structural analyses, summarized in this FSAR, support the conclusion that the confinement, criticality control, radiation shielding, and retrievability criteria set forth under 10CFR72.236(l), 10CFR72.124(a), 10CFR72.104, 10CFR72.106, and 10CFR72.122(l) shall be met by the storage system. In particular, the design basis information contained in the previous two chapters and in this chapter provides the necessary data to permit all needed structural evaluations for demonstrating compliance with the requirements of 10CFR72.236(a), (b), (d) (e), (f), (g),and (1). To facilitate regulatory review, the assumptions and conservatisms inherent in the analyses are identified along with a concise description of the analytical methods, models, and acceptance criteria. A summary of the system's ability to maintain its structural integrity under other slow acting (degenerative) or precipitous (sudden) effects that may contribute to structural failure, such as, corrosion, fatigue, buckling, and non-ductile fracture is also provided. The information presented herein is intended to comply with the guidelines of NUREG-1536 and ISG-21 pertaining to use of finite element codes.

In particular, every Computational Modeling Software (CMS) deployed to perform the structural analyses is identified and its implementation appropriately justified as suggested in ISG-21. The information on benchmarking and validation of each Computational Modeling Software is also provided (in Subsection 3.6.2).

Where appropriate, the structural analyses have been performed using classical strength materials solution. Such calculations are presented in this FSAR in transparent detail.

Furthermore, the input data and analyses using Computational Modeling Software (CMS) are described in sufficient detail to enable an independent evaluation of safety conclusions reached in this chapter.

[†] This chapter has been prepared in the format and section organization set forth in Regulatory Guide 3.61. However, the material content of this chapter also fulfills the requirements of NUREG-1536. Pagination and numbering of sections, figures, and tables are consistent with the convention set down in Chapter 1, Section 1.0, herein. Finally, all terms-of-art used in this chapter are consistent with the terminology of the Glossary.

3.1 STRUCTURAL DESIGN

3.1.1 Discussion

The HI-STORM FW system consists of the Multi-Purpose Canister (MPC) and the storage overpack (Figure 1.1.1). The components subject to certification on this docket consist of the HI-STORM FW system components and the HI-TRAC VW transfer cask (please see Table 1.0.1). A complete description of the design details of these three components are provided in Section 1.2. This section discusses the structural aspects of the MPC, the storage overpack, and the HI-TRAC VW transfer cask. Detailed licensing drawings for each component are provided in Section 1.5.

(i) The Multi-Purpose Canister (MPC)

The design of the MPC seeks to attain three objectives that are central to its functional adequacy:

- Ability to Dissipate Heat: The thermal energy produced by the stored spent fuel must be transported to the outside surface of the MPC to maintain the fuel cladding and fuel basket metal walls below the regulatory temperature limits.

- Ability to Withstand Large Impact Loads: The MPC, with its payload of nuclear fuel, must withstand the large impact loads associated with the non-mechanistic tipover event.

- Restraint of Free End Expansion: The MPC structure is designed so that membrane and bending (primary) stresses produced by constrained thermal expansion of the fuel basket do not arise.

As stated in Chapter 1, the MPC Enclosure Vessel is a confinement vessel designed to meet the stress limits in ASME Code, Section III, Subsection NB. The enveloping canister shell, baseplate, and the lid system form a complete Confinement Boundary for the stored fuel that is referred to as the "Enclosure Vessel". Within this cylindrical shell confinement vessel is an egg-crate assemblage of Metamic-HT plates that form prismatic cells with square cross sectional openings for fuel storage, referred to as the fuel basket. All multi-purpose canisters designed for deployment in the HI-STORM FW have identical external diameters. The essential difference between the different MPCs lies in the fuel baskets, each of which is designed to house different types of fuel assemblies. All fuel basket designs are configured to maximize structural integrity through extensive inter-cell connectivity. Although all fuel basket designs are structurally similar, analyses for each of the MPC types is carried out separately to ensure structural compliance.

The design criteria of components in the HI-STORM FW system important to safety are defined in Chapter 2.

The principal structural functions of the MPC in storage mode are:

i. To position the fuel in a subcritical configuration, and

ii. To provide a leak tight Confinement Boundary.

The key structural functions of the overpack during storage are:

i. To serve as a missile barrier for the MPC,

ii. To provide flow paths for natural convection,

iii. To provide a kinematically stable SNF storage configuration,

iv. To provide fixed and reliable radiation shielding, and

v. To allow safe translocation of the overpack with a loaded MPC inside.

Some structural features of the MPCs that allow the system to perform these functions are summarized below:

- There are no gasketed ports or openings in the MPC. The MPC does not rely on any mechanical sealing arrangement except welding. The absence of any gasketed or flanged joints makes the MPC structure immune from joint leaks. The Confinement Boundary contains no valves or other pressure relief devices.

- The closure system for the MPCs consists of two components, namely, the MPC lid and the closure ring. The MPC lid can be either a single thick circular plate continuously welded to the MPC shell along its circumference or a two-piece lid, dual lids welded around their common periphery. When using a two piece lid only the top portion of the lid is considered as part of the closure system, the bottomportion is only for shielding purposes. The MPC closure system is shown in the licensing drawings in Section 1.5. The MPC lid is equipped with vent and drain ports, which are used both for evacuating moisture and air from the MPC following fuel loading and subsequent backfilling with an inert gas (helium) at a specified mass. The vent and drain ports are covered by a cover plate and welded before the closure ring is installed. The closure ring is a circular annular plate edge-welded to the MPC lid and shell. The two closure members are interconnected by welding around the inner diameter of the ring. Lift points for the MPC are provided on the MPC lid.

- The MPC fuel baskets consist of an array of interconnecting plates. The number of storage cells formed by this interconnection process varies depending on the type of fuel being stored. Basket configurations designed for both PWR and BWR fuel are explained in detail in Section 1.2. All baskets are designed to fit into the same MPC shell.

- The MPC basket is separated from its lateral supports (basket shims) by a small, calibrated gap designed to prevent thermal stressing associated with the thermal expansion mismatches between the fuel basket and the basket support structure. The gap is designed to ensure that the basket remains unconstrained when subjected to the thermal heat generated by the spent nuclear fuel.

The MPC fuel basket maintains the spent nuclear fuel in a subcritical arrangement. Its safe operation is assured by maintaining the physical configuration of the storage cell cavities intact in the aftermath of a non-mechanistic tipover event. This requirement is satisfied if the MPC fuel basket plates undergo a minimal deflection (see Table 2.2.11). The fuel basket strains are shown in Subsection 3.4.4.1.4 to remain essentially elastic, and, therefore, there is no impairment in the recoverability or retrievability of the fuel and the subcriticality of the stored fuel is unchallenged.

The MPC Confinement Boundary contains no valves or other pressure relief devices. In addition, the analyses presented in Subsections 3.4.3, 3.4.4.1.5, and 3.4.4.1.6 show that the MPC Enclosure Vessel meets the stress intensity criteria of the ASME Code, Section III, Subsection NB for all service conditions. Therefore, the demonstration that the MPC Enclosure Vessel meets Subsection NB stress limits ensures that there will be no discernible release of radioactive materials from the MPC.

(ii) Storage Overpack

The HI-STORM FW storage overpack is a steel cylindrical structure consisting of inner and outer low carbon steel shells, a lid, and a baseplate. Between the two shells is a thick cylinder of un-reinforced (plain) concrete. Plain concrete is also installed in the lid to minimize skyshine. The storage overpack serves as a missile and radiation barrier, provides flow paths for natural convection, provides kinematic stability to the system, and acts as a shock absorber for the MPC in the event of a postulated tipover accident. The storage overpack is not a pressure vessel since it contains cooling vents. The structural steel weldment of the HI-STORM FW overpack is designed to meet the stress limits of the ASME Code, Section III, Subsection NF, Class 3 for normal and off-normal loading conditions and Regulatory Guide 3.61 for handling conditions.

As discussed in Chapters 1 and 2, the principal shielding material utilized in the HI-STORM FW overpack is plain concrete. The plain concrete in the HI-STORM FW serves a structural function only to the extent that it may participate in supporting direct compressive or punching loads. The allowable compression/bearing resistance is defined and quantified in ACI -318-05 [3.3.5]. Strength analyses of the HI-STORM FW overpack and its confined concrete have been carried out in Subsections 3.4.4.1.3 and 3.4.4.1.4 to show that the concrete is able to perform its radiation protection function and that retrievability of the MPC subsequent to any postulated accident condition of storage or handling is maintained.

(iii) Transfer Cask

The HI-TRAC VW transfer cask is the third component type subject to certification. Strictly speaking, the transfer cask is an ancillary equipment which serves to enable the *short term operations* to be carried out safely and ALARA. Specifically, the transfer cask provides a missile and radiation barrier during transport of the MPC from the fuel pool to the HI-STORM FW overpack. Because of its critical role in insuring a safe dry storage implementation, the transfer cask is subject to certification under 10CFR 72 even though it is not a device for storing spent fuel.

The HI-TRAC VW body is a double-walled steel cylinder that constitutes its structural system. Contained between the two steel shells is an intermediate lead cylinder. Integral to the exterior of the HI-TRAC VW body outer shell is a water jacket that acts as a radiation barrier. The HI-TRAC VW is not a pressure vessel since it contains penetrations and openings. The structural steel components of the HI-TRAC VW are subject to the stress limits of the ASME Code, Section III, Subsection NF, Class 3 for normal and off-normal loading conditions.

Since the HI-TRAC VW may serve as an MPC carrier, its lifting attachments are designed to meet the design safety factor requirements of NUREG-0612 [3.1.1] and Regulatory Guide 3.61 [1.0.2] for single-failure-proof lifting equipment.

3.1.2 Design Criteria and Applicable Loads

Principal design criteria for normal, off-normal, and accident/environmental events are discussed in Section 2.2. In this section, the loads, load combinations, and the structural performance of the HI-STORM FW system under the required loading events are presented.

Consistent with the provisions of NUREG-1536, the central objective of the structural analysis presented in this chapter is to ensure that the HI-STORM FW system possesses sufficient structural capability to withstand normal and off-normal loads and the worst case loads under natural phenomenon or accident events. Withstanding such loadings implies that the HI-STORM FW system will successfully preclude the following:

- unacceptable risk of criticality
- unacceptable release of radioactive materials
- unacceptable radiation levels
- impairment of ready retrievability of the SNF

The above design objectives for the HI-STORM FW system can be particularized for individual components as follows:

- The objectives of the structural analysis of the MPC are to demonstrate that:

  i. Confinement of radioactive material is maintained under normal, off-normal, accident conditions, and natural phenomenon events.

  ii. The MPC basket does not deform under credible loading conditions such that the subcriticality or retrievability of the SNF is jeopardized.

- The objectives of the structural analysis of the storage overpack are to demonstrate that:

  i. Large energetic missiles such as tornado-generated missiles do not compromise the integrity of the MPC Confinement Boundary.

  ii. The radiation shielding remains properly positioned in the case of any normal, off-normal, or natural phenomenon or accident event.

  iii. The flow path for the cooling airflow shall remain available under normal and off-normal conditions of storage and after a natural phenomenon or accident event.

  iv. The loads arising from normal, off-normal, and accident level conditions exerted on the contained MPC do not violate the structural design criteria of the MPC.

  v. No geometry changes occur under any normal, off-normal, and accident level conditions of storage that preclude ready retrievability of the contained MPC.

  vi. A freestanding storage overpack loaded with a MPC can safely withstand a non-mechanistic tip-over event.

  vii. The inter-cask transfer of a loaded MPC can be carried out without exceeding the structural capacity of the HI-STORM FW overpack, provided all required auxiliary equipment and components specific to an ISFSI site comply with their design criteria set forth in this FSAR and the handling operations are in full compliance with operational limits and controls prescribed in this FSAR.

- The objective of the structural analysis of the HI-TRAC VW transfer cask is to demonstrate that:

    i. Tornado generated missiles do not compromise the integrity of the MPC Confinement Boundary while the MPC is contained within HI-TRAC VW.

    ii. No geometry changes occur under any postulated handling or storage conditions that may preclude ready retrievability of the contained MPC.

    iii. The structural components perform their intended function during lifting and handling with the loaded MPC.

    iv. The radiation shielding remains properly positioned under all applicable handling service conditions for HI-TRAC VW.

The above design objectives are deemed to be satisfied for the MPC, the overpack, and the HI-TRAC VW, if stresses (or stress intensities or strains, as applicable) calculated by the appropriate structural analyses are less than the allowables defined in Subsection 3.1.2.3, and if the diametral change in the storage overpack (or HI-TRAC VW), if any, after any event of structural consequence to the overpack (or transfer cask), does not preclude ready retrievability of the contained MPC.

Stresses arise in the components of the HI-STORM FW system due to various loads that originate under normal, off-normal, or accident conditions. These individual loads are combined to form load combinations. Stresses, strains, displacements, and stress intensities, as applicable, resulting from the load combinations are compared to their respective allowable limits. The following subsections present loads, load combinations, and the allowable limits germane to them for use in the structural analyses of the MPC, the overpack, and the HI-TRAC VW transfer cask.

3.1.2.1 Applicable Loadings

The individual loads applicable to the HI-STORM FW system and the HI-TRAC VW cask are defined in Section 2.2 of this FSAR. Load combinations are developed by assembling the individual loads that may act concurrently, and possibly, synergistically. In this subsection, the individual loads are further clarified as appropriate and the required load combinations are identified. Table 3.1.1 contains the governing load cases and the affected components. Loadings are applied to the mathematical models of the MPCs, the overpack, and the HI-TRAC VW. Results of the analyses carried out under bounding load combinations are compared with their respective allowable limits. The analysis results from the bounding load combinations are also evaluated to ensure satisfaction of the functional performance criteria discussed in the foregoing.

The individual loads that address each design criterion applicable to the structural design of the HI-STORM FW system are cataloged in Tables 2.2.6, 2.2.7, and 2.2.13 for the handling, normal, off-normal, and accident (Design Basis Loads) conditions, respectively. The magnitude of loadings

associated with accident condition and natural phenomena-induced events, in general, do not have a regulatory limit. For example, the impact load from a tornado-borne missile, or the overturning load under flood or tsunami, cannot be prescribed as design basis values with absolute certainty that all ISFSI sites will be covered. Therefore, as applicable, representative magnitudes of such loadings are drawn from regulatory and industry documents (such as for tornado missiles and wind from Reg. Guide 1.76). In the following, the essential characteristics of both credible and non-credible loadings analyzed in this FSAR are explained.

a. Tip-Over

The freestanding HI-STORM FW storage overpack, containing a loaded MPC, must not tip over as a result of postulated natural phenomenon events, including tornado wind, a tornado-generated missile, a seismic or a hydrological event (flood). However, to demonstrate the defense-in-depth features of the design, a *non-mechanistic* tip-over scenario per NUREG-1536 is analyzed (Subsection 2.2.3) in this chapter. For MPC transfers that will occur outside of a Part 50 controlled structure, the potential of the HI-STORM FW overpack tipping over during the lowering (or raising) of the loaded MPC from (or into) the mounted HI-TRAC VW cask is ruled out because of the safeguards and devices mandated by this FSAR for such operations (Subsection 2.3.3). The physical and procedural barriers imposed during MPC handling operations, as described in this FSAR, prevent overturning of the HI-STORM/HI-TRAC assemblage with an extremely high level of certainty. Among the physical barriers to prevent the overturning of the HI-STORM/HI-TRAC stack during MPC transfer is the use of the Canister Transfer Facility illustrated in Figure 1.1.2 which secures the HI-STORM FW inside an engineered pit.

b. Handling Accident

The handling of all heavy loads that are within Part 72 jurisdiction must be carried out using single failure-proof equipment and lifting devices that comply with the stress limits of ANSI N14.6 to render an uncontrolled lowering of the payload non-credible (please see Subsection 2.2.3).

c. Flood

Flood at an ISFSI is designated as an extreme environmental event and is described in Subsection 2.2.3 (f).

The postulated flood event has two discrete potential structural consequences; namely,

i. stability of the HI-STORM FW system due to flood water velocity, and
ii. structural effects of hydrostatic pressure and water velocity induced lateral pressure.

The maximum hydrostatic pressure on the cask in a flood where the water level is conservatively set per Table 2.2.8 is calculated as follows:

Using p = the maximum hydrostatic pressure on the system (psi),
γ = weight density of water = 62.4 lb/ft^3,
h = the height of the water level = 125 ft;

The maximum hydrostatic pressure is

$$p = \gamma h = (62.4 \text{ lb/ft}^3)(125 \text{ ft})(1 \text{ ft}^2/144 \text{ in}^2) = 54.2 \text{ psi}$$

It is noted that the accident condition design external pressure for the MPC (Table 2.2.1) bounds the maximum hydrostatic pressure exerted by the flood.

The maximum acceptable water velocity for a moving flood water scenario is computed using the procedure in Subsection 3.4.4.1.1.

d. Explosion

Explosion, by definition, is a transient event. Explosive materials (except for the short duration when a limited quantity of motive fuel for placing the loaded MPC on the ISFSI pad is present in the tow vehicle or transporter) are prohibited in the controlled area by specific stipulation in the HI-STORM FW Technical Specification. However, pressure waves emanating from explosions in areas outside the ISFSI are credible.

Pressure waves from an explosive blast in a property near the ISFSI site result in an impulsive aerodynamic loading on the stored HI-STORM FW overpacks. Depending on the rapidity of the pressure build-up, the inside and outside pressures on the HI-STORM FW METCON™ shell may not equalize, leading to a net lateral loading on the upright overpack as the pressure wave traverses the overpack. The magnitude of the dynamic pressure wave is conservatively set to a value below the magnitude of the pressure differential that would cause a tip-over of the cask if the pulse duration were set infinite.

The allowable pressure from explosion, p_e, can be computed from static equilibrium to prevent sliding or tipping of the cask. A simplified inequality to ensure that the cask will not slide is given by

$$p_e \, D \, L \leq \mu W$$

where:

D: diameter of the cask
L: height of the cask above the ISFSI pad
μ: limiting value of the interface friction coefficient
W: weight of the cask (lower bound weight, assuming that the MPC has only one fuel assembly)

$$p_e \leq \frac{\mu W}{DL} \qquad \text{(A)}$$

The inequality for protection against tipping is obtained by moment equilibrium.

$$p_e \, D \frac{L^2}{2} \leq \frac{W \, D}{2}$$

or $$p_e \leq \frac{W}{L^2} \qquad \text{(B)}$$

The allowable value of p_e must be lesser of the two values given by inequalities (A) and (B) above.

In contrast to the overpack, the MPC is a closed pressure vessel. Because of the enveloping overpack around it, the explosive pressure wave would manifest as an external pressure on the external surface of the MPC.

The maximum overpressure on the MPC resulting from an explosion is limited by the HI-STORM FW Technical Specification to be equal to or less than the accident condition design external pressure specified in Table 2.2.1.

e. Tornado

The tornado loading is described in Subsection 2.2.3 (e). The three components of a tornado load are:

1. pressure changes,
2. wind loads, and
3. tornado-generated missiles.

Reference values of wind speeds and tornado-induced pressure drop are specified in Table 2.2.4. Tornado missiles are listed in Table 2.2.5. A central functional objective of a storage overpack is to maintain the integrity of the "Confinement Boundary", namely, the multi-purpose canister stored inside it. This operational imperative requires that the mechanical loadings associated with a tornado at the ISFSI do not jeopardize the physical integrity of the loaded MPC. Potential consequences of a tornado on the cask system are:

- Instability (tip-over) due to tornado missile impact plus either steady wind or impulse from the pressure drop

- Loadings applied on the MPC transmitted to the inside of the overpack through its openings or as a secondary effect of loading on the enveloping overpack structure.

- Excessive storage overpack permanent deformation that may prevent ready retrievability of the MPC.

- Excessive storage overpack permanent deformation that may significantly reduce the shielding effectiveness of the storage overpack.

Analyses must be performed to ensure that, due to the tornado-induced loadings:

- The overpack does not deform plastically such that the retrievability of the stored MPC is threatened.

- The MPC Confinement Boundary is not breached.

- The MPC fuel basket does not deform beyond the permitted limit (Table 2.2.11) to preserve its subcriticality margins (requires evaluation if the overpack tips over).

f. Earthquake

The earthquake loading and the associated acceptance criteria are presented in Subsection 2.2.3(g).

The Design Basis Earthquake for an ISFSI site shall be obtained *on the top surface of the pad* using an appropriate soil-structure interaction Code such as SHAKE2000 [3.1.7]. The seismic analysis methodology is provided in Subsection 3.4.4.1.2.

g. Lightning

The HI-STORM FW overpack contains over 50,000 lb of highly conductive carbon steel with over 700 square feet of external surface area. It is known from experience that such a large surface area and metal mass is adequate to dissipate any lightning that may strike the HI-STORM FW system. There are no combustible materials on the HI-STORM FW surface. Therefore, a postulated lightning strike event will not impair the structural performance of components of the HI-STORM FW system that are important-to-safety.

h. Fire

The fire event applicable to an ISFSI is described in Subsection 2.2.3(c) wherein the acceptance criteria are also presented.

i. 100% Fuel Rod Rupture

The sole effect of the postulated 100% fuel rod rupture is to increase the internal pressure in the MPC. Calculations in Chapter 4 show that the accident internal pressure limit set in Chapter 2 bounds the pressure from 100% fuel rod rupture. Therefore, 100% rod rupture does not define a new controlling loading event.

3.1.2.2 Design Basis Loads and Load Combinations

As discussed in Subsection 2.2.7, the number of discrete loadings for each situational condition (i.e., normal, off-normal, etc.) is consolidated by defining bounding loads for certain groups of loadings. Thus, the accident condition pressure P_o^* bounds the surface loadings arising from accident and extreme natural phenomenon events, namely, tornado wind W', flood F, and explosion E^*. These bounding loads are referred to as "Design Basis Loads".

The Design Basis Loads are analyzed in combination with other permanent loads, i.e., loads that are present at all times. The permanent loads consist of:

- The dead load of weight of each component.
- Internal pressure in the MPC.

For conservatism, the upper or lower bound of the dead load, D, of a component is used for a DBL to maximize the response. Thus, the lower bound value of D is used in the stability of the HI-STORM FW system under flood. Likewise, the value of internal pressure in the MPC is represented by the Design Pressure (Table 2.2.1), which envelops the actual internal pressure under each service condition.

As noted previously, certain loads, namely earthquake E, flowing water under flood condition F, force from an explosion pressure pulse F*, and tornado missile M, act to destabilize a cask. Additionally, these loads act on the overpack and produce essentially localized stresses at the HI-STORM FW system to ISFSI interface. Table 3.1.1 provides the load combinations that are relevant to the stability analyses of freestanding casks.

The major constituents in the HI-STORM FW system are: (i) the fuel basket, (ii) the Enclosure Vessel, (iii) the HI-STORM FW overpack, and (iv) the HI-TRAC VW transfer cask. The fuel basket and the Enclosure Vessel (EV) together constitute the multi-purpose canister. A complete account of analyses and results for all applicable loadings for all four constituent parts is provided in Section 3.4 as suggested in Regulatory Guide 3.61.

In the following, the loadings listed as applicable for each situational condition are addressed in meaningful load combinations for the fuel basket, Enclosure Vessel, and the overpack. Each component is considered separately.

a. Fuel Basket

Table 3.1.1 summarizes the loading cases (derived from Tables 2.2.6, 2.2.7, and 2.2.13) that are germane to demonstrating compliance of the loaded fuel baskets inside the MPC Enclosure Vessel.

The fuel basket is not a pressure vessel; therefore, the pressure loadings are not meaningful loads for the basket. Further, the basket is physically disconnected from the Enclosure Vessel. The gap between the basket and the Enclosure Vessel is sized to ensure that no constraint of free-end thermal expansion of the basket occurs. The demonstration of the adequacy of the basket-to-Enclosure Vessel (EV) gap to ensure absence of interference due to differential thermal expansion is addressed in Chapter 4.

The normal handling of the MPC within the HI-STORM FW system or the HI-TRAC VW transfer cask does not produce any significant stresses in the fuel basket because the operating procedures preclude horizontal handling.

b. Enclosure Vessel

Table 3.1.1 summarizes all load cases that are applicable to structural analysis of the Enclosure Vessel to ensure integrity of the Confinement Boundary.

The Enclosure Vessel is a pressure retaining device consisting of a cylindrical shell, a thick circular baseplate at the bottom, and a thick circular lid at the top. This pressure vessel must be shown to meet the primary stress intensity limits per ASME Section III Class 1 at the design temperature and primary plus secondary stress intensity limits under the combined action of pressure plus thermal loads (Level A service condition in the Code).

Normal handling of the Enclosure Vessel is considered in Section 2.2; the handling loads are independent of whether the Enclosure Vessel is within the storage overpack or HI-TRAC VW cask.

c. Storage Overpack

Table 3.1.1 identifies the load cases to be considered for the overpack. The following acceptance criteria apply:

i. Normal Conditions

- The dead load of the HI-TRAC VW with the heaviest loaded MPC (dry) on top of the HI-STORM FW overpack must be shown to be able to be supported by the metal-concrete (METCON™) structure consisting of the two concentric steel shells and the radial ribs.

- The stress field in the steel structure of the overpack must meet Level A (Subsection NF) limits.

ii. Accident Conditions

- Maximum flood water velocity for the overpack with a near empty MPC (only one SNF stored) shall not cause sliding or tip-over of the cask.

- Tornado missile plus wind on an overpack (with an empty MPC) (see Table 2.2.4) must not lead to violation of the acceptance criteria in 3.1.2.1(e).

- Large or medium penetrant missiles (see Table 2.2.5) must not be able to access the MPC. The small missile must be shown not to penetrate the MPC pressure vessel boundary since, in principle, it can enter the overpack cavity through the (curvilinear) vent inlet vent passages.

- Under seismic conditions, a freestanding HI-STORM FW overpack must be demonstrated to not tip over under the DBE events. The maximum sliding of the overpack must demonstrate that casks will not impact each other.

- Under a non-mechanistic tip-over of a fully loaded, freestanding HI-STORM FW overpack, the overpack lid must not dislodge.

- Accident condition induced gross general deformations of the storage overpack must be limited to values that do not prevent ready retrievability of the MPC.

d. HI-TRAC VW Transfer Cask

Table 3.1.1 culled from Tables 2.2.6, 2.2.7 and 2.2.13 identifies load cases applicable to the HI-TRAC VW transfer cask.

The HI-TRAC VW transfer cask must provide radiation protection, must act as a handling cask when carrying a loaded MPC, and in the event of a postulated accident must not suffer permanent deformation to the extent that ready retrievability of the MPC is compromised.

3.1.2.3 Allowables

The important-to-safety (ITS) components of the HI-STORM FW system are identified on the drawings in Section 1.5. Allowable stresses, as appropriate, are tabulated for these components for all service conditions.

In Section 2.2, the applicable service level from the ASME Code for determination of allowables is listed. Tables 2.2.6, 2.2.7 and 2.2.13 (condensed in Table 3.1.1) provide a tabulation of loadings for normal, off-normal, and accident conditions and the applicable acceptance criteria.

Relationships for allowable stresses and stress intensities for NB and NF components are provided in Tables 2.2.10 and 2.2.12, respectively. Tables 3.1.2 through 3.1.8 contain numerical values of the allowable stresses/stress intensities for all MPC, overpack, and HI-TRAC VW load bearing Code materials as a function of temperature. The tabulated values for the allowable stresses/stress intensities are used in Subsections 3.4.3 and 3.4.4, as applicable, to compute factors of safety for the ITS components of the HI-STORM FW system for various loadings.

In all tables the terms S, S_m, S_y, and S_u, respectively, denote the design stress, design stress intensity, minimum yield strength, and the ultimate strength. Property values at intermediate temperatures that are not reported in the ASME Code are obtained by linear interpolation. Property values are not extrapolated beyond the limits of the Code in any structural calculation.

Additional terms relevant to the stress analysis of the HI-STORM FW system extracted from the ASME Code (see Figure NB-3222-1, for example) are listed in Table 3.1.10.

3.1.2.4 Brittle Fracture

Section 8.4.3 discusses the low temperature ductility of the HI-STORM FW system materials. Table 3.1.9 provides a summary of impact testing requirements to insure prevention of brittle fracture.

3.1.2.5 Fatigue

Fatigue is a consequence of a cyclic state of stress applied on a metal part. Failure from fatigue occurs if the combination of amplitude of the cyclic stress, σ_a, and the number of cycles, n_f, reaches a threshold value at which failure occurs. ASME Code, Section III, Subsection NCA provides the σ_a-n_f curves for a number of material types. At $n_f = 10^6$, the required σ_a is referred to as the "Endurance Limit". The Endurance Limit for stainless steel (the material used in the MPC) according to the ASME Code, Section III, Div. 1, Appendices, Table I.9.2, is approximately 28 ksi.

The causative factors for fatigue expenditure in a non-active system (i.e., no moving parts) such as the HI-STORM FW system may be:

i. rapid temperature changes
ii. significant pressure changes

The HI-STORM FW system is exposed to the fluctuating thermal state of the ambient environment. Effect of wind and relative humidity also play a role in affecting the temperature of the cask components. However, the most significant effects are the large thermal inertia of the system and the relatively low heat transfer coefficients that act to smooth out the daily temperature cycles. As a result, the amplitude of the cyclic stresses, to the extent that they are developed, remains orders of magnitude below the cask material's Endurance Limit.

The second causative factor, namely, pressure pulsation, is limited to the only pressure vessel in the system – the MPC. Pressure produces several types of stresses in the MPC (see Table 3.1.10), all of which are equally effective in causing fatigue expenditure in the metal. However, the amplitude of stress from the pressure cycling (due to the changes in the ambient conditions) is quite small and well below the endurance limit of the stainless steel material.

Therefore, failure from fatigue is not a credible concern for the HI-STORM FW system components.

3.1.2.6 Buckling

Buckling is caused by a compressive stress acting on a slender section. In the HI-STORM FW system, the steel weldment in the overpack is not slender; its height-to-diameter ratio being less than 2. There is no source of compressive stress except from the self-weight of the shell and the overpack weight of the HI-TRAC VW in the stacked condition, which produces a modest state of compressive stress. The state of a small compressive stress combined with a low slenderness ratio makes the HI-STORM FW overpack safe from the buckling mode of failure. The same statement also applies to the HI-TRAC VW transfer cask, which is a radially buttressed triple shell (in comparison to the dual shell construction in HI-STORM FW) structure.

The MPC Enclosure Vessel is protected from buckling of by the permanent tensile stress in both hoop and longitudinal directions due to internal pressure.

Finally, the fuel basket, which is an egg-crate structure, as shown in Figures 1.1.6 and1.1.7 (an intrinsically resistant structural form to buckling from axial compressive loads), is subject to minor compressive stresses from its own weight. The absence of buckling in the Metamic-HT fuel basket is based on the fact that there are no causative scenarios (normal or accident) that produce a significant in-plane compressive stress in the basket structure. A lower bound Euler Buckling strength for the Metamic-HT fuel basket can be obtained by assuming that the basket walls are fully continuous[1] over the entire height of the MPC fuel basket, neglecting the strengthening effect of the honeycomb completely, and treating the Metamic-HT basket wall as an end-loaded plate 199.5" high by 8.94" wide by 0.59" thick (corresponding to the maximum height MPC-37 fuel basket). The top and

1 In reality, the basket walls are not fully continuous in the vertical direction since the fuel basket is assembled by vertically stacking narrow width Metamic-HT panels in a honeycomb pattern (see drawing 6506 in Chapter 1 of HI-STORM FW SAR). For the above buckling strength evaluation, the assumption that the basket walls are continuous over the full height of the fuel basket is extremely conservative since the critical buckling load is inversely proportional to the square of the height.

bottom edges are assumed to be pinned and the lateral edges are assumed to be free to minimize the permissible buckling load (a particularly severe modeling artifice to minimize buckling strength). The Euler buckling load for this geometry is given by (see Timoshenko et al., "Theory of ElasticStability", 2nd Edition):

$$P_{cr} = \frac{\pi^2 EI}{h^2} = 133lbf$$

where E = Young's Modulus of Metamic-HT at 500°C = 3,500 ksi,
I = moment of inertia of 8.94" wide by 0.59" thick plate = 0.153 in^4,
h = maximum height of fuel basket = 199.5"

The corresponding compressive axial stress is given by:

$$\sigma_{cr} = \frac{P_{cr}}{A} = \frac{133lbf}{(8.94in)(0.59in)} = 25.2psi$$

The factor of safety against buckling is given by (where σ_b is the compressive stress in the basket due to self weight):

$$SF = \frac{\sigma_{cr}}{\sigma_b} = \frac{25.2psi}{19.5psi} = 1.29$$

Thus, even with an exceedingly conservative model, the safety margin against buckling is more than 25%.

Therefore, buckling is ruled out as a credible failure mechanism in the HI-STORM FW system components. Nevertheless, a Design Basis Load consisting of external pressure is specified in Table 2.2.1 with the (evidently, non-mechanistic) conservative assumption that the internal pressure, which will counteract buckling behavior, is zero psig. (In reality, internal pressure cannot be zero because of the positive helium fill pressure established at the time of canister backfill.)

3.1.2.7 Consideration of Manufacturing and Material Deviations

Departure from the assumed values of material properties in the safety analyses clearly can have a significant effect on the computed margins. Likewise, the presence of deviations in manufacturing that inevitably occur in custom fabrication of capital equipment may detract from the safety factors reported in this chapter. In what follows, the method and measures adopted to insure that deviations in material properties or in the fabricated hardware will not undermine the structural safety conclusions are summarized.

That the yield and ultimate strengths of materials used in manufacturing the HI-STORM FW components will be greater than that assumed in the structural analyses is insured by the requirement

in the ASME Code which mandates all Code materials to meet the minimum certified property values set down in the Code tables. Holtec International requires the material supplier to provide a Certified Mill Test Report in the format specified in the Code to insure compliance of all physical properties of the supplied material with the specified Code minimums. The same protocol to insure that the actual property values are above the minimum specified values is followed in the manufacture of Metamic-HT (Appendix 1.B and Subsection 10.1.3). An additional margin in the actual physical properties vis-à-vis the Code values exists in the case of the MPC Confinement Boundary material by virtue of the Alloy X definition (Appendix 1.A): The physical properties of Alloy X at each temperature are set down at the lowest of that property value in the Code from a group of austenitic stainless steels.

The above measures make the probability of an actual material strength property to be falling below the assumed value in the structural analysis in this chapter to be non-credible. On the contrary, Holtec's manufacturing experience suggests that the actual properties are likely to be uniformly and substantially greater than the assumed values.

A similarly conservative approach is used to insure that the fabrication processes do not degrade the computed safety margins. Towards this end, the fabrication documents (drawings, travelers and shop procedures) implement a number of pro-active measures to prevent all known sources of development of a strength-adverse condition, such as:

i. All welding procedures are qualified to yield better physical properties than the Code minimums. All essential variables that affect weld quality are tightly controlled.

ii. Only those craftsmen who have passed the welding skill criteria implemented in the shop are permitted to weld.

iii. A rigorous weld material quality overcheck program is employed to insure that every weld wire spool meets its respective Code specification.

iv. All welds are specified as minimums: In practice, most exceed the specified minimums significantly. All primary structural welds are subject to Q.C. overcheck and sign-off.

v. The Threaded Anchor Locations (TALs) are machined to a depth greater than the specified minimum. The stress analyses utilize the minimum thread depths/lengths per the licensing drawings.

In the event of a deviation that may depress the computed safety margin, a non-conformance report is prepared by the manufacturer and subject to a safety analysis by Holtec International's corporate engineering using the same methodology as that described in this FSAR. The item is accepted only if the safety evaluation musters part 72.48 acceptance criteria. A complete documentation of the life cycle of the NCR is archived in the Company's Permanent Filing System and shared with the designated system user.

The above processes and measures have been in place at the Holtec Manufacturing Division to insure that an unacceptable reduction in the safety factors due to variation in material properties and manufacturing processes does not occur. The manufacturing experience over the past 20 years corroborates the effectiveness of the above measures.

3.1.3 Stress Analysis Models

To evaluate the effect of loads on the HI-STORM FW system components, finite element models for stress and deformation analysis are developed. The essential attributes of the finite element models for the HI-STORM overpack and the MPC are presented in this subsection. These models are used to perform the structural analysis of the system components under the loadings listed in Tables 2.2.6, 2.2.7 and 2.2.13, and summarized in Table 3.1.1 herein for handling, normal, off-normal, and accident conditions, respectively. The HI-TRAC VW transfer cask, on the other hand, is conservatively analyzed using strength of materials principles, as described in Subsection 3.1.3.3.

All finite element models are three-dimensional and are prepared to the level of discretization appropriate to the problem to be solved. The models are suitable for implementation in ANSYS and LS-DYNA general purpose codes, which are described in Subsection 3.6.2.

In the following, the finite element models of the HI-STORM overpack (body and lid) and the MPC (Confinement Boundary and the fuel baskets) are presented. Pursuant to ISG-21, the description of the computational model for each component addresses the following areas:

- Description of the model, its key attributes and its conservative aspects
- Types of finite elements used and the rationale for their selection
- Material properties and applicable temperature ranges
- Modeling simplifications and their underlying logic

In subsequent subsections, where the finite element models are deployed to analyze the different load cases, the presentation includes the consideration of:

- Geometric compliance of the simulation with the physics of the problem
- Boundary conditions
- Effect of tolerances on the results
- Convergence (numerical) of the solutions reported in this FSAR

The input files prepared to implement the finite element solutions as well as detailed results are archived in the Calculation Packages [3.4.11, 3.4.13] within the Company's Configuration Control

System. Essential portions of the results for each loading case necessary to draw safety conclusions are extracted from the Calculation Packages and reported in this FSAR. Specifically, the results summarized from the finite element solutions in this chapter are self-contained to enable an independent assessment of the system's safety. Input data is provided in tabular form as suggested in ISG-21. For consistency, the following units are employed to document input data throughout this chapter:

- Time: second
- Mass: pound
- Length: inch

3.1.3.1 HI-STORM FW Overpack

The physical geometry and materials of construction of the HI-STORM FW overpack are provided in Sections 1.1 and 1.2 and the drawings in Section 1.5. The finite element simulation of the overpack consists of two discrete models, one for the overpack body and the other for the top lid.

The models are initially developed using the finite element code ANSYS [3.4.1], and then, depending on the load case, numerical simulations are performed either in ANSYS or in LS-DYNA [3.1.8]. For example, the handling loads (Load Case 9) and the snow load (Load Case 10) are simulated in ANSYS, and the non-mechanistic tipover event (Load Case 4) is simulated in LS-DYNA. For the non-mechanistic tipover analysis, two distinct finite element models are created: one for the HI-STORM FW overpack carrying the maximum length MPC-37 and one for the HI-STORM FW overpack carrying the maximum length MPC-89 (Figures 3.4.10A and 3.4.10B).

The key attributes of the HI-STORM FW overpack models (implemented in ANSYS) are:

i. The finite element discretization of the overpack is sufficiently detailed to accurately articulate the primary membrane and bending stresses as well as the secondary stresses at locations of gross structural discontinuity. The finite element layout of the HI-STORM FW overpack body and the top lid are pictorially illustrated in Figures 3.4.3 and 3.4.5, respectively. The overpack model consists of over 70,000 nodes and 50,000 elements, which exceed the number of nodes and elements in the HI-STORM 100 tipover model utilized in [3.1.4]. Table 3.1.11 summarizes the key input data that is used to create the finite element models of the HI-STORM FW overpack body and top lid.

ii. The overpack baseplate, anchor blocks, and the lid studs are modeled with SOLID45 elements. The overpack inner and outer shells, bottom vent shells, and the lifting ribs are modeled with SHELL63 elements. A combination of SOLID45, SHELL63, and SOLSH190 elements is used to model the steel components in the HI-STORM FW lid. These element types are well suited for the overpack geometry and loading conditions, and they have been used successfully in previous cask licensing applications [3.1.10, 3.3.2].

iii. All overpack steel members are represented by their linear elastic material properties (at 300°F) based on the data provided in Section 3.3. The concrete material in the overpack body is not explicitly modeled. Its mass, however, is accounted for by applying a uniformly distributed pressure on the baseplate annular area between the inner and outer shells (see Figure 3.4.26). The plain concrete in the HI-STORM FW lid is explicitly modeled in ANSYS using SOLID65 elements along with the input parameters listed in Table 3.1.12.

iv. To implement the ANSYS finite element model in LS-DYNA, the SOLID45, SHELL63, and SOLSH190 elements are converted to solid, shell, and thick shell elements, respectively, in LS-DYNA. The SOLID65 elements used to model the plain concrete in the HI-STORM FW lid are replaced by MAT_PSEUDO_TENSOR (or MAT_016) elements in LS-DYNA. The plain concrete in the overpack body is also modeled in LS-DYNA using MAT_PSEUDO_TENSOR elements.

v. In LS-DYNA, all overpack steel members are represented by their applicable nonlinear elastic-plastic true stress-strain relationships. The methodology used for obtaining a true stress-strain curve from a set of engineering stress-strain data (e.g., strength properties from [3.3.1]) is provided in [3.1.9], which utilizes the following power law relation to represent the flow curve of metal in the plastic deformation region:

$$\sigma = K\varepsilon^n$$

where n is the strain-hardening exponent and K is the strength coefficient. Table 3.1.13 provides the values of K and n that are used to model the behavior of the overpack steel materials in LS-DYNA. Further details of the development of the true stress-strain relations for these materials are found in [3.4.11]. The concrete material is modeled in LS-DYNA using a non-linear material model (i.e., MAT_PSEUDO_TENSOR or MAT_016) based on the properties listed in Section 3.3.

3.1.3.2 Multi-Purpose Canister (MPC)

The two constituent parts of the MPC, namely (i) the Enclosure Vessel and (ii) the Fuel Basket, are modeled separately. The model for the Enclosure Vessel is focused to quantify its stress and strain field under the various loading conditions. The model for the Fuel Basket is focused on characterizing its strain and displacement behavior during a non-mechanistic tipover event. For the non-mechanistic tipover analysis, two distinct finite element models are created: one for the maximum length MPC-37 and one for the maximum length MPC-89 (Figures 3.4.11 and 3.4.12).

The key attributes of the MPC finite element models (implemented in ANSYS) are:

i. The finite element layout of the Enclosure Vessel is pictorially illustrated in Figure 3.4.1. The finite element discretization of the Enclosure Vessel is sufficiently detailed to accurately articulate the primary membrane and bending stresses as well as the secondary stresses at

locations of gross structural discontinuity, particularly at the MPC shell to baseplate juncture. This has been confirmed by comparing the ANSYS stress results with the analytical solution provided in [3.4.16] (specifically Cases 4a and 4b of Table 31) for the discontinuity stress at the junction between a cylindrical shell and a flat circular plate under internal pressure (100 psig). The two solutions agree within 3% indicating that the finite element mesh for the Enclosure Vessel is adequately sized. Table 3.1.14 summarizes the key input data that is used to create the finite element model of the Enclosure Vessel.

ii. The Enclosure Vessel shell, baseplate, and upper and lower lids are meshed using SOLID185 elements. The MPC lid-to-shell weld and the reinforcing fillet weld at the shell-to-baseplate juncture are also explicitly modeled using SOLID185 elements (see Figure 3.4.1).

iii. Consistent with the drawings in Section 1.5, the MPC lid is modeled as two separate plates, which are joined together along their perimeter edge. The upper lid is conservatively modeled as 4.5" thick, which is less than the minimum thickness specified on the licensing drawing (see Section 1.5). "Surface-to-surface" contact is defined over the interior interface between the two lid plates using CONTA173 and TARGE170 contact elements.

iv. The materials used to represent the Enclosure Vessel are assumed to be isotropic and are assigned linear elastic material properties based on the Alloy X material data provided in Section 3.3. The Young's modulus value varies throughout the model based on the applied temperature distribution, which is shown in Figure 3.4.27 and conservatively bounds the normal operating temperature distribution for the maximum length MPC-37 as determined by the thermal analyses in Chapter 4.

v. The fuel basket models (Figures 3.4.12A and 3.4.12B), which are implemented in LS-DYNA, are assembled from intersecting plates per the licensing drawings in Section 1.5, include all potential contacts and allow for relative rotations between intersecting plates. For conservatism, a bounding gap is assumed at contact interfaces between any two perpendicular basket plates to allow for impacts and, therefore, maximize the stress and deformation of the fuel basket plate. The fuel basket plates are modeled in LS-DYNA using thick shell elements, which behave like solid elements in contact, but can also accurately simulate the bending behavior of the fuel basket plates. To ensure numerical accuracy, full integration thick shell elements with 10 through-thickness integration points are used. This modeling approach is consistent with the approach taken in [3.1.10] to qualify the F-32 and F-37 fuel baskets.

vi. In LS-DYNA, the fuel basket plates are represented by their applicable nonlinear elastic-plastic true stress-strain relationships in the same manner as the steel members of the HI-STORM FW overpack (see Subsection 3.1.3.1). Table 3.1.13 provides the values of K and n that are used to model the behavior of the fuel basket plates in LS-DYNA. Details of the development of the true stress-strain relations are found in [3.4.11].

3.1.3.3 HI-TRAC VW Transfer Cask

The stress analysis of the transfer cask addresses three performance features that are of safety consequence. They are:

i. Performance of the water jacket as a pressure retaining enclosure under an accident condition leading to overheating of water.
ii. Performance of the threaded anchor locations in the HI-TRAC VW top flange under the maximum lifted load.
iii. Performance of the HI-TRAC VW bottom lid under its own self weight plus the weight of the heaviest MPC.

The above HI-TRAC VW components are analyzed separately using strength of materials formula, the details of which are provided in Subsections 3.4.3 and 3.4.4.

Table 3.1.1

GOVERNING CASES AND AFFECTED COMPONENTS

Case	Loading Case I.D. from Tables 2.2.6, 2.2.7 and 2.2.13	Loading Event	Affected Components			Objective of the Analysis	For additional discussion, refer to Subsection
			HI-STORM	MPC	HI-TRAC		
1	AD	Moving Flood Moving Floodwater with loaded HI-STORM on the pad.	X	—	—	Determine the flood velocity that will not overturn the overpack.	2.2.3
2.	AE	Design Basis Earthquake (DBE) Loaded HI-STORMs arrayed on the ISFSI pad subject to ISFSI's DBE	X	X	—	Determine the maximum magnitude of the earthquake that meets the acceptance criteria of 2.2.3(g).	2.2.3
3	AC	Tornado Missile A large, medium or small tornado missile strikes a loaded HI-STORM on the ISFSI pad or HI-TRAC.	X	X	X	Demonstrate that the acceptance criteria of 2.2.3(e) will be met.	2.2.3
4	AA	Non-Mechanistic Tip-Over A loaded HI-STORM is assumed to tip over and strike the pad.	X	X	—	Satisfy the acceptance criteria of 2.2.3(b).	2.2.3
5	NB	Design Internal Pressure MPC under the normal condition Design Internal Pressure	—	X	—	Demonstrate that the MPC meets "NB" stress intensity limits.	2.2.1
6	NB	Maximum Internal Pressure Under the Accident Condition MPC under the accident condition internal pressure (from Table 2.2.1)	—	X	—	Demonstrate that the Level D stress intensity limits are met.	2.2.1

Table 3.1.1 (continued)

GOVERNING CASES AND AFFECTED COMPONENTS

Case	Loading Case I.D. from Tables 2.2.6, 2.2.7 and 2.2.13	Loading Event	Affected Components			Objective of the Analysis	For additional discussion, refer to Subsection
7	AH	Design External Pressure MPC under the accident condition external pressure (from Table 2.2.1)	—	X	—	The Enclosure Vessel must not buckle.	2.2.3
8	AJ	HI-TRAC Non-Mechanistic Heat-Up Postulate the water jacket's internal pressure reaches the Design Pressure (defined in Table 2.2.1)	—	—	X	Demonstrate that the stresses in the water jacket meet the ASME Code Section III Subsection Class 3 limits for the Design Condition.	2.2.1
9.	HA, HB, and HC	Handling of Components	X	X	X	Demonstrate that the tapped anchor locations (TALs) meet the Regulatory Guide 3.61 and NUREG-0612 stress limits (as applicable).	2.2.1
10.	NA	Snow Load	X	—	—	Demonstrate that the top lid's steel structure meets "NF" stress limit for normal condition.	2.2.1
11.	NA	MPC Reflood Event	—	X	—	Demonstrate that there is no breach of the fuel rod cladding.	12.3.1

Table 3.1.2

DESIGN AND LEVEL A: STRESS

Reference Code: ASME NF
Material: SA36
Service Conditions: Design and Normal
Item: Stress

Temp. (Deg. F)	Classification and Value (ksi)		
	S	Membrane Stress	Membrane plus Bending Stress
-20 to 650	16.6	16.6	24.9
700	15.6	15.6	23.4

Notes:

1. S = Maximum allowable stress values from Table 1A of ASME Code, Section II, Part D.
2. Stress classification per Paragraph NF-3260.
3. Limits on values are presented in Table 2.2.12.

Table 3.1.3

LEVEL B: STRESS

Reference Code: ASME NF
Material: SA36
Service Conditions: Off-Normal
Item: Stress

Temp. (Deg. F)	Classification and Value (ksi)	
	Membrane Stress	Membrane plus Bending Stress
-20 to 650	22.1	33.1
700	20.7	31.1

Notes:

1. Limits on values are presented in Table 2.2.12 with allowables from Table 3.1.2.

Table 3.1.4

DESIGN AND LEVEL A SERVICE CONDITIONS: ALLOWABLE STRESS

Code: ASME NF
Material: SA516 (SA515) Grade 70, SA350-LF3 (SA350-LF2)
Service Conditions: Design and Normal
Item: Allowable Stress

Temp. (Deg. F)	Classification and Value (ksi)		
	S	Membrane Stress	Membrane plus Bending Stress
-20 to 400	20.0	20.0	30.0
500	19.6	19.6	29.4
600	18.4	18.4	27.6
650	17.8	17.8	26.7
700	17.2	17.2	25.8

Notes:

1. S = Maximum allowable stress values from Table 1A of ASME Code, Section II, Part D.
2. Stress classification per Paragraph NF-3260.
3. Limits on values are presented in Table 2.2.12.
4. Maximum allowable stress values are the lowest of all values for the candidate materials (SA516 (SA515) Grade 70, SA350-LF3 (SA350-LF2)) at corresponding temperature.

Table 3.1.5

LEVEL B: ALLOWABLE STRESS

Code: ASME NF
Material: SA516 (SA515) Grade 70, SA350-LF3 (SA350-LF2)
Service Conditions: Off-Normal
Item: Allowable Stress

Temp. (Deg. F)	Classification and Value (ksi)	
	Membrane Stress	Membrane plus Bending Stress
-20 to 400	26.6	39.9
500	26.1	39.1
600	24.5	36.7
650	23.7	35.5
700	22.9	34.3

Notes:

1. Limits on values are presented in Table 2.2.12 with allowables from Table 3.1.4.
2. Maximum allowable stress values are the lowest of all values for the candidate materials (SA516 (SA515) Grade 70, SA350-LF3 (SA350-LF2)) at corresponding temperature.

Table 3.1.6

LEVEL D: STRESS INTENSITY

Code: ASME NF
Material: SA516 (SA515) Grade 70
Service Conditions: Accident
Item: Stress Intensity

Temp. (Deg. F)	Classification and Value (ksi)		
	S_m	P_m AMAX ($1.2S_y$, $1.5S_m$), but < $0.7\ S_u$	$P_m + P_b$ 150% of P_m
-20 to 100	23.3	45.6	68.4
200	23.2	41.8	62.7
300	22.4	40.3	60.4
400	21.6	39.0	58.5
500	20.6	37.2	55.8
600	19.4	34.9	52.4
650	18.8	33.8	50.7
700	18.1	32.9	49.4

Notes:

1. Level D allowable stress intensities per Appendix F, Paragraph F-1332.
2. S_m = Stress intensity values per Table 2A of ASME, Section II, Part D.
3. P_m and P_b are defined in Table 3.1.10.

Table 3.1.7

DESIGN, LEVELS A AND B: STRESS INTENSITY

Code: ASME NB
Material: Alloy X
Service Conditions: Design, Levels A and B (Normal and Off-Normal)
Item: Stress Intensity

Temp. (Deg. F)	Classification and Numerical Value					
	S_m	P_m†	P_L†	$P_L + P_b$†	$P_L + P_b + Q$††	P_e††
-20 to 100	20.0	20.0	30.0	30.0	60.0	60.0
200	20.0	20.0	30.0	30.0	60.0	60.0
300	20.0	20.0	30.0	30.0	60.0	60.0
400	18.6	18.6	27.9	27.9	55.8	55.8
500	17.5	17.5	26.3	26.3	52.5	52.5
600	16.5	16.5	24.75	24.75	49.5	49.5
650	16.0	16.0	24.0	24.0	48.0	48.0
700	15.6	15.6	23.4	23.4	46.8	46.8
750	15.2	15.2	22.8	22.8	45.6	45.6
800	14.8	14.8	22.2	22.2	44.4	44.4

Notes:

1. S_m = Stress intensity values per Table 2A of ASME II, Part D.
2. Alloy X S_m values are the lowest values for each of the candidate materials at corresponding temperature.
3. Stress classification per NB-3220.
4. Limits on values are presented in Table 2.2.10.
5. P_m, P_L, P_b, Q, and P_e are defined in Table 3.1.10.

† Evaluation required for Design condition only.
†† Evaluation required for Levels A, B conditions only. P_e not applicable to vessels.

Table 3.1.8

LEVEL D: STRESS INTENSITY

Code:	ASME NB
Material:	Alloy X
Service Conditions:	Level D (Accident)
Item:	Stress Intensity

Temp. (Deg. F)	Classification and Value (ksi)		
	P_m	P_L	$P_L + P_b$
-20 to 100	48.0	72.0	72.0
200	48.0	72.0	72.0
300	46.3	69.45	69.45
400	44.6	66.9	66.9
500	42.0	63.0	63.0
600	39.6	59.4	59.4
650	38.4	57.6	57.6
700	37.4	56.1	56.1
750	36.5	54.8	54.8
800	35.5	53.25	53.25

Notes:

1. Level D stress intensities per ASME NB-3225 and Appendix F, Paragraph F-1331.
2. The average primary shear strength across a section loaded in pure shear may not exceed 0.42 S_u.
3. Limits on values are presented in Table 2.2.10.
4. P_m, P_L, and P_b are defined in Table 3.1.10.

Table 3.1.9

FRACTURE TOUGHNESS TEST REQUIREMENTS FOR HI-STORM FW OVERPACK

Material	Test Requirement	Test Temperature	Acceptance Criterion
Bolting (SA193 B7)	Not required per NF-2311(b)(13) and Note (e) to Figure NF-2311(b)-1	-	-
Material with a nominal section thickness of 5/8" and less	Not required per NF-2311(b)(1)	-	-
Normalized SA516 Gr. 70 (thicknesses 2-1/2" and less)	Not required per NF-2311(b)(10) for service temperatures greater than or equal to 0°F (i.e., handling operations), and per NF-2311(b)(7) for service temperatures less than 0°F and greater than or equal to -40°F (i.e., non-handling operations)	-	-
Normalized SA516 Gr. 70 used for HI-STORM FW base plate (thickness greater than 2-1/2")	Not required per NF-2311(b)(7)	-	-
As rolled SA516 Gr. 70 used for HI-STORM FW inner and outer shells, base plate, top plate, inlet shell plate, inlet vent top plate, gamma shield plate, lid lower shim plate, and lid gusset	Not required per NF-2311(b)(7)	-	-
SA36 (thickness greater than 5/8")	Not required per NF-2311(b)(7)	-	-
SA350-LF2 (thickness greater than 5/8") and as rolled SA516 Gr. 70 used for HI-STORM FW lifting rib	Per NF-2331	-40°F (Also must meet ASME Section IIA requirements)	Table NF-2331(a)-3 or Figure NF-2331(a)-2 (Also must meet ASME Section IIA requirements)
Weld material	Test per NF-2430 if: (1) either of the base materials of the production weld requires impact testing, or; (2) either of the base materials is SA516 Gr. 70 with nominal section thickness greater than 5/8".	-40°F	Per NF-2331

Table 3.1.9 (continued)

FRACTURE TOUGHNESS TEST REQUIREMENTS FOR HI-TRAC VW TRANSFER CASK

Material	Test Requirement	Test Temperature	Acceptance Criterion
Bolting (SA193 B8 Class 2)	Not required per NF-2311(b)(5)	-	-
Material with a nominal section thickness of 5/8" and less	Not required per NF-2311(b)(1)	-	-
Normalized SA516 Gr. 70 (thicknesses 2-1/2" and less)	Not required per NF-2311(b)(10)	-	-
Normalized SA516 Gr. 70 used for HI-TRAC VW bottom lid (thickness greater than 2-1/2")	Not required per NF-2311(b)(7)	-	-
As rolled SA516 Gr. 70 used for HI-TRAC VW inner and outer shells, extended rib, short rib, bolt recess cap, and bottom lid	Not required per NF-2311(b)(7)	-	-
SA36 (thickness greater than 5/8")	Not required per NF-2311(b)(7)	-	-
SA515 Gr. 70, SA106 Gr. C, and SA350-LF3 (thickness greater than 5/8")	Per NF-2331	0°F (Also must meet ASME Section IIA requirements)	Table NF-2331(a)-3 or Figure NF-2331(a)-2 (Also must meet ASME Section IIA requirements)
Weld material	Test per NF-2430 if: (1) either of the base materials of the production weld requires impact testing, or; (2) either of the base materials is SA516 Gr. 70 with nominal section thickness greater than 5/8".	0°F	Per NF-2331

Table 3.1.10

ORIGIN, TYPE AND SIGNIFICANCE OF STRESSES IN THE HI-STORM FW SYSEM

Symbol	Description	Notes
P_m	Primary membrane stress	Excludes effects of discontinuities and concentrations. Produced by pressure and mechanical loads. Primary membrane stress develops in the MPC Enclosure Vessel shell. Limits on P_m exist for normal (Level A), off-normal (Level B), and accident (Level D) service conditions.
P_L	Local membrane stress	Considers effects of discontinuities but not concentrations. Produced by pressure and mechanical loads, including earthquake inertial effects. P_L develops in the MPC Enclosure Vessel wall due to impact between the overpack guide tubes and the MPC (near the top of the MPC) under an earthquake (Level D condition) or non-mechanistic tip-over event. However, because there is no Code limit on P_L under Level D event, a limit on the local strain consistent with the approach in the HI-STORM 100 docket is used (see Subsection 3.4.4.1.4).
P_b	Primary bending stress	Component of primary stress proportional to the distance from the centroid of a solid section. Excludes the effects of discontinuities and concentrations. Produced by pressure and mechanical loads, including earthquake inertial effects. Primary bending stress develops in the top lid and baseplate of the MPC, which is a pressurized vessel. Lifting of the loaded MPC using the so-called "lift cleats" also produces primary bending stress in the MPC lid. Similarly, the top lid of the HI-STORM FW module, a plate-type structure, withstands the snow load (Table 2.2.8) by developing primary bending stress.
P_e	Secondary expansion stress	Stresses that result from the constraint of free-end displacement. Considers effects of discontinuities but not local stress concentration (not applicable to vessels). It is shown that there is no interference between component parts due to free thermal expansion. Therefore, P_e does not develop within any HI-STORM FW component.
Q	Secondary membrane plus bending stress	Self-equilibrating stress necessary to satisfy continuity of structure. Occurs at gross structural discontinuities. Can be caused by pressure, mechanical loads, or differential thermal expansion. The junction of MPC shell with the baseplate and top lid locations of gross structural discontinuity, where secondary stresses develop as a result of internal pressure. Secondary stresses would also develop at the two extremities of the MPC shell if a thermal gradient were to exist. However, because the top and bottom regions of the MPC cavity also serve as the top and bottom plenums, respectively, for the recirculating helium, the temperature field in the regions of gross discontinuity is essentially uniform, and as a result, the thermal stress adder is insignificant and neglected (see Paragraph 3.1.2.5).
F	Peak stress	Increment added to primary or secondary stress by a concentration (notch), or, certain thermal stresses that may cause fatigue but not distortion. Because fatigue is not a credible source of failure in a passive system with gradual temperature changes, fatigue damage is not computed for HI-STORM FW components.

Table 3.1.11

KEY INPUT DATA FOR FINITE ELEMENT MODEL OF HI-STORM FW OVERPACK

Item	Value
Overall height of HI-STORM FW (including top lid)	221.5 in (for maximum length BWR fuel) 239.5 in (for maximum length PWR fuel)
Height of overpack body	199.25 (for maximum length BWR fuel) 217.25 in (for maximum length PWR fuel)
Height of top lid above top of overpack body	22.25 in
Top lid diameter	103 in
Inside diameter of HI-STORM FW storage cavity	81 in
Outside diameter of HI-STORM FW overpack	139 in
Inner shell thickness	0.75 in
Outer shell thickness	0.75 in
Lifting rib thickness	1 in
Baseplate thickness	3 in
Material	Various (see licensing drawings in Section 1.5)
Ref. temperature for material properties	300°F (implemented in ANSYS) Table 3.1.13 (implemented in LS-DYNA)
Concrete density	200 lbf/ft^3

Table 3.1.12

INPUT PARAMETERS FOR SOLID65 CONCRETE ELEMENTS
USED IN HI-STORM FW LID MODEL

Input Parameter	Value
Density	200 lbf/ft^3
Poisson's ratio	0.17
Compressive strength	3,000 psi
Young's modulus	3.122×10^6 psi
Shear transfer coefficient for open cracks	0.1
Shear transfer coefficient for closed cracks	0.3

Table 3.1.13

VALUES OF "K" AND "n" USED TO MODEL ELASTIC-PLASTIC BEHAVIOR OF HI-STORM SYSTEM COMPONENTS IN LS-DYNA

Component	Material	Ref. Temperature	K† (psi)	n†
Fuel Basket	Metamic-HT	365°C	1.542×10^4	0.069
		350°C	1.676×10^4	0.063
		325°C	1.897×10^4	0.056
		300°C	2.116×10^4	0.051
		250°C	2.417×10^4	0.064
		200°C	2.712×10^4	0.075
MPC Lid	Alloy X	500°F	1.055×10^5	0.235
MPC Shell	Alloy X	450°F	1.152×10^5	0.244
MPC Baseplate	Alloy X	350°F	1.161×10^5	0.236
HI-STORM Anchor Block	SA-350 LF2	250°F	1.160×10^5	0.189
HI-STORM Lid Stud	SA-193 B7	250°F	1.399×10^5	0.082
HI-STORM Inlet Shield Pipe	SA-53	250°F	9.464×10^4	0.161
HI-STORM Body††	SA-516 Gr. 70	300°F	1.144×10^5	0.181
HI-STORM Lid	SA-516 Gr. 70	250°F	1.139×10^5	0.179
HI-STORM Inlet Shell Plate, Inlet Vent Top Plate, & Lid	SA-36	250°F	8.952×10^4	0.150

† K and n are defined in Subsection 3.1.3.1.

†† Includes all components in HI-STORM overpack body made from SA-516 Gr. 70 material (e.g., baseplate, inner and outer shells, lifting ribs, etc.).

Table 3.1.14

KEY INPUT DATA FOR ANSYS MODEL OF MPC ENCLOSURE VESSEL

Item	Value
Overall Height of MPC	195 in (for maximum length BWR fuel) 213 in (for maximum length PWR fuel)
Outside diameter of MPC	75.5 in
MPC upper lid thickness	4.5 in
MPC lower lid thickness	4.5 in
MPC shell thickness	0.5 in
MPC baseplate thickness	3.0 in
Material	Alloy X
Ref. temperature for material properties	Figure 3.4.27 (implemented in ANSYS) Table 3.1.13 (implemented in LS-DYNA)

3.2 WEIGHTS AND CENTERS OF GRAVITY

As stated in Chapter 1, while the diameters of the MPC, HI-STORM FW, and HI-TRAC VW are fixed, their height is dependent on the length of the fuel assembly. The MPC cavity height (which determines the external height of the MPC) is set equal to the nominal fuel length (along with control components, if any) plus Δ, where Δ is between 1.5" (minimum), 2" (maximum), Δ is increased above 1.5" so that the MPC cavity height is a full inch or half-inch number. Thus, for the PWR reference fuel (Table 1.0.4), whose length including control components is 167.2" (Table 2.1.1), Δ = 1.8" so that the MPC cavity height, c, becomes 169". Δ is provided to account for irradiation and thermal growth of the fuel in the reactor. Table 3.2.1 provides the height of the internal cavities and bottom-to-top external dimension of all system components. Table 3.2.2 provides the parameters that affect the weight of cask components and their range of values assumed in this FSAR.

The cavity heights of the HI-STORM FW overpack and the HI-TRAC VW transfer cask are set greater than the MPC height by fixed amounts to account for differential thermal expansion and manufacturing tolerances. Table 3.2.1 provides the height data on HI-STORM FW, HI-TRAC VW, and the MPC as the adder to the MPC cavity length.

Table 3.2.5 provides the reference weight of the HI-STORM FW overpack for storing MPC-37 and MPC-89 containing reference PWR and BWR fuel, respectively. The weight of the HI-STORM FW overpack body is provided for two discrete concrete densities and for two discrete heights for PWR and BWR fuel. The weight at any other density and any other height can be obtained by linear interpolation. Similarly the weight of the HI-STORM FW lid is provided for two discrete values of concrete density. The weight corresponding to any other density can be computed by linear interpolation.

As discussed in Section 1.2, the weight of the HI-TRAC VW transfer cask is maximized for a particular site to take full advantage of the plant's crane capacity within the architectural limitations of the Fuel Building. Accordingly, the thickness of the lead shield and outer diameter of the water jacket can be increased to maximize shielding. The weight of the empty HI-TRAC VW cask in Table 3.2.4 is provided for three lengths corresponding to PWR fuel. Using the data for three lengths, the transfer cask's weight corresponding to any other length can be obtained by linear interpolation (or extrapolation). For MPC-89, the weight data is provided for the minimum and reference fuel lengths, as well as the reference fuel assembly with a DFC and therefore likewise the transfer cask's weight corresponding to any other length can be obtained by linear interpolation (or extrapolation).

The approximate change in the empty weight of HI-TRAC VW (in kilo pounds) of a certain height, h (inch), by virtue of changing the thickness of the lead by an amount, δ (inch), is given by the formula:

$$\Delta W_{lead} = 0.1128(h - 13.5)\,\delta$$

The approximate change in the empty weight of HI-TRAC VW (in kilo pounds) of a certain length, h (inch), by virtue of changing the thickness of the water layer by δ (inch) is given by:

$$\Delta W_{water} = 0.01077\,(h - 13.5)\,\delta$$

The above formulas serve as a reasonable approximation for the weight change whether the thickness of lead (or water) is being increased or decreased.

The weights of the loaded MPCs containing "reference SNF" with and without water are provided in Table 3.2.3. All weights in the aforementioned tables are nominal values computed using the SOLIDWORKS™ computer code or using standard material density and geometric shapes for the respective subcomponents of the equipment.

Table 3.2.5 provides the loaded weight of the HI-STORM FW system on the ISFSI pad for two different concrete densities for both PWR and BWR reference fuel. Table 3.2.6 contains the weight data on loaded HI-TRAC VW under the various handling scenarios expected during loading.

The maximum and minimum locations of the centers of gravity (CGs) are presented (in dimensionless form) in Table 3.2.7. The radial eccentricity, ϕ, of a cask system is defined as:

$$\phi = \frac{\Delta_r}{D} \times 100 \ (\phi \text{ is dimensionless})$$

where Δ_r is the radial offset distance between the CG of the cask system and the geometric centerline of the cask, and D is the outside diameter of the cask. In other words, the value of ϕ defines a circle around the axis of symmetry of the cask within which the CG lies (see Figure 3.2.1). All centers of gravity are located close to the geometric centerline of the cylindrical cask since the non-axisymmetric effects of the cask system and its contents are very small. The vertical eccentricity, Ψ, of a cask system is defined similarly as:

$$\Psi = \frac{\Delta_v}{H} \times 100 \ (\Psi \text{ is dimensionless})$$

Where Δ_v is the vertical offset distance between the CG of the cask system and the geometric center of the cask (i.e., cask mid-height), and H is the overall height of the cask. A positive value of Ψ indicates that the CG is located above the cask mid-height, and a negative value indicates that the CG is located below the cask mid-height. Figure 3.2.2 illustrates how Ψ is defined.

The values of ϕ and Ψ given in Table 3.2.7are bounding values, which take into consideration material and fabrication tolerances. The tabulated values of ϕ and Ψ can be converted into dimensionless form using the equations above. For example, from Table 3.2.7 the empty HI-STORM FW with lid installed has maximum eccentricities of $\phi = 2.0$ and $\Psi = \pm 3.0$. Therefore, the maximum radial and vertical offset distances are (D=140", H=207.75" for PWR reference fuel):

$$\Delta_r = \frac{\phi D}{100} = \frac{(2.0)(140in)}{100} = 2.8in$$

$$\Delta_v = \frac{\Psi H}{100} = \frac{(\pm 3.0)(207.75in)}{100} = \pm 6.23in \text{ (CG height relative to H/2)}$$

The C.G. information provided above shall be used in designing the lifting and handling ancillary for the HI-STORM FW cask components. In addition, the maximum CG height per Table 3.2.7 shall be used for the stability analysis of the HI-STORM FW under DBE conditions. Using the weight data in the previously mentioned tables, Table 3.2.8 has been constructed to provide the bounding weights for structural analyses so that every load case is analyzed using the most conservative data (to *minimize the computed safety margins*). The weight data in Table 3.2.8 is used in all structural analyses in this chapter.

Table 3.2.1 OPTIMIZED MPC, HI-TRAC, AND HI-STORM HEIGHT DATA FOR A SPECIFIC UNIRRADIATED FUEL LENGTH, ℓ [†]	
MPC Cavity Height, c	$\ell + \Delta$ [‡]
MPC Height (including top lid), h	c + 12"
HI-TRAC VW Cavity Height	h + 1"
HI-TRAC VW Total Height	h + 6.5"
HI-STORM FW Cavity Height	h + 3.5"
HI-STORM FW Body Height (height from the bottom of the HI-STORM FW to the top surface of the shear ring at the top of the HI-STORM FW body)	h + 4.5"
HI-STORM FW Height (loaded over the pad)	h + 27"

[†] Fuel Length, ℓ, shall be based on the fuel assembly length with or without a damaged fuel container (DFC). Users planning to store fuel in DFCs shall adjust the length ℓ to include the additional height of the DFC. The maximum additional height for the DFC shall be 5". Note that users who plan to store any fuel in a DFC will need to utilize a system designed for the additional length and will need to use fuel shims to reduce the gap between the fuel without a DFC and the enclosure cavity.

[‡] Δ shall be selected as 1.5" < Δ < 2" so that c is an integral multiple of 1/2 inch (add 1.5" to the fuel length and round up to the nearest 1/2" or full inch).

Table 3.2.2 LIMITING PARAMETERS			
	Item	PWR	BWR
1.	Minimum fuel assembly length, inch	157	171
2.	Maximum fuel assembly length, inch	199.2	181.5[3]
3.	Nominal thickness of the lead cylinder in the lowest weight HI-TRAC VW, inch	2.75	2.50
4.	Maximum nominal thickness of the lead cylinder, inch	4.25	4.25
5.	Nominal (radial) thickness of the water in the external jacket, inch	4.75	4.75

[3] Maximum fuel assembly length for the BWR fuel assembly refers to the maximum fuel assembly length plus an additional 5" to account for a Damage Fuel Container (DFC).

Table 3.2.3

MPC WEIGHT DATA (COMPUTED NOMINAL VALUES)

Item	BWR Fuel Based on length below			PWR Fuel Based on length below		
	Reference	Shortest from Table 3.2.2	Longest from Table 3.2.2	Reference	Shortest from Table 3.2.2	Longest from Table 3.2.2
Enclosure Vessel	27,500	27,100	27,800	28,600	27,800	31,100
Fuel Basket	8,600	8,300	8,800	7,900	7,400	9,400
Water in the MPC @ SG = 1 (See Note 1)	16,700	16,200	18,900	15,400	14,400	18,700
Water mass displaced by a closed MPC Enclosure Vessel (SG = 1)	30,800	29,900	31,600	29,300	27,600	34,500

SG = Specific Gravity

Note 1: Water weight in the MPC assumes that water volume displaced by the fuel is equal to the fuel weight divided by an average fuel assembly density of 0.396 lb/in3. The fuel weights used for calculating the fuel volumes for Reference/Shortest/Longest PWR and BWR fuel assemblies are 1750/1600/2050 and 750/700/850 pounds respectively.

Table 3.2.4

HI-TRAC VW WEIGHT DATA (COMPUTED NOMINAL VALUES)

Item	BWR Fuel Based on length below			PWR Fuel Based on length below		
	Reference	Shortest from Table 3.2.2	Longest from Table 3.2.2	Reference	Shortest from Table 3.2.2	Longest from Table 3.2.2
HI-TRAC VW Body (no Bottom Lid, water jacket empty)	84,000	81,700	86,200	85,200	80,400	99,600
HI-TRAC VW Bottom Lid	11,300	11,300	11,300	11,300	11,300	11,300
MPC with Basket	36,100	35,400	36,600	36,500	35,200	40,500
Fuel Weight (assume 50% with control components or channels, as applicable)	66,800 (750 lb per assembly average)	64,600 (725 lb per assembly average)	71,200 (800 lb per assembly average)	62,000 (1,675 lb per assembly average)	59,200 (1,600 lb per assembly average)	69,400 (1,875 lb per assembly average)
Water in the Annulus	600	600	600	600	600	700
Water in the Water Jacket	8,800	8,500	9,000	8,400	7,900	9,900
Displaced Water Mass by the Cask in the Pool (Excludes MPC)	18,900	18,400	19,400	18,600	17,600	21,600

Table 3.2.5

ON-ISFSI WEIGHT OF LOADED HI-STORM FW

Scenario		Weight of Cask Body (kilo-pounds)	Weight of HI-STORM FW Lid (kilo-pounds)
Fuel Type	**HI-STORM FW Concrete Density (lb/cubic feet)**		
Ref. PWR	150	198.0	20.1
Ref. PWR	200	246.2	23.3
Maximum length – PWR	150	229.0	20.1
Maximum length – PWR	200	286.1	23.3
Ref. BWR	150	206.7	20.1
Ref. BWR	200	257.4	23.3
Maximum length – BWR	150	211.6	20.1
Maximum length – BWR	200	263.7	23.3

Table 3.2.6

HI-TRAC VW OPERATING WEIGHT DATA FOR REFERENCE FUEL

Scenario			HI-TRAC VW[4] Weight in Kilo-Pounds	
Water in the MPC	**Water in the Water Jacket**	**Cask in (pool) Water/Air**	**Ref. PWR Fuel**	**Ref. BWR Fuel**
Yes	Yes	Water	167.7	173.3
Yes	Yes	Air	215.5	222.9
Yes	No	Water	159.4	164.6
No	No	Water	143.7	147.9
No	Yes	Air	199.9	206.2
No	No	Air	191.5	197.5

Weights above include the weight of the fuel assembly alone and do not include any additional weight for non-fuel hardware or damaged fuel containers.

[4] Add 4,000 lbs for the weight of the lift yoke.

Table 3.2.7

LOCATION OF C.G. WITH RESPECT TO THE CENTERPOINT ON THE EQUIPMENT'S GEOMETRIC CENTERLINE

	Item	Radial eccentricity (dimensionless) [5], ϕ	Vertical eccentricity (dimensionless), Above (+)* or Below (-), ψ
1.	Empty HI-STORM FW with lid installed	2.0	±3.0
2.	Empty HI-STORM FW without top lid	2.0	±3.0
3.	HI-STORM FW with fully loaded stored MPC without top lid	2.0	±2.0
4.	HI-STORM FW with lid and a fully loaded MPC	2.0	±3.0
5.	HI-TRAC VW with Bottom lid and loaded MPC	2.0	±2.0
6.	Empty HI-TRAC VW without bottom lid	2.0	±2.0

[5] ϕ and Ψ are dimension values as explained in Section 3.2.

Table 3.2.8

BOUNDING WEIGHTS FOR STRUCTURAL ANALYSES
(Height from Tables 3.2.1 and 3.2.2)

	Case	Purpose	Assumed Weight (Kilo-pounds)
1.	Loaded HI-STORM FW on the pad containing maximum length/weight fuel and 200 lb/cubic feet concrete – maximum possible weight scenario	Sizing and analysis of lifting and handling locations and cask stability analysis under overturning loads such as flood and earthquake	425.7
2.	Loaded HI-STORM FW on the pad with 150 lb concrete, shortest length MPC	Stability analysis under missile strike	302.1
3.	Loaded HI-TRAC VW with maximum length fuel and maximum lead and water shielding	Analysis for NUREG-0612 compliance of lifting and handling locations (TALs)	270.0
4.	Loaded HI-TRAC VW with shortest length MPC and minimum lead and water shielding	Stability analysis under missile strike	186.0
5.	Loaded MPC containing maximum length/weight fuel – maximum possible weight scenario	Analysis for NUREG-0612 compliance of lifting and handling locations (TALs)	116.4

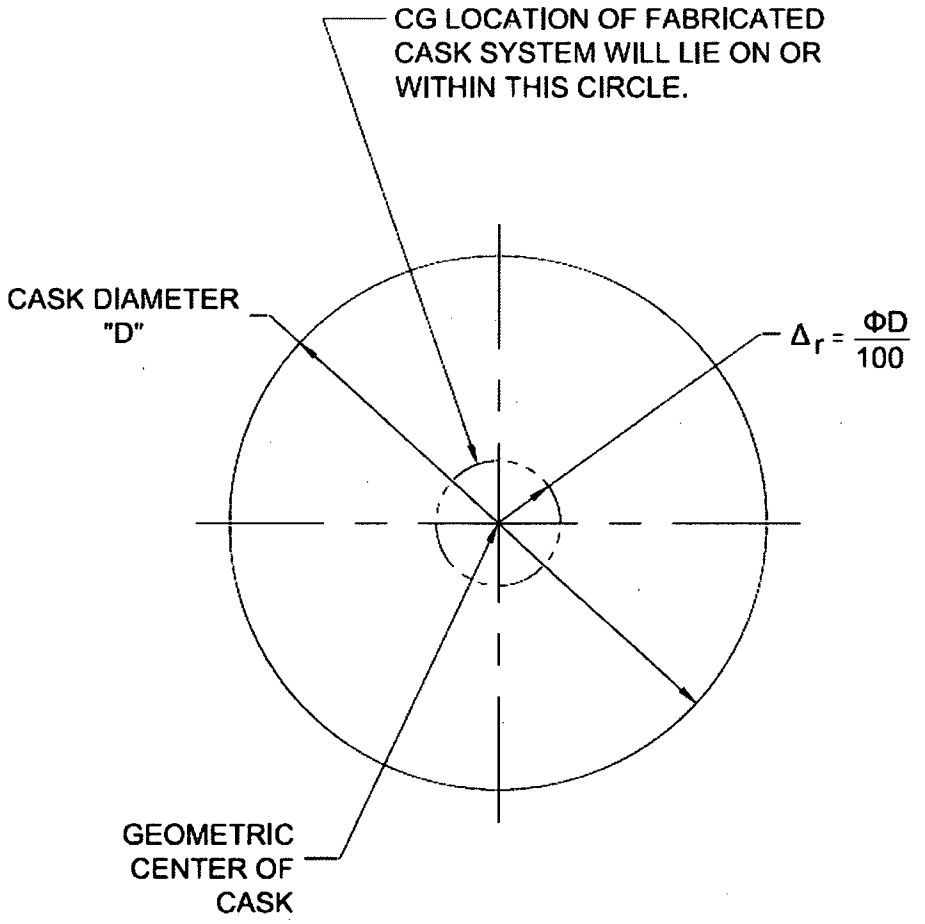

Top View of Cask

Figure 3.2.1: Radial Eccentricity of Cask Center of Gravity

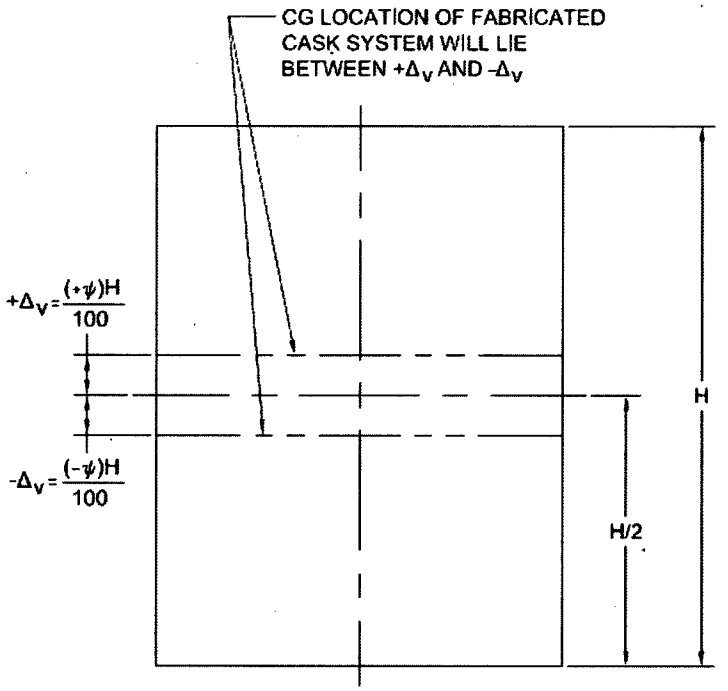

Elevation View of Cask

Figure 3.2.2: Vertical Eccentricity of Cask Center of Gravity

3.3 MECHANICAL PROPERTIES OF MATERIALS

This section provides the mechanical properties used in the structural evaluation. The properties include yield stress, ultimate stress, modulus of elasticity, Poisson's ratio, weight density, and coefficient of thermal expansion. Values are presented for a range of temperatures which envelopes the maximum and minimum temperatures under all service conditions applicable to the HI-STORM FW system components.

The materials selected for use in the MPC, HI-STORM FW overpack, and HI-TRAC VW transfer cask are presented on the drawings in Section 1.5. In this chapter, the materials are divided into two categories, structural and nonstructural. Structural materials are materials that act as load bearing members and are, therefore, significant in the stress evaluations. Materials that do not support mechanical loads are considered nonstructural. For example, the HI-TRAC VW inner shell is a structural material, while the lead between the inner and outer shell is a nonstructural material. For nonstructural materials, the principal property that is used in the structural analysis is weight density. In local deformation analysis, however, such as the study of penetration from a tornado-borne missile, the properties of lead in HI-TRAC VW and plain concrete in HI-STORM FW are included.

3.3.1 Structural Materials

a. Alloy X

A hypothetical material termed Alloy X is defined for the MPC pressure retaining boundary. The material properties of Alloy X are the least favorable values from the set of candidate alloys. The purpose of a least favorable material definition is to ensure that all structural analyses are conservative, regardless of the actual MPC material. For example, when evaluating the stresses in the MPC, it is conservative to work with the minimum values for yield strength and ultimate strength. This guarantees that the material used for fabrication of the MPC will be of equal or greater strength than the hypothetical material used in the analysis.

Table 3.3.1 lists the numerical values for the material properties of Alloy X versus temperature. These values, taken from the ASME Code, Section II, Part D [3.3.1], are used in all structural analyses. As is shown in Chapter 4, the maximum metal temperature for Alloy X used at or within the Confinement Boundary remains below 1000°F under all service modes. As shown in ASME Code Case N-47-33 (Class 1 Components in Elevated Temperature Service, 2007 Code Cases, Nuclear Components), the strength properties of austenitic stainless steels do not change due to exposure to 1000°F temperature for up to 10,000 hours. Therefore, there is no risk of a significant effect on the mechanical properties of the confinement or boundary material during the short time duration loading. A further description of Alloy X, including the materials from which it is derived, is provided in Appendix 1.A.

Two properties of Alloy X that are not included in Table 3.3.1 are weight density and Poisson's ratio. These properties are assumed constant for all structural analyses, regardless of temperature. The values used are shown in the table below.

PROPERTY	VALUE
Weight Density (lb/in^3)	0.290
Poisson's Ratio	0.30

b. Metamic-HT

Metamic-HT is a composite of nano-particles of aluminum oxide (alumina) and finely ground boron carbide particles dispersed in the metal matrix of pure aluminum. Metamic-HT is the principal constituent material of the HI-STORM FW fuel baskets. Metamic-HT neutron absorber is an enhanced version of the Metamic (classic) product widely used in dry storage fuel baskets [3.1.4, 3.3.2] and spent fuel storage racks [3.3.3, 3.3.4]. The enhanced properties of Metamic-HT derive from the strengthening of its aluminum matrix with ultra fine-grained (nano-particle size) alumina (Al_2O_3) particles that anchor the grain boundaries. The strength properties of Metamic-HT have been characterized through a comprehensive test program, and Minimum Guaranteed Values suitable for structural design are archived in [1.B.1]. The Metamic-HT metal matrix composite thus exhibits excellent mechanical strength properties (notably creep resistance) in addition to the proven thermal and neutron absorption properties that are intrinsic to borated aluminum materials. The specific Metamic-HT composition utilized in this FSAR has 10% (min.) B_4C by weight.

Appendix 1.B provides detailed information on Metamic-HT. Mechanical properties are provided in Table 1.B.1

c. Carbon Steel, Low-Alloy and Nickel Alloy Steel

The carbon steels in the HI-STORM FW system are SA516 Grade 70, SA515 Grade 70, and SA36. The low alloy steel is SA350-LF3. The material properties of SA516 Grade 70 and SA515 Grade 70 are shown in Tables 3.3.2. The material properties of SA350-LF2 and SA350-LF3 are given in Table 3.3.3. The material properties of SA36 are shown in Table 3.3.6.

Two properties of these steels that are not included in Tables 3.3.2, 3.3.3 and 3.3.6 are weight density and Poisson's ratio. These properties are assumed constant for all structural analyses. The values used are shown in the table below.

PROPERTY	VALUE
Weight Density (lb/in^3)	0.283
Poisson's Ratio	0.30

d. Bolting Materials

Material properties of the bolting materials used in the HI-STORM FW system are given in Table 3.3.4.

e. Weld Material

All weld materials utilized in the welding of the Code components comply with the provisions of the appropriate ASME subsection (e.g., Subsection NB for the MPC enclosure vessel) and Section IX. All non-code welds will be made using weld procedures that meet Section IX of the ASME Code. The minimum tensile strength of the weld wire and filler material (where applicable) will be equal to or greater than the tensile strength of the base metal listed in the ASME Code.

3.3.2 Nonstructural Materials

a. Concrete

The primary function of the plain concrete in the HI-STORM FW storage overpack is shielding. Concrete in the HI-STORM FW overpack is not considered as a structural member, except to withstand compressive, bearing, and penetrant loads. Therefore the mechanical behavior of concrete must be quantified to determine the stresses in the structural members (steel shells surrounding it) under accident conditions. Table 3.3.5 provides the concrete mechanical properties. Allowable, bearing strength in concrete for normal loading conditions is calculated in accordance with ACI 318-05 [3.3.5]. The procedure specified in ASTM C-39 is utilized to verify that the assumed compressive strength will be realized in the actual in-situ pours. Appendix 1.D in the HI-STORM 100 FSAR [3.1.4] provides additional information on the requirements on plain concrete for use in HI-STORM FW storage overpack.

To enhance the shielding performance of the HI-STORM FW storage overpack, high density concrete can be used during fabrication. The permissible range of concrete densities is specified in Table 1.2.5. The structural calculations consider the most conservative density value (i.e., maximum or minimum weight), as appropriate.

b. Lead

Lead is not considered as a structural member of the HI-STORM FW system. Its load carrying capacity is neglected in all structural analysis, except in the analysis of a tornado missile strike where it acts as a missile barrier. Applicable mechanical properties of lead are provided in Table 3.3.5.

Table 3.3.1

ALLOY X MATERIAL PROPERTIES

Temp. (Deg. F)	Alloy X			
	S_y	S_u[†]	α	E
-40	30.0	75.0 (70.0)	--	28.88
100	30.0	75.0 (70.0)	8.6	28.12
150	27.5	73.0 (68.1)	8.8	27.81
200	25.0	71.0 (66.3)	8.9	27.5
250	23.7	68.6 (64.05)	9.1	27.25
300	22.4	66.2 (61.8)	9.2	27.0
350	21.55	65.3 (60.75)	9.4	26.7
400	20.7	64.4 (59.7)	9.5	26.4
450	20.05	63.9 (59.45)	9.6	26.15
500	19.4	63.4 (59.2)	9.7	25.9
550	18.85	63.35 (59.1)	9.8	25.6
600	18.3	63.3 (59.0)	9.8	25.3
650	17.8	62.85 (58.6)	9.9	25.05
700	17.3	62.4 (58.3)	10.0	24.8
750	16.9	62.1 (57.9)	10.0	24.45
800	16.5	61.7 (57.6)	10.1	24.1

Definitions:

S_y = Yield Stress (ksi)
α = Mean Coefficient of thermal expansion (in./in. per degree F x 10^{-6})
S_u = Ultimate Stress (ksi)
E = Young's Modulus (psi x 10^6)

Notes:

1. Source for S_y values is Table Y-1 of [3.3.1].
2. Source for S_u values is Table U of [3.3.1].
3. Source for α values is Table TE-1 of [3.3.1].
4. Source for E values is material group G in Table TM-1 of [3.3.1].

[†] The ultimate stress of Alloy X is dependent on the product form of the material (i.e., forging vs. plate). Values in parentheses are based on SA-336 forged materials (type F304, F304LN, F316, and F316LN), which are used solely for the one-piece construction MPC lids. All other values correspond to SA-240 plate material.

Table 3.3.2

SA516 AND SA515, GRADE 70 MATERIAL PROPERTIES

Temp. (Deg. F)	SA516 and SA515, Grade 70			
	S_y	S_u	α	E
-40	38.0	70.0	---	29.98
100	38.0	70.0	6.5	29.26
150	35.7	70.0	6.6	29.03
200	34.8	70.0	6.7	28.8
250	34.2	70.0	6.8	28.55
300	33.6	70.0	6.9	28.3
350	33.05	70.0	7.0	28.1
400	32.5	70.0	7.1	27.9
450	31.75	70.0	7.2	27.6
500	31.0	70.0	7.3	27.3
550	30.05	70.0	7.3	26.9
600	29.1	70.0	7.4	26.5
650	28.2	70.0	7.5	26.0
700	27.2	70.0	7.6	25.5
750	26.3	69.1	7.7	24.85

Definitions:

S_y = Yield Stress (ksi)
α = Mean Coefficient of thermal expansion (in./in. per degree F x 10^{-6})
S_u = Ultimate Stress (ksi)
E = Young's Modulus (psi x 10^6)

Notes:
1. Source for S_y values is Table Y-1 of [3.3.1].
2. Source for S_u values is Table U of [3.3.1].
3. Source for α values is material group 1 in Table TE-1 of [3.3.1].
4. Source for E values is "Carbon steels with C less than or equal to 0.30%" in Table TM-1 of [3.3.1]

Table 3.3.3

SA350-LF3 AND SA350-LF2 MATERIAL PROPERTIES

Temp. (Deg. F)	SA350-LF3 (SA350-LF2)			SA350-LF3 (SA350-LF2)	
	S_m	S_y	S_u	E	α
-20	23.3	37.5 (36.0)	70.0	28.22 (29.88)	---
100	23.3	37.5 (36.0)	70.0	27.64 (29.26)	6.5
200	22.9 (22.0)	34.3 (33.0)	70.0 (70.0)	27.1 (28.8)	6.7
300	22.1 (21.2)	33.2 (31.8)	70.0 (70.0)	26.7 (28.3)	6.9
400	21.4 (20.5)	32.0 (30.8)	70.0 (70.0)	26.2 (27.9)	7.1
500	20.3 (19.6)	30.4 (29.3)	70.0 (70.0)	25.7 (27.3)	7.3
600	18.8 (18.4)	28.2 (27.6)	70.0 (70.0)	25.1 (26.5)	7.4
700	16.9 (17.2)	25.3 (25.8)	66.5 (70.0)	24.6 (25.5)	7.6

Definitions:

S_m = Design Stress Intensity (ksi)
S_y = Yield Stress (ksi)
S_u = Ultimate Stress (ksi)
α = Mean Coefficient of Thermal Expansion (in./in. per degree F x 10^{-6})
E = Young's Modulus (psi x 10^6)

Notes:

1. Source for S_m values is Table 2A of [3.3.1].
2. Source for S_y values is Table Y-1 of [3.3.1].
3. Source for S_u values is ratioing S_m values.
4. Source for α values is group 1 alloys in Table TE-1 of [3.3.1].
5. Source for E values is material group B (for SA350-LF3) and "Carbon steels with C less than or equal to 0.30%" (for SA350-LF2) in Table TM-1 of [3.3.1].
6. Values for LF2 are given in parentheses where different from LF3.

Table 3.3.4

BOLTING MATERIAL PROPERTIES

SB637-N07718 (less than or equal to 6 inches diameter)					
Temp. (Deg. F)	S_y	S_u	E	α	S_m
-100	150.0	185.0	29.9	---	50.0
-20	150.0	185.0	29.43	---	50.0
70	150.0	185.0	28.9	7.1	50.0
100	150.0	185.0	28.76	7.1	50.0
200	144.0	177.6	28.3	7.2	48.0
300	140.7	173.5	27.9	7.3	46.9
400	138.3	170.6	27.5	7.5	46.1
500	136.8	168.7	27.2	7.6	45.6
600	135.3	166.9	26.8	7.7	45.1
SA193 Grade B7 (2.5 to 4 inches diameter)					
Temp. (Deg. F)	S_y	S_u	E	α	S_m
100	95.0	115.0	29.46	6.5	31.7
200	88.5	115.0	29.0	6.7	29.5
300	85.1	115.0	28.5	6.9	28.4
400	82.7	115.0	28.0	7.1	27.6
500	80.1	115.0	27.4	7.3	26.7
600	77.1	115.0	26.9	7.4	25.7

Definitions:

S_m = Design stress intensity (ksi)
S_y = Yield Stress (ksi)
α = Mean Coefficient of thermal expansion (in./in. per degree F x 10^{-6})
S_u = Ultimate Stress (ksi)
E = Young's Modulus (psi x 10^6)

Notes:

1. Source for S_m values is Table 4 of [3.3.1].
2. Source for S_y values is ratioing design stress intensity values and Table Y-1 of [3.3.1], as applicable.
3. Source for S_u values is ratioing design stress intensity values and Table U of [3.3.1], as applicable.
4. Source for α values is Tables TE-1 and TE-4 of [3.3.1], as applicable.
5. Source for E values is Tables TM-1 and TM-4 of [3.3.1], as applicable.

Table 3.3.4 (CONTINUED)

BOLTING MATERIAL PROPERTIES

Temp. (Deg. F)	S_y	S_u	E	α	S_m
SA193 Grade B8 Class 2 (less than or equal to 2 inches diameter)					
100	75.0	95.0	28.12	8.6	---
200	62.5	89.93	27.5	8.9	---
300	56.0	83.85	27.0	9.2	---
400	51.75	81.07	26.4	9.5	---
500	48.5	80.31	25.9	9.7	---
600	46.0	80.31	25.3	9.8	---

Definitions:

S_m = Design stress intensity (ksi)
S_y = Yield Stress (ksi)
α = Mean Coefficient of thermal expansion (in./in. per degree F x 10^{-6})
S_u = Ultimate Stress (ksi)
E = Young's Modulus (psi x 10^6)

Notes:
1. Source for S_y values is ratioing S_y values of SA193 B8 Class 1 bolt material obtained from Table Y-1 of [3.3.1].
2. Source for S_u values is ratioing S_u values of SA193 B8 Class 1 bolt material obtained from Table U of [3.3.1].
3. Source for α values is group 3 alloys in Table TE-1 of [3.3.1].
4. Source for E values is material group G in Table TM-1 of [3.3.1].

Table 3.3.5

CONCRETE AND LEAD MECHANICAL PROPERTIES

PROPERTY	**VALUE**					
CONCRETE:						
Compressive Strength (psi)	3,300 psi					
Nominal Density (lb/ft^3)	150 lb/cubic feet					
Allowable Bearing Stress (psi)	1,543[†]					
Allowable Axial Compression (psi)	1,042[†]					
Allowable Flexure, extreme fiber tension (psi)	158[†,††]					
Allowable Flexure, extreme fiber compression (psi)	1,543[†]					
Mean Coefficient of Thermal Expansion (in/in/deg. F)	5.5E-06					
Modulus of Elasticity (psi)	57,000 (compressive strength (psi))$^{1/2}$					
LEAD:	-40°F	-20°F	70°F	200°F	300°F	600°F
Yield Strength (psi)	700	680	640	490	380	20
Modulus of Elasticity (ksi)	2.4E+3	2.4E+3	2.3E+3	2.0E+3	1.9E+3	1.5E+3
Coefficient of Thermal Expansion (in/in/deg. F)	15.6E-6	15.7E-6	16.1E-6	16.6E-6	17.2E-6	20.2E-6
Poisson's Ratio	0.40					
Density (lb/cubic ft.)	708					

Notes:
1. Concrete allowable stress values based on ACI 318-05.
2. Lead properties are from [3.3.7].

[†] Values listed correspond to concrete compressive stress = 3,300 psi.
[††] No credit for tensile strength of concrete is taken in the calculations.

Table 3.3.6

SA36 MATERIAL PROPERTIES

Temp. (Deg. F)	SA36			
	S_y	S_u	α	E
-40	36.0	58.0	---	29.98
100	36.0	58.0	6.5	29.26
150	33.8	58.0	6.6	29.03
200	33.0	58.0	6.7	28.8
250	32.4	58.0	6.8	28.55
300	31.8	58.0	6.9	28.3
350	31.3	58.0	7.0	28.1
400	30.8	58.0	7.1	27.9
450	30.05	58.0	7.2	27.6
500	29.3	58.0	7.3	27.3
550	28.45	58.0	7.3	26.9
600	27.6	58.0	7.4	26.5
650	26.7	58.0	7.5	26.0
700	25.8	58.0	7.6	25.5

Definitions:

S_y = Yield Stress (ksi)
α = Mean Coefficient of thermal expansion (in./in./^{0}F x 10^{-6})
S_u = Ultimate Stress (ksi)
E = Young's Modulus (psi x 10^6)

Notes:
1. Source for S_y values is Table Y-1 of [3.3.1].
2. Source for S_u values is Table U of [3.3.1].
3. Source for α values is group 1 alloys in Table TE-1 of [3.3.1].
4. Source for E values is "Carbon steels with C less than or equal to 0.30%" in Table TM-1 of [3.3.1].

3.4 GENERAL STANDARDS FOR CASKS

3.4.1 Chemical and Galvanic Reactions

Chapter 8 provides discussions on chemical and galvanic reactions, material compatibility and operating environments. Section 8.12 provides a summary of compatibility all HI-STORM FW system materials with the operating environment.

3.4.2 Positive Closure

There are no quick-connect/disconnect ports in the Confinement Boundary of the HI-STORM FW system. The only access to the MPC is through the storage overpack lid, which weighs over 10 tons (see Table 3.2.5). The lid is fastened to the storage overpack with large bolts. Inadvertent opening of the storage overpack is not feasible because opening a storage overpack requires mobilization of special tools and heavy-load lifting equipment.

3.4.3 Lifting Devices

3.4.3.1 Identification of Lifting Devices and Required Safety Factors

The safety of the lifting and handling operations involving HI-STORM FW system components is considered in this section. In particular, the compliance of the appurtenances integral to the cask components used in the lifting operations to NUREG-0612, Reg. Guide 3.61, and the ASME Code is evaluated.

The following design features of Threaded Anchor Locations (TALs) are relevant to their stress analysis:

i. All TALs consist of vertically tapped penetrations in the solid metal blocks. For example, the HI-STORM FW overpack body and overpack lid (like all HI-STORM models) have tapped holes in the "anchor blocks" that are engaged for lifting. The loaded MPC (like all previous MPC designs) is lifted at four threaded penetrations in the top lid. Likewise, four vertically tapped holes in the top flange provide the lift points for HI-TRAC VW transfer cask.

   Specifically, trunnions are not used in the HI-STORM FW system components because of the radiation streaming paths introduced by their presence and high stresses produced at the trunnion's root by the cantilever action during lifting.

ii. Operations involving loaded HI-STORM FW cask components involve handling evolutions in the vertical orientation. While the lifting devices used by a specific nuclear site shall be custom engineered to meet the architectural constraints of the site, all lifting devices are required to engage the tapped connection points using a vertical tension member such as a threaded rod. Thus, the loading on the cask during lifting is purely vertical.

iii. There are no rotation trunnions in the HI-STORM FW components. All components are upended and downended at the nuclear plant site using "cradles" of the same design used at the factory (viz., the Holtec Manufacturing Division) during their manufacturing.

The stress analysis of the HI-STORM FW components, therefore, involves applying a vertical load equal to D*/n at each of the n TAL locations. Thus, for the case of the HI-STORM FW overpack, n = 4 (four "anchor blocks" as shown in the licensing drawings in Section 1.5).

The stress limits for individual components are as follows:

i. Lift points (MPC and HI-TRAC VW): The stress in the threads must be the lesser of $1/3^{rd}$ of the material's yield strength and $1/10^{th}$ of its ultimate strength pursuant to NUREG-0612 and Reg. Guide 3.61.

ii. Lift points (HI-STORM FW): The stress in the threads must be less than $1/3^{rd}$ of the material's yield strength pursuant to Reg. Guide 3.61. This acceptance criterion is consistent with the stress limits used for the lifting evaluation of the HI-STORM 100 overpack in [3.1.4].

iii. Balance of the components: The maximum primary stress (membrane plus bending) must be below the Level A service condition limit using ASME Code, Section III, Subsection NF (2007 issue) as the reference code.

To incorporate an additional margin of safety in the reported safety factors, the following assumptions are made:

i. As the system description in Chapter 1 indicates, the heights of the MPCs, HI-STORM FW and HI-TRAC VW are variable. Further, the quantity of lead shielding installed in HI-TRAC VW and the density of concrete can be increased to maximize shielding. All lift point capacity evaluations are performed using the maximum possible weights for each component, henceforth referred to as the "heaviest weight configuration". Because a great majority of site applications will utilize lower weight components (due to shorter fuel length and other architectural limitations such as restricted crane capacity or DAS slab load bearing capacity, or lack of floor space in the loading pit), there will be an additional margin of safety in the lifting point's capacity at specific plant sites.

ii. All material yield strength and ultimate strength values used are the minimum from the ASME Code. Actual yield and tensile data for manufactured steel usually have up to 20% higher values.

The stress analysis of the lifting operation is carried out using the load combination D+H, where H is the "handling load". The term D denotes the dead load. Quite obviously, D must be taken as the bounding value of the dead load of the component being lifted. In all lifting analyses considered in this document, the handling load H is assumed to be 0.15D. In other words, the inertia amplifier during the lifting operation is assumed to be equal to 0.15g. This value is consistent with the

guidelines of the Crane Manufacturer's Association of America (CMAA), Specification No. 70, 1988, Section 3.3, which stipulates a dynamic factor equal to 0.15 for slowly executed lifts. Thus, the "apparent dead load" of the component for stress analysis purposes is $D^* = 1.15D$. Unless otherwise stated, all lifting analyses in this FSAR use the "apparent dead load", D^*, as the lifted load.

Unless explicitly stated otherwise, all analyses of lifting operations presented in this FSAR follow the load definition and allowable stress provisions of the foregoing. Consistent with the practice adopted throughout this chapter, results are presented in dimensionless form, as safety factors, defined as

$$\text{Safety Factor, } \beta = \frac{\text{Allowable Stress}}{\text{Computed Stress}}$$

In the following subsections, the lifting device stress analyses performed to demonstrate compliance with regulations are presented. Summary results are presented for each of the analyses.

3.4.3.2 Analysis of Lifting Scenarios

In the following, the safety analyses of the HI-STORM FW components under the following lifting conditions are summarized.

a. MPC Lifts

The governing condition for the MPC lift is when it is being raised or lowered in a radiation shielded space defined by the HI-TRAC VW or HI-STORM FW stack. In this condition, the four tapped holes in the MPC lid (Alloy X material) serve to carry the weight.

The criteria derived from NUREG-0612, Reg. Guide 3.61, and the ASME Code Level A condition, stated earlier, apply. The stress analysis is carried out in two parts.

i. Strength analysis of the TALs (connection points) using classical strength-of-materials.

ii. A finite element analysis of the MPC as a cylindrical vessel with the weight of the fuel and basket applied on its baseplate which along with the weight of the Confinement Boundary metal is equilibrated by the reaction loads at the our lift points.

The primary stress intensities must meet the Level A stress limits for "NB" Class 3 plate and shell structures.

Case (i): Stress Analysis of MPC Threaded Anchor Locations (TALs)

Per Table 3.2.8, the maximum weight of a loaded MPC is

D = 116,400 lb

Per the above, the apparent dead load of the MPC during handling operations is

$D^* = 1.15 \times D = 133{,}860$ lb

The MPC lid has 4 TALs as shown on the drawings in Section 1.5. Therefore, the lifted load per TAL is equal to

$$\frac{D^*}{4} = 33{,}465 lb$$

Per Machinery's Handbook [3.4.12], the shear area of the internal threads (1 3/4" - 5UNC x 3.5" Lg.) at each TAL is

$A = 13.7$ in^2

Finally, the shear stress on the TALs is computed as follows

$$\tau = \frac{D^*}{4A} = 2{,}443 psi$$

The MPC lid is made from Alloy X material, whose mechanical properties are listed in Table 3.3.1. Based on a design temperature of 600°F (Table 2.2.3), and assuming the yield and ultimate strengths in shear to be 60% of the corresponding tensile strengths, the allowable stress in the threads is determined as follows

$$Sa = 0.6 \times \min\left(\frac{Sy}{3}, \frac{Su}{10}\right) = 3{,}540 psi$$

Therefore, the safety factor against shear failure of the TALs in the MPC lid is

$$SF = \frac{Sa}{\tau} = 1.45$$

Case (ii): Finite Element Analysis of MPC Enclosure Vessel

The stress analysis of the MPC Enclosure Vessel under normal handling conditions is performed using ANSYS [3.4.1]. The finite element model, which is shown in Figure 3.4.1, is ¼ -symmetric, and it represents the maximum height MPC as defined by Tables 3.2.1 and 3.2.2. The maximum height MPC is analyzed because it is also the heaviest MPC. The key attributes of the ANSYS finite element model of the MPC Enclosure Vessel are described in Subsection 3.1.3.2.

The loads are statically applied to the finite element model in the following manner. The self weight

of the Enclosure Vessel is simulated by applying a constant acceleration of 1.15g in the vertical direction. The apparent dead weight of the stored fuel inside the MPC cavity (which includes a 15% dynamic amplifier) is accounted for by applying a uniformly distributed pressure of 18.8 psi on the top surface of the MPC baseplate. The amplified weight of the fuel basket and the fuel basket shims is applied as a ring load on the MPC baseplate at a radius equal to the half-width of the fuel basket cross section. The magnitude of the ring load is equal to 100.4 lbf/in. All internal surfaces of the MPC storage cavity are also subjected to an internal pressure of 95 psig, which exceeds the normal operating pressure per Table 4.4.5. Finally, the model is constrained by fixing one node on the top surface of the ¼-symmetric MPC lid, which coincides with the TAL. Symmetric boundary conditions are applied to the two vertical symmetry planes. The boundary conditions and the applied loads are graphically depicted in Figure 3.4.28.

The resulting stress intensity distribution in the Enclosure Vessel under the applied handling loads is shown in Figure 3.4.2. Figures 3.4.29 and 3.4.30 plot the thru-thickness variation of the stress intensity at the baseplate center and at the baseplate-to-shell juncture, respectively. The maximum primary and secondary stress intensities in the MPC Enclosure Vessel are compared with the applicable stress intensity limits from Subsection NB of the ASME Code [3.4.4]. The allowable stress intensities are taken at 450°F for the MPC shell and MPC lids, 300°F for the baseplate, and 250°F at the baseplate-to-shell juncture. These temperatures bound the operating temperatures for these parts under normal operating conditions (Table 4.4.3). The maximum calculated stress intensities and the corresponding safety factors are summarized in Table 3.4.1.

The shear stress in the MPC lid-to-shell weld under normal handling conditions is independently calculated, as shown below.

Per Table 3.2.8, the maximum weight of a loaded MPC is

$W_{MPC} = 116{,}400$ lb

The diameter and weight of the MPC lid assembly are

$D = 74.5$ in

$W_{lid} = 11{,}500$ lb

From Table 4.4.5, the bounding pressure inside the MPC cavity under normal operating conditions is

$P = 95$ psig

Thus, the total force acting on the MPC lid-to-shell weld is

$$F = 1.15 \cdot (W_{MPC} - W_{lid}) + P \cdot \left(\frac{\pi \cdot D^2}{4} \right) = 534{,}755 lb$$

which includes a 15% dynamic amplifier. The MPC lid-to-shell weld is a ¾" partial groove weld, which has an effective area equal to

$$A = \pi \cdot D \cdot \left(t_w - \frac{1}{8}\text{in} \right) \cdot 0.8 = 117.0\text{in}^2$$

where t_w is the weld size (= 0.75in). The calculated weld area includes a strength reduction factor of 0.8 per ISG-15 [3.4.17]. Thus, the average shear stress in the MPC lid-to-shell weld is

$$\tau = \frac{F}{A} = 4{,}571\text{psi}$$

The MPC Enclosure Vessel is made from Alloy X material, whose mechanical properties are listed in Table 3.3.1. Based on a temperature of 450°F (Table 4.4.3), and assuming that the weld strength is equal to the base metal ultimate strength, the allowable shear stress in the weld under normal conditions is

$$\tau_a = 0.3 \times S_u = 19{,}170\text{psi}$$

Therefore, the safety factor against shear failure of the MPC lid-to-shell weld is

$$SF = \frac{\tau_a}{\tau} = 4.19$$

b. Heaviest Weight HI-TRAC VW Lift

The HI-TRAC VW transfer cask is at its heaviest weight when it is being lifted out of the loading pit with the MPC full of fuel and water and the MPC lid lying on it for shielding protection (Table 3.2.8). The threaded lift points provide for the anchor locations for lifting.

The stress analysis of the transfer cask consists of two steps:

i. A strength evaluation of the tapped connection points to ensure that it will not undergo yielding at 3 times D* and failure at 10 times D*.

ii. A strength evaluation of the HI-TRAC VW vessel using strength of materials formula to establish the stress field under D*. The primary membrane plus primary bending stresses throughout the HI-TRAC VW body and the bottom lid shall be below the Level A stress limits for "NF" Class 3 plate and shell structures.

Case (i): Stress Analysis of HI-TRAC VW Threaded Anchor Locations (TALs)

Per Table 3.2.8, the maximum lifted weight of a loaded HI-TRAC VW is

D = 270,000 lb

Per the above, the apparent dead load of the HI-TRAC VW during handling operations is

D* = 1.15 x D = 310,500 lb

The HI-TRAC VW top flange has 8 TALs as shown on the drawing in Section 1.5. Therefore, the lifted load per TAL is equal to

$$\frac{D^*}{8} = 38{,}813 lb$$

Per Machinery's Handbook [3.4.12], the shear area of the internal threads (2" - 4.5UNC x 4" Lg.) at each TAL is

A = 18.1 in^2

Finally, the shear stress on the TALs is computed as follows

$$\tau = \frac{D^*}{8A} = 2{,}144 psi$$

The HI-TRAC VW top flange is made from SA-350 LF3 material, whose mechanical properties are listed in Table 3.3.3. Based on a design temperature of 400°F (Table 2.2.3), and assuming the yield and ultimate strengths in shear to be 60% of the corresponding tensile strengths, the allowable stress in the threads is determined as follows

$$Sa = 0.6 \times \min\left(\frac{Sy}{3}, \frac{Su}{10}\right) = 4{,}200 psi$$

Therefore, the safety factor against shear failure of the TALs in the HI-TRAC VW top flange is

$$SF = \frac{Sa}{\tau} = 1.96$$

Case (ii): Stress Analysis of HI-TRAC VW Body

The stress analysis of the HI-TRAC VW steel structure during lifting operations is performed using strength of materials. All structural members in the load path are evaluated for the maximum lifted weight (Table 3.2.8). In particular, the following stresses are calculated:

- the shear stress in the welds between the top flange and the inner and outer shells
- the primary membrane stress in the inner and outer shells
- the tensile stress in the bottom lid bolts
- the primary bending stress in the bottom lid

To determine the bending stress in the bottom lid, the weight of the loaded MPC (Table 3.2.8) plus the weight of the water inside the HI-TRAC VW cavity (Table 3.2.4) is applied as a uniformly distributed pressure on the top surface of the lid. The bending stress is calculated at the center of the bottom lid assuming that the lid is simply supported at the bolt circle diameter. The calculated stresses are compared with the Level A stress limits for "NF" Class 3 plate and shell structures. The detailed calculations are documented in [3.4.13]. Table 3.4.2 summarizes the stress analysis results for the HI-TRAC VW steel structure under the maximum lifted load.

c. HI-STORM FW Overpack Related Lifts

Two related lift conditions are:

i. HI-STORM FW loaded with the heaviest MPC and closure lid installed being lifted (heaviest weight configuration).

ii. HI-STORM FW lid being lifted (heaviest weight configuration)

Case (i): HI-STORM FW Lift Using Anchor Block Connections

Calculations to establish the margin of safety in the TALs and the HI-STORM FW overpack's steel structure are summarized below.

Per Table 3.2.8, the maximum weight of a loaded HI-STORM FW is

D = 425,700 lb

Per the above, the apparent dead load of the HI-STORM FW during handling operations is

D* = 1.15 x D = 489,555 lb

The HI-STORM FW overpack has 4 TALs as shown on the drawing in Section 1.5. Therefore, the lifted load per TAL is equal to

$$\frac{D^*}{4} = 122{,}389 lb$$

Per Machinery's Handbook [3.4.12], the shear area of the internal threads (3 1/4" - 4UNC x 6.5" Lg.) at each TAL is

$A = 48.3\ in^2$

Finally, the shear stress on the TALs is computed as follows

$$\tau = \frac{D^*}{4A} = 2{,}534 psi$$

The HI-STORM FW anchor blocks are made from SA-350 LF2 material, whose mechanical properties are listed in Table 3.3.3. Based on a design temperature of 350°F (Table 2.2.3), and assuming the yield strength in shear to be 60% of the corresponding tensile yield strength, the allowable stress in the threads is determined as follows

$$Sa = 0.6 \times \frac{Sy}{3} = 6{,}260 psi$$

Therefore, the safety factor against shear failure of the TALs in the HI-STORM FW overpack is

$$SF = \frac{Sa}{\tau} = 2.47$$

The stress analysis of the overpack body under normal handling conditions is performed using ANSYS [3.4.1]. The finite element model, which is shown in Figure 3.4.3, is ¼-symmetric, and it represents the maximum height HI-STORM FW as defined by Tables 3.2.1 and 3.2.2. The concrete density is also maximized (Table 3.2.5) in the ANSYS model. The key attributes of the ANSYS finite element model of the HI-STORM FW overpack are described in Subsection 3.1.3.1.

The self weight of the overpack is simulated by applying a constant acceleration of 1.15g in the vertical direction. The apparent dead weight of the fully loaded MPC (which includes a 15% dynamic amplifier) is accounted for by applying a uniformly distributed pressure of 23.8 on the top surface of the HI-STORM FW baseplate. Finally, the model is constrained by fixing four nodes on the top surface of the HI-STORM FW, which coincide with the TALs. Symmetric boundary conditions are applied to the two vertical symmetry planes. The boundary conditions and the applied loads are graphically depicted in Figure 3.4.26.

The resulting stress distribution in the overpack under the applied handling loads is shown in Figure 3.4.4. The maximum primary stresses in the HI-STORM overpack body are compared with the applicable stress limits from Subsection NF of the ASME Code [3.4.2]. The allowable stresses for the load-bearing members are taken at 300°F, which exceeds the maximum operating temperature for the overpack under normal operating conditions (Table 4.4.3). The maximum stresses and the corresponding safety factors are summarized in Table 3.4.3.

Case (ii): Lid Lift Analysis

The weight of the HI-STORM FW lid is dependent on the shielding concrete's density. The maximum possible weight of the lid is provided in Table 3.2.5. The HI-STORM FW lid is lifted using the four equally spaced TALs on the lid top surface, which are shown on the licensing drawing in Section 1.5. Calculations to establish the margin of safety in the TALs and the lid's steel structure are summarized below.

Per Table 3.2.5, the maximum weight of the HI-STORM FW lid is

D = 23,300 lb

Per the above, the apparent dead load of the HI-STORM FW lid during handling operations is

D* = 1.15 x D = 26,795 lb

The HI-STORM FW lid has 4 TALs as shown on the drawing in Section 1.5. Therefore, the lifted load per TAL is equal to

$$\frac{D^*}{4} = 6{,}699\text{lb}$$

Per Machinery's Handbook [3.4.12], the shear area of the internal threads (1 1/2" - 6UNC x 3" Lg.) at each TAL is

$A = 10.7\ \text{in}^2$

Finally, the shear stress on the TALs is computed as follows

$$\tau = \frac{D^*}{4A} = 626\text{psi}$$

The HI-STORM FW lid anchor blocks are made from carbon steel material, whose yield and ultimate strengths at 450°F (Table 2.2.3) are conservatively input as 15,000 psi and 40,000 psi, respectively. Assuming the yield and ultimate strengths in shear to be 60% of the corresponding tensile strengths, the allowable stress in the threads is determined as follows

$$Sa = 0.6 \times \min\left(\frac{Sy}{3}, \frac{Su}{10}\right) = 2{,}400\text{psi}$$

Therefore, the safety factor against shear failure of the TALs in the HI-STORM FW lid is

$$SF = \frac{Sa}{\tau} = 3.83$$

The global stress analysis of the overpack lid under normal handling conditions is performed using ANSYS [3.4.1]. Figure 3.4.5 shows the finite element model of the lid, which incorporates the maximum concrete density (Table 3.2.5). The key attributes of the ANSYS finite element model of the HI-STORM FW lid are described in Subsection 3.1.3.1.

The self weight of the overpack lid is simulated by applying a constant acceleration of 1.15g in the vertical direction. The model is constrained by fixing four nodes on the top surface of the HI-STORM FW lid, which coincide with the TALs.

The resulting stress distribution in the steel structure of the overpack lid under the applied handling load is shown in Figure 3.4.6. The maximum stresses and the corresponding safety factors are summarized in Table 3.4.4. For conservatism, the maximum calculated stress at any point on the lid, including secondary stress contributions, is compared against the primary membrane and primary bending stress limits per Subsection NF of the ASME Code for Level A conditions. The allowable stresses are taken at 300°F, which exceeds the maximum operating temperature for the overpack top lid under normal operating conditions.

3.4.3.3 Safety Evaluation of Lifting Scenarios

As can be seen from the above, the computed factors of safety have a large margin over the allowable (of 1.0) in every case. In the actual fabricated hardware, the factors of safety will likely be much greater because of the fact that the actual material strength properties are generally substantially greater than the Code minimums. Minor variations in manufacturing, on the other hand, may result in a small subtraction from the above computed factors of safety. A part 72.48 safety evaluation will be required if the cumulative effect of manufacturing deviation and use of the CMTR (or CoC) material strength in a manufactured hardware renders a factor of safety to fall below the above computed value. Otherwise, a part 72.48 evaluation is not necessary. The above criterion applies to all lift calculations covered in this FSAR.

3.4.4 Heat

The thermal evaluation of the HI-STORM FW system is reported in Chapter 4.

a. Summary of Pressures and Temperatures

Design pressures and design temperatures for all conditions of storage are listed in Tables 2.2.1 and 2.2.3, respectively.

b. Differential Thermal Expansion

The effect of differential thermal expansion among the constituent components in the HI-STORM FW system is considered in Chapter 4 wherein the temperatures necessary to perform the differential thermal expansion analyses for the MPC in the HI-STORM FW and HI-TRAC VW casks are computed. The material presented in Section 4.4 demonstrates that a constraint to free expansion due to differential growth between discrete components of the HI-STORM FW system (e.g., storage overpack and enclosure vessel) will not develop under any operating condition.

i. Normal Hot Environment

Results presented in Section 4.4 demonstrate that initial gaps between the HI-STORM FW storage overpack or the HI-TRAC VW transfer cask and the MPC canister, and between the MPC canister and the fuel basket, will not close due to thermal expansion of the system components normal operating conditions.

The clearances between the MPC basket and canister structure, as well as between the MPC shell and storage overpack or HI-TRAC VW inside surface, are shown in Section 4.4 to be sufficient to preclude a temperature induced interference from differential thermal expansions under normal operating conditions.

ii. Fire Accident

It is shown in Chapter 4 that the fire accident has a small effect on the MPC temperatures because of the short duration of the fire accidents and the large thermal inertia of the storage overpack. Therefore, a structural evaluation of the MPC under the postulated fire event is not required. The conclusions reached in item (i) above are also appropriate for the fire accident with the MPC housed in the storage overpack. Analysis of fire accident temperatures of the MPC housed within the HI-TRAC VW for thermal expansion is unnecessary, as the HI-TRAC VW, directly exposed to the fire, expands to increase the gap between the HI-TRAC VW and MPC.

As expected, the external surfaces of the HI-STORM FW storage overpack that are directly exposed to the fire event experience maximum rise in temperature. The outer shell and top plate in the top lid are the external surfaces that are in direct contact with heated air from fire. Table 4.6.2 provides the maximum temperatures attained at the key locations in HI-STORM FW storage overpack under the

postulated fire event.

The following conclusions are evident from the above table.

- The maximum metal temperature of the carbon steel shell most directly exposed to the combustion air is well below 700°F (Table 2.2.3 applicable short-term temperature limit). 700°F is the permissible temperature limit in the ASME Code for the outer shell material.

- The bulk temperature of concrete is well below the normal condition temperature limit of 300°F specified in Table 2.2.3. ACI-349-85 [3.3.6] permits 350°F as the short-term temperature limit; the shielding concrete in the HI-STORM FW overpack. As the detailed information in Section 4.6 shows, the radial extent in the concrete where the local temperature exceeds 350°F begins at the outer shell/concrete interface and ends in less than one-inch. Therefore, the potential loss in the shielding material's effectiveness is less than 4% of the concrete shielding mass in the overpack annulus.

- The metal temperature of the inner shell does not exceed 300°F at any location, which is well below the accident condition temperature specified in Table 2.2.3 for the inner shell.

- The presence of a vented space at the top of the overpack body ensures that there will be no pressure buildup in the concrete annulus due to the evaporation of vapor and gaseous matter from the shielding concrete.

Thus, it is concluded that the postulated fire event will not jeopardize the structural integrity of the HI-STORM FW overpack or significantly diminish its shielding effectiveness.

The above conclusions, as relevant, also apply to the HI-TRAC VW fire considered in Chapter 4. Water jacket over-pressurization is prevented by the pressure relief devices. The non-structural effects of loss of water have been evaluated in Chapter 5 and shown to meet regulatory limits. Therefore, it is concluded that the postulated fire event will not cause a state of non-compliance with the regulations to materialize.

3.4.4.1 Safety Analysis

Calculations of the stresses and displacements in the different components of the HI-STORM FW system from the effects of mechanical load case assembled in Table 3.1.1 for the MPC, the HI-STORM FW storage overpack and the HI-TRAC VW transfer cask are presented in the following. The purpose of the analyses summarized herein is to provide the necessary assurance that there will be no unacceptable risk of criticality, unacceptable release of radioactive material, unacceptable radiation levels, or impairment of ready retrievability of fuel from the MPC (for normal and off-normal conditions of storage) and the MPC from the HI-STORM FW storage overpack or from the HI-TRAC VW transfer cask.

Because many of the analyses must be performed for a particular ISFSI to demonstrate the acceptability of site-specific loads under the provisions of 10CFR72.212, the analyses presented here also set down the acceptable methodologies. Accordingly, the analysis methodologies are configured to exaggerate the severity of response. Also, because the weight and height of all three components (overpack, MPC, and HI-TRAC VW) can vary between specified ranges (see tables in Section 3.2), each analysis is carried out for the dimensional and weight condition of the component that maximizes response. Thus, for example, the seismic stability analysis of the loaded HI-STORM FW (Load Case 2 in Table 3.1.1) is performed for the case of maximum height, but the stability under the impact of a large tornado missile (Load Case 3) is analyzed assuming maximum height and minimum weight (MPC is assumed to contain only one fuel assembly).

Each load case in Table 3.1.1 is considered sequentially and all affected components are analyzed to determine the factors of safety.

All factors of safety reported in this FSAR utilize nominal dimensions and minimum material strengths. Actual factors of safety in the manufactured hardware are apt to be considerably larger than those reported herein chiefly because of the actual material strengths being much greater than the values used in the safety analyses. A part 72.48 safety assessment will be required if the combined effect of the actual material strength and manufacturing deviation produces a lower safety factor for a design basis loading than that referenced in the safety evaluation in this FSAR.

3.4.4.1.1 Load Case 1: Moving Floodwater

The object of the analysis is to determine the maximum floodwater velocity that a loaded HI-STORM FW on the ISFSI pad can withstand before tipping over or sliding. The flood data for the ISFSI shall be based on a 40-year (minimum) return flood. The kinematic stability analysis consists of writing static equilibrium equations for tipping and sliding.

The flood condition subjects the HI-STORM FW system to external pressure, together with a horizontal load due to water velocity. Because the HI-STORM FW storage overpack is equipped with ventilation openings, the hydrostatic pressure from flood submergence acts only on the MPC. As stated in Subsection 2.2.3, the design external pressure for the MPC bounds the hydrostatic pressure from flood submergence.

The water velocity associated with flood produces a horizontal drag force, which may act to cause sliding or tip-over. In accordance with the provisions of ANSI/ANS 57.9, the acceptable upper bound flood velocity, V, must provide a minimum factor of safety of 1.1 against overturning and sliding.

The overturning horizontal force, F, due to hydraulic drag, is given by the classical formula:

$$F = Cd\ A\ V^* \qquad \text{[Equation 1]}$$

where:

V^* = velocity head = $\frac{\rho V^2}{2g}$ (ρ is water weight density, and g is acceleration due to gravity).

A = projected area of the HI-STORM FW cylinder perpendicular to the fluid velocity vector, equal to D times h, where h is the height of the floodwater.

Cd = drag coefficient

The value of Cd for flow past a cylinder at Reynolds number above 5E+05 is given as 0.5 in the literature (viz. Hoerner, Fluid Dynamics, 1965).

The drag force tending to cause HI-STORM FW's sliding is opposed by the friction force, which is given by

$$F_f = \mu\ W^* \qquad \text{[Equation 2]}$$

where:

μ = limiting value of the friction coefficient at the HI-STORM FW/ISFSI pad interface is assumed to be equal to 0.53 (the NRC-approved value in Docket No. 72-1014).

W* = apparent (buoyant) weight of HI-STORM FW with an empty MPC.

i. Sliding Factor of Safety

The factor of safety against sliding, β_1, is given by

$$\beta_1 = \frac{F_f}{F} = \frac{\mu W^*}{Cd\ A\ V^*} = \frac{2g\mu W^*}{Cd(Dh)\rho V^2} \qquad \text{[Equation 3]}$$

The factor of safety, β_1, must be greater than 1.1. For $g = 32.2$ ft/sec^2, $Cd = 0.5$, and $\rho = 62.4$ lbf/ft^3, the maximum value of V as a function of the floodwater height h is given by

$$V = \sqrt{\frac{1.876\mu W^*}{Dh}} \qquad \text{[Equation 4]}$$

ii. Overturning Factor of Safety

For determining the margin of safety against overturning, β_2, the cask is assumed to pivot about a fixed point located at the outer edge of the contact circle at the interface between HI-STORM FW and the ISFSI. The overturning moment due to the hydraulic force F_T is balanced by a restoring moment from the buoyant weight acting at radius D/2.

Overturning moment, $M_o = Fh/2$ where F is given by Equation 1 above.

Restoring moment, $M_r, = W^* D/2$ [Equation 5]

For stability against tipping $M_o \leq M_r$

or $Fh \leq W^*D$

Hence the factor of safety against overturning is

$$\beta_2 = \frac{W^*D}{Fh} = \frac{W^*D}{Cd\,A\,V^*h} = \frac{2gW^*}{Cdh^2\rho V^2} \qquad \text{[Equation 6]}$$

β_2 must be greater than 1.1. For $g = 32.2$ ft/sec^2, $Cd = 0.5$, and $\rho = 62.4$ lbf/ft^3, the maximum value of V as a function of the floodwater height h is given by

$$V = \frac{\sqrt{1.876W^*}}{h} \qquad \text{[Equation 7]}$$

The smaller of the value of V from Equations 4 and 7 defines the maximum permissible flood velocity for the site. For the HI-STORM FW system, Equation 4 governs since the coefficient of friction (μ) is less than the smallest value of D/h for the limiting overpack geometry (maximum height). The numerical value of V is computed as follows:

From Tables 3.2.1 and 3.2.2 and the drawings in Section 1.5, the diameter and maximum height of the overpack are

D = 139 in = 11.6 ft

h = 240 in = 20.0 ft

From Tables 3.2.3 and 3.2.5, the minimum weight of the HI-STORM FW overpack with an empty MPC (based on Ref. PWR fuel length and 150 pcf concrete density) is

W = 254,600 lbf

Finally, assuming that W* = 0.87W, the acceptable upper bound flood velocity is determined from Equation 4 as

$$V = \sqrt{\frac{1.876(0.53)(0.87 \times 254{,}600)}{(11.6)(20.0)}} = 30.8 \text{ft/sec}$$

3.4.4.1.2 Load Case 2: Design Basis Earthquake

In Subsection 2.2.3 (g), the combination of vertical and horizontal ZPA of the earthquake that would cause incipient loss of kinematic stability is derived using static equilibrium. The resulting inequality defines the threshold of the so-called low intensity earthquake for which the HI-STORM FW system is qualified without a dynamic analysis. However, an earthquake is a cyclic loading event which would produce rattling of the MPC inside the overpack and possibly large strains in the Confinement Boundary at the location of rattling impact between the MPC and the overpack guide tubes.

For earthquakes stronger than that defined by the inequalities in Subsection 2.2.3(g), it is necessary to perform a dynamic analysis. The dynamic stability analysis may be performed using either one of the following two approaches:

i. Using the nomographs developed in NUREG/CR-6865 [3.4.7] to predict the cask rotation and sliding.

ii. Performing a time history analysis for the cask modeled with 6 degrees-of-freedom and subjected to 3-dimensional seismic accelerations.

The first approach, although limited in its applications, is simple and conservative for the seismic stability evaluation of the HI-STORM FW storage cask as explained below. The nomograph developed in NUREG/CR-6865 [3.4.7] for cylindrical casks are based on extensive parametric study of the seismic response of HI-STORM 100 with a series of seismic inputs fitting three different spectral shapes. The seismic response is predicted through transient finite element analyses where the cask is supported on a flexible concrete pad founded on three substrates ranging from soft soil to rock. The NUREG study offers two sets of nomographs depending on the match of the site-specific free field horizontal spectrum with the three spectral shapes utilized in the study (after normalization to the Peak (Zero Period) Ground Acceleration (PGA)). The power law for the HI-STORM 100 response "y" (either peak cask top displacement or peak cask rotation) in terms of the ground motion parameter "x" at confidence band "m" standard deviations above the median response is:

$$y = A x^B \exp\left(m S_{Y|x}\right)$$

In the above equation, "A" and "B" are the nomograph curve fitting parameters, and "S" is the conditional standard deviation of the result data after undergoing a logarithmic transformation. The value for "m" is 0 (for the median curve), +1 (for the 84% confidence level) and –1 (for the 16%

confidence level). The units of "A" are meters (for displacement) and degrees (for rotation). The values for the coefficients are given below, as reproduced from [3.4.7]. The nomograph parameters are affected by the cask/pad coefficient of friction, but are independent of substrate stiffness.

Curve Fitting Parameters for Cylindrical Cask, NUREG/CR-0098 Earthquakes, PGA

	A (disp.)	B (disp.)	$S_{\gamma_1 x}$ (disp.)	A (rot.)	B (rot.)	$S_{\gamma_1 x}$ (rot.)
μ=0.2	0.216	2.60	0.409	0.0217	0.689	0.718
μ=0.55	0.911	4.06	0.814	6.70	3.94	0.794
μ=0.8	1.150	4.16	0.796	9.01	4.09	0.765

Curve Fitting Parameters for Cylindrical Cask, Regulatory Guide 1.60 Earthquakes, PGA

	A (disp.)	B (disp.)	$S_{\gamma_1 x}$ (disp.)	A (rot.)	B (rot.)	$S_{\gamma_1 x}$ (rot.)
μ=0.2	0.837	2.52	0.465	0.0733	1.71	0.785
μ=0.55	8.96	4.80	1.03	62.5	4.71	0.956
μ=0.8	15.4	5.04	1.13	114	4.94	1.12

Curve Fitting Parameters for Cylindrical Cask, NUREG/CR-6728 Earthquakes, PGA

	A (disp.)	B (disp.)	$S_{T_1 x}$ (disp.)	A (rot.)	B (rot.)	$S_{T_1 x}$ (rot.)
μ=0.2	0.0897	1.88	0.377	0.0456	1.17	0.777
μ=0.55	0.219	2.63	0.543	1.64	2.53	0.583
μ=0.8	0.253	2.71	0.631	2.11	2.68	0.606

Curve Fitting Parameters for Cylindrical Cask, All Spectral Shapes, 1 Hz PSA

	A (disp.)	B (disp.)	$S_{T_1 x}$ (disp.)	A (rot.)	B (rot.)	$S_{T_1 x}$ (rot.)
μ=0.2	0.271	2.15	0.532	0.0335	0.769	0.91
μ=0.55	0.979	3.20	1.07	7.07	3.10	1.04
μ=0.8	1.29	3.31	1.11	10.1	3.25	1.09

The use of the above nomographs for HI-STORM FW seismic stability analysis is conservative, as long as the h/r ratio (h = height to cask centroid, r = radius of the cask at interface with the pad) of HI-STORM FW is smaller than that of HI-STORM 100 cask, which is true in most cases. The nomographs should not be used when the substrate characteristics indicate that liquefaction will occur under a seismic event [3.4.7]. The basic analysis procedure is as follows:

i. Demonstrate that the cask h/r ratio is less than that of HI-STORM 100 cask. If this condition is not satisfied, this approach cannot be used for the seismic stability analysis.

ii. Evaluate the site-specific substrate data to ensure that the site-specific substrate is within the range considered in the NUREG and that there is no potential for soil liquefaction under a seismic event.

iii. Compare the site-specific horizontal free-field response spectrum for 5% damping with those employed in the NUREG (after normalizing the site-specific data to 1g).

a. If the site-specific spectrum is a good match with one of the spectrums employed, then use the nomograph appropriate to the matched spectrum and site-specific input at the ZPA to predict cask displacement and rotation.

b. If the site-specific spectrum is not a good match with any of the spectra, then use the nomograph developed for all spectra with site-specific input at 1 Hz and 5% damping to predict cask displacement and rotation.

If the previously described NUREG/CR-6865 approach is not appropriate to use for a specific ISFSI site, the second approach should be used to perform the seismic stability evaluation for HI-STORM FW casks. The time history analysis approach, which is free of the limitations associated with NUREG/CR-6865, was used and approved by the USNRC to demonstrate the seismic stability of HI-STORM 100 casks at the Private Fuel Storage ISFSI. The input seismic acceleration time histories shall meet the relevant requirements specified in the SRP 3.7.1 [3.4.8] and shall be baseline corrected.

Finally, a small clearance between the MPC and the MPC guide tubes may lead to a high localized strain in the region of the shell where impacts from rattling of the canister under a seismic event occur. The extent of local strain from impact is minimized by locating the guide tube in the vertical direction such that its impact footprint is aligned with the surface of the closure lid which has been shimmed to close the crevice between the lid and the shell. Thus the impact between the guide tubes and the MPC lid will occur at a location where the maximum damage to the MPC shell will be local denting in the region where it is buttressed by the edge of a (thick) MPC lid. Therefore, a through-wall damage of the MPC shell is not credible. Furthermore, the force of impact will evidently be greater in the non-mechanistic tip-over case. Therefore, the seismic impact case is designated as non-governing for the guide tube/MPC impact scenario.

3.4.4.1.3 Load Case 3: Tornado-Borne Projectiles

During a tornado event, the HI-STORM FW overpack and the HI-TRAC VW are assumed to be subjected to a constant wind force. They are also subject to impacts by postulated missiles. The maximum wind speed is specified in Table 2.2.4, and the three missiles, designated as large, intermediate, and small, are described in Table 2.2.5.

a. Large Missile

Overturning Analysis

The large tornado missile acting at the top region of the cask (HI-STORM FW or HI-TRAC VW) to produce maximum overturning effect (Table 3.1.1) is analyzed to determine whether the cask will remain stable. Because the site-specific large missile is apt to be different from the one analyzed herein, the method of analysis presented here will provide the means for the site-specific safety evaluation pursuant to 10CFR72.212.

The overturning analysis of the cask under the tornado wind load and large missile impact is performed by solving the 1-DOF equation of motion for the cask angular rotation, which is same methodology used in the HI-STORM 100 FSAR (Docket No. 72-1014). Specifically, the solution of the post-impact dynamics problem is obtained by solving the following equation of motion:

$$I_r\alpha = \left(-W_c\frac{a}{2}\right) + F_{max}\left(\frac{L}{2}\right)$$

where:

I_r = cask moment of inertia about the pivot point
α = angular acceleration of the cask
W_c = lower bound weight of the cask
a = diameter of cask at its base (see Figure 3.4.7)
F_{max} = force on the cask due to tornado wind/instantaneous pressure drop
L = height of the cask (see Figure 3.4.7)

The impacting missile enters into the above through the post-strike angular velocity of the cask, which is the relevant initial condition for the cask equation of motion. The solution gives the post-impact position of the cask centroid as a function of time, which indicates whether the cask remains stable.

The following assumptions are made in the analysis:

i. The cask is assumed to be a rigid solid cylinder, with uniform mass distribution. This assumption implies that the cask sustains no plastic deformation (i.e. no absorption of energy through plastic deformation of the cask occurs).

ii. The angle of incidence of the missile is assumed to be such that its overturning effect on the cask is maximized (see Figure 3.4.7).

iii. The analysis considers the maximum height cask per Tables 3.2.1 and 3.2.2. The missile is assumed to strike at the highest point of the cask (see Figure 3.4.7), again maximizing the overturning effect.

iv. The cask is assumed to pivot about a point at the bottom of the base plate opposite the location of missile impact and the application of wind force in order to conservatively maximize the propensity for overturning (see Figure 3.4.7).

v. Inelastic impact is assumed, with the missile velocity reduced to zero after impact. This assumption conservatively lets the missile impart the maximum amount of angular momentum to the cask, and it is in agreement with missile impact tests conducted by EPRI [3.4.14].

vi. The analysis is performed for a cask without fuel in order to provide a conservative solution. A lighter cask will tend to rotate further after the missile strike. The weight of the missile is not included in the total post-impact weight.

vii. Planar motion of the cask is assumed; any loads from out-of-plane wind forces are neglected.

viii. The drag coefficient for a cylinder in turbulent cross flow is used.

ix. The missile and wind loads are assumed to be perfectly aligned in direction.

The results for the post-impact response of the HI-STORM FW overpack and the HI-TRAC VW transfer cask are summarized in Table 3.4.5. The table shows that both casks remain in a vertical upright position (i.e., no overturning) in the aftermath of a large missile impact. The complete details of the tornado wind and large missile impact analyses for the HI-STORM FW overpack and the HI-TRAC VW transfer cask are provided in Appendix 3.A.

Sliding Analysis

A conservative calculation of the extent of sliding of the HI-STORM FW overpack and the HI-TRAC VW cask due to the impact of a large missile (Table 2.2.5) and tornado wind (Table 2.2.4) is obtained using a common formulation as explained below. A more realistic impact simulation using LS-DYNA, with less bounding assumptions, has been used in Subsection 3.4.4.1.4 to qualify the HI-STORM overpack for a non-mechanistic tip over event. While it is not necessary for demonstrating adequate safety margins for this problem, an LS-DYNA analysis could also be used to calculate the sliding potential of the HI-STORM FW and HI-TRAC VW for a large missile impact. In what follows, both HI-STORM FW and HI-TRAC VW are identified by the generic term "cask".

The principal assumptions that render these calculations for sliding conservative are:

i. The weight of the cask used in the analysis is assumed to be the lowest per Table 3.2.8.

ii. The cask is assumed to absorb the energy of impact purely by sliding. In other words, none of the impact energy is dissipated by the noise from the impact, from local plastic deformation in the cask at the location of impact, or from the potential tipping action of the cask.

iii. The missile impact and high wind, which applies a steady drag force on the cask, are assumed to act synergistically to maximize the movement of the cask.

iv. The cask is assumed to be freestanding on a concrete surface. The interface friction coefficient is assumed to be equal to that endorsed in the HI-STORM 100 FSAR (USNRC Docket No. 72-1014) and adopted here in the HI-STORM FW FSAR.

v. The dynamic effect of the impact is represented by the force-time curve developed in the Bechtel topical report "Design of Structures for Missile Impact" [3.4.9], previously used to qualify the HI-STORM 100 System (USNCR Docket No. 72-1014).

The analysis for sliding under the above assumptions reduces to solving Newton's equation of motion of the form:

$$m\frac{d^2x}{dt^2} = F(t) + F_{dp} - \mu mg$$

where

m: mass of the cask,

t: time coordinate with its origin set at the instant when the sum of the missile impact force and wind drag force overcomes the static friction force,

x: displacement as a function of time coordinate t,

$F(t)$: missile impact force as a function of time (from [3.4.9]),

F_{dp}: drag force from high wind,

μ: interface friction set as 0.53 for freestanding cask on a reinforced concrete pad in Docket No. 72-1014,

g: acceleration due to gravity.

The above second-order differential equation is solved numerically in [3.4.15] for the HI-STORM FW overpack and the HI-TRAC VW transfer cask, and the calculated sliding displacements are summarized in Table 3.4.16.

Referring to the spacing dimensions for HI-STORM FW arrays in Table 1.4.1, the minimum space between HI-STORM FW overpacks and the minimum distance of the overpack to the edge of the pad are calculated. The above table demonstrates the HI-STORM FW overpack will not collide with another overpack, and the overpack will not slide off the pad due to the combined effects of a large tornado missile impact and high wind.

No generic limits for sliding are established for the HI-TRAC VW. Therefore, the sliding result for the HI-TRAC VW transfer cask in Table 3.4.16 is strictly informational.

b. Small and Intermediate Missiles

The small and intermediate missiles (Table 2.2.5) are analyzed to determine the extent to which they will penetrate the HI-STORM FW overpack or the HI-TRAC VW and cause potential damage to the MPC Enclosure Vessel. Classical energy balance methods are used to compute the depth of

penetration at the following impact locations:

- on the HI-STORM FW outer shell (with concrete backing)
- on the HI-STORM FW lid top plate (with concrete backing)
- on the HI-TRAC VW outer shell (with lead backing)
- on the top surface of the MPC upper lid

The MPC upper lid is analyzed for a direct missile impact because, when the MPC is placed inside the HI-TRAC VW, the MPC lid is theoretically accessible to a vertically downward directed small or intermediate missile.

The following assumptions are made in the analysis:

i. The intermediate missile and the small missile are assumed to be unyielding, and hence the entire initial kinetic energy is assumed to be absorbed by local yielding and denting of the cask surface.

ii. No credit is taken for the missile resistance offered by the HI-TRAC VW water jacket shell. It is assumed a priori that the small and intermediate missiles will penetrate the water jacket shell (with no energy loss). Therefore, in the analysis 100% of the missile impact energy is applied directly to the HI-TRAC VW outer shell.

iii. For missile strikes on the side and top lid of the overpack, the analysis credits the structural resistance in compression offered by the concrete material that backs the outer shell and the lid.

iv. The resistance from the concrete is conservatively assumed to act over an area equal to the target area of impact. In other words, no diffusion of the load is assumed to occur through the concrete.

The analyses documented in Appendix 3.B show that the depth of penetration of the small missile is less than the thinnest section of material on the exterior surface of the HI-STORM FW or the HI-TRAC VW. Therefore, the small missile will dent, but not penetrate, the cask. The 1-inch missile can enter the air inlet/outlet vents in the HI-STORM FW overpack, but geometry prevents a direct impact with the MPC.

For the intermediate missile, the analyses documented in Appendix 3.B show that there will be no penetration through the concrete surrounding the inner shell of the storage overpack or penetration of the top lid. Likewise, the intermediate missile will not penetrate the lead surrounding the HI-TRAC VW inner shell. Therefore, there will be no impairment to the Confinement Boundary due to tornado-borne missile strikes. Furthermore, since the HI-STORM FW and HI-TRAC VW inner shells are not compromised by the missile strike, there will be no permanent deformation of the inner shells and ready retrievability of the MPC will be assured.

The penetration results for the small and intermediate missile are summarized in Table 3.4.6.

3.4.4.1.4 Load Case 4: Non-Mechanistic Tipover

The non-mechanistic tipover event, as described in Subsection 2.2.3(b), is site-dependent only to the extent that the stiffness of the target (ISFSI pad) affects the severity of the impact impulse. To bound the majority of ISFSI pad sites, the tipover analyses are performed using a stiff target foundation, which is defined in Table 2.2.9. The objectives of the analyses are to demonstrate that the plastic deformation in the fuel basket is sufficiently limited to permit the stored SNF to be retrieved by normal means and that there is no significant loss of radiation shielding in the storage system. Furthermore, the maximum lateral deflection of the lateral surface of the fuel basket is within the limit assumed in the criticality analyses (Chapter 6), and therefore, the lateral deflection does not have an adverse effect on criticality safety.

The tipover event is an artificial construct wherein the HI-STORM FW overpack is assumed to be perched on its edge with its C.G. directly over the pivot point A (Figure 3.4.8). In this orientation, the overpack begins its downward rotation with zero initial velocity. Towards the end of the tip-over, the overpack is horizontal with its downward velocity ranging from zero at the pivot point (point A) to a maximum at the farthest point of impact. The angular velocity at the instant of impact defines the downward velocity distribution along the contact line.

In the following, an explicit expression for calculating the angular velocity of the cask at the instant when it impacts on the ISFSI pad is derived. Referring to Figure 3.4.8, let r be the length AC where C is the cask centroid. Therefore,

$$r = \left(\frac{d^2}{4} + h^2 \right)^{1/2}$$

The mass moment of inertia of the HI-STORM FW system, considered as a rigid body, can be written about an axis through point A, as

$$I_A = I_c + \frac{W}{g} r^2$$

where I_c is the mass moment of inertia about a parallel axis through the cask centroid C, and W is the weight of the cask (W = Mg).

Let $\theta_1(t)$ be the rotation angle between a vertical line and the line AC. The equation of motion for rotation of the cask around point A, during the time interval prior to contact with the ISFSI pad, is

$$I_A \frac{d^2\theta_1}{dt^2} = Mgr \sin\theta_1$$

This equation can be rewritten in the form

$$\frac{I_A}{2} \frac{d(\dot{\theta}_1)^2}{d\theta_1} = Mgr \sin\theta_1$$

which can be integrated over the limits $\theta_1 = 0$ to $\theta_1 = \theta_{2f}$ (Figure 3.4.8). The final angular velocity θ_1 at the time instant just prior to contact with the ISFSI pad is given by the expression

$$\dot{\theta}_1(t_B) = \sqrt{\frac{2\,Mgr}{I_A}(1-\cos\theta_{2f})}$$

where, from Figure 3.4.8,

$$\theta_{2f} = \cos^{-1}\left(\frac{d}{2r}\right)$$

This equation establishes the initial conditions for the final phase of the tip-over analysis; namely, the portion of the motion when the cask is decelerated by the resistive force at the ISFSI pad interface. Using the data germane to HI-STORM FW (Table 3.4.11) and the above equations, the angular velocity of impact is calculated as

$$\dot{\theta}_1(t_B) = 1.45 \text{ rad/sec}$$

The LS-DYNA analysis to characterize the response of the HI-STORM FW system under the non-mechanistic tipover event is focused on two principal demonstrations, namely:

(i) The lateral deformation of the basket panels in the active fuel region is less than the limiting value in Table 2.2.11.

(ii) The impact between the MPC guide tubes and the MPC does not cause a thru-wall penetration of the MPC shell.

Two LS-DYNA finite element models are developed to simulate the postulated tipover event of HI-STORM FW storage cask with loaded MPC-37 and MPC-89, respectively. The two LS-DYNA models are constructed according to the dimensions specified in the licensing drawings included in Section 1.5; the tallest configuration for each MPC type is considered to ensure a bounding tipover analysis. Because of geometric and loading symmetries, a half model of the loaded cask and impact target (i.e., the ISFSI pad) is considered in the analysis. The LS-DYNA models of the HI-STORM FW overpack and the MPC are described in Subsections 3.1.3.1 and 3.1.3.2, respectively.

The ISFSI pad LS-DYNA model, which consists of a 320"×100"×36" concrete pad and the underlying subgrade (800"×275"×470" in size) with non-reflective lateral and bottom surface boundaries, is identical to that used in the HI-STORM 100 tipover analysis documented in the HI-STORM 100 FSAR [3.1.4]. All structural members of the loaded cask are explicitly modeled so that any violation of the acceptance criteria can be found by examining the LS-DYNA simulation results (note: the fuel assembly, which is not expected to fail in a tipover event, is modeled as an elastic rectangular body). This is an improvement compared with the approach taken in the HI-STORM 100 tipover analysis, where the loaded MPC was modeled as a cylinder and therefore the structural integrity of the MPC and fuel basket had to be analyzed separately based on the rigid body deceleration result of the cask. Except for the fuel basket, which is divided into four parts based on the temperature distribution of the basket, each structural member of the cask is modeled as an independent part in the LS-DYNA model. Note that the critical weld connection between the MPC shell and the MPC lid is treated as a separate part and modeled with solid elements. Each of the two LS-DYNA models consists of forty-two parts, which are discretized with sufficiently high mesh density; very fine grids are used in modeling the MPC enclosure vessel, especially in the areas where high stress gradients are expected (e.g., initial impact location with the overpack). To ensure numerical accuracy, full integration thin shell and thick shell elements with 10 though-thickness integration points or multi-layer solid elements are used. The LS-DYNA tipover model consists of over 470,000 nodes and 255,000 elements for HI-STORM FW with loaded MPC-37, and the model for the cask with loaded MPC-89 consists of over 689,000 nodes and 350,000 elements.

The same ISFSI concrete pad material model used for the HI-STORM 100 tipover analysis reported in [3.1.4] is repeated for the HI-STORM FW tipover analysis. Specifically, the concrete pad behavior is characterized using the same LS-DYNA material model (i.e., MAT_PSEUDO_TENSOR or MAT_016) as for the end drop and tipover analyses of the HI-STORM 100 storage cask (the only difference between the HI-STORM FW reference ISFSI concrete pad model and the model of the HI-STORM 100 Set B ISFSI concrete pad is thickness). Moreover, the subgrade is also conservatively modeled as an elastic material as before. Note that this ISFSI pad material modeling approach was originally taken in the USNRC approved storage cask tipover and end drop LS-DYNA analyses [3.4.5] where a good correlation was obtained between the analysis results and the test results.

To assess the potential damage of the cask caused by the tipover accident, an LS-DYNA nonlinear material model with strain rate effect is used to model the responses of all HI-STORM FW cask structural members based on the true stress-strain curves of the corresponding materials. Note that the strain rate effect for the fuel basket material, i.e., Metamic HT, is not considered for

conservatism.

Figures 3.4.9 to 3.4.14 depict the two finite-element tipover analysis models developed for the bounding HI-STORM FW cask configurations with loaded MPC-37 and MPC-89, respectively.

As shown in Figure 3.4.15, the fuel basket does not experience any plastic deformation in the active fuel region; plastic deformation is limited locally in one periphery cell near the top of the basket beyond the active fuel region for both MPC-37 and MPC-89 baskets. The fuel basket is considered to be structurally safe since it can continue maintaining appropriate spacing between fuel assemblies after the tipover event. The MPC enclosure vessel experiences minor plastic deformation at the impact locations with the overpack guide tubes; the maximum local plastic strain (9.9%, see Figure 3.4.16) is well below the failure strain of the material and smaller than the plastic strain limit (i.e., at least 0.2 for stainless steel) recommended by [3.4.6] for ASME NB components. Similarly, local plastic deformation occurs in the overpack shear ring near the cask-to-pad impact location as shown in Figure 3.4.17. However, the shielding capacity of overpack will not be compromised by the tipover accident and there is no gross plastic deformation in the overpack inner shell to affect the retrievablilty of the MPC. In addition, the cask closure lid bolts are demonstrated to be structurally safe after the tipover event, only a negligibly small plastic strain is observed in the bolt near the impact location (see Figure 3.4.18). Therefore, the cask lid will not dislodge after the tipover event. Finally, Figures 3.4.19 and 3.4.20 present the deceleration time history results of the cask lid predicted by LS-DYNA. The peak rigid body decelerations, measured for the HI-STORM FW lid concrete, are shown to be 63.8 g's in the vertical direction and 18.5 g's in the horizontal direction, respectively. Note that the deceleration time histories are filtered using the LS-DYNA built-in Butterworth filter with a cut-off frequency of 350 Hz; the same filter was used for the HI-STORM 100 non-mechanistic tipover analysis [3.1.4].

The structural integrity of the HI-STORM FW lid cannot be ascertained from the LS-DYNA tipover analyses since some components of the lid, namely the lid outer shell and the lid gussets, are defined as rigid members in order to simplify the modeling effort and maintain proper connectivity. Therefore, a separate tipover analysis has been performed for the HI-STORM FW lid using ANSYS, wherein the peak rigid body decelerations determined from LS-DYNA are statically applied to the lid. The finite element model is identical to the one used in Subsection 3.4.3 to simulate a vertical lift of the HI-STORM FW lid (Figure 3.4.5), except that the eight circumferential gussets are conservatively neglected (i.e., deleted from the finite element model).

The resulting stress distribution in the HI-STORM FW lid is shown in Figure 3.4.21. Per Subsection 2.2.3, the HI-STORM FW lid should not suffer any gross loss of shielding as a result of the non-mechanistic tipover event. To satisfy this criterion, the primary membrane stresses in the lid components are compared against the material yield strength. The most heavily loaded component is the upper shim plate closest to the point of impact (Figure 3.4.21). In order to determine the primary membrane stress in the upper shim plate, the stresses are linearized along a path that follows the outside vertical edge of the upper shim plate (see Figure 3.4.21 for path definition). Figure 3.4.22 shows the linearized stress results. Since the membrane stress is less than the yield strength of the material at 300°F (Table 3.3.6), it is concluded that the lid will not suffer any gross loss of

shielding as a result of the non-mechanistic tipover event. The complete details of the lid tipover analysis are provided in [3.4.13].

Finally, to evaluate the potential for crack propagation and growth for the MPC fuel baskets under the non-mechanistic tipover event, a crack propagation analysis is carried out for the MPC-37 fuel basket using the same methodology utilized in Attachment D of [1.B.1] to evaluate the HI-STAR 180 F-37 fuel basket in support of the HI-STAR 180 SAR [3.1.10]. The crack propagation analysis for the MPC-37 is bounding for the MPC-89 fuel basket due to its smaller storage cell width, lower reference metal temperature, and lower fuel assembly weight (see Table 3.4.13).

To begin the analysis, the stress distribution in the MPC-37 fuel basket is determined by implementing the fuel basket finite element model (see Subsection 3.1.3) in ANSYS and performing a static stress analysis of the fuel basket structure for a bounding load of 65-g. The resulting stress distribution in the horizontally oriented Metamic-HT basket panels is shown in Figure 3.4.36. The maximum stress occurs at one of the basket notches, which are conservatively modeled as sharp (90 degree) corners in the finite element model. This peak stress is used as input to the following crack propagation analysis.

Per [1.B.1] the critical stress intensity factor of Metamic-HT panels is estimated to be

$$K_{IC} = 30ksi\sqrt{in}$$

based on Charpy V-notch absorbed energy (CVE) correlations for steels. The estimated value is consistent with the range for aluminum alloys, which is 20 to 50 $MPa\sqrt{m}$ or 18.2 to 45 $ksi\sqrt{in}$ per Table 3 of [3.4.19]. Next the minimum crack size, amin, for crack propagation to occur is calculated below using the formula for a through-thickness edge crack given in [3.1.5]. Although the formula is derived for a straight-edge specimen, the use of the peak stress, σ max, at a notch in the fuel basket panel (instead of the average stress in the panel as required by the formula) essentially compensates for the geometric difference between the basket panel and the specimen. Moreover, the maximum size of a pre-existing crack (1/16") in the fuel basket panel is less than 1/9th of the basket panel thickness (0.59"). Thus, the assumption of a through-thickness edge crack is very conservative. The result is

$$a_{\min} = \frac{\left(\frac{K_{IC}}{1.12\sigma_{\max}}\right)^2}{\pi} = \frac{\left[\frac{30ksi\sqrt{in}}{1.12(17.98ksi)}\right]^2}{\pi} = 0.706in$$

And the safety factor against crack propagation (based on a 1/16" minimum detectable flaw size) is

$$SF = \frac{a_{\min}}{a_{\det}} = \frac{0.706in}{0.0625in} = 11.3$$

The calculated minimum crack size is more than 11 times greater than the maximum possible pre-existing crack size in the fuel basket (based on 100% surface inspection of each panel). The large safety factor ensures that crack propagation in the HI-STORM FW fuel baskets will not occur due to the non-mechanistic tipover event.

3.4.4.1.5 Load Case 5: Design Internal Pressure

The MPC Enclosure Vessel, which is designed to meet the stress intensity limits of ASME Subsection NB [3.4.4], is analyzed for design internal pressure (Table 2.2.1) using the ANSYS finite element code [3.4.1]. Except for the applied loads and the boundary conditions, the finite element model of the MPC Enclosure Vessel used for this load case is identical to the model described in Subsections 3.1.3.2 and 3.4.3.2 for the MPC lifting analysis.

The only load applied to the finite element model for this load case is the MPC design internal pressure for normal conditions (Table 2.2.1). All internal surfaces of the MPC storage cavity are subjected to the design pressure. The center node on the top surface of the MPC upper lid is fixed against translation in all directions. Symmetric boundary conditions are applied to the two vertical symmetry planes. This set of boundary conditions allows the MPC Enclosure Vessel to deform freely under the applied pressure load. Figure 3.4.31 graphically depicts the applied pressure load and the boundary conditions for Load Case 5.

The stress intensity distribution in the MPC Enclosure Vessel under design internal pressure is shown in Figure 3.4.23. Figures 3.4.32 and 3.4.33 plot the thru-thickness variation of the stress intensity at the baseplate center and at the baseplate-to-shell juncture, respectively. The maximum primary and secondary stress intensities in the MPC Enclosure Vessel are compared with the applicable stress intensity limits from Subsection NB of the ASME Code. The allowable stress intensities are taken at 450°F for the MPC shell and MPC lids, 300°F for the baseplate, and 250°F at the baseplate-to-shell juncture. The maximum calculated stress intensities in the MPC Enclosure Vessel, and their corresponding allowable limits, are summarized in Table 3.4.7 for Load Case 5.

Since the stress intensity distribution in the MPC Enclosure Vessel is a linear function of the internal pressure, and the stress intensity limits for normal and off-normal conditions are the same (Table 3.1.7), the minimum calculated safety factor from Table 3.4.7 is used to establish the internal pressure limit for off-normal conditions (Table 2.2.1).

3.4.4.1.6 Load Case 6: Maximum Internal Pressure Under Accident Conditions

The maximum pressure in the MPC Enclosure Vessel under accident conditions is specified in Table 2.2.1. The stress analysis under this pressure condition uses the same model as the one described in the preceding subsection. The only change is the magnitude of the applied pressure. Figure 3.4.34 graphically depicts the applied pressure load and the boundary conditions for Load Case 6.

The stress intensity distribution in the MPC Enclosure Vessel under accident internal pressure is shown in Figure 3.4.24. The maximum primary stress intensities in the MPC Enclosure Vessel are

compared with the applicable stress intensity limits from Subsection NB of the ASME Code [3.4.4]. The allowable stress intensities are taken at 450°F for the MPC shell and MPC lids, 300°F for the baseplate, and 250°F at the baseplate-to-shell juncture. These temperatures bound the calculated temperatures under normal operating conditions for the respective MPC components based on the thermal evaluations in Chapter 4. The allowable stress intensities are determined based on normal operating temperatures since the MPC accident internal pressure is dictated by the 100% fuel rod rupture accident, which does not cause any significant rise in MPC temperatures. In fact, the temperatures inside the MPC tend to decrease as a result of the 100% fuel rod rupture accident due to the increase in the density and internal pressure of the circulating gas. The maximum calculated stress intensities in the MPC Enclosure Vessel, and their corresponding allowable limits, are summarized in Table 3.4.8 for Load Case 6.

3.4.4.1.7 Load Case 7: Accident External Pressure

The only affected component for this load case is the MPC Enclosure Vessel. The accident external pressure (Table 2.2.1) is selected sufficiently high to envelop hydraulic-pressure in the case of flood or explosion-induced pressure at all ISFSI Sites.

The main effect of an external pressure on the MPC is to cause compressive stress in the MPC shell. Therefore, the potential of buckling must be investigated. The methodology used for this investigation is from ASME Code Case N-284-2 (Metal Containment Shell Buckling Design Methods, Section III, Division 1, Class MC (1/07)). This Code Case has been previously used by Holtec in [3.1.4] and accepted by the NRC as a valid method for evaluation of stability in vessels.

The detailed evaluation of the MPC shell under accident external pressure is provided in Appendix 3.C. It is concluded that positive safety margins exist so that elastic or plastic instability of the maximum height MPC shell does not occur under the applied pressure.

3.4.4.1.8 Load Case 8: Non-Mechanistic Heat-Up of the HI-TRAC VW Water Jacket

Even though the analyses presented in Chapter 4 indicate that the temperature of water in the water jacket shall not reach boiling and the rupture disks will not open, it is (non-mechanistically) assumed that the hydraulic pressure in the water jacket reaches the relief devices' set point. The object of this analysis is to demonstrate that the stresses in the water jacket and its welds shall be below the limits set down in an appropriate reference ASME Boiler and Pressure Vessel Code (Section II Class 3) for the Level D service condition. The accident pressure inside the water jacket is given in Table 2.2.1.

The HI-TRAC VW water jacket is analyzed using classical strength-of-materials. Specifically, the unsupported span of the water jacket shell between radial ribs is treated as a curved beam, with clamped ends, under a uniformly distributed radial pressure. The force and moment reactions at the ends of the curved beam for this type of loading are calculated using the formula for Case 5j of Table 18 in [3.4.16]. The primary membrane plus bending stress is then calculated using the formula for Case 1 of Table 16 in [3.4.16]. Figure 3.4.35 depicts the curved beam model that is used to analyze the water jacket shell and defines the key input variables. The input values that are used in

the calculations are provided in Table 3.4.12.

The bottom flange, which serves as the base of the water jacket, is conservatively analyzed as an annular plate clamped at the water jacket inside diameter and simply supported at the water jacket outside diameter. The maximum bending stress in the bottom flange is calculated using the following formula from [3.4.18, Art. 23]:

$$\sigma_{max} = k\frac{q \cdot a^2}{h^2}$$

where q is the internal pressure inside the water jacket (= 73.65 psi), a is the outside radius of the water jacket (= 47.5 in), and h is the thickness of the bottom flange (= 2.0 in). The analyzed pressure accounts for the accident internal pressure inside the water jacket (Table 2.2.1) plus the hydrostatic pressure at the base of the water jacket. The value of k is dependent on the diameter ratio of the annular plate and the boundary conditions. Per Table 5 of [3.4.18], k is equal to 0.122 for a bounding diameter ratio of 1.25 and simply supported-clamped boundary conditions (Case 4). Therefore, the maximum bending stress in the bottom flange is:

$$\sigma_{max} = 5{,}068 \text{ psi}$$

Per Table 3.1.6, the allowable primary membrane plus bending stress intensity for SA-516 Gr. 70 material (at 400°F) is 58,500 psi, which means the factor of safety is greater than 10.

The maximum stresses in the various water jacket components, including the connecting welds, are summarized in Table 3.4.9.

3.4.4.1.9 Load Case 9: Handling of Components

The stress analyses of the MPC, the HI-STORM FW overpack, and the HI-TRAC VW transfer cask under normal handling conditions are presented in Subsection 3.4.3.

3.4.4.1.10 Load Case 10: Snow Load

In accordance with Table 3.1.1, the HI-STORM FW lid is analyzed using ANSYS to demonstrate that the design basis snow load (Table 2.2.8) does not cause stress levels in the overpack lid to exceed ASME Subsection NF stress limits for Level A. The finite element model is identical to the one used in Subsection 3.4.3 to simulate a vertical lift of the HI-STORM FW lid (see Figure 3.4.5). For conservatism, a pressure load of 10 psig is used in the finite element analysis. The stress distribution in the lid under the bounding snow load is shown in Figure 3.4.25. The maximum stress results are summarized in Table 3.4.10. For conservatism, the maximum calculated stress at any point on the lid, including secondary stress contributions, is compared against the primary membrane and primary bending stress limits per ASME Subsection NF.

3.4.4.1.11 Load Case 11: MPC Reflood Event

During a MPC reflood event, water is introduced to the MPC cavity through the lid drain line to cooldown the MPC internals and support fuel unloading. This quenching operation induces thermal stresses and strains in the fuel rod cladding, which are maximum at the boundary interface between the rising water and the dry (gaseous) cavity. The following analysis demonstrates that the maximum total strain in the fuel cladding due to the reflood event is well below the failure strain limit of the material. Thus, the fuel rod cladding will not be breached due to the MPC reflood event.

The analysis is carried out using the finite element code ANSYS [3.4.1]. The model, which is shown in Figure 3.4.37, is constructed using 4-node plastic large strain elements (SHELL43) based on the cladding dimensions of the PWR reference fuel type. The overall length of the model is equal to 30 times the outside diameter of the fuel cladding. As seen in Figure 3.4.37, the mesh size is reduced at the boundary between the wetted fuel rod and the dry fuel rod, where the highest stresses and strains occur. To account for the gas pressure inside the fuel rod, the top end of the fuel rod is fixed in the vertical direction, and an equivalent axial force is applied at the bottom end. A radial pressure is also applied to the inside surface of the fuel cladding (see Figure 3.4.38). The fuel cladding material is modeled as a bi-linear isotropic hardening material with temperature dependent properties. The key input data used to develop the finite element model are summarized in Table 3.4.14.

The MPC reflood pressure, which is restricted to below the normal condition pressure limit, is too low to have and adverse effect on the fuel cladding, the reflood water pressure acts to produce compressive hoop stresses which help reduce the tensile hoop stress (albeit by a small amount) from the internal gas pressure in the rods. Therefore, the MPC flooding pressure has no harmful consequence to the fuel cladding and is neglected in the analysis.

At t = 0 sec, the uniform temperature throughout the entire fuel rod is set at 752°F (400°C), which equals the fuel cladding temperature limit under normal operating conditions. At t = 0.1 sec, the temperature assigned to the lower half of the fuel rod model is suddenly reduced to 80°F to simulate the water quenching (see Figure 3.4.39). The resulting stress and strain distributions in the fuel rod are shown in Figures 3.4.40 and 3.4.41, respectively. The maximum stress and strain values are summarized in Table 3.4.15. The maximum total strain in the fuel rod is well below the failure strain limit of 1.7% for the cladding material per [3.4.20]. In fact, the maximum stress and strain in the fuel rod remain in the elastic range.

The analysis described above makes a number of assumptions that significantly overstate the computed thru-wall strain in the fuel cladding. The major assumptions are:

1. Even though the peak cladding temperature occurs at a localized location, the fuel rod is modeled as a pressurized tube with closed ends at a uniform temperature that is greater than the maximum peak cladding temperature value reported in Chapter 4 when the MPC is in the HI-TRAC under the Design Basis heat load condition.
2. The rapid thermal straining of the pressurized tube (fuel rod) due to the quenching effect of water is simulated as a step transient wherein the temperature of the quenched portion of the

tube is assumed to drop down to the injected water temperature (assumed to be 80°F) causing a step change in the cladding wall temperature in the longitudinal direction at its interface with the "dry" portion of the tube. This assumption is extremely conservative because in actuality the immersed portion of the fuel rod is blanketed by vapor which acts to retard the severity of the thermal transient.

3. Even though, as the rod is gradually immersed in water, the axial heat conduction will tend to cool the un-immersed portion of the tube thus reducing the ΔT at the quenched/dry interface, no credit for axial conduction is taken.
4. The cooling of the fuel rod by gradual immersion in the water has the beneficial effect of reducing the internal pressure (per the ideal gas law) and thus the magnitude of pressure induced stress in the fuel cladding. As the peak cladding temperature in the MPC is reached in the upper half of the fuel rods (see Chapter 4), a substantial amount of rod is cooled by water (as its level gradually rises inside the MPC) before the vulnerable zone (where the peak cladding temperature exists) is subjected to the thermal transient from quenching. No credit for this amelioration of the pressure stresses due to the gradual cooling of the rod is taken in the analysis.

In summary, even though the analysis presented above is highly conservative, the maximum stress and strain in the fuel rod remain elastic. Moreover, the maximum strain is less than the failure strain limit by a factor of 6. Thus, the MPC reflood event will not cause a breach of the fuel rod cladding.

3.4.5 Cold

A discussion of the resistance to failure due to brittle fracture is provided in Subsection 3.1.2.

The value of the ambient temperature has two principal effects on the HI-STORM FW system, namely:

i. The steady-state temperature of all material points in the cask system will go up or down by the amount of change in the ambient temperature.

ii. As the ambient temperature drops, the absolute temperature of the contained helium will drop accordingly, producing a proportional reduction in the internal pressure in accordance with the Ideal Gas Law.

In other words, the temperature gradients in the system under steady-state conditions will remain the same regardless of the value of the ambient temperature. The internal pressure, on the other hand, will decline with the lowering of the ambient temperature. Since the stresses under normal storage condition arise principally from pressure and thermal gradients, it follows that the stress field in the MPC under –40 degree F ambient would be smaller than the "heat" condition of storage, treated in the preceding subsection. Additionally, the allowable stress limits tend to increase as the component temperatures decrease.

Therefore, the stress margins computed in Subsection 3.4.4 can be conservatively assumed to apply to the "cold" condition as well.

Finally, it can be readily shown that the HI-STORM FW system is engineered to withstand "cold" temperatures (-40 degrees F) without impairment of its storage function.

Unlike the MPC, the HI-STORM FW storage overpack is an open structure; it contains no pressure. Its stress field is unaffected by the ambient temperature, unless low temperatures produce brittle fracture due to the small stresses which develop from self-weight of the structure and from the minute difference in the thermal expansion coefficients in the constituent parts of the equipment (steel and concrete). To prevent brittle fracture, all steel material in HI-STORM FW is qualified by impact testing pursuant to the ASME Code (Table 3.1.9).

The structural material used in the MPC (Alloy X) is recognized to be completely immune from brittle fracture in the ASME Codes.

As no liquids are included in the HI-STORM FW storage overpack design, loads due to expansion of freezing liquids are not considered. The HI-TRAC VW transfer cask utilizes demineralized water in the water jacket. However, the specified lowest service temperature for the HI-TRAC VW is 0 degrees F and a 25% ethylene glycol solution is required for the temperatures from 0 degrees F to 32 degrees F. Therefore, loads due to expansion of freezing liquids are not considered.

There is one condition, however, that does require examination to ensure ready retrievability of the fuel. Under a postulated loading of an MPC from a HI-TRAC VW transfer cask into a cold HI-STORM FW storage overpack, it must be demonstrated that sufficient clearances are available to preclude interference when the "hot" MPC is inserted into a "cold" storage overpack. To this end, a bounding analysis for free thermal expansions has been performed in Subsection 4.4.6, wherein the MPC shell is postulated at its maximum design basis temperature and the thermal expansion of the overpack is ignored. The results from the evaluation of free thermal expansion are summarized in Table 4.4.6. The final radial clearance is sufficient to preclude jamming of the MPC upon insertion into a cold HI-STORM FW storage overpack.

3.4.6 Miscellaneous Evaluations

3.4.6.1 Structural Integrity of Damaged Fuel Containers (DFCs)

The Damaged Fuel Container (DFC) is used to store fuel that is physically impaired such that it cannot be handled by normal means. The DFC, as shown in the licensing drawings, is equipped with a handle welded to a square cellular box with a perforated baseplate structurally capable of supporting the weight of the fuel while permitting water (but not particulates) to pass through. All load bearing members of the DFC are designed to meet Level A service limit when holding a spent fuel assembly.

Because the DFC is always handled under water, there are no radiation release-related issues

associated with it.

3.4.7 Service Life of HI-STORM FW and HI-TRAC VW

The term of the 10CFR72, Subpart L C of C, granted by the NRC is 20 years; therefore, the License Life (see Glossary) of all components is 20 years. Nonetheless, the HI-STORM FW storage overpack and the HI-TRAC VW transfer cask are engineered for 60 years of design life, while satisfying the conservative design requirements defined in Chapter 2, including the regulatory requirements of 10CFR72. In addition, the storage overpack and HI-TRAC VW are designed, fabricated, and inspected under the comprehensive Quality Assurance Program approved by the USNRC and in accordance with the applicable requirements of the ACI and ASME Codes. This assures high design margins, high quality fabrication, and verification of compliance through rigorous inspection and testing, as described in Chapter 10 and the licensing drawings in Section 1.5. Technical Specifications defined in Chapter 13 assure that the integrity of the cask and the contained MPC are maintained throughout the components' design life. The design life of a component, as defined in the Glossary, is the minimum duration for which the equipment or system is engineered to perform its intended function if operated and maintained in accordance with the FSAR. The design life is essentially the lower bound value of the service life, which is the expected functioning life of the component or system. Therefore, component longevity should be: licensed life < design life < service life. (The licensed life, enunciated by the USNRC, is the most pessimistic estimate of a component's life span). For purposes of further discussion, we principally focus on the service life of the HI-STORM FW system components that, as stated earlier, is the reasonable expectation of equipment's functioning life span.

The service life of the storage overpack and HI-TRAC VW transfer cask is further discussed in the following.

3.4.7.1 Storage Overpack

The principal design considerations that bear on the adequacy of the storage overpack for the service life are addressed as follows:

Exposure to Environmental Effects

All exposed surfaces of the HI-STORM FW overpack are made from ferritic steels that are readily painted. Concrete, which serves strictly as a shielding material, is completely encased in steel. Therefore, the potential of environmental vagaries such as spalling of concrete, are ruled out for HI-STORM FW. Under normal storage conditions, the bulk temperature of the HI-STORM FW storage overpack will, because of its large thermal inertia, change very gradually with time. Therefore, material degradation from rapid thermal ramping conditions is not credible for the HI-STORM FW storage overpack. Similarly, corrosion of structural steel embedded in the concrete structures due to salinity in the environment at coastal sites is not a concern for HI-STORM FW because HI-STORM FW does not rely on rebars (indeed, it contains no rebars). As discussed in Appendix 1.D of HI-STORM 100 FSAR, the aggregates, cement and water used in the storage cask concrete are carefully

controlled to provide high durability and resistance to temperature effects. The configuration of the storage overpack assures resistance to freeze-thaw degradation. In addition, the storage overpack is specifically designed for a full range of enveloping design basis natural phenomena that could occur over the 60-year design life of the storage overpack as defined in Subsection 2.2.3 and evaluated in Chapter 12. Chapter 8 provides further discussions on chemical and galvanic reactions, material compatibility and operating environments.

Material Degradation

As discussed in Chapter 8, the relatively low neutron flux to which the storage overpack is subjected cannot produce measurable degradation of the cask's material properties and impair its intended safety function. Exposed carbon steel components are coated to prevent corrosion. The controlled environment of the ISFSI storage pad mitigates damage due to direct exposure to corrosive chemicals that may be present in other industrial applications.

Maintenance and Inspection Provisions

The requirements for periodic inspection and maintenance of the storage overpack throughout the 60-year design life are defined in Chapter 10. These requirements include provisions for routine inspection of the storage overpack exterior and periodic visual verification that the ventilation flow paths of the storage overpack are free and clear of debris. ISFSIs located in areas subject to atmospheric conditions that may degrade the storage cask or canister should be evaluated by the licensee on a site-specific basis to determine the frequency for such inspections to assure long-term performance. In addition, the HI-STORM FW system is designed for easy retrieval of the MPC from the storage overpack should it become necessary to perform more detailed inspections and repairs on the storage overpack.

The above findings are consistent with those of the NRC's Waste Confidence Decision Review [3.4.10], which concluded that dry storage systems designed, fabricated, inspected, and operated in accordance with such requirements are adequate for a 100-year service life while satisfying the requirements of 10CFR72.

3.4.7.2 Transfer Cask

The principal design considerations that bear on the adequacy of the HI-TRAC VW transfer cask for the service life are addressed as follows:

Exposure to Environmental Effects

All transfer cask materials that come in contact with the spent fuel pool are coated to facilitate decontamination. The HI-TRAC VW is designed for repeated normal condition handling operations with high factor of safety to assure structural integrity. The resulting cyclic loading produces stresses that are well below the endurance limit of the cask's materials, and therefore, will not lead to a fatigue failure in the transfer cask. All other off-normal or postulated accident conditions are

infrequent or one-time occurrences that do not contribute significantly to fatigue. In addition, the transfer cask utilizes materials that are not susceptible to brittle fracture during the lowest temperature permitted for loading, as discussed in Subsection 8.4.3.

Chapter 8 provides further discussions on chemical and galvanic reactions, material compatibility and operating environments.

Material Degradation

As discussed in Chapter 8, all transfer cask materials that are susceptible to corrosion are coated. The controlled environment in which the HI-TRAC VW is used mitigates damage due to direct exposure to corrosive chemicals that may be present in other industrial applications. The infrequent use and relatively low neutron flux to which the HI-TRAC VW materials are subjected do not result in radiation embrittlement or degradation of the HI-TRAC's shielding materials that could impair the HI-TRAC's intended safety function. The HI-TRAC VW transfer cask materials are selected for durability and wear resistance for their deployment.

Maintenance and Inspection Provisions

The requirements for periodic inspection and maintenance of the HI-TRAC VW transfer cask throughout the 60-year design life are defined in Chapter 10. These requirements include provisions for routine inspection of the HI-TRAC VW transfer cask for damage prior to each use, including an annual inspection of the lifting attachments. Precautions are taken during lid handling operations to protect the sealing surfaces of the bottom lid. The leak tightness of the liquid neutron shield is verified periodically. The water jacket pressure rupture discs and other fittings used can be easily removed.

3.4.8 MPC Service Life

The term of the 10CFR72, Subpart L C of C, granted by the NRC (i.e., licensed life) is 20 years. Nonetheless, the HI-STORM FW MPCs are designed for 60 years of design life, while satisfying the conservative design requirements defined in Chapter 2, including the regulatory requirements of 10CFR72. Additional assurance of the integrity of the MPC and the contained SNF assemblies throughout the 60-year life of the MPC is provided through the following:

- Design, fabrication, and inspection invoke the pertinent requirements of the ASME Code, as applicable, assures high inherent design margins in operating modes.
- Fabrication and inspection performed in accordance with the comprehensive Quality Assurance program assures competent compliance with the fabrication requirements.
- Use of materials with known characteristics, verified through rigorous inspection and testing, as described in Chapter 10, assures component compliance with design requirements.

- Use of welding procedures in full compliance with Section III of the ASME Code ensures high-quality weld joints.

Technical Specifications, as defined in Chapter 13, have been developed and imposed on the MPC that assure that the integrity of the MPC and the contained SNF assemblies are maintained throughout the 60-year design life of the MPC.

The principal design considerations bearing on the adequacy of the MPC for the service life are summarized below.

Corrosion

All MPC materials are fabricated from corrosion-resistant austenitic stainless steel and passivated aluminum. The corrosion-resistant characteristics of such materials for dry SNF storage canister applications, as well as the protection offered by these materials against other material degradation effects, are well established in the nuclear industry. The moisture in the MPC is removed to eliminate all oxidizing liquids and gases and the MPC cavity is backfilled with dry inert helium at the time of closure to maintain an atmosphere in the MPC that provides corrosion protection for the SNF cladding throughout the dry storage period. The preservation of this non-corrosive atmosphere is assured by the inherent sealworthiness of the MPC Confinement Boundary integrity (there are no gasketed joints in the MPC).

Structural Fatigue

The passive non-cyclic nature of dry storage conditions does not subject the MPC to conditions that might lead to structural fatigue failure. Ambient temperature and insolation cycling during normal dry storage conditions and the resulting fluctuations in MPC thermal gradients and internal pressure is the only mechanism for fatigue. These low-stress, high-cycle conditions cannot lead to a fatigue failure of the MPC that is made from stainless alloy stock (endurance limit well in excess of 20,000 psi). All other off-normal or postulated accident conditions are infrequent or one-time occurrences, which cannot produce fatigue failures. Finally, the MPC uses materials that are not susceptible to brittle fracture.

Maintenance of Helium Atmosphere

The inert helium atmosphere in the MPC provides a non-oxidizing environment for the SNF cladding to assure its integrity during long-term storage. The preservation of the helium atmosphere in the MPC is assured by the robust design of the MPC Confinement Boundary described in Section 7.1. Maintaining an inert environment in the MPC mitigates conditions that might otherwise lead to SNF cladding failures. The required mass quantity of helium backfilled into the canister at the time of closure and the associated fabrication and closure requirements for the canister are specifically set down to assure that an inert helium atmosphere is maintained in the canister throughout the 60-year design life.

Allowable Fuel Cladding Temperatures

The helium atmosphere in the MPC promotes heat removal and thus reduces SNF cladding temperatures during dry storage. In addition, the SNF decay heat will substantially attenuate over a 60-year dry storage period. Maintaining the fuel cladding temperatures below allowable levels during long-term dry storage mitigates the damage mechanism that might otherwise lead to SNF cladding failures. The allowable long-term SNF cladding temperatures used for thermal acceptance of the MPC design are conservatively determined, as discussed in Section 4.3.

Neutron Absorber Boron Depletion

The effectiveness of the fixed borated neutron absorbing material used in the MPC fuel basket design requires that sufficient concentrations of boron be present to assure criticality safety during worst case design basis conditions over the 60-year design life of the MPC. Information on the characteristics of the borated neutron absorbing material used in the MPC fuel basket is provided in Subsection 1.2.1 and Chapter 8. The relatively low neutron flux, to which this borated material is subjected and will continue to decay over time, does not result in significant depletion of the material's available boron to perform its intended safety function. In addition, the boron content of the material used in the criticality safety analysis is conservatively based on the minimum specified boron areal density (rather than the nominal), which is further reduced by 25% for analysis purposes, as described in Section 6.1. Analysis discussed in Section 6.3 demonstrates that the boron depletion in the neutron absorber material is negligible over a 60-year duration. Thus, sufficient levels of boron are present in the fuel basket neutron absorbing material to maintain criticality safety functions over the 60-year design life of the MPC.

The above findings are consistent with those of the NRC's Waste Confidence Decision Review, which concluded that dry storage systems designed, fabricated, inspected, and operated in the manner of the requirements set down in this document are adequate for a 100-year service life, while satisfying the requirements of 10CFR72.

3.4.9 Design and Service Life

The discussion in the preceding sections seeks to provide the logical underpinnings for setting the design life of the storage overpacks, the HI-TRAC VW transfer cask, and the MPCs as sixty years. Design life, as stated earlier, is a lower bound value for the expected performance life of a component (service life). If operated and maintained in accordance with this Safety Analysis Report, Holtec International expects the service life of HI-STORM FW casks to substantially exceed their design life values.

Table 3.4.1

STRESS INTENSITY RESULTS FOR MPC ENCLOSURE VESSEL – NORMAL HANDLING

Item	Calculated Value (ksi)	Allowable Limit (ksi)	Safety Factor
Lid – Primary Membrane Stress Intensity	6.94	18.05	2.60
Lid – Local Membrane Plus Primary Bending Stress Intensity	6.94	27.1	3.90
Baseplate – Primary Membrane Stress Intensity	8.32	20.0	2.40
Baseplate – Local Membrane Plus Primary Bending Stress Intensity	21.8	30.0	1.38
Shell – Primary Membrane Stress Intensity	13.14	18.05	1.37
Shell – Local Membrane Plus Primary Bending Plus Secondary Stress Intensity	56.50	60.0	1.06

Table 3.4.2 STRESS RESULTS FOR HI-TRAC VW – NORMAL HANDLING			
Item	Calculated Value (ksi)	Allowable Limit (ksi)	Safety Factor
Top Flange-to-Inner/Outer Shell Weld – Primary Shear Stress	5.79	17.4	3.01
Inner/Outer Shell – Primary Membrane Stress	1.72	19.6	11.4
Bottom Lid Bolts – Tensile Stress	9.14	41.2	4.51
Bottom Lid – Primary Bending Stress	3.80	30.0	7.90

Table 3.4.3

STRESS RESULTS FOR HI-STORM FW – NORMAL HANDLING

Item	Calculated Value (ksi)	Allowable Limit (ksi)	Safety Factor
Inner/Outer Shell – Primary Membrane Stress	1.92	20.0	10.4
Inner/Outer Shell – Primary Membrane Plus Bending Stress	3.42	30.0	8.77
Baseplate – Primary Membrane Stress	1.97	20.0	10.2
Baseplate – Primary Membrane Plus Bending Stress	3.42	30.0	8.77
Lifting Rib – Primary Membrane Stress	4.79	20.0	4.18
Lifting Rib – Primary Membrane Plus Bending Stress	6.22	30.0	4.82
Shell-to-Baseplate Weld – Primary Shear Stress	4.56	21.0	4.60

Table 3.4.4

STRESS RESULTS FOR HI-STORM FW LID – NORMAL HANDLING

Item	Calculated Value (ksi)	Allowable Limit (ksi)	Safety Factor
Maximum Primary Membrane Stress	1.57	16.6	10.6
Maximum Primary Membrane Plus Bending Stress	1.57	24.9	15.9

Table 3.4.5

CASK ROTATIONS DUE TO LARGE MISSILE IMPACT

Event	Calculated Value (deg)	Allowable Limit (deg)	Safety Factor
Missile Impact plus Tornado Wind on HI-STORM FW	3.37	30.3	8.99
Missile Impact plus Pressure Drop on HI-STORM FW	3.91	30.3	7.75
Missile Impact plus Tornado Wind on HI-TRAC VW	14.40	23.6	1.64
Missile Impact plus Pressure Drop on HI-TRAC VW	12.32	23.6	1.92

Table 3.4.6

MISSILE PENETRATION RESULTS –
SMALL AND INTERMEDIATE MISSILE

Missile Type – Impact Location	Calculated Value (in)	Allowable Limit (in)	Safety Factor
Small Missile – All Impact Locations	< 0.4 in	> 0.5 in (MPC shell thickness)[†]	> 1.25
Intermediate Missile – Side Strike on HI-STORM FW Outer Shell (away from Inlet)	8.39	29.00	3.46
Intermediate Missile – Side Strike on HI-STORM FW Outer Shell (at Inlet)	11.69	24.00	2.05
Intermediate Missile – End Strike on HI-STORM FW Lid	10.46	19.25	1.84
Intermediate Missile – Side Strike on HI-TRAC VW Outer Shell	0.50	1.50	3.00
Intermediate Missile – End Strike on MPC Closure Lid	0.23	9.00	39.13

[†] In reality, a maximum velocity impact between the small projectile missile and the MPC shell is not credible due to the geometry of the HI-STORM FW inlet and outlet vents (i.e., no direct line of sight).

Table 3.4.7

STRESS INTENSITY RESULTS FOR MPC ENCLOSURE VESSEL – DESIGN INTERNAL PRESSURE

Item	Calculated Value (ksi)	Allowable Limit (ksi)	Safety Factor
Lid – Primary Membrane Stress Intensity	5.98	18.05	3.02
Lid – Local Membrane Plus Primary Bending Stress Intensity	5.98	27.1	4.53
Baseplate – Primary Membrane Stress Intensity	7.12	20.0	2.81
Baseplate – Local Membrane Plus Primary Bending Stress Intensity	18.65	30.0	1.61
Shell – Primary Membrane Stress Intensity	11.50	18.05	1.57
Shell – Local Membrane Plus Primary Bending Plus Secondary Stress Intensity	50.10	60.0	1.20

Table 3.4.8

STRESS INTENSITY RESULTS FOR MPC ENCLOSURE VESSEL – ACCIDENT INTERNAL PRESSURE

Item	Calculated Value (ksi)	Allowable Limit (ksi)	Safety Factor
Lid – Primary Membrane Stress Intensity	11.97	43.3	3.62
Lid – Local Membrane Plus Primary Bending Stress Intensity	11.97	64.95	5.43
Baseplate – Primary Membrane Stress Intensity	14.25	46.3	3.25
Baseplate – Local Membrane Plus Primary Bending Stress Intensity	37.29	69.45	1.86
Shell – Primary Membrane Stress Intensity	22.99	43.3	1.88

Table 3.4.9

STRESS RESULTS FOR HI-TRAC VW WATER JACKET – ACCIDENT INTERNAL PRESSURE

Item	Calculated Value (ksi)	Allowable Limit (ksi)	Safety Factor
Bottom Flange – Primary Membrane Plus Bending Stress	5.07	58.5	11.54
Water Jacket Shell – Primary Membrane Plus Bending Stress	7.97	58.5	7.34
Water Jacket Rib – Primary Membrane Stress	4.72	39.0	8.26
Water Jacket Shell-to-Bottom Flange Weld – Primary Shear Stress	3.70	29.4	7.94

Table 3.4.10 STRESS RESULTS FOR HI-STORM FW LID – SNOW LOAD			
Item	Calculated Value (ksi)	Allowable Limit (ksi)	Safety Factor
Maximum Primary Membrane Stress	1.81	16.6	9.16
Maximum Primary Membrane Plus Bending Stress	1.81	24.9	13.7

Table 3.4.11

INPUT DATA USED FOR CALCULATING ANGULAR VELOCITY OF OVERPACK DURING NON-MECHANISTIC TIPOVER (LOAD CASE 4)

Item	Value
Maximum weight of loaded HI-STORM FW (W)	426,300 lbf[†]
Mid-height of maximum length HI-STORM FW (h)	119.75 in
Outer diameter of HI-STORM FW (d)	140 in
Distance between cask pivot point and cask center (r)	138.709 in
Mass moment of inertia of loaded HI-STORM FW about cask pivot point (I_A)	1.076×10^{10} lb-in^2

[†] Bounds value in Table 3.2.8.

Table 3.4.12

INPUT VALUES USED FOR CALCULATING STRESS IN WATER JACKET SHELL (LOAD CASE 8)

Item	Value
Mean radius of water jacket shell (R)	47.25 in
Thickness of water jacket shell (d)	0.5 in
Width of beam strip (b)	1 in
Extreme fiber distance of beam cross-section (c)	0.25 in
Unsupported span of water jacket shell (θ)	45 deg
Distributed load on water jacket shell (w)	-75 lbf/in[†]
Span of distributed load on water jacket shell (ϕ)	45 deg

Note: Variables are defined in Figure 3.4.35.

[†] Bounds accident internal pressure in Table 2.2.1 for HI-TRAC water jacket.

Table 3.4.13

PARAMETERS SIGNIFICANT TO CRACK PROPAGATION OF METAMIC-HT FUEL BASKETS

	HI-STAR 180 F-37 (Attachment D of [1.B.1])	HI-STORM FW MPC-37	HI-STORM FW MPC-89
Storage cell width, w (in)	8.11	8.94	6.01
Panel thickness, t (in)	0.59	0.59	0.40
Reference metal temperature (°C)	275	365	325
Design basis g-load under lateral loading event*, acc (g)	95	59.14	63.03
Fuel dead load per unit length, f (lbf/in)	8.04	9.79	4.25
Panel stress**, σ(ksi)	13.35	11.15	7.55

* For HI-STORM FW MPCs, the limiting lateral loading is from the non-mechanistic tip-over scenario.

** To facilitate comparison, panel stress is computed according to the following formula (parameters are defined in first column of table):

$$\sigma = \frac{3 \cdot acc \cdot f \cdot w}{4 \cdot t^2}$$

which assumes that the storage cell wall acts as a simply supported beam strip under a uniformly distributed load equal to the amplified fuel weight.

Table 3.4.14

KEY INPUT DATA FOR FUEL ROD INTEGRITY ANALYSIS DURING MPC REFLOOD EVENT (LOAD CASE 11)

Item	Input Value	Source
Cladding Thickness (for reference PWR fuel), in	0.022	SAR Tables 1.0.4 and 2.1.2
Cladding OD (for reference PWR fuel), in	0.377	SAR Tables 1.0.4 and 2.1.2
Fuel Rod Pressure, psi	2,000	Ref. [3.4.24] (upper bound value)
Yield Strength of Zircaloy, psi	100,000 (at 80°F) 50,500 (at 750°F)	Ref. [3.4.21]
Tensile Strength of Zircaloy, psi	112,100 (at 80°F) 68,200 (at 750°F)	Ref. [3.4.21]
Elastic Modulus of Zircaloy, $\times 10^6$ psi	13.42 (at 80°F) 10.4 (at 750°F)	Ref. [3.4.21]
Coefficient of Thermal Expansion of Zircaloy, $\times 10^{-6}$ in/in/°F	3.3 (at 80°F) 4.5 (at 750°F)	Ref. [3.4.22]
Poisson's Ratio of Zircaloy	0.4	Appendix C of Ref. [3.4.23]

Table 3.4.15 MAXIMUM RESULTS FOR FUEL ROD INTEGRITY ANALYSIS DURING MPC REFLOOD EVENT (LOAD CASE 11)	
Result	Value
Maximum Stress in Fuel Rod Cladding	29,995 psi
Maximum Strain in Fuel Rod Cladding	2.66×10^{-3}

Table 3.4.16

CASK SLIDING DISPLACEMENTS DUE LARGE MISSILE IMPACT (LOAD CASE 3)

Cask	Calculated Sliding Displacement (ft)	Allowable Sliding Displacement (ft)	Safety Factor
HI-STORM FW	0.352	3.33 (cask to cask) 6.2 (cask to edge of ISFSI pad)	9.46 17.6
HI-TRAC VW	1.07	None Established	-

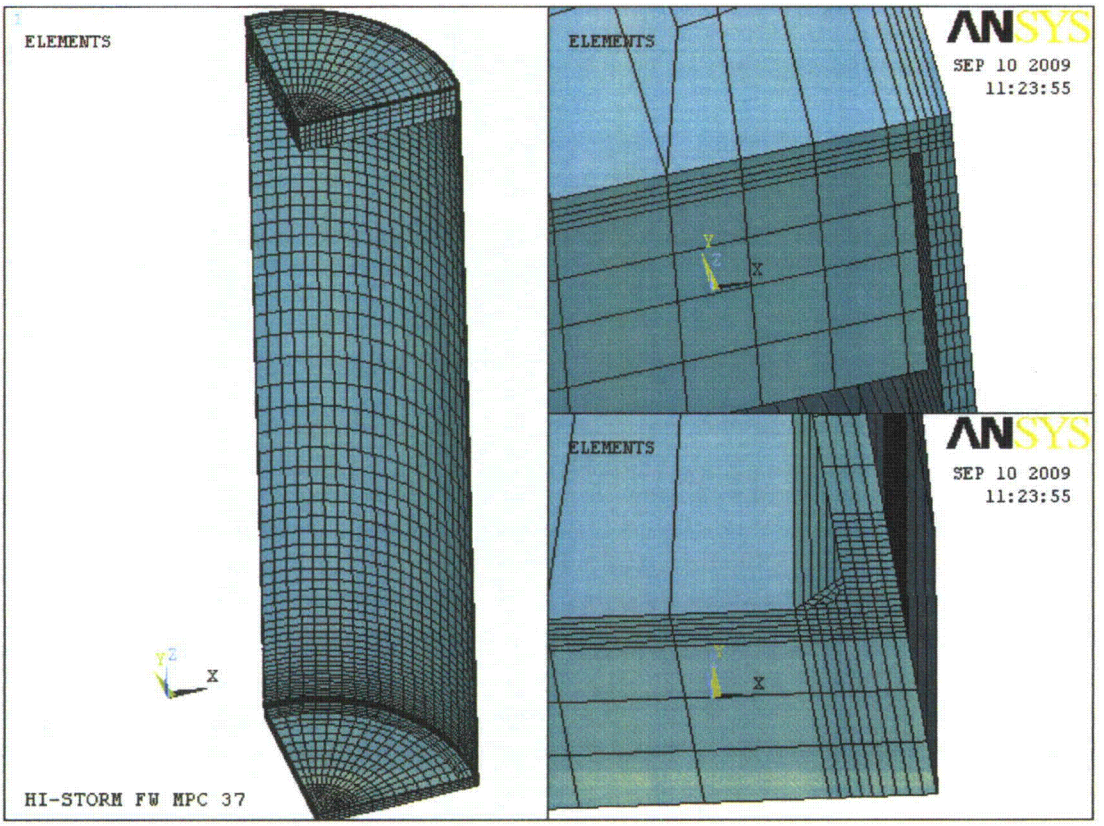

Figure 3.4.1: ANSYS Model of MPC Enclosure Vessel – Normal Handling

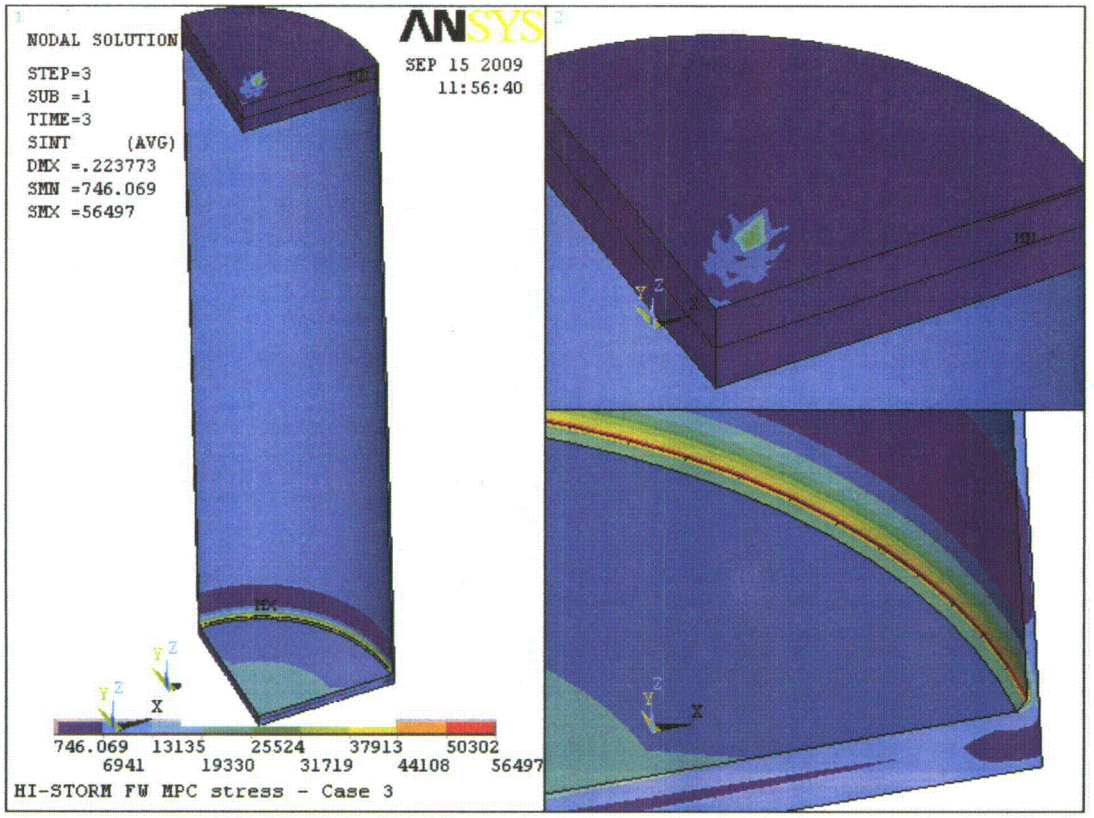

Figure 3.4.2: Stress Intensity Distribution in MPC Enclosure Vessel – Normal Handling

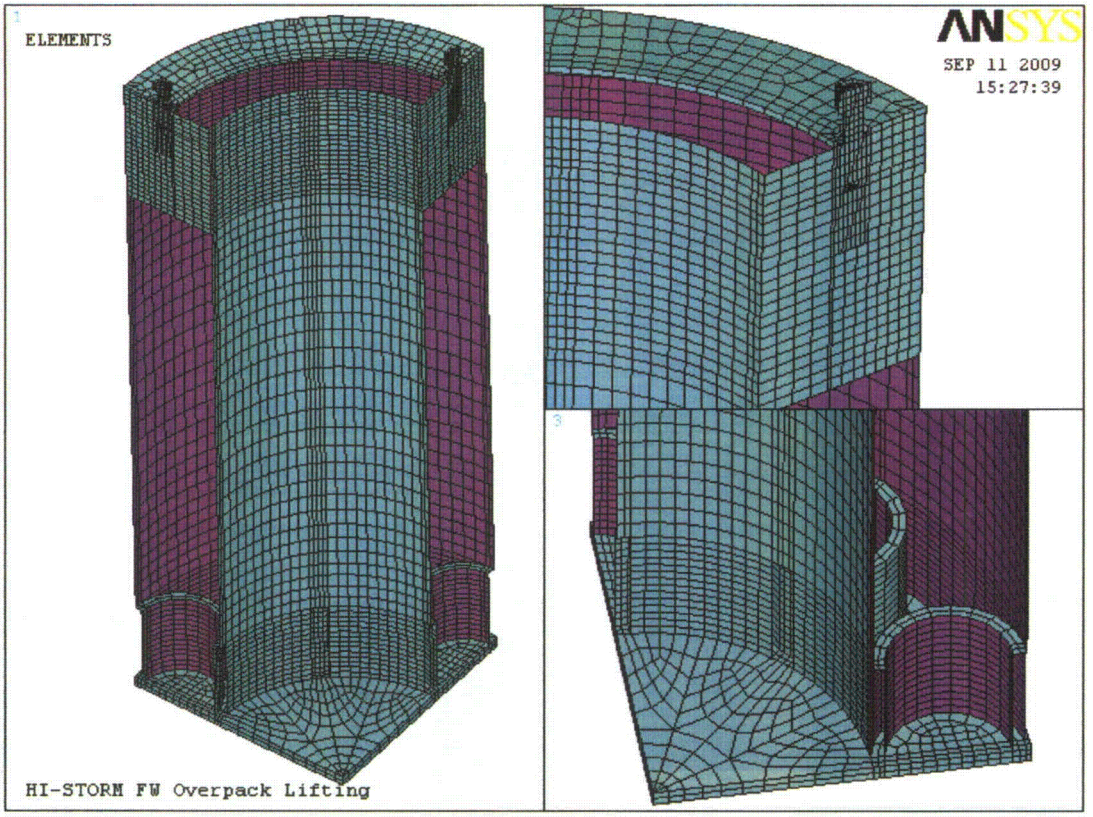

Figure 3.4.3: ANSYS Model of HI-STORM FW Overpack – Normal Handling

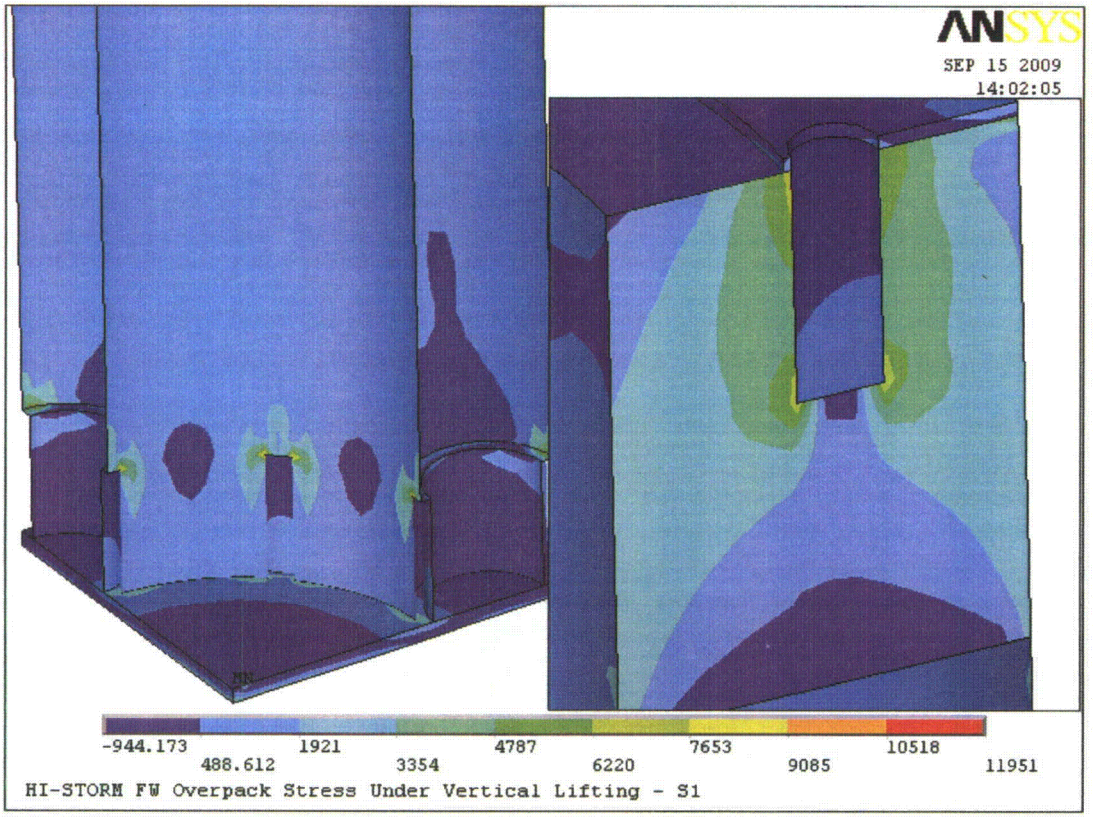

Figure 3.4.4: Stress Distribution in HI-STORM FW Overpack – Normal Handling

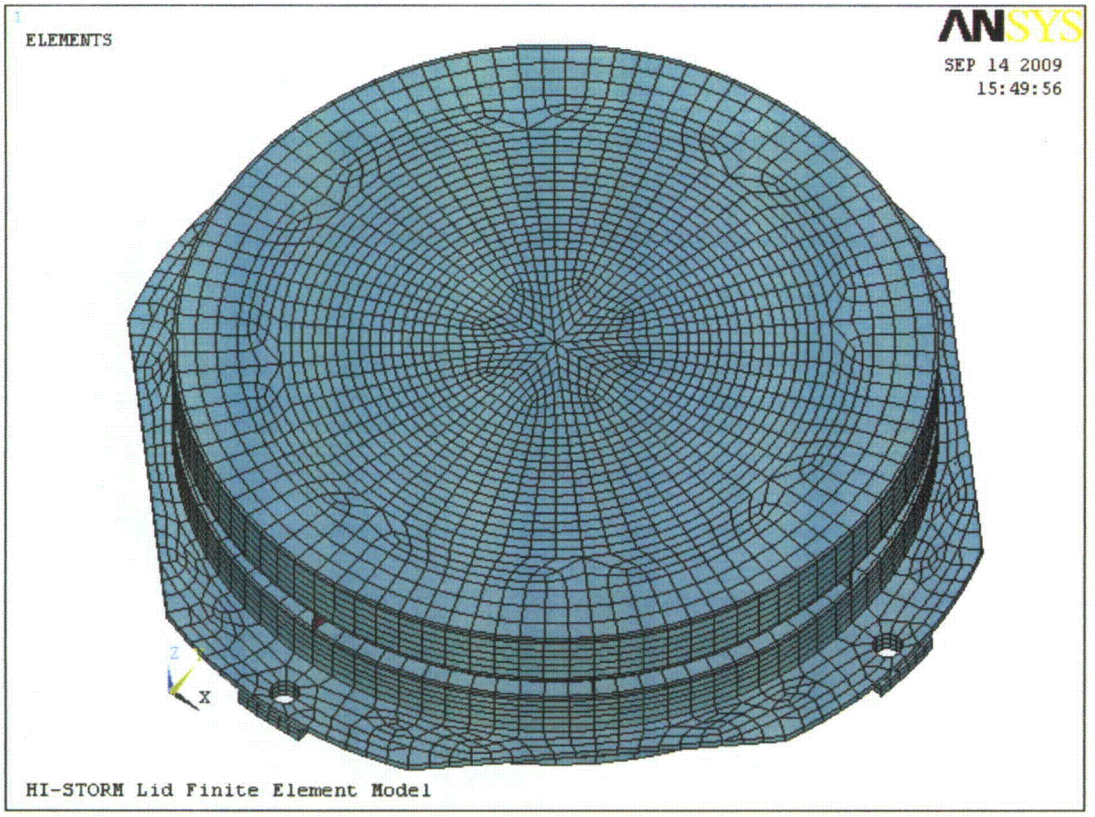

Figure 3.4.5: ANSYS Model of HI-STORM FW Lid – Normal Handling

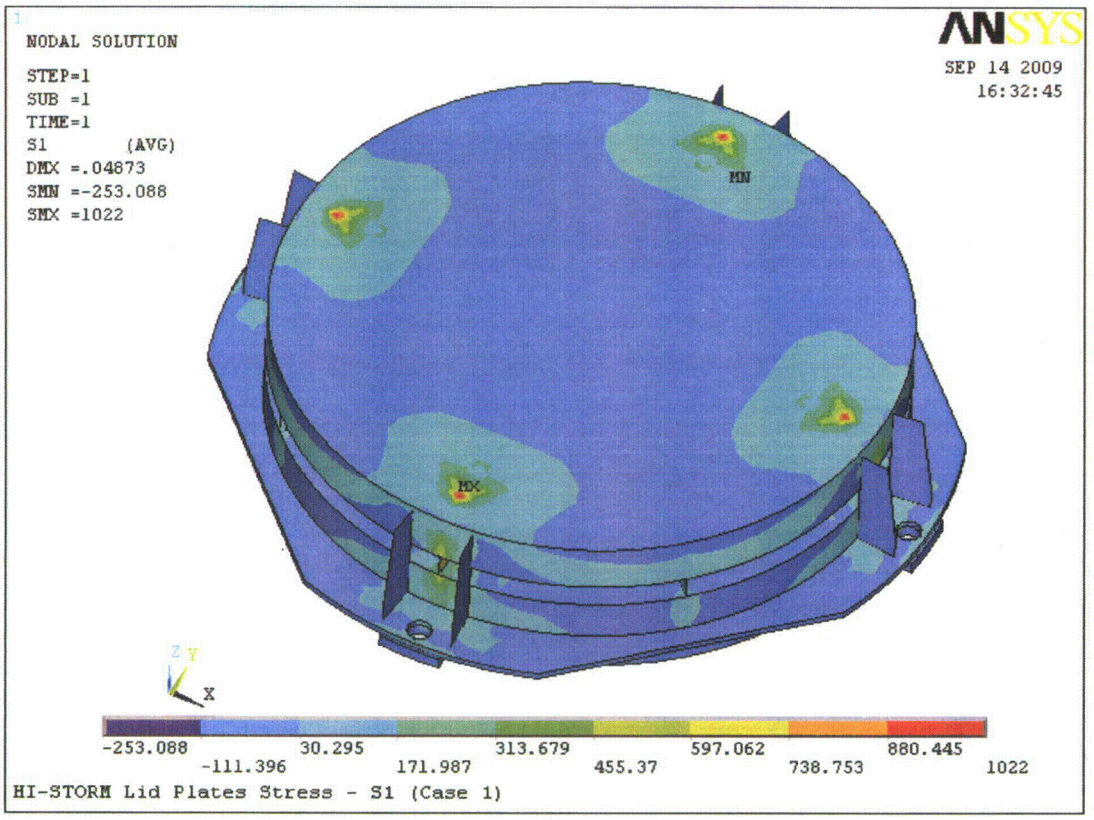

Figure 3.4.6: Stress Distribution in HI-STORM FW Lid – Normal Handling

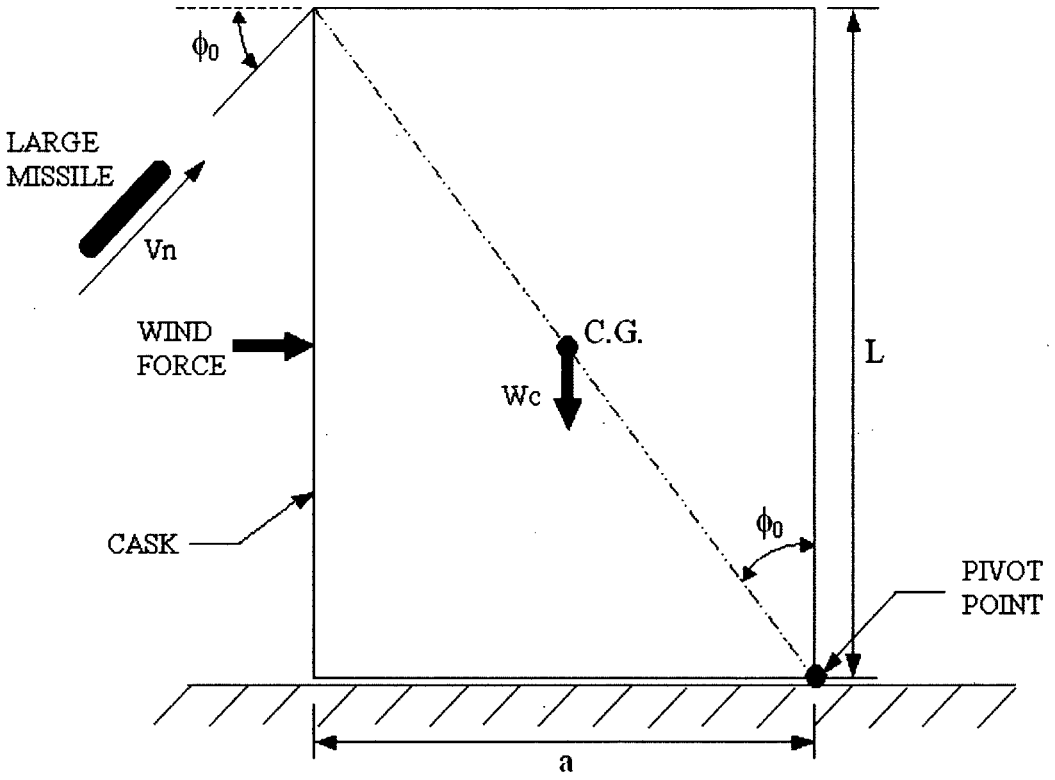

Figure 3.4.7: Free Body Diagram of Cask for Large Missile Strike/Tornado Event

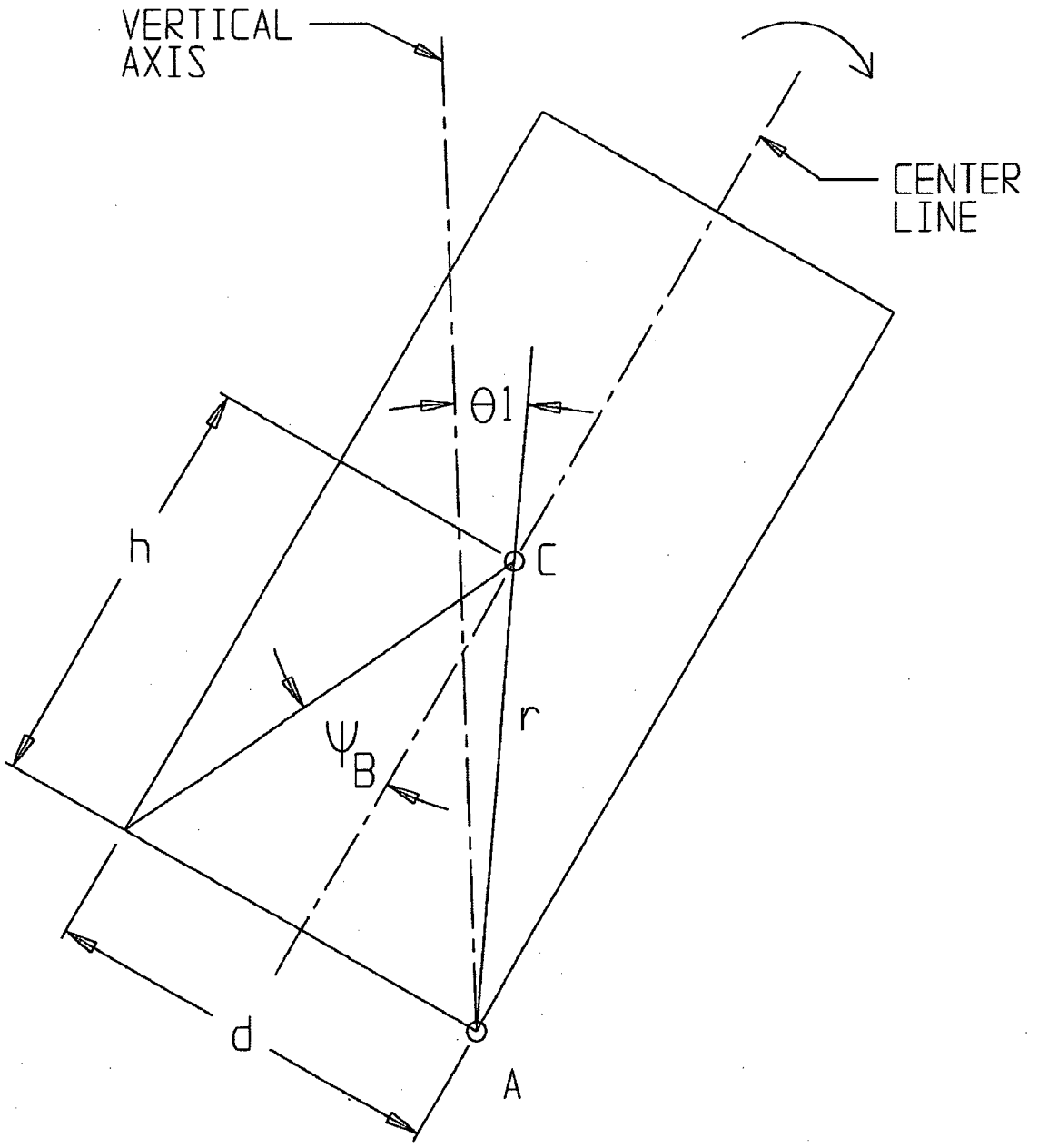

Figure 3.4.8: Cask Configuration at Incipient Tipping

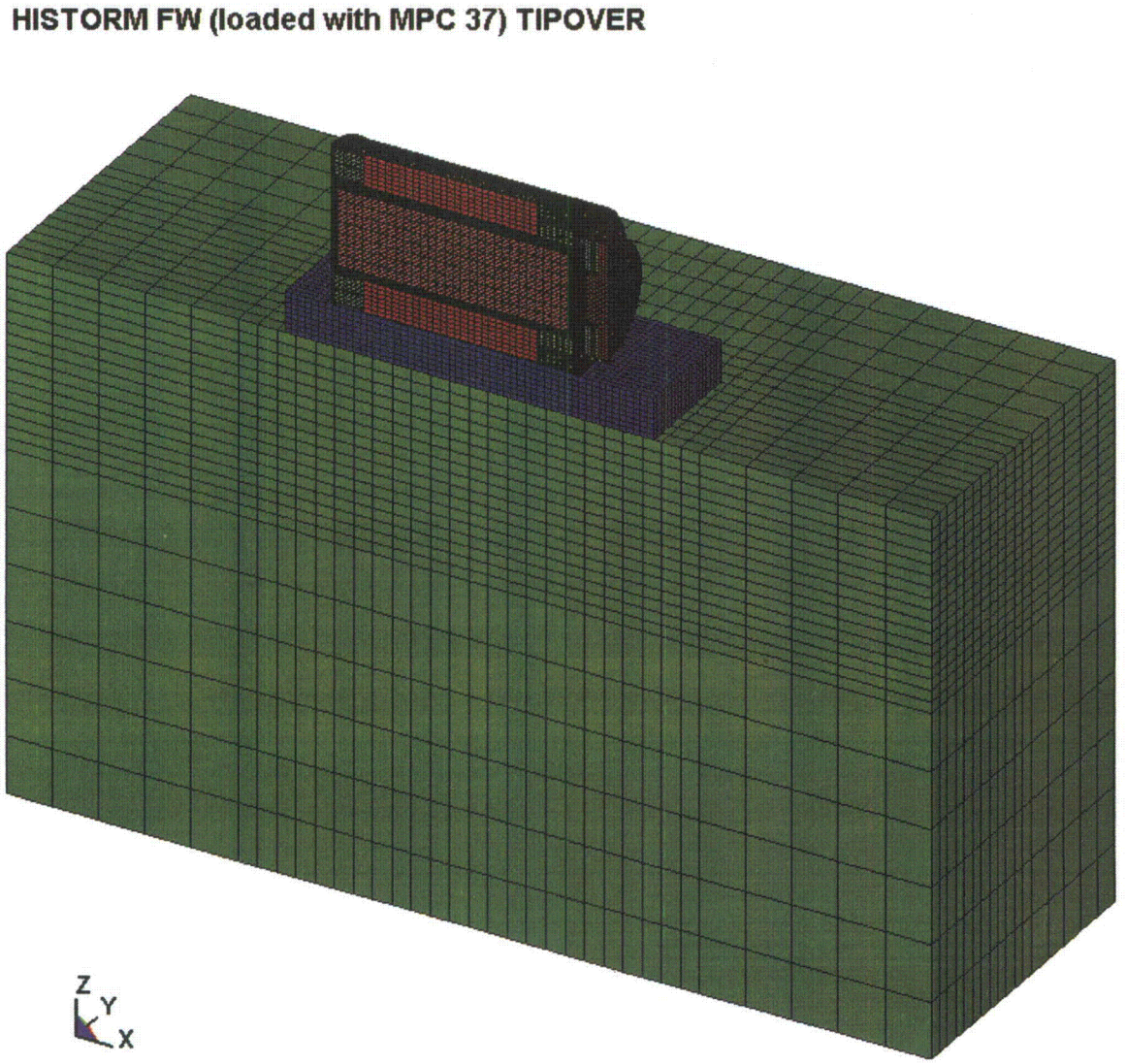

Figure 3.4.9A: LS-DYNA Tipover Model – HI-STORM FW Loaded with MPC-37

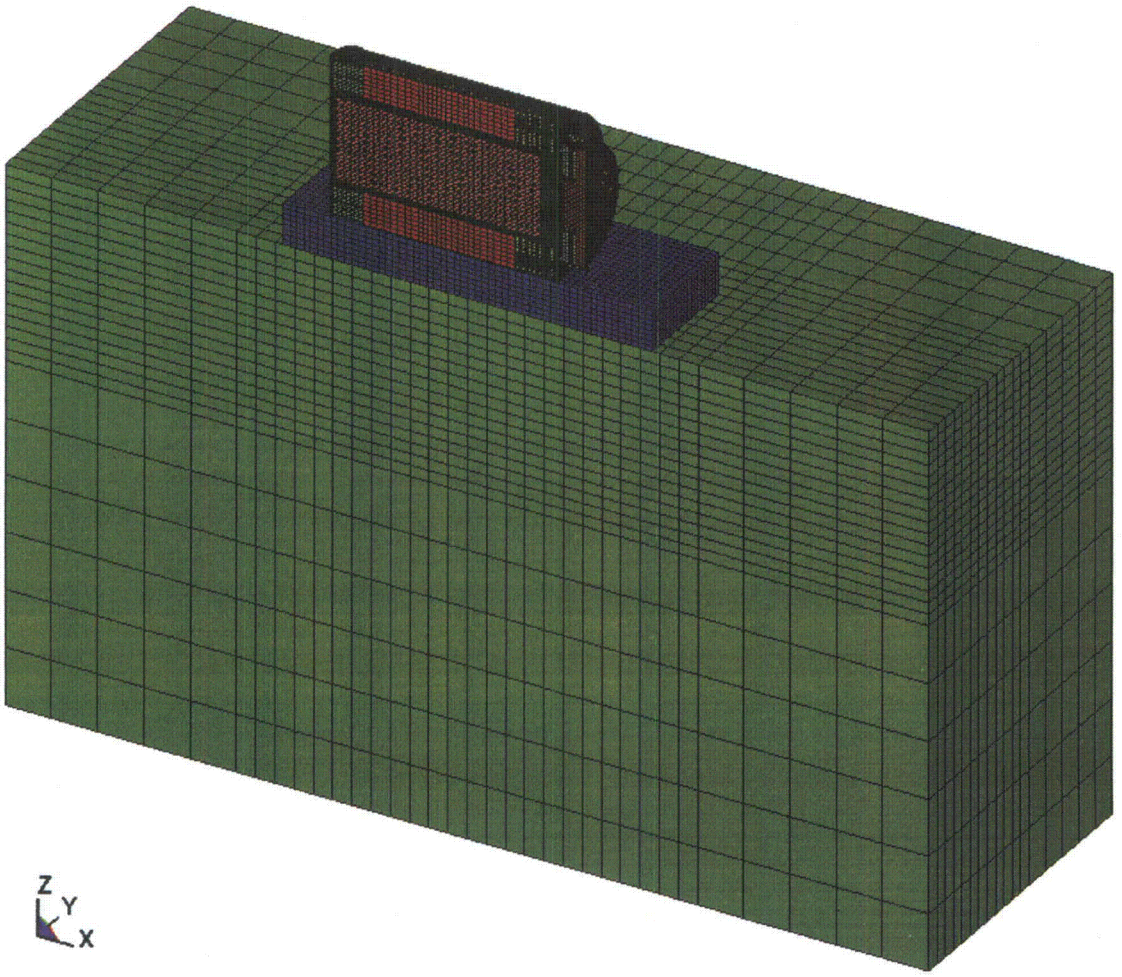

Figure 3.4.9B: LS-DYNA Tipover Model – HI-STORM FW Loaded with MPC-89

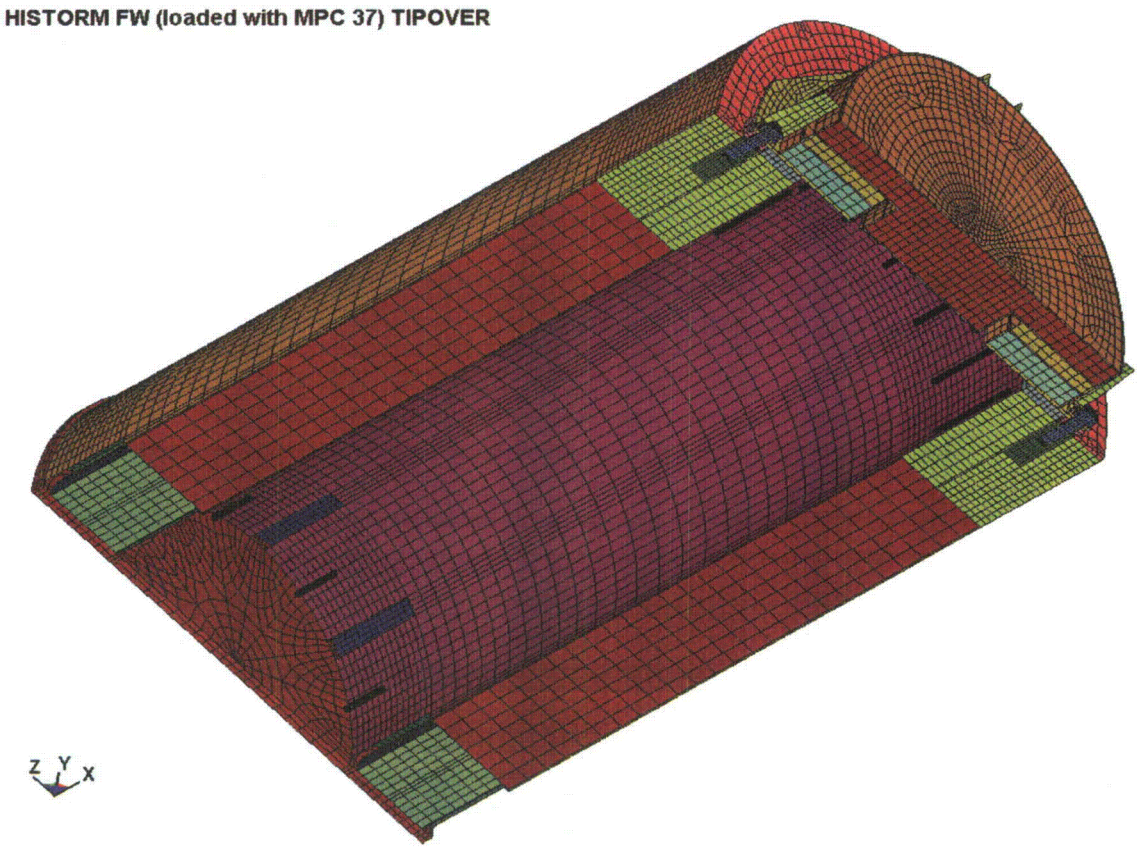

Figure 3.4.10A: LS-DYNA Model – HI-STORM FW for MPC-37

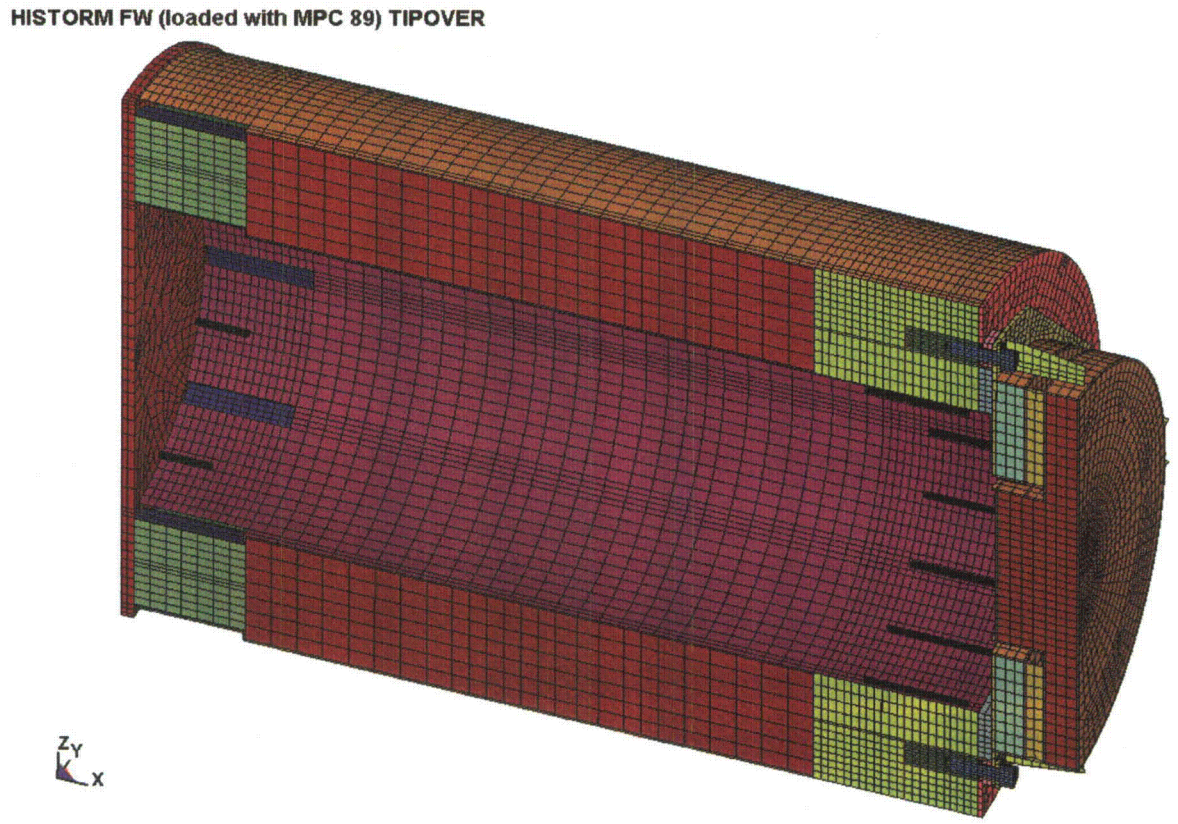

Figure 3.4.10B: LS-DYNA Model – HI-STORM FW for MPC-89

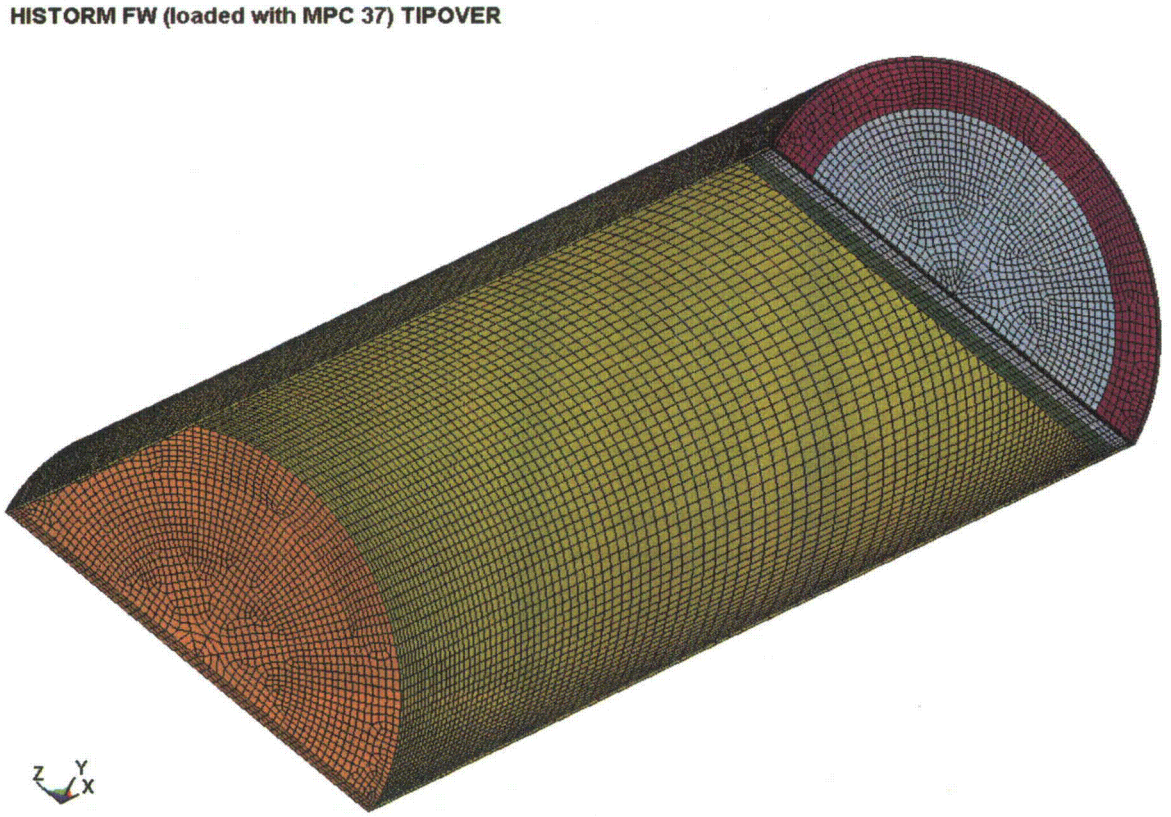

Figure 3.4.11A: LS-DYNA Model – MPC-37 Enclosure Vessel

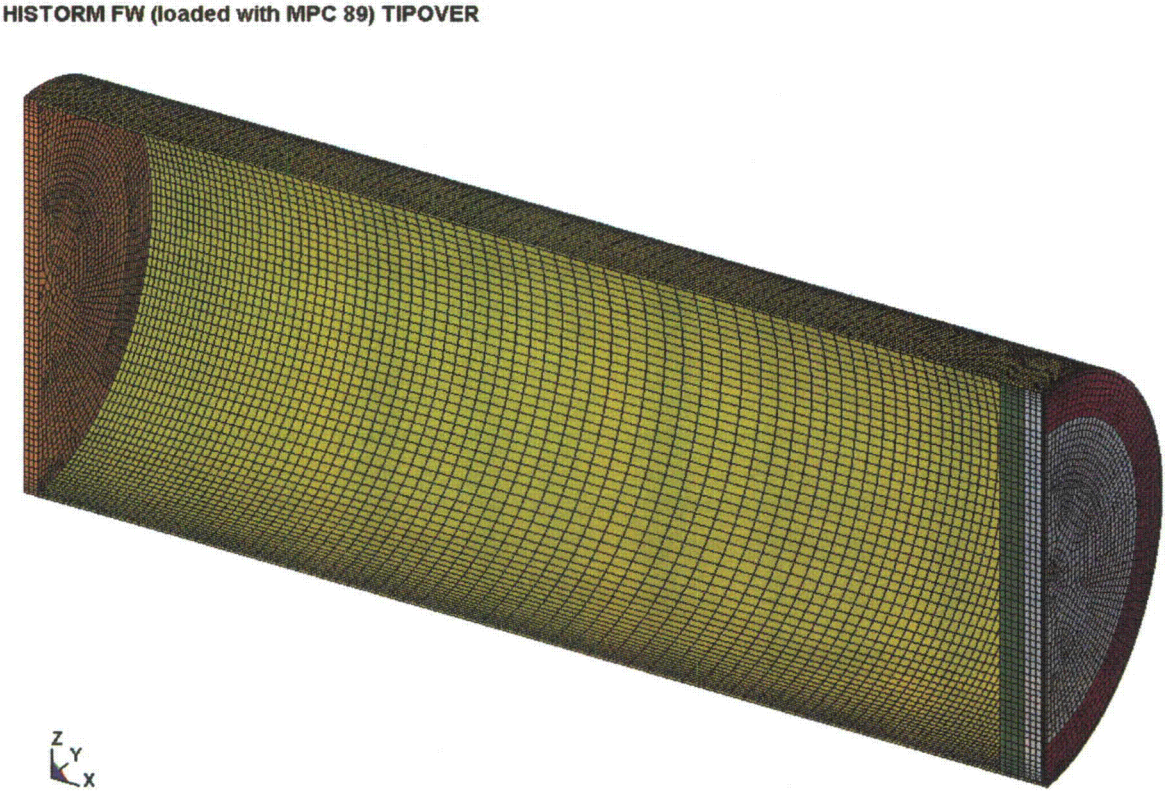

Figure 3.4.11B: LS-DYNA Model – MPC-89 Enclosure Vessel

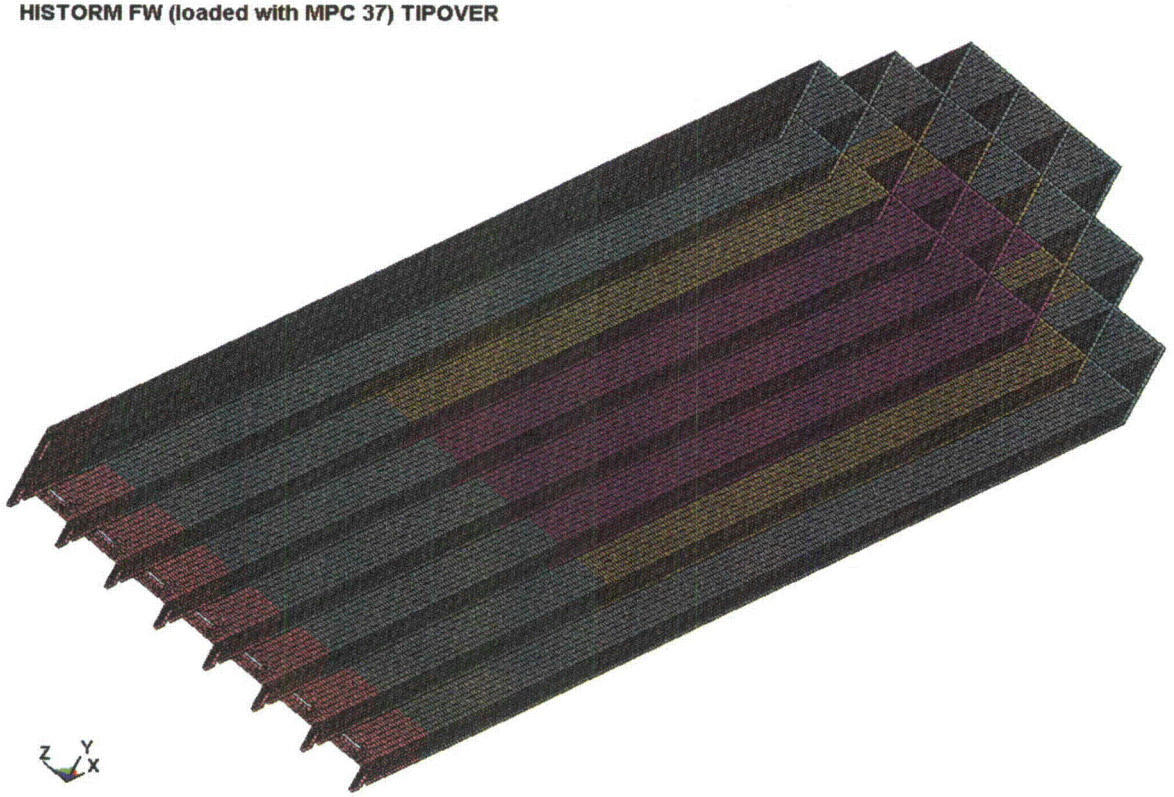

Figure 3.4.12A: LS-DYNA Model – MPC-37 Fuel Basket
(note: the different colors represent regions with bounding temperatures of 340°C, 325°C, 300°C and 250°C, respectively)

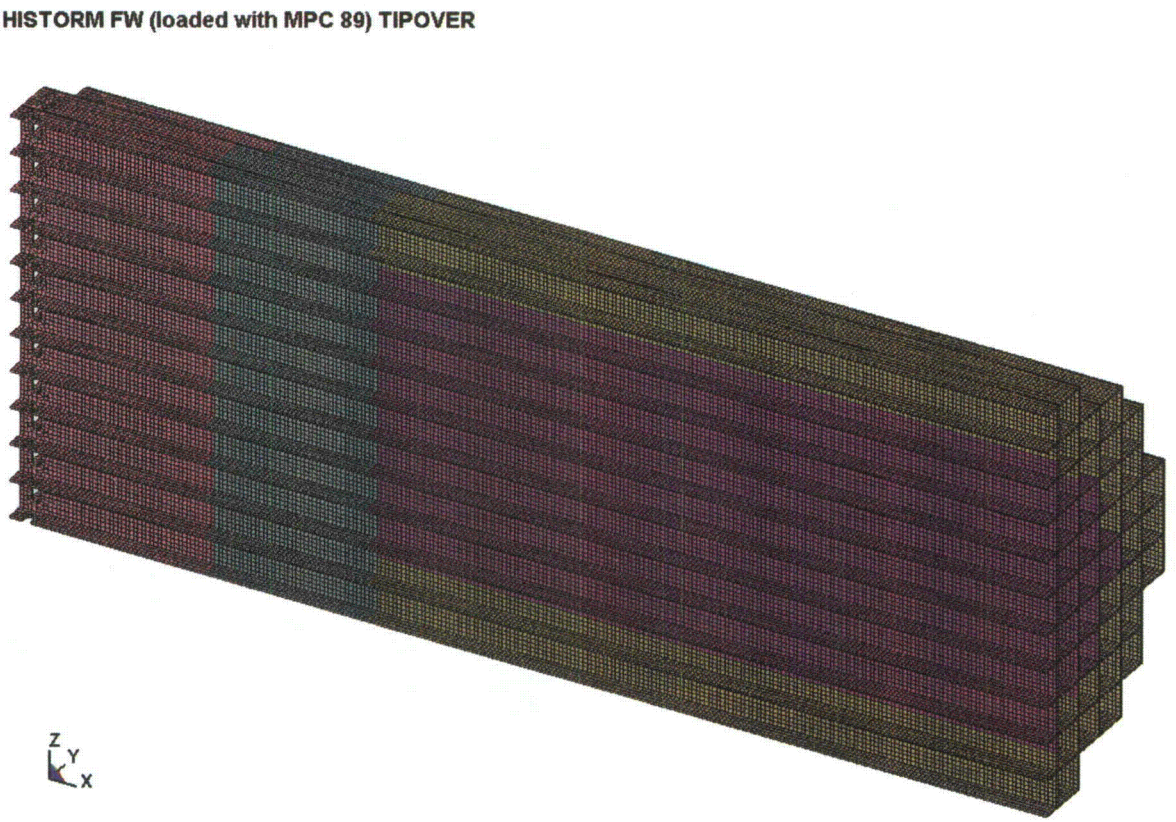

Figure 3.4.12B: LS-DYNA Model – MPC-89 Fuel Basket
(note: the different colors represent regions with bounding temperatures of 325°C, 300°C, 250°C and 200°C, respectively)

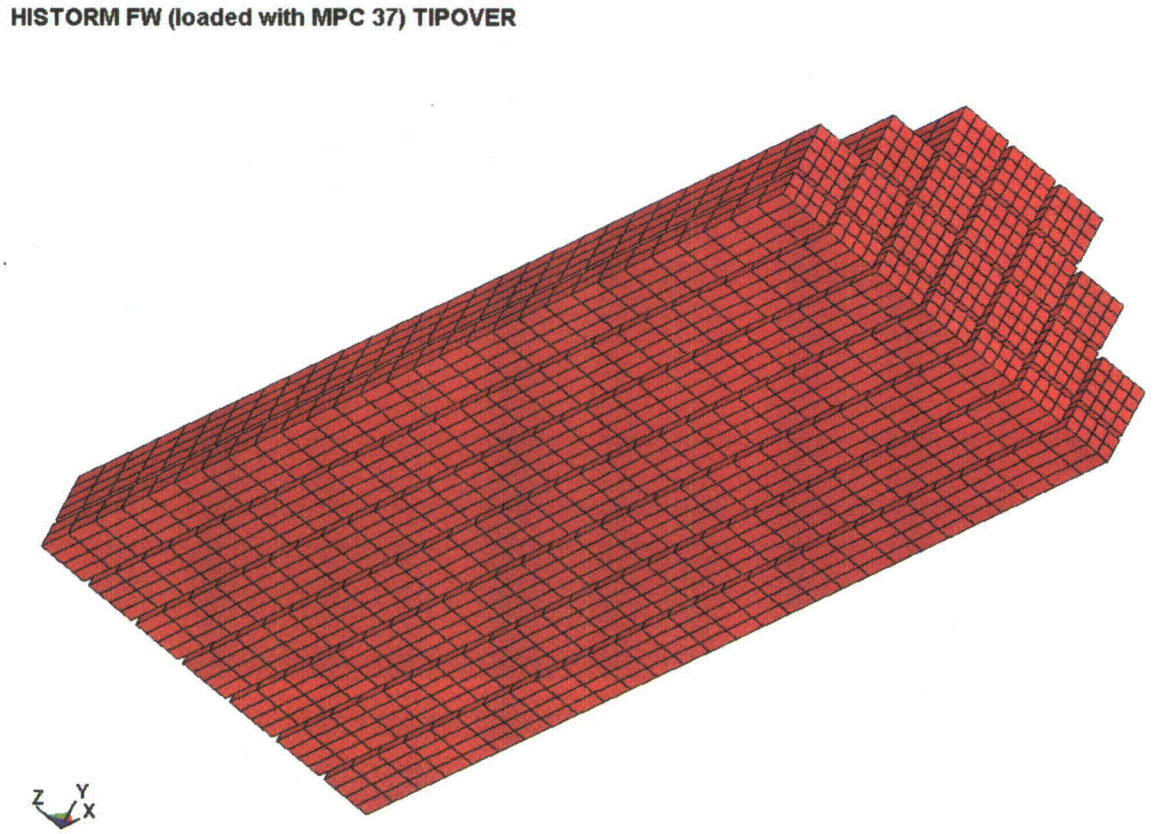

Figure 3.4.13A: LS-DYNA Model – PWR Fuel Assemblies

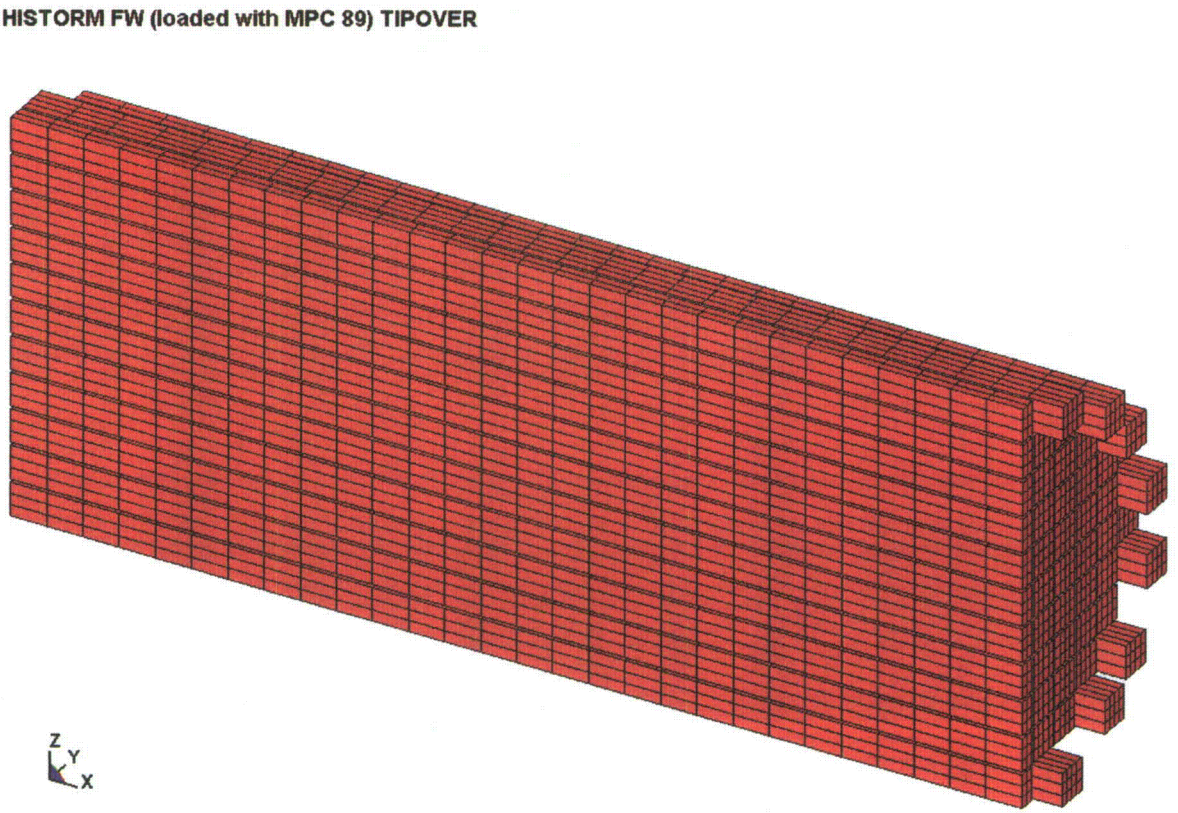

Figure 3.4.13B: LS-DYNA Model – BWR Fuel Assemblies & Damaged Fuel Containers

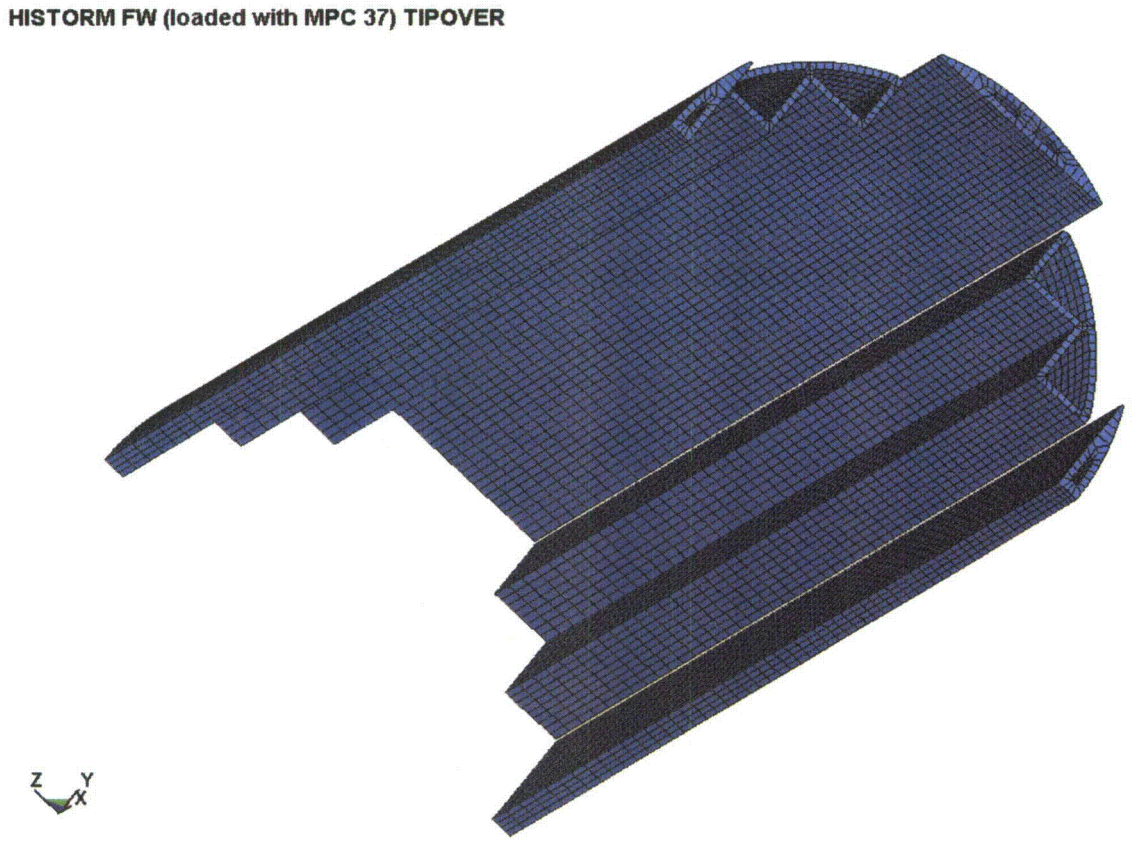

Figure 3.4.14A: LS-DYNA Model – MPC-37 Fuel Basket Shims

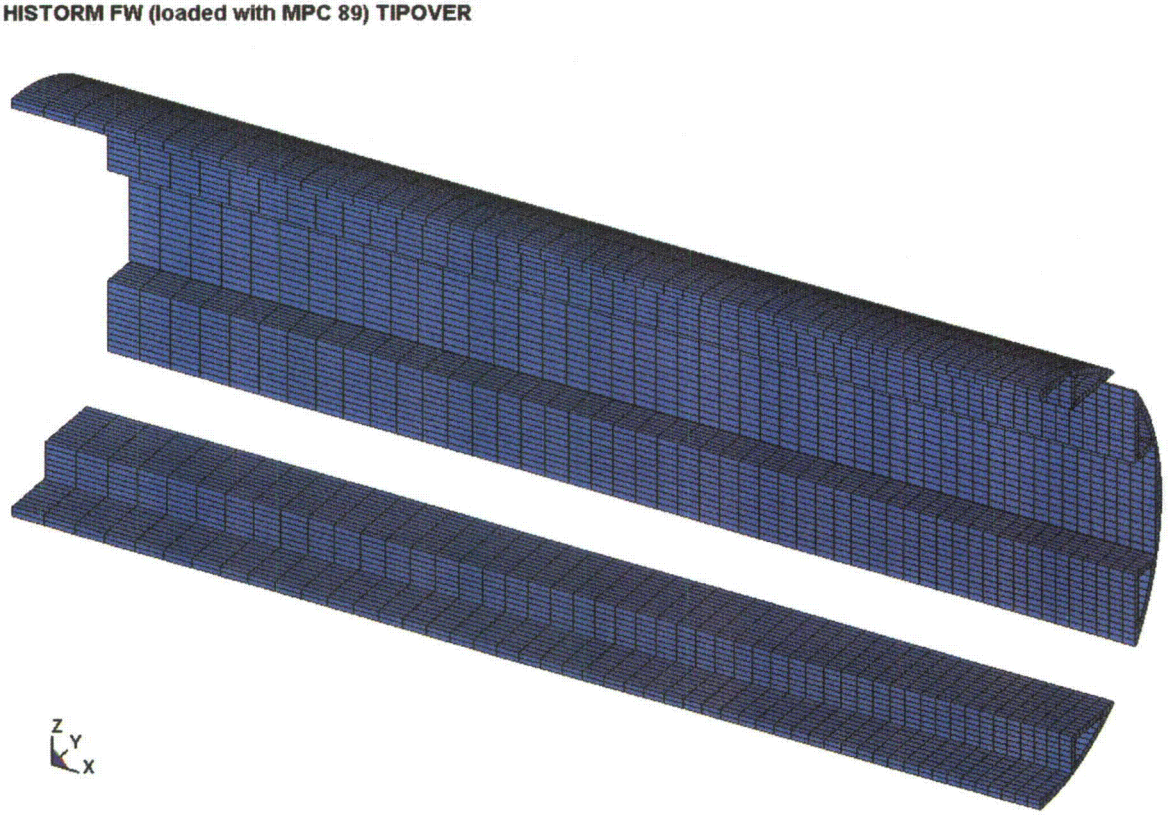

Figure 3.4.14B: LS-DYNA Model – MPC-89 Fuel Basket Shims

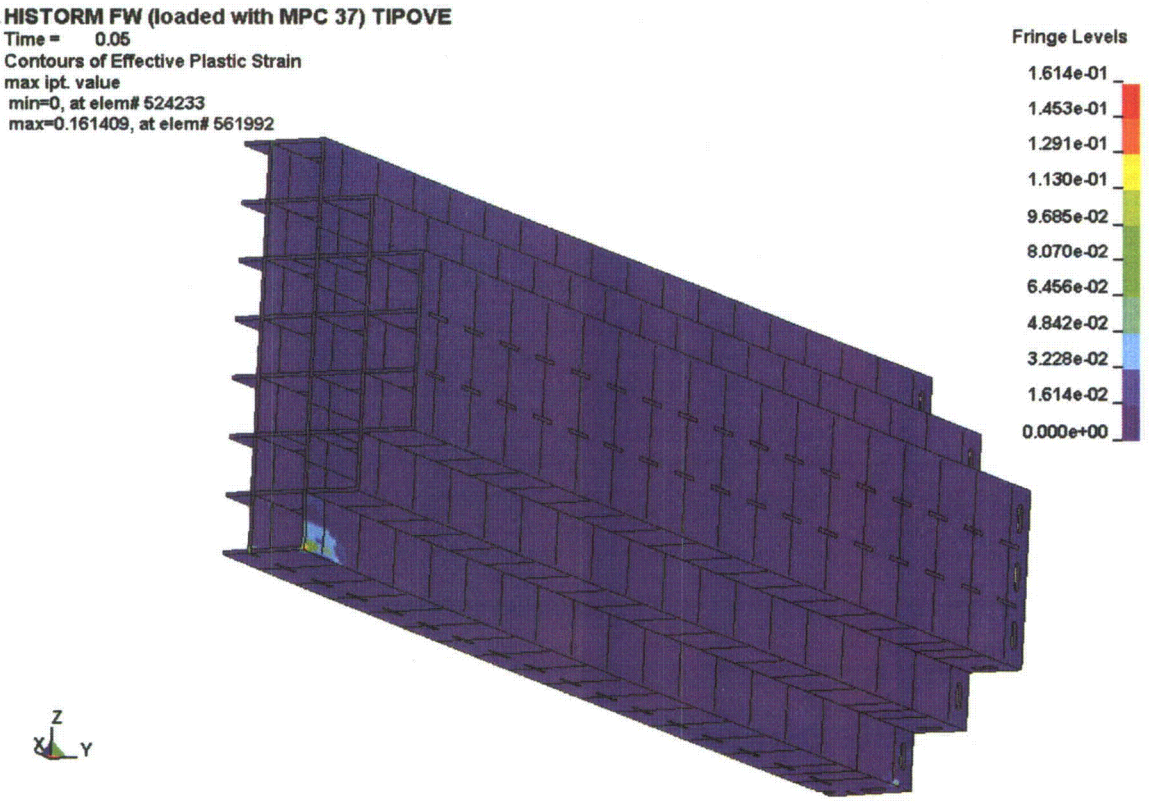

Figure 3.4.15A: Maximum Plastic Strain – MPC-37 Fuel Basket

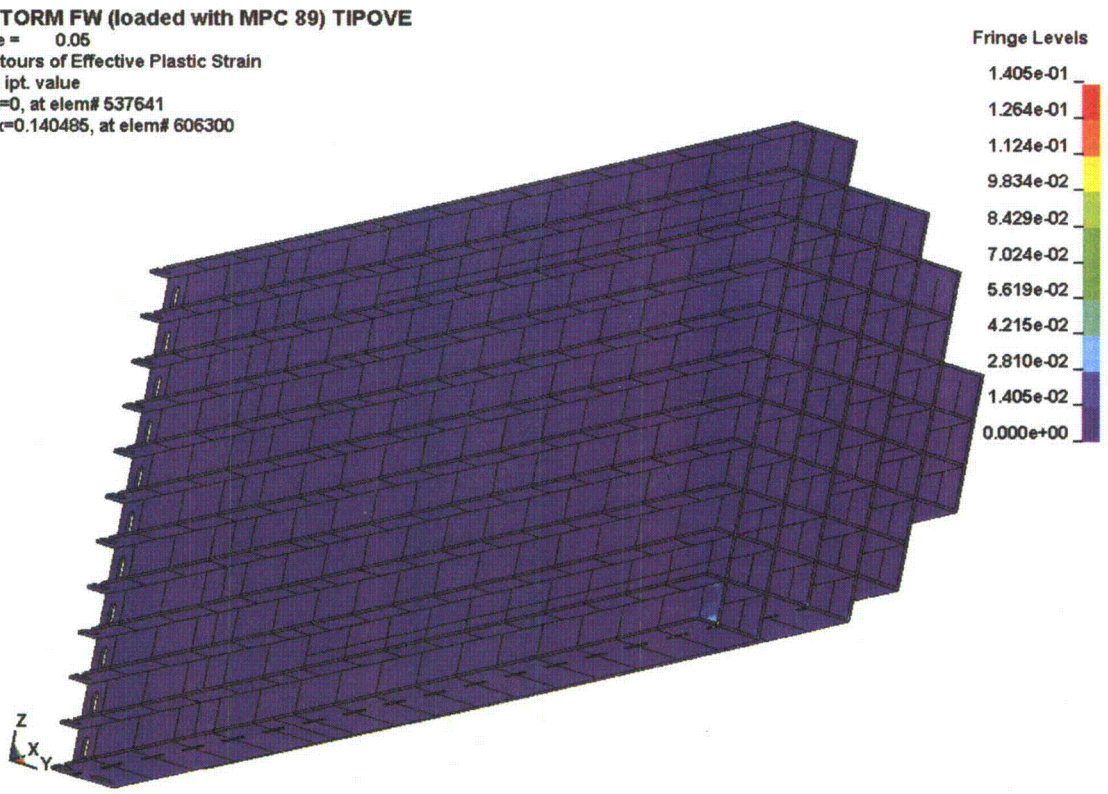

Figure 3.4.15B: Maximum Plastic Strain – MPC-89 Fuel Basket

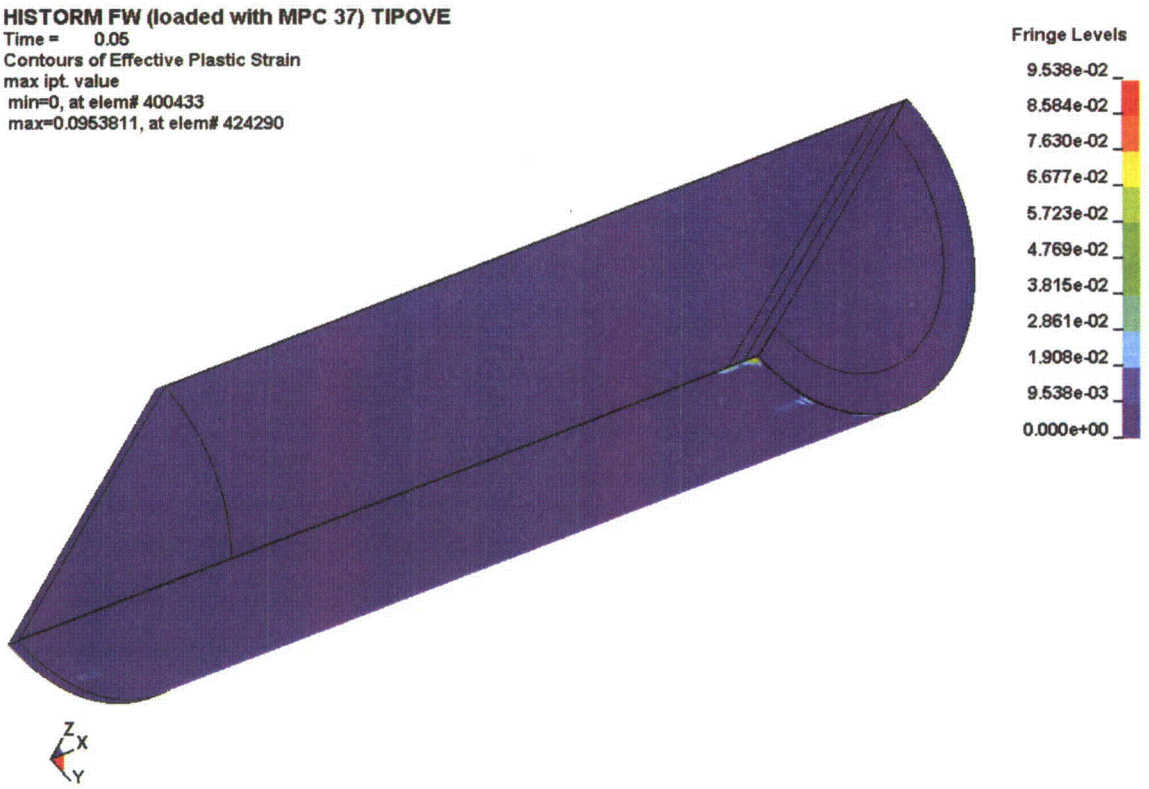

Figure 3.4.16A: Maximum Plastic Strain – MPC-37 Enclosure Vessel

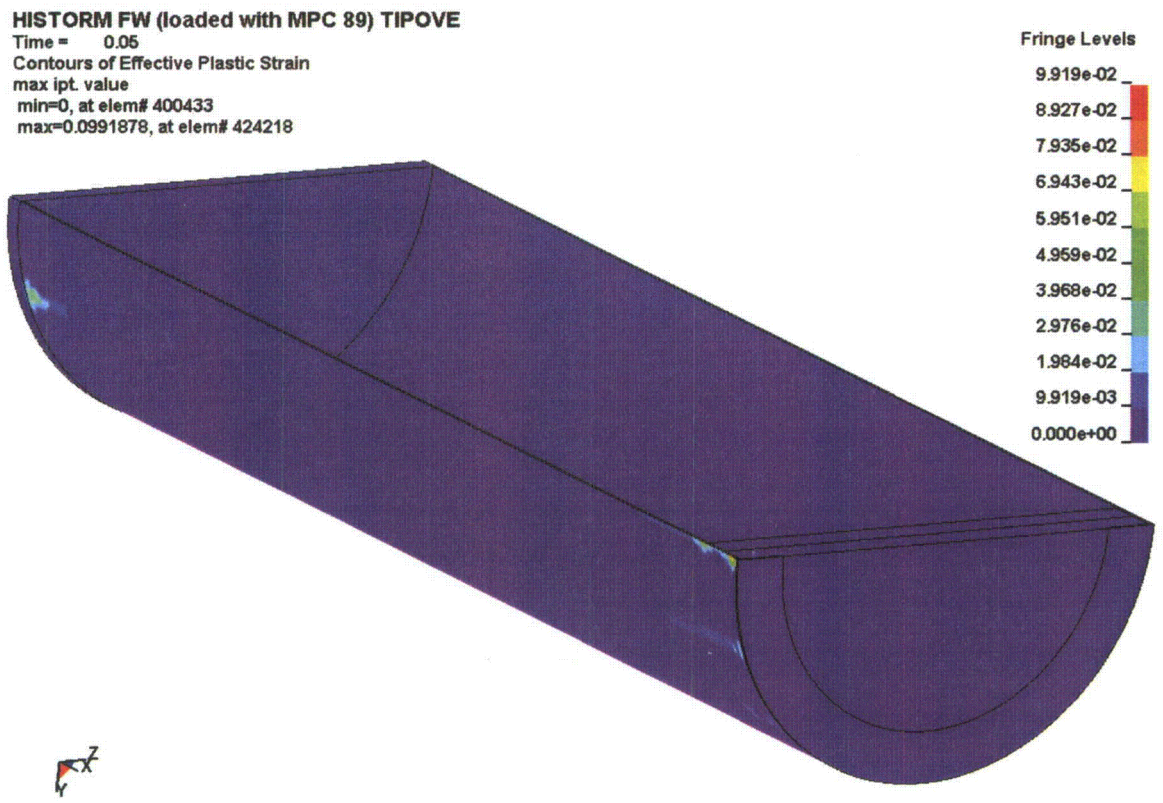

Figure 3.4.16B: Maximum Plastic Strain – MPC-89 Enclosure Vessel

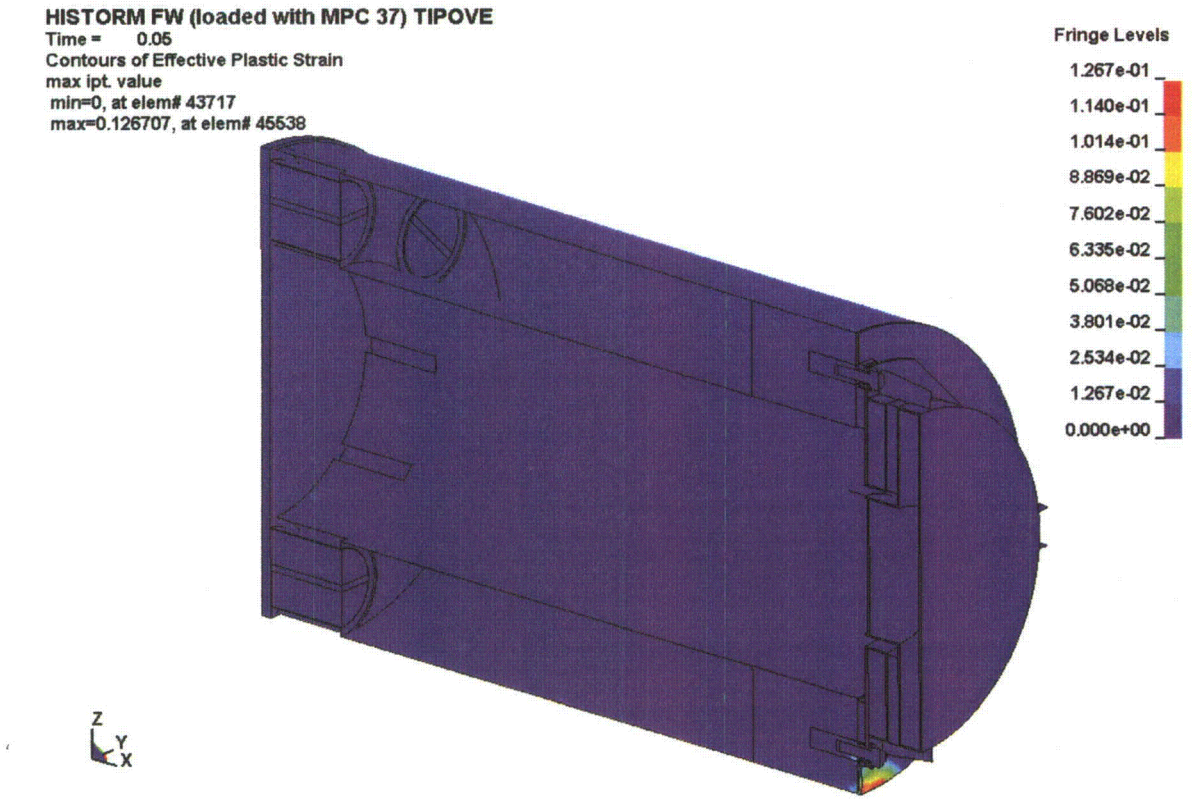

Figure 3.4.17A: Maximum Plastic Strain – HI-STORM FW Overpack
(for MPC-37, Excluding MPC Guide Tubes)

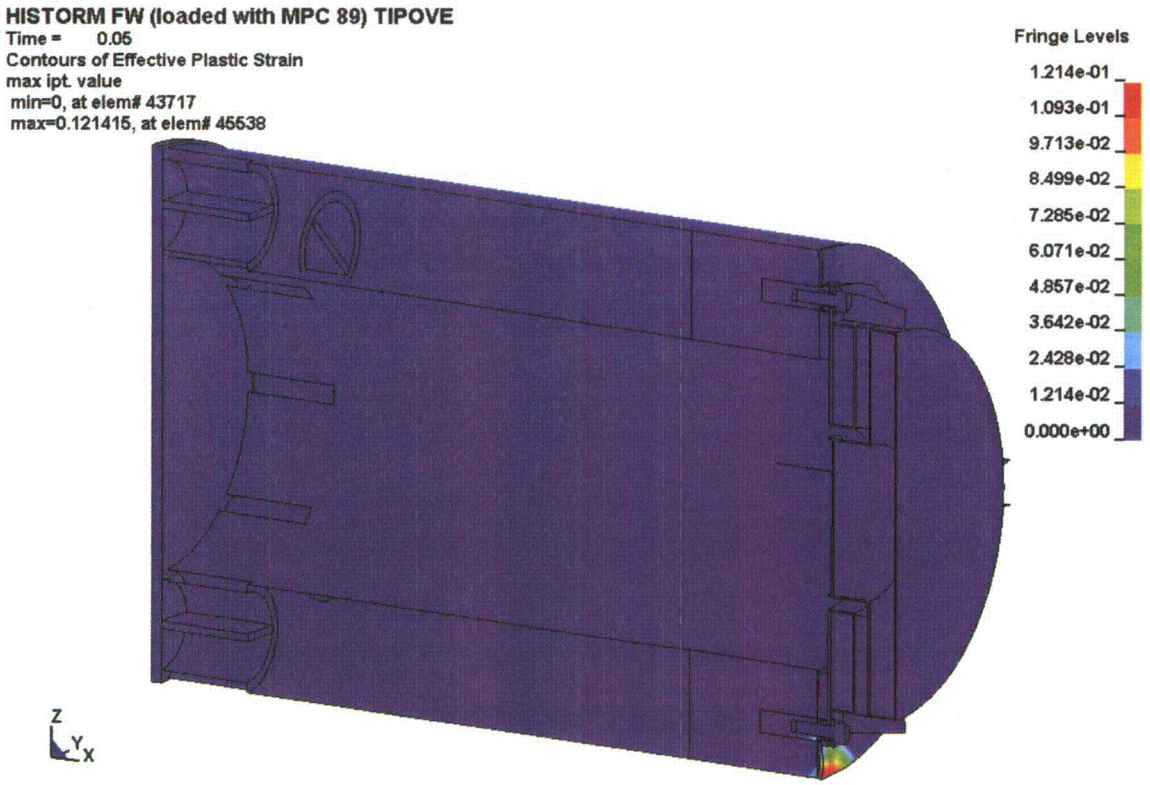

Figure 3.4.17B: Maximum Plastic Strain – HI-STORM FW Overpack
(for MPC-89, Excluding MPC Guide Tubes)

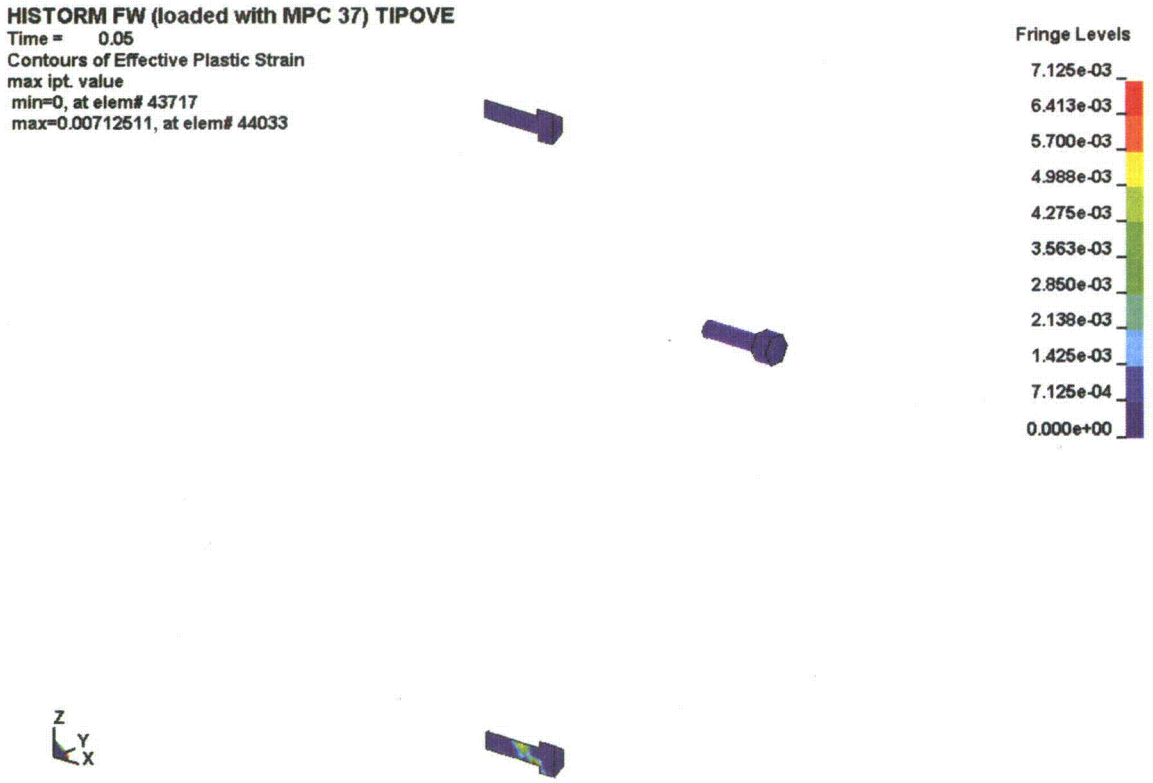

Figure 3.4.18A: Maximum Plastic Strain –
HI-STORM FW Overpack (for MPC-37) Closure Lid Bolts

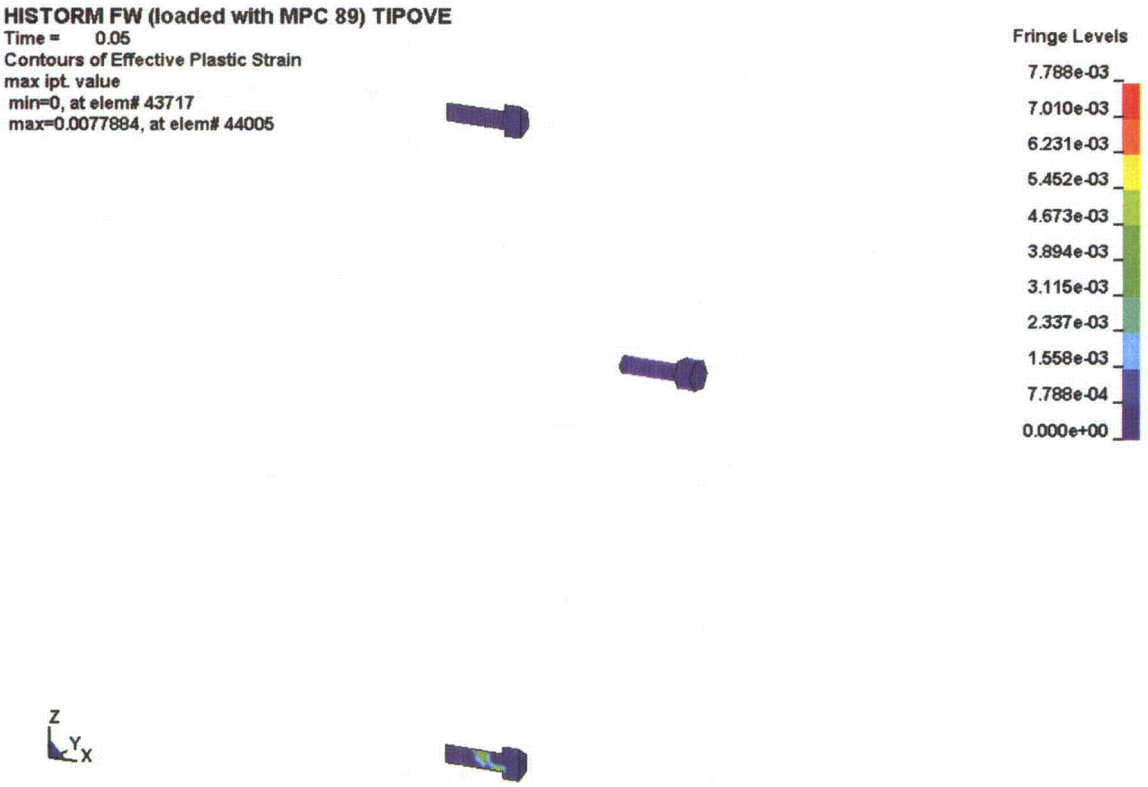

Figure 3.4.18B: Maximum Plastic Strain –
HI-STORM FW Overpack (for MPC-37) Closure Lid Bolts

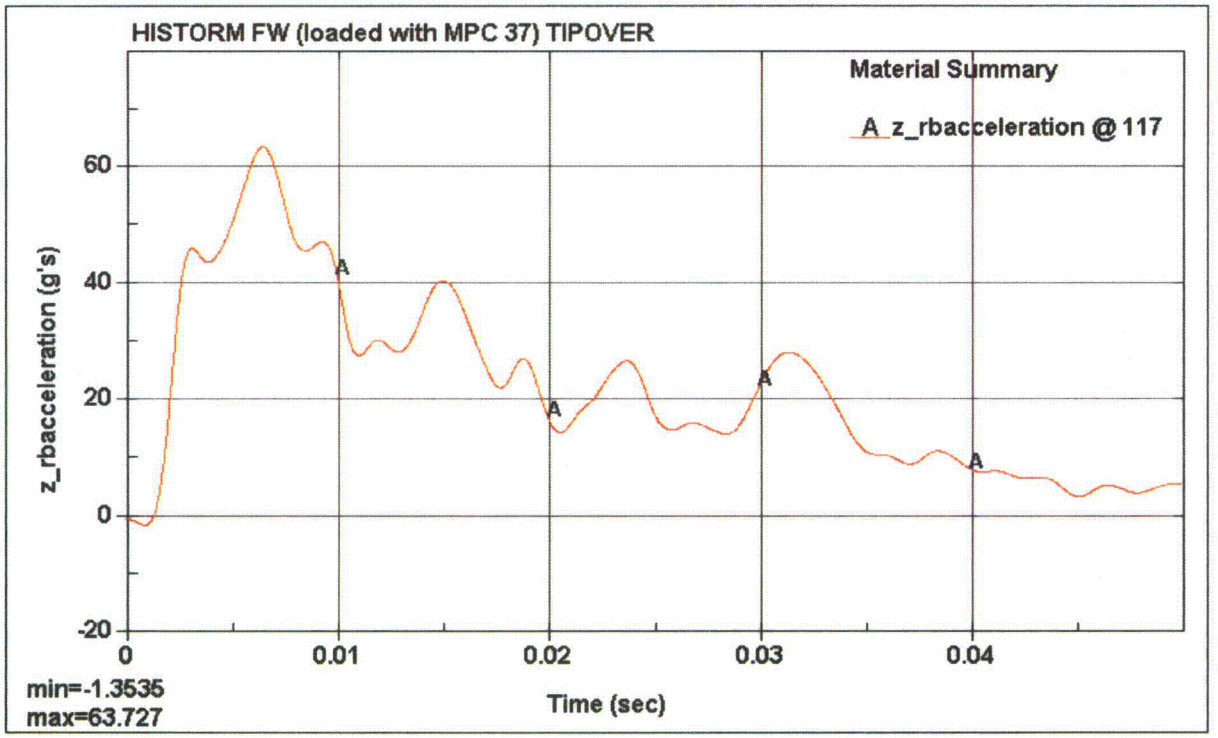

Figure 3.4.19A: Vertical Rigid Body Deceleration Time History –
Cask Lid Concrete (for HI-STORM FW Loaded with MPC-37)

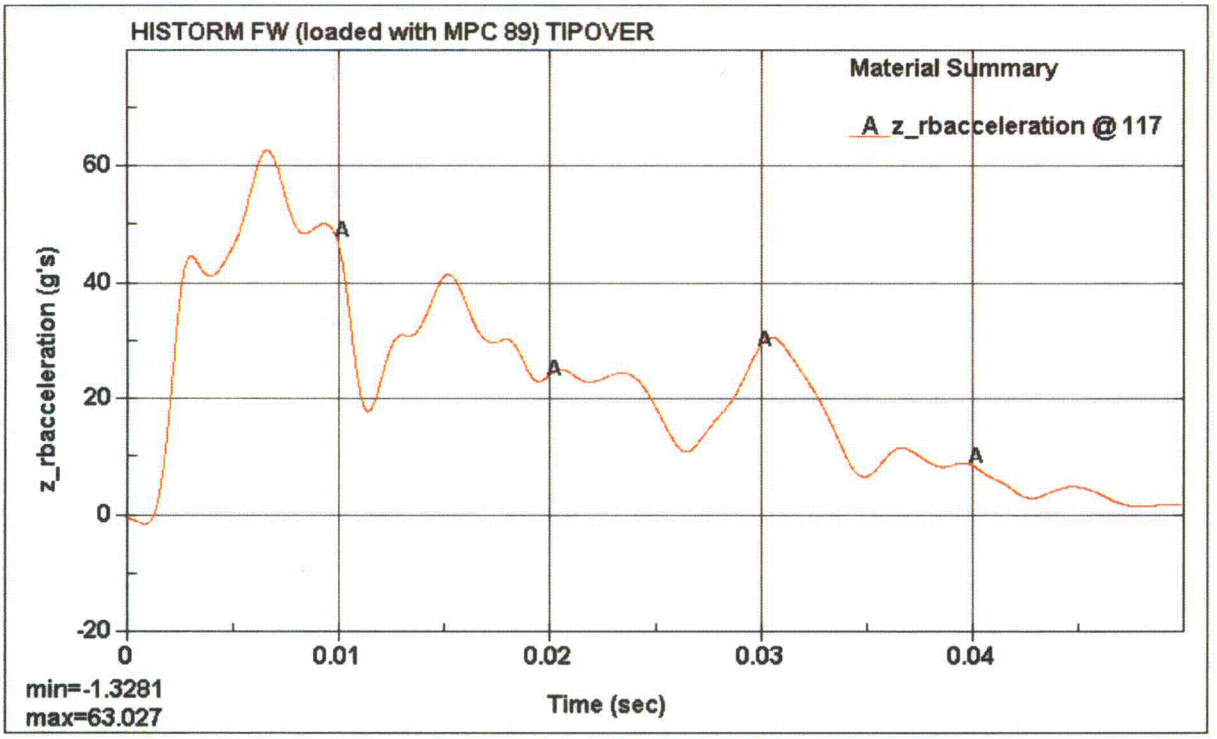

Figure 3.4.19B: Vertical Rigid Body Deceleration Time History –
Cask Lid Concrete (for HI-STORM FW Loaded with MPC-89)

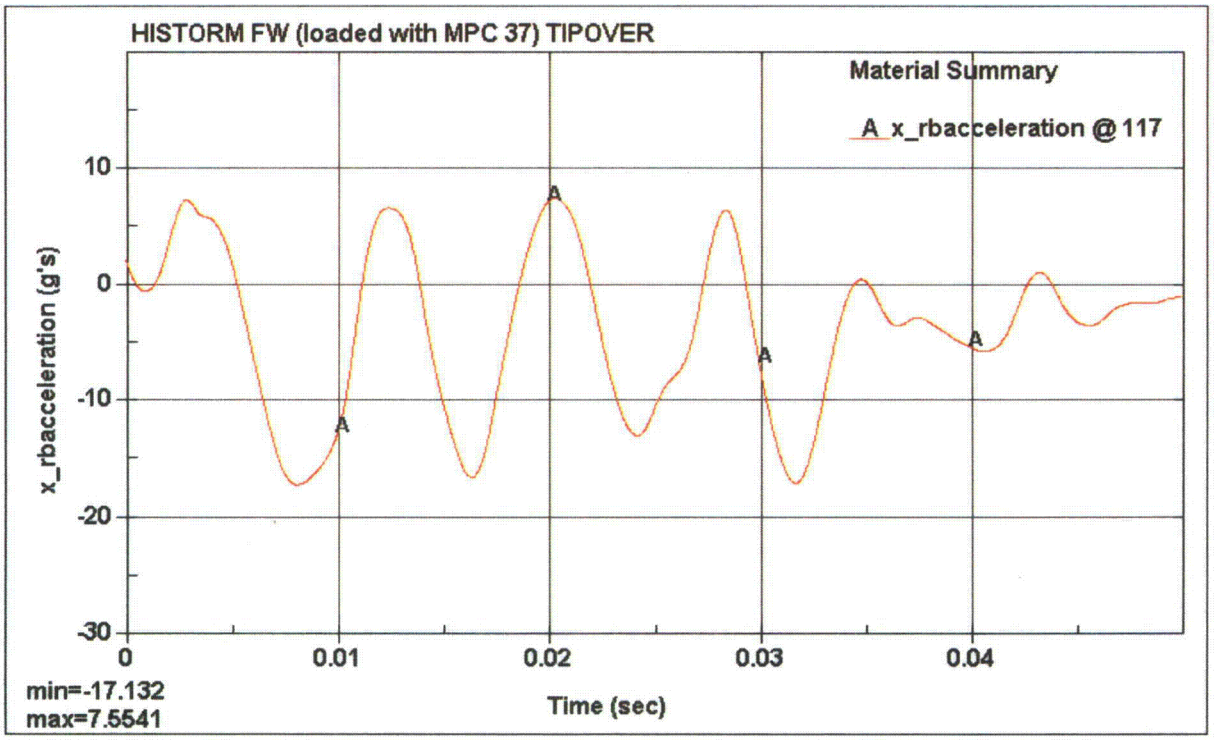

Figure 3.4.20A: Horizontal Rigid Body Deceleration Time History – Cask Lid Concrete (for HI-STORM FW Loaded with MPC-37)

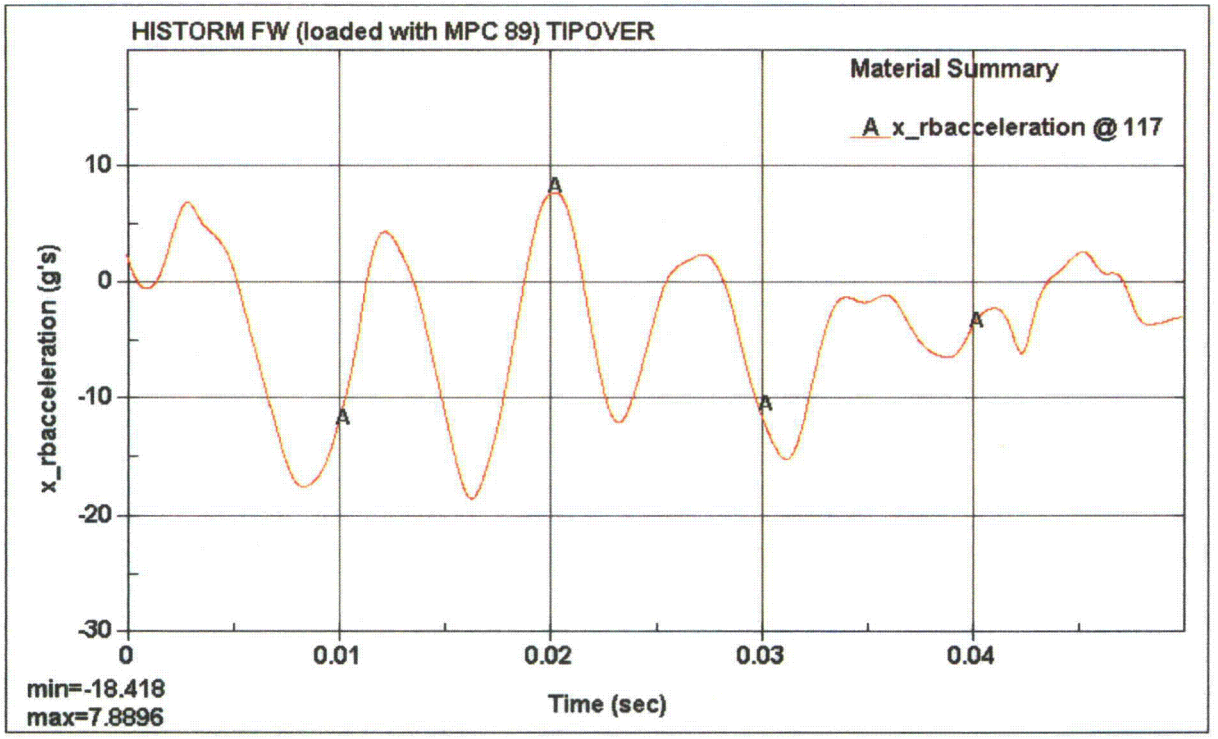

Figure 3.4.20B: Horizontal Rigid Body Deceleration Time History – Cask Lid Concrete (for HI-STORM FW Loaded with MPC-89)

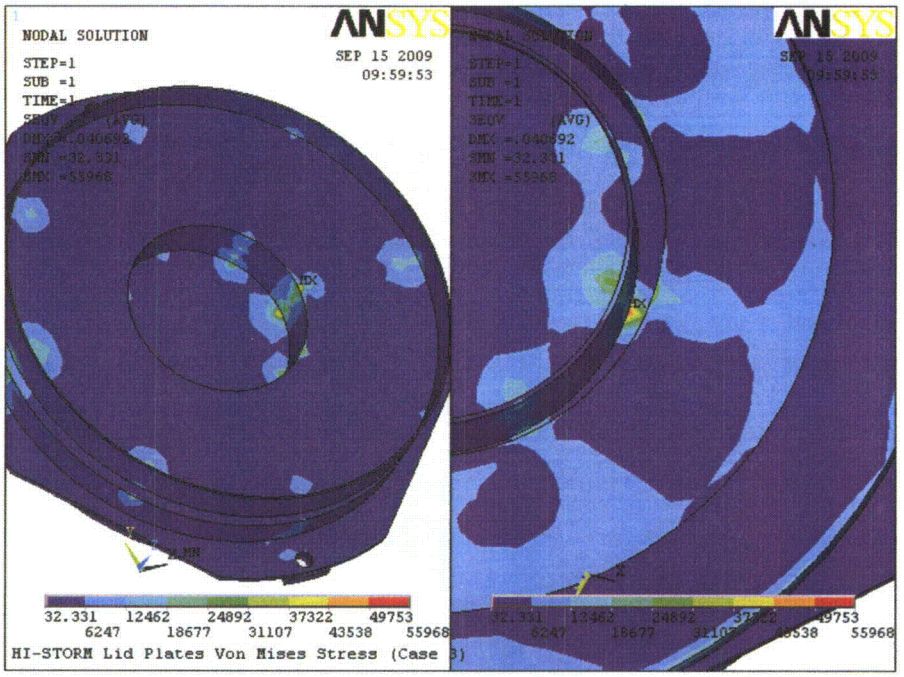

(a) Steel Weldment (Excluding Upper Shim Plates)

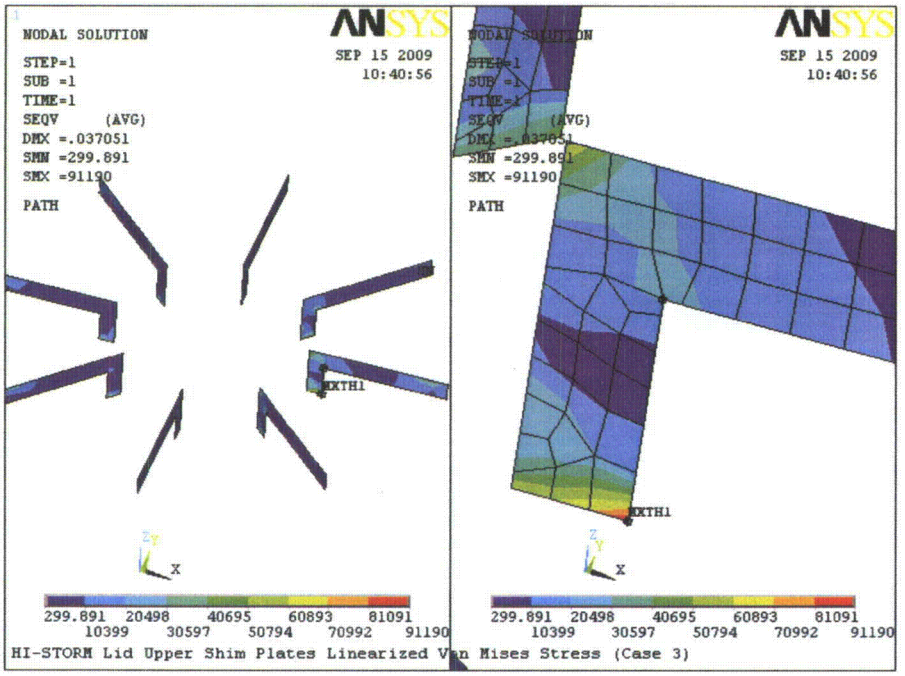

(b) Upper Shim Plates

Figure 3.4.21: Stress Distribution in HI-STORM FW Lid – Non-Mechanistic Tipover

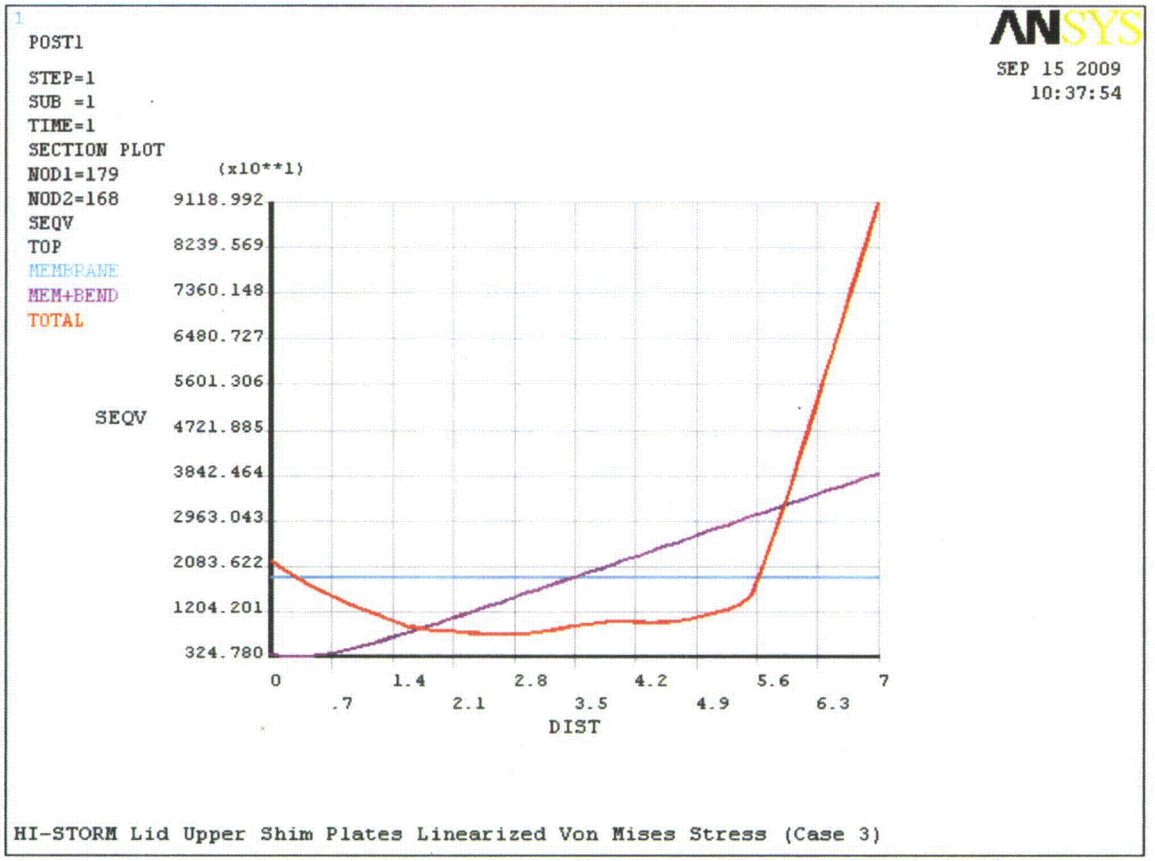

Figure 3.4.22: Linearized Stress Results for Upper Shim Plate – Non-Mechanistic Tipover

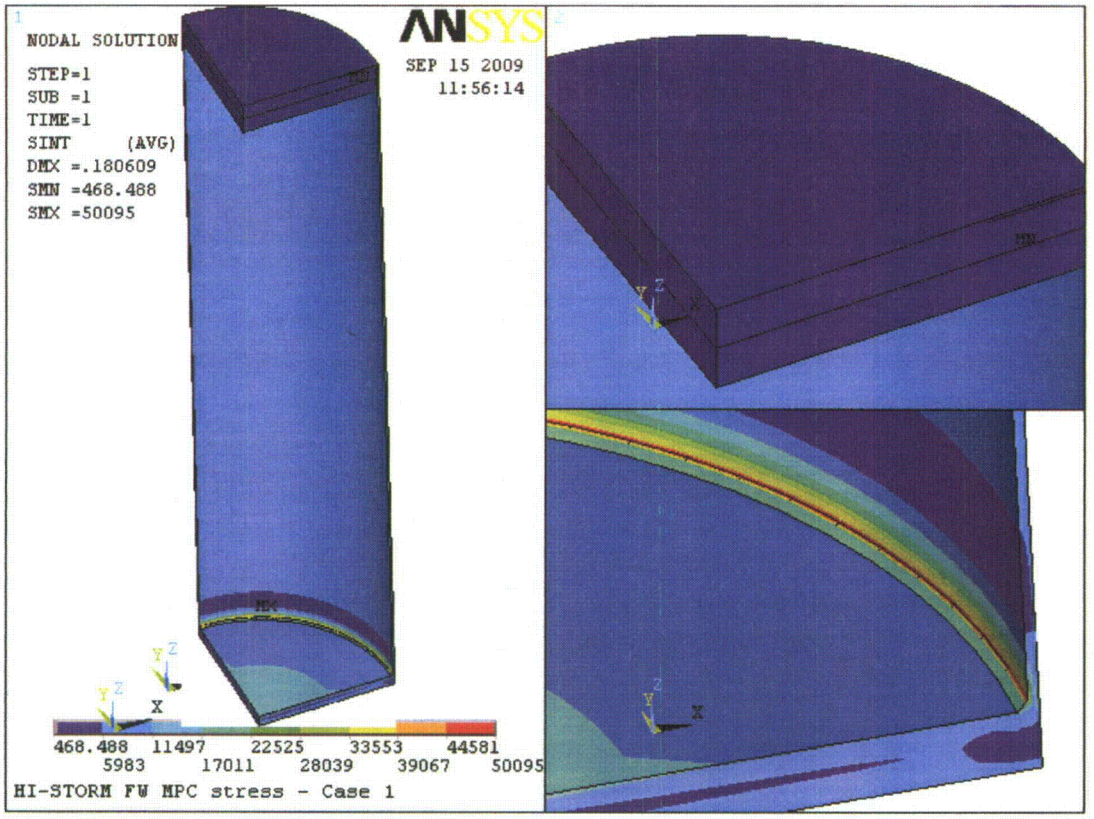

Figure 3.4.23: Stress Intensity Distribution in MPC Enclosure Vessel – Design Internal Pressure

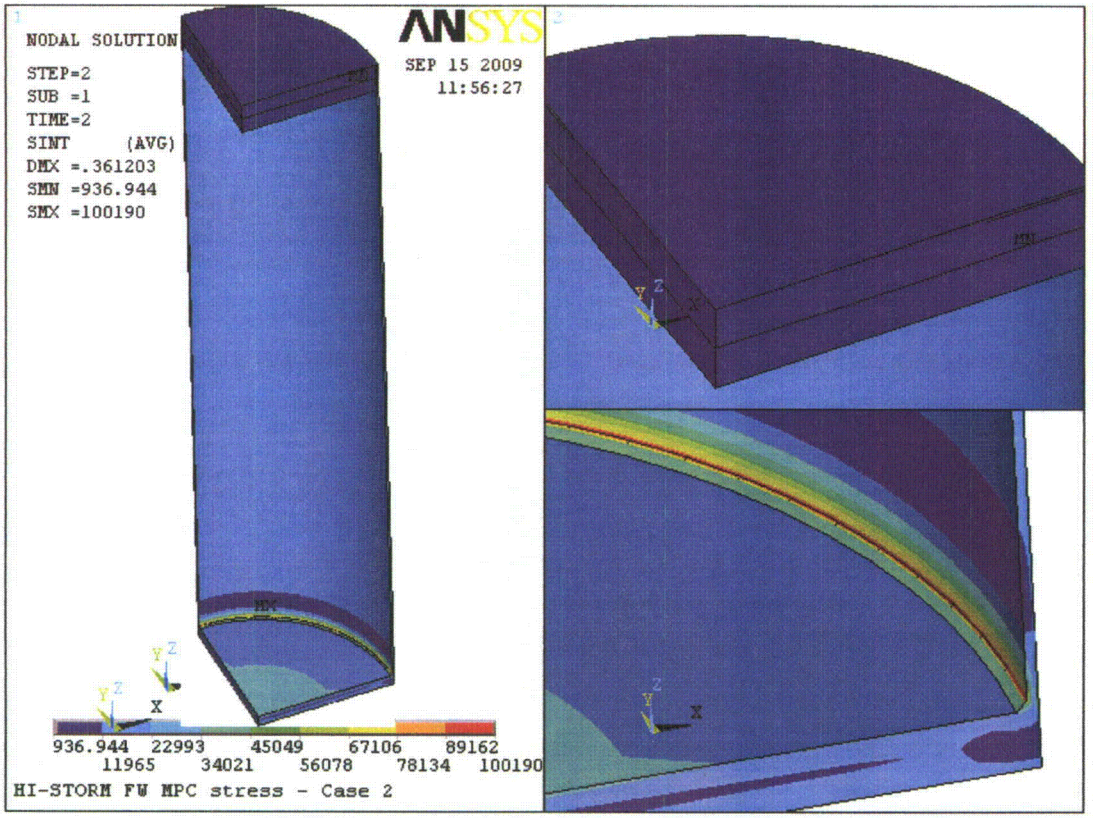

Figure 3.4.24: Stress Intensity Distribution in MPC Enclosure Vessel – Accident Internal Pressure

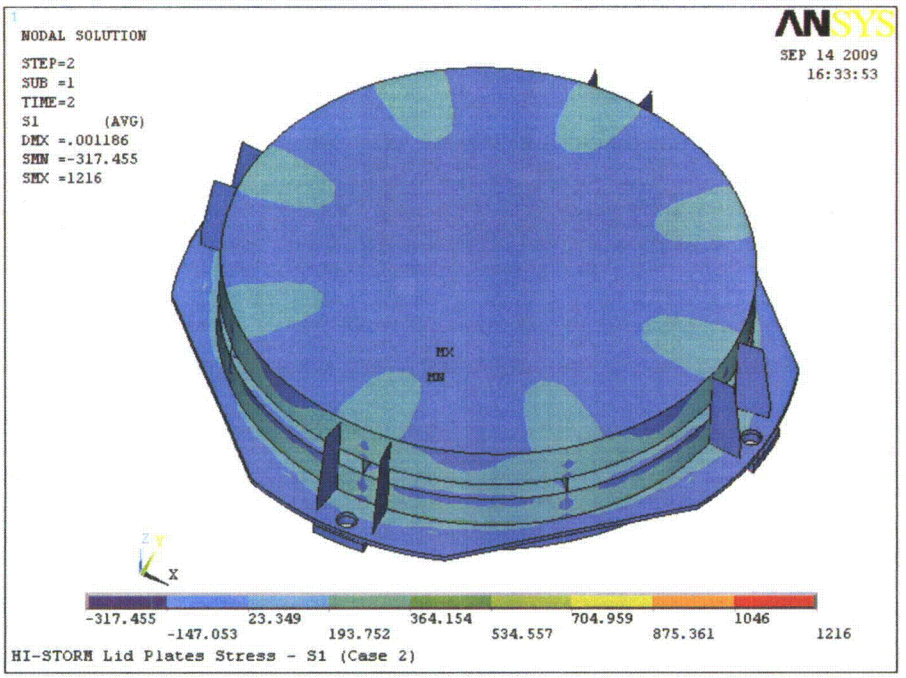

(a) S1 Principal Stress

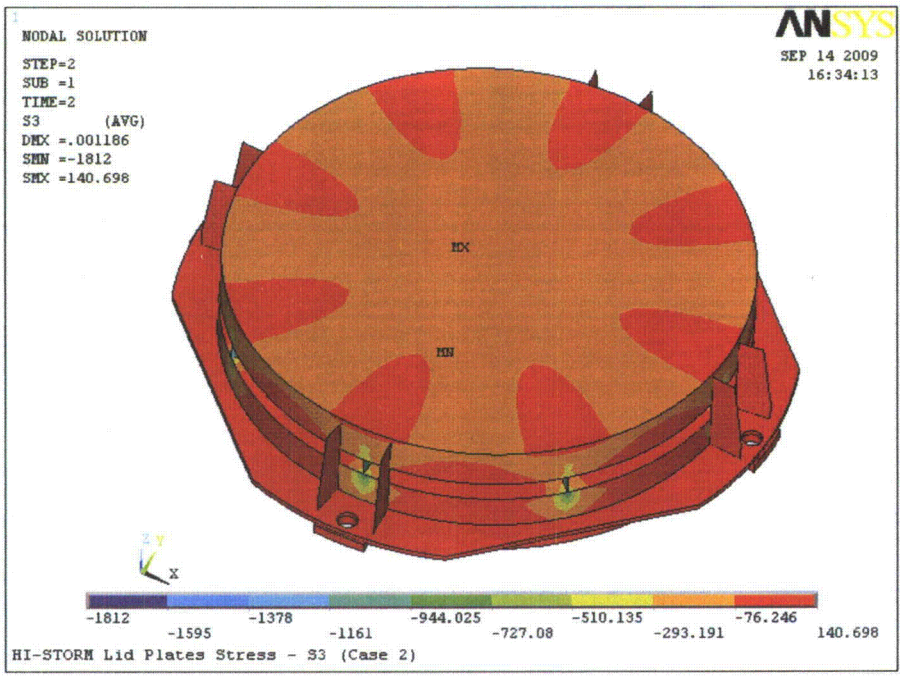

(b) S3 Principal Stress

Figure 3.4.25: Stress Distribution in HI-STORM FW Lid – Snow Load

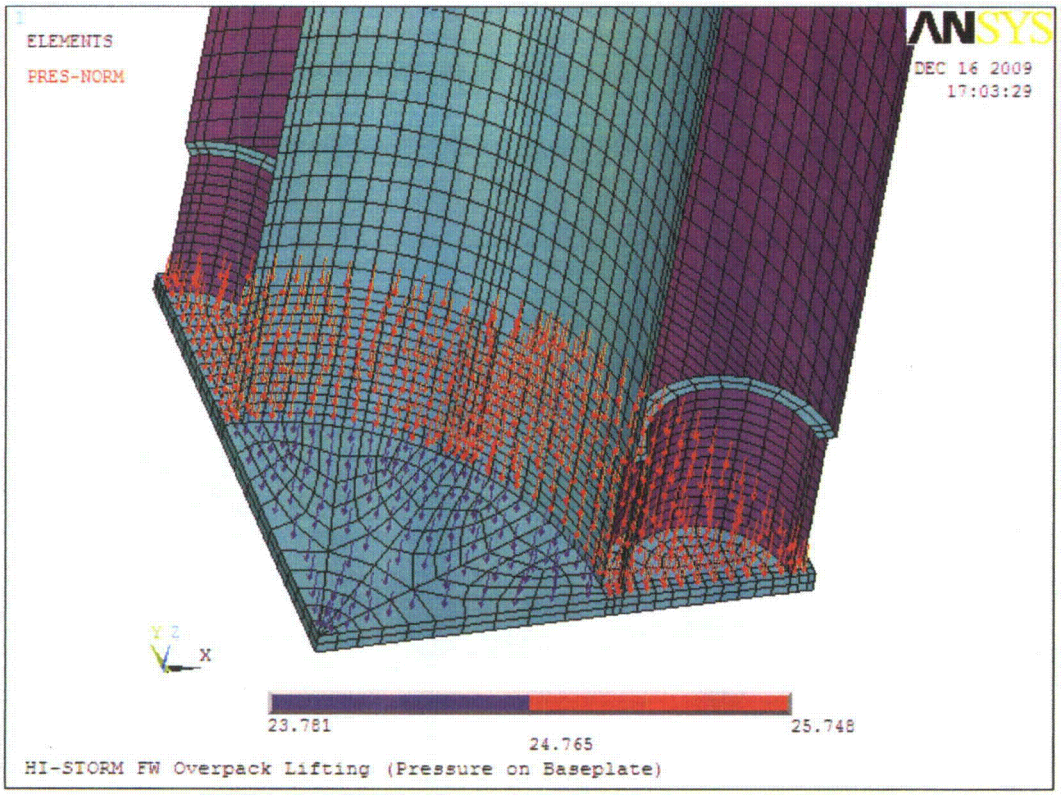

Figure 3.4.26: Applied Pressure on HI-STORM Baseplate Simulating Concrete Shielding and Loaded MPC

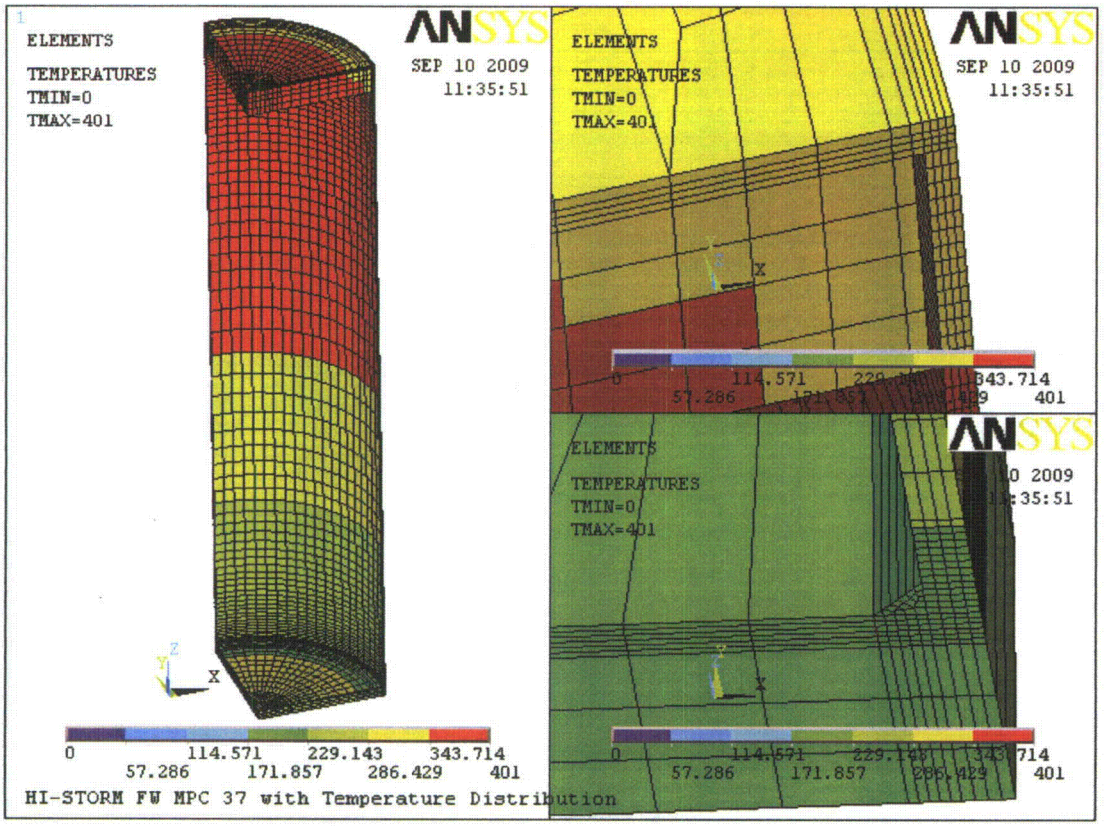

Figure 3.4.27: Normal Operating Temperature Distribution in MPC Enclosure Vessel

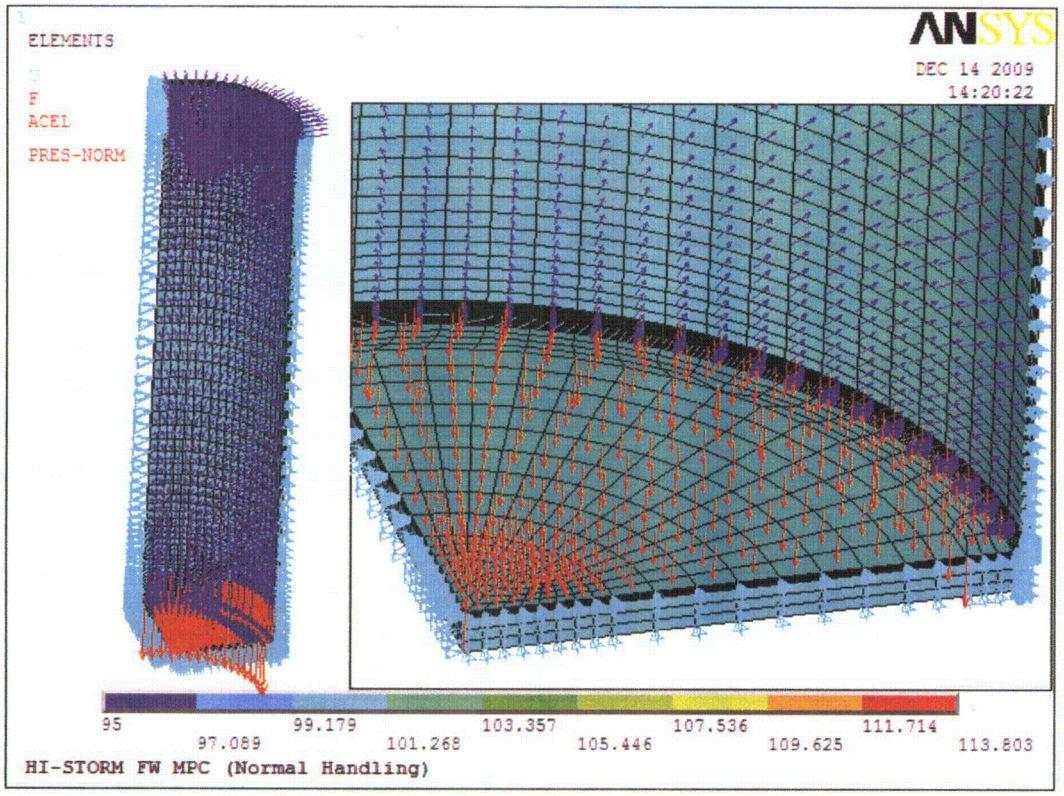

Figure 3.4.28: Normal Handling of MPC Enclosure Vessel – Boundary Conditions and Applied Loads

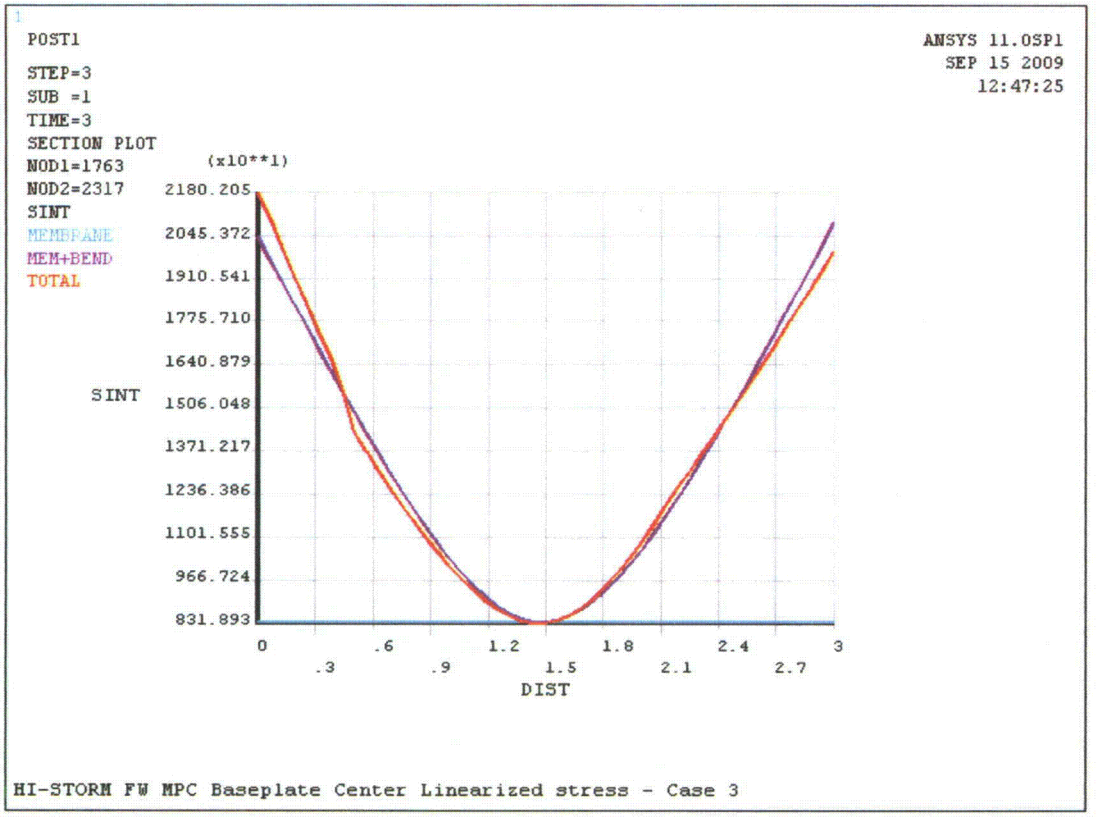

Figure 3.4.29: Normal Handling of MPC Enclosure Vessel –
Thru-Thickness Stress Intensity Plot at Baseplate Center

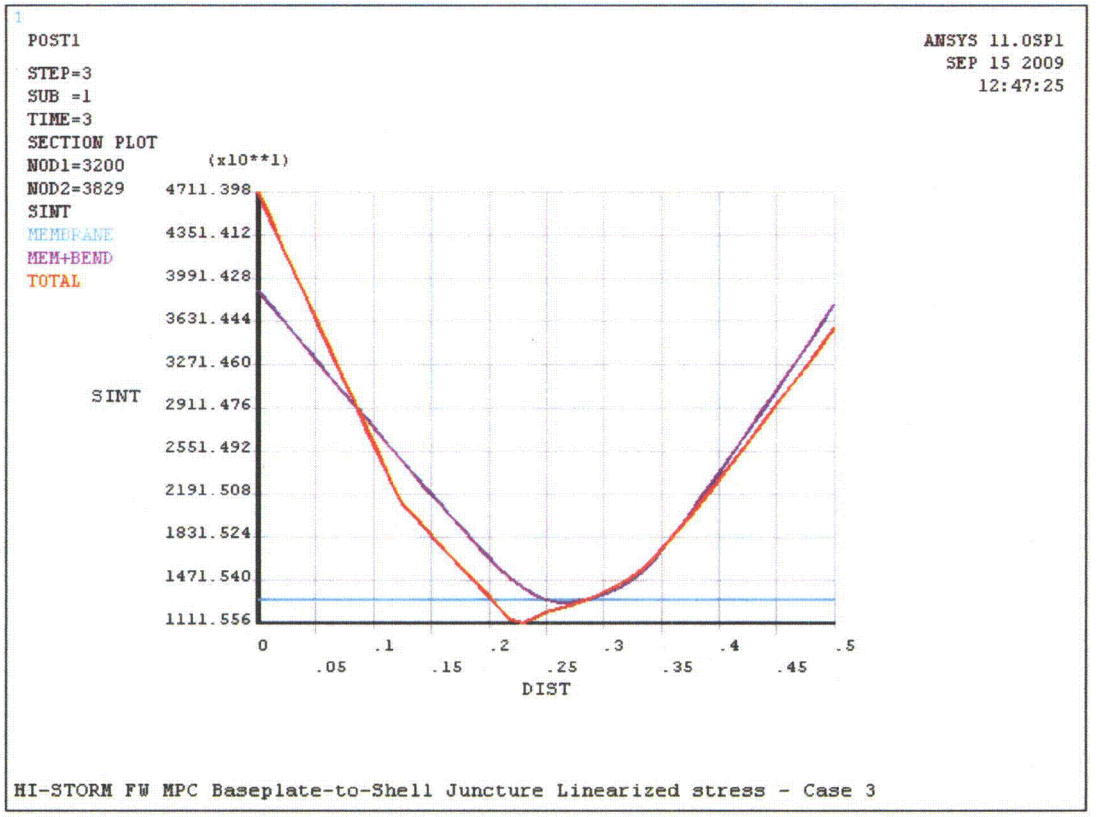

Figure 3.4.30: Normal Handling of MPC Enclosure Vessel –
Thru-Thickness Stress Intensity Plot at Baseplate-to-Shell Juncture

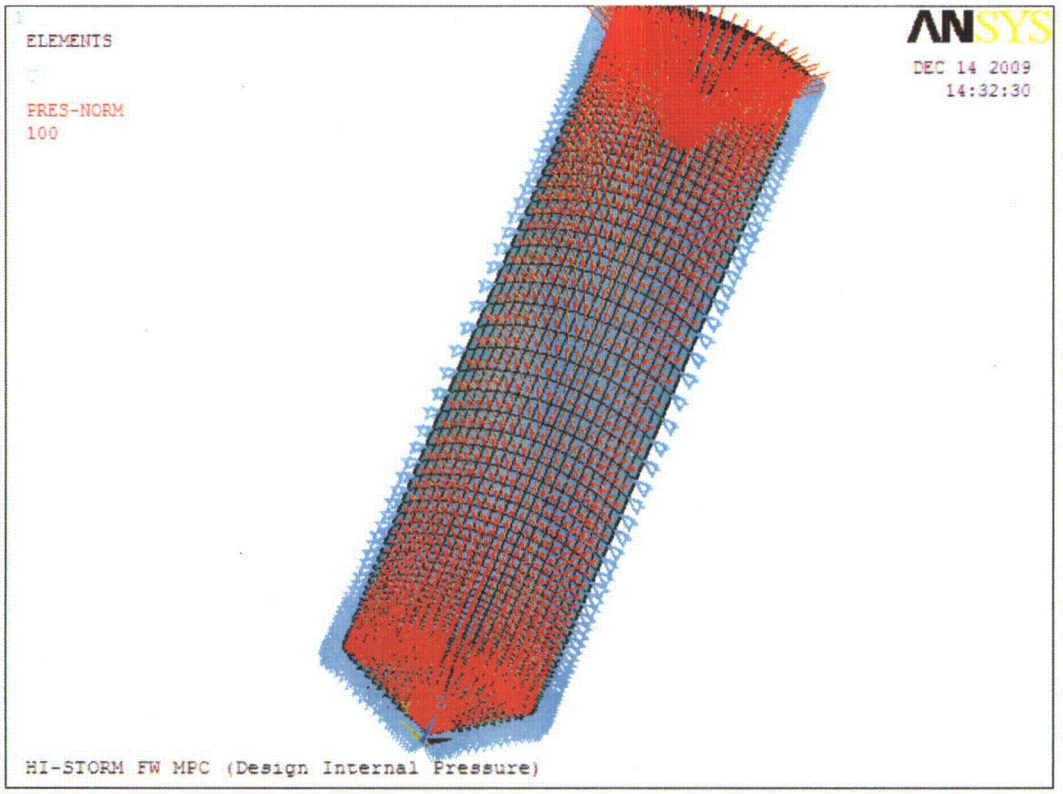

Figure 3.4.31: MPC Design Internal Pressure (Load Case 5) – Boundary Conditions and Applied Loads

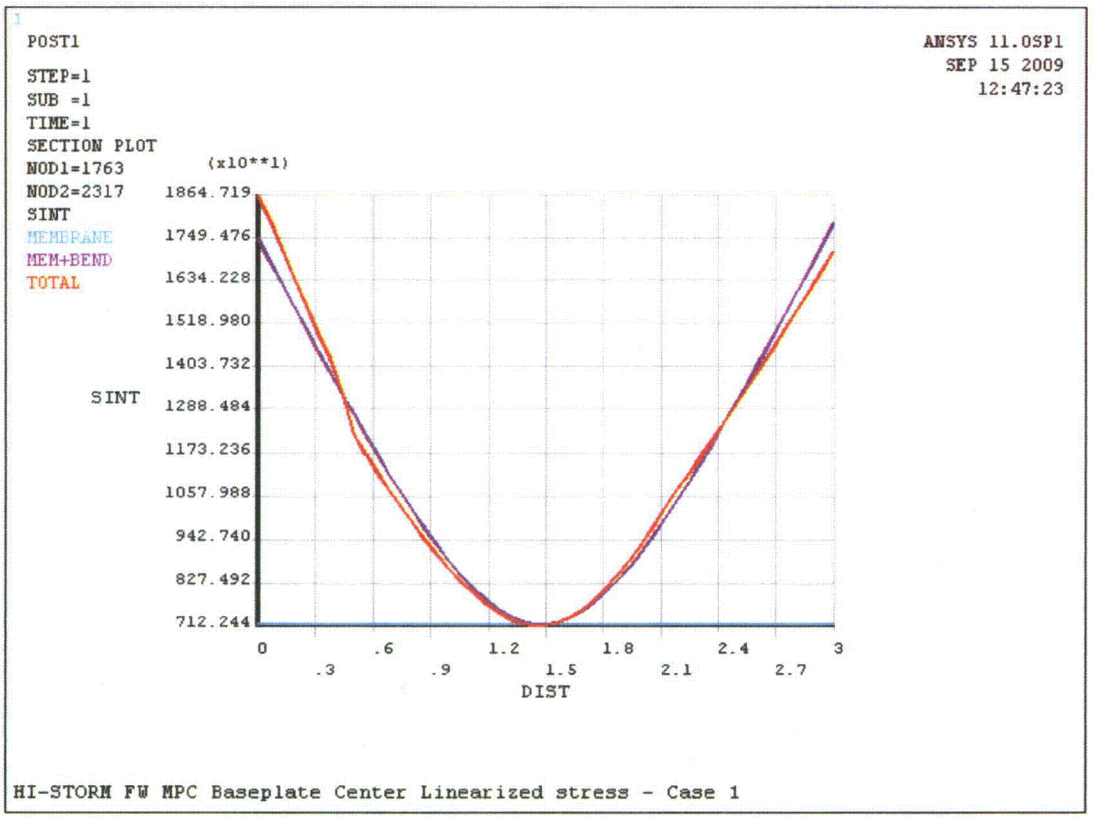

Figure 3.4.32: MPC Design Internal Pressure (Load Case 5) –
Thru-Thickness Stress Intensity Plot at Baseplate Center

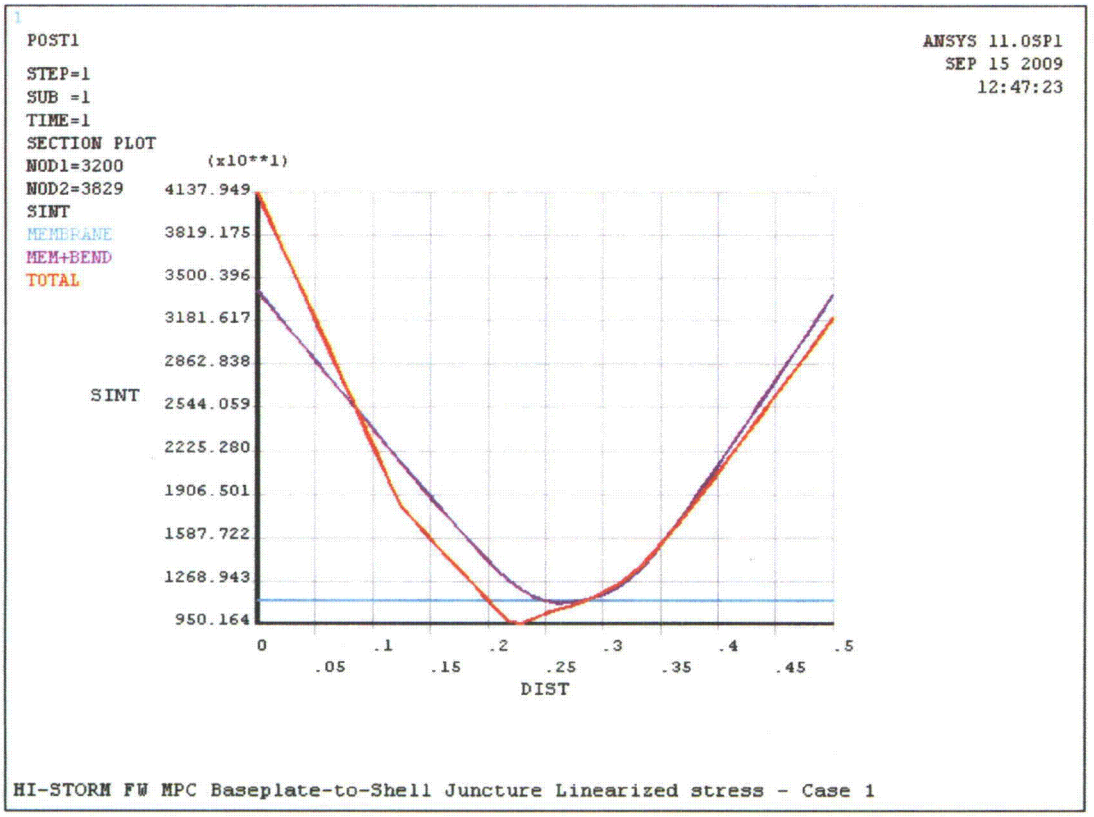

Figure 3.4.33: MPC Design Internal Pressure (Load Case 5) –
Thru-Thickness Stress Intensity Plot at Baseplate-to-Shell Juncture

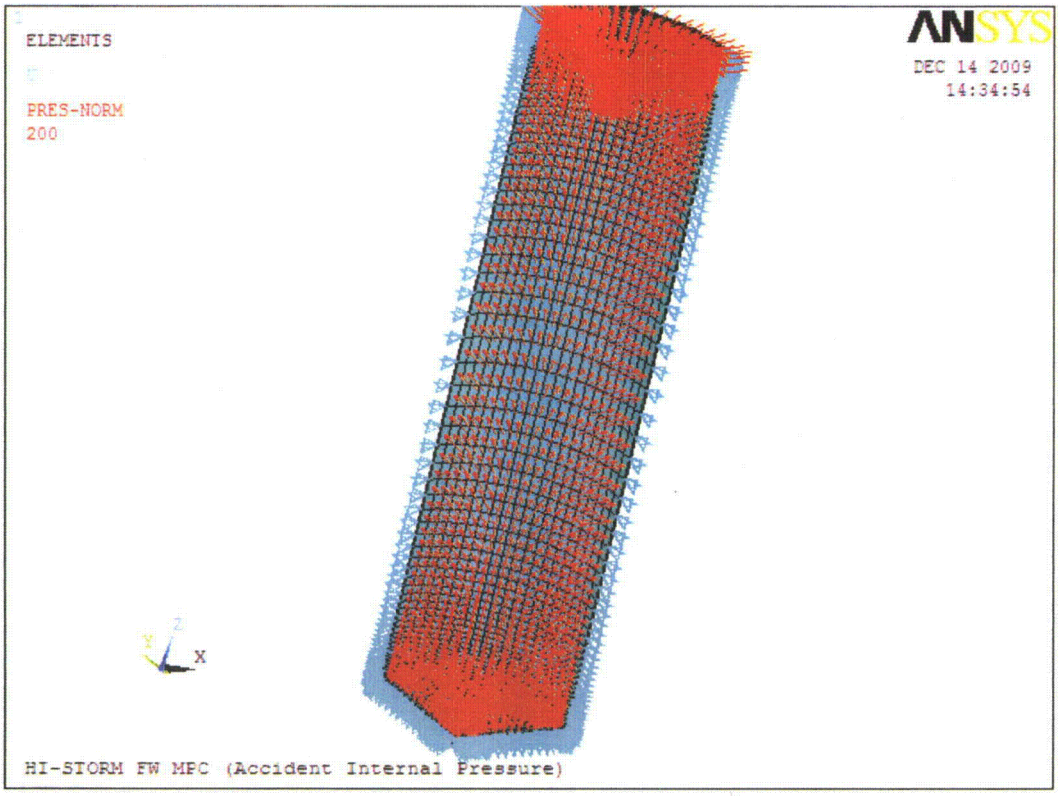

Figure 3.4.34: MPC Accident Internal Pressure (Load Case 6) – Boundary Conditions and Applied Loads

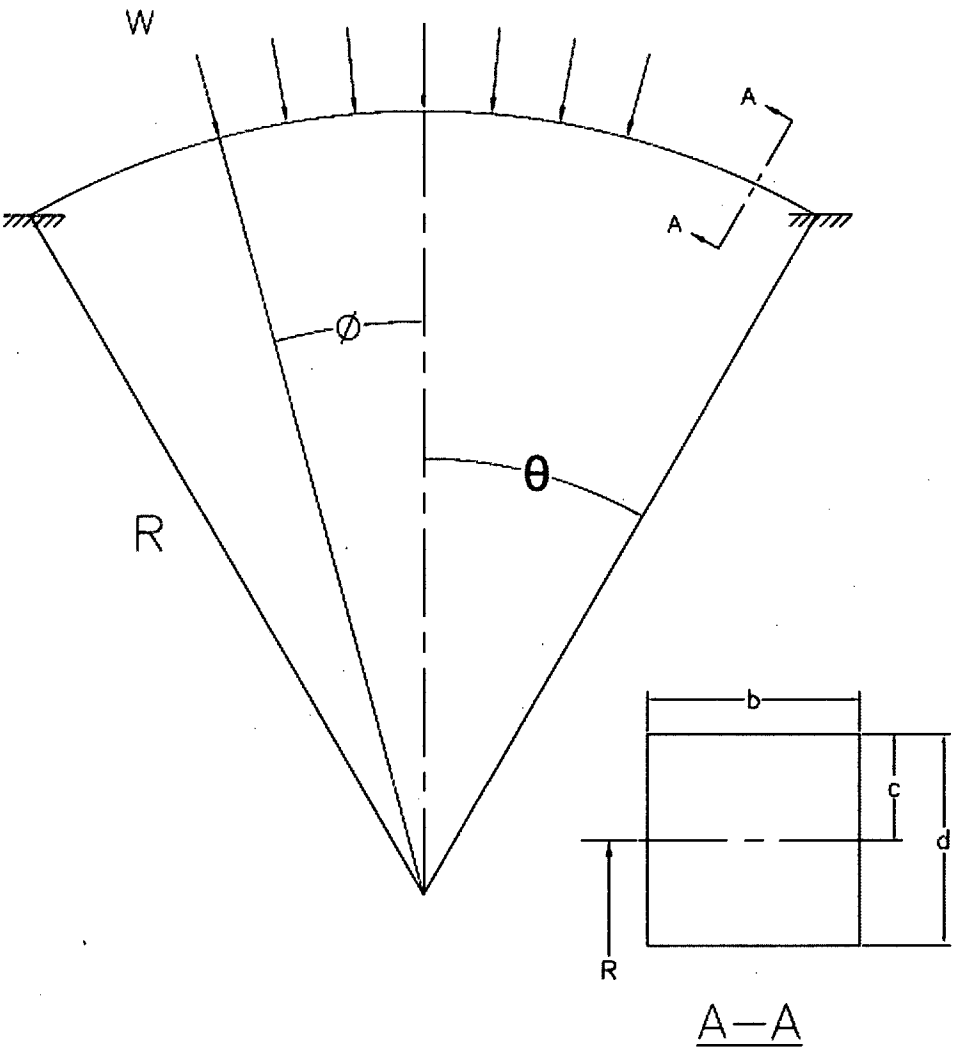

Figure 3.4.35: Analytical Model of HI-TRAC Water Jacket Shell (Load Case 8)

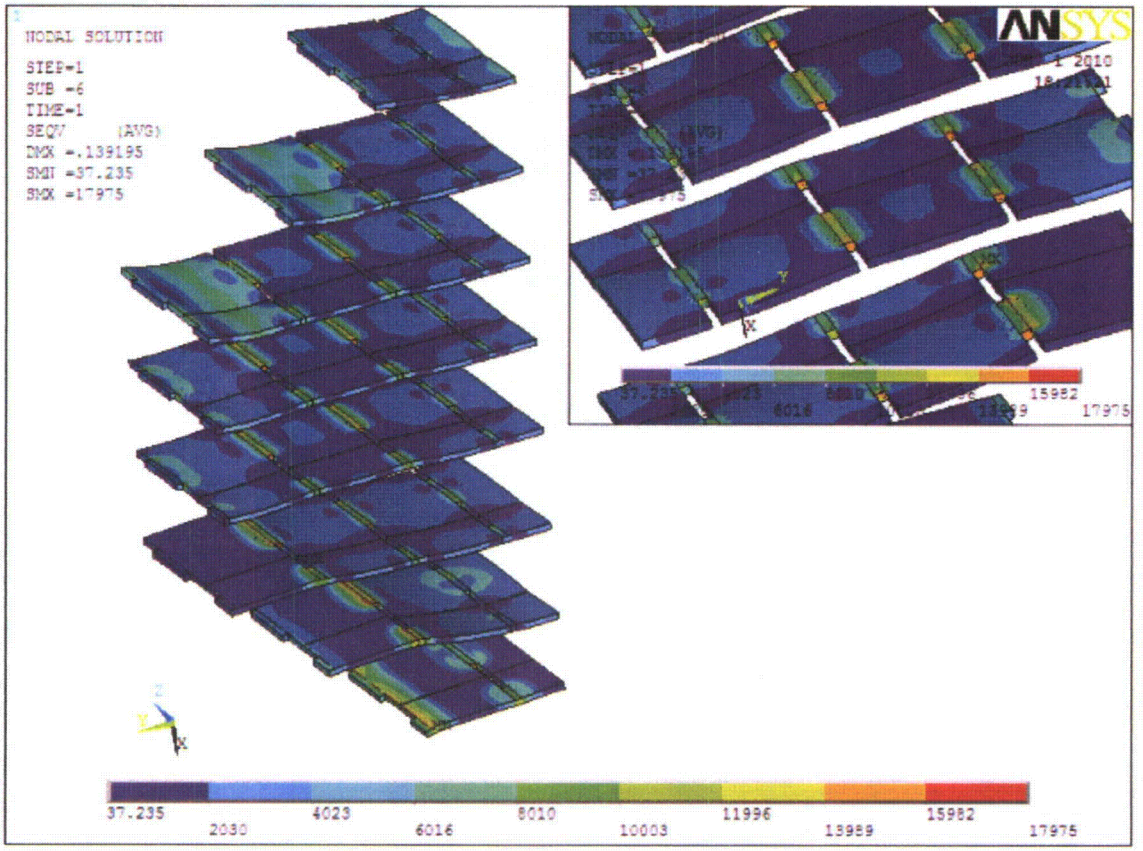

Figure 3.4.36: Stress Distribution in MPC-37 Fuel Basket (Horizontal Panels Only) under 65-g Static Load

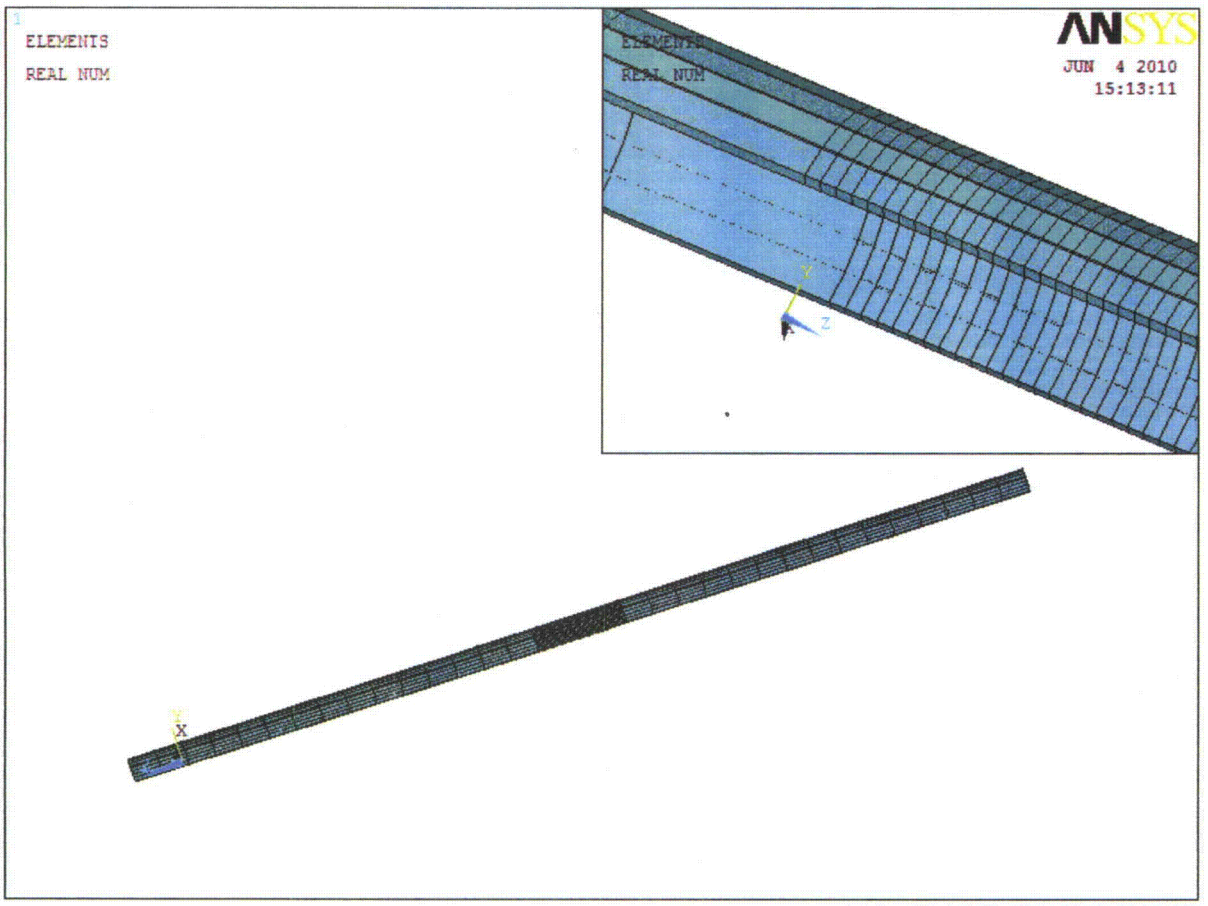

Figure 3.4.37: Finite Element Model for Fuel Rod Integrity Analysis (Load Case 11)

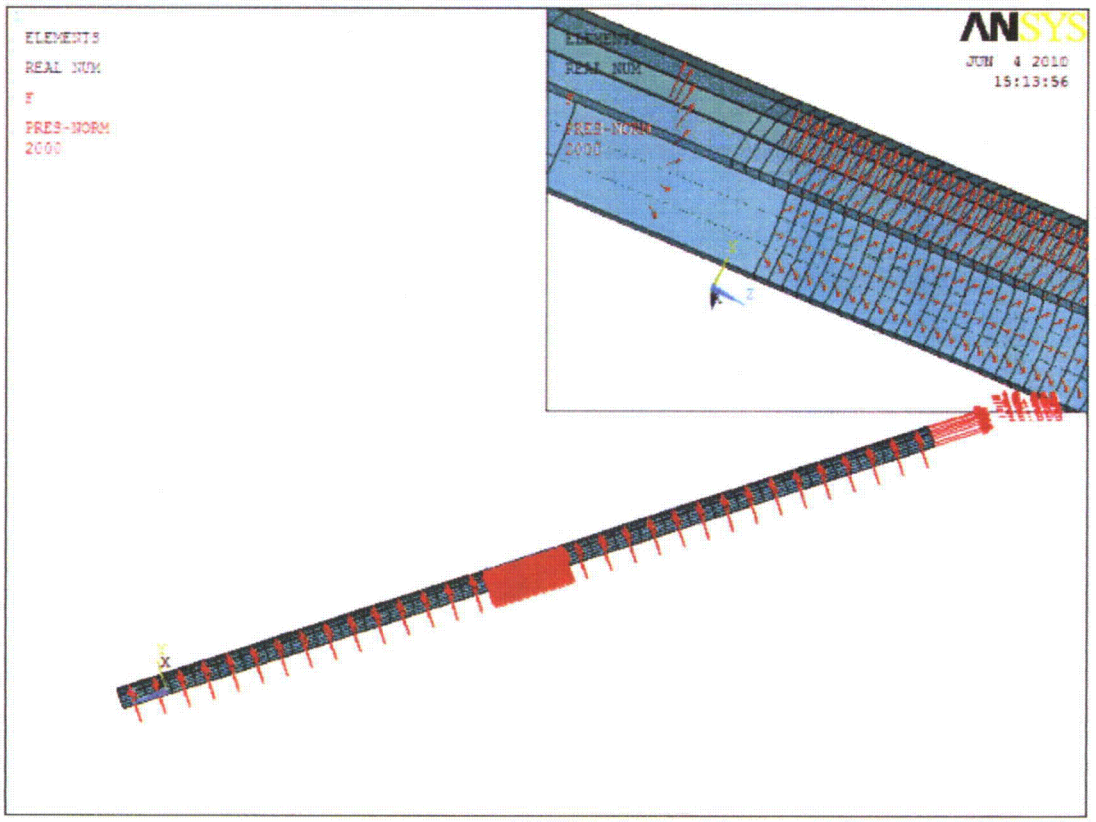

Figure 3.4.38: Applied Loads for Fuel Rod Integrity Analysis (Load Case 11)

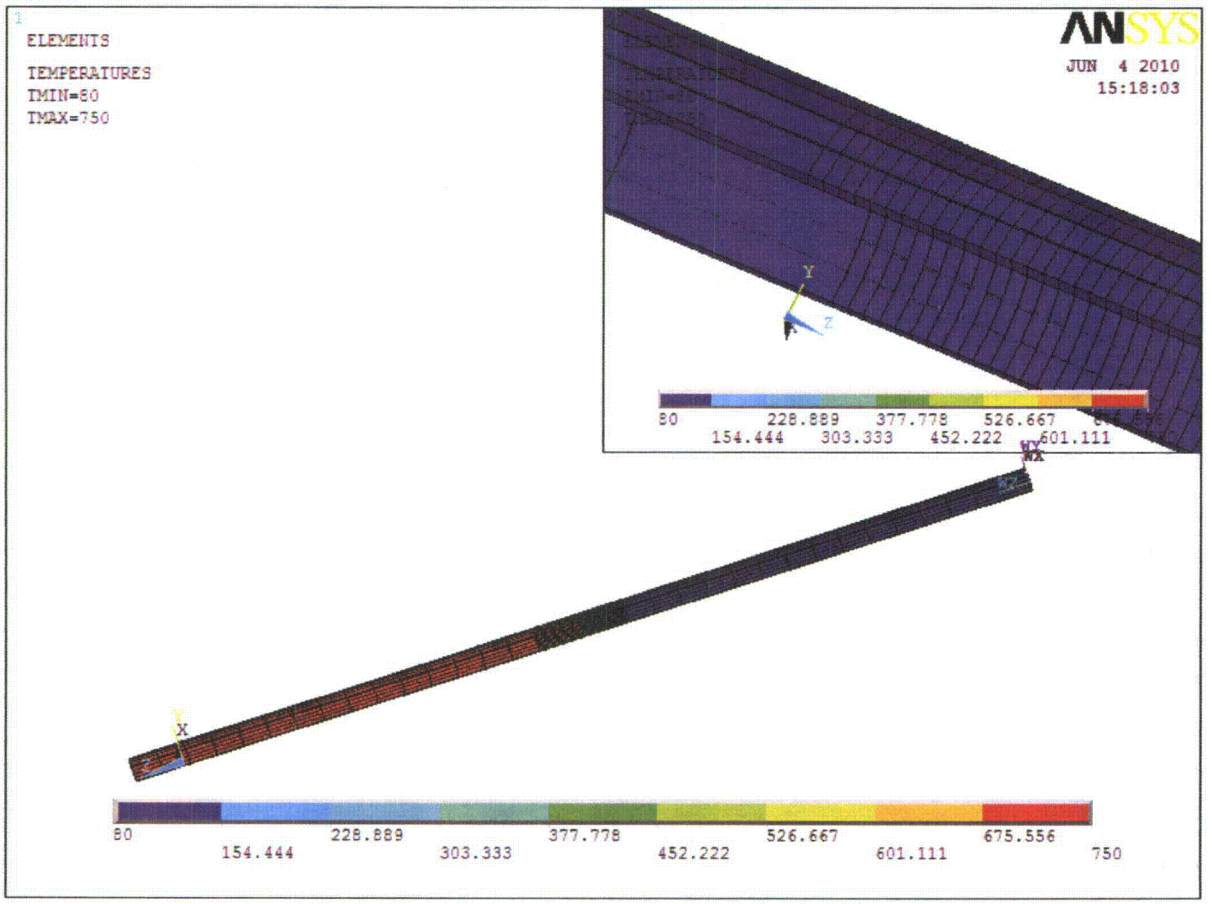

Figure 3.4.39: Applied Temperatures for Fuel Rod Integrity Analysis (Load Case 11)

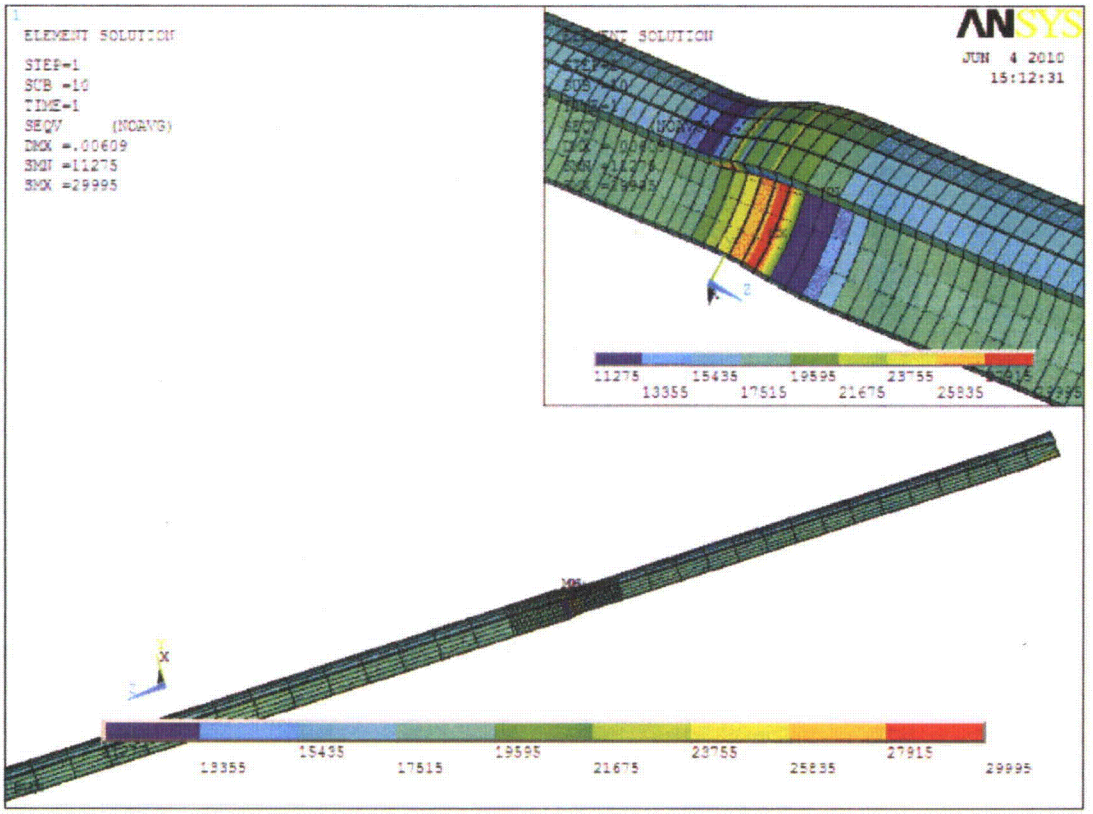

Figure 3.4.40: Stress Distribution in Fuel Rod Due to MPC Reflood (Load Case 11)

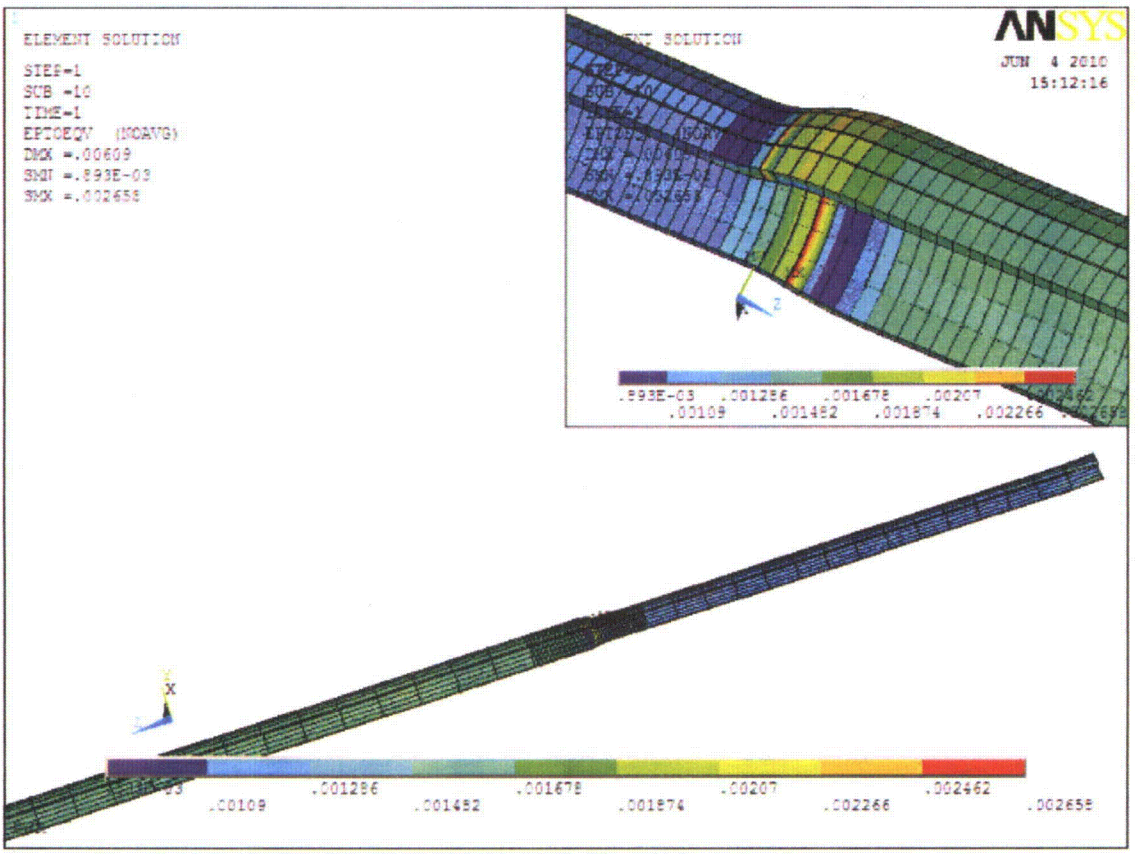

Figure 3.4.41: Strain Distribution in Fuel Rod Due to MPC Reflood (Load Case 11)

3.5 FUEL RODS

The regulations governing spent fuel storage cask approval and fabrication (10 CFR 72.236) require that a storage cask system "will reasonably maintain confinement of radioactive material under normal, off-normal, and credible accident conditions" (§72.236(l)). Although the cladding of intact fuel rods does provide a barrier against the release of radioactive fission products, the confinement evaluation for the HI-STORM FW system (Chapter 7) takes no credit for fuel cladding integrity in satisfying the regulatory confinement requirement.

As described in Section 7.1, the Confinement Boundary in the HI-STORM FW system consists of the MPC Enclosure Vessel. The Enclosure Vessel is designed and, to the extent practicable, manufactured in accordance with the most stringent ASME B&PV Code (Section III, Subsection NB). As required by NB, all materials are 100% UT inspected and all butt welds are subjected to 100% volumetric inspection. The field closure features redundant barriers (the MPC lid and port cover plates are the primary barriers, the closure ring is the secondary barrier). Section 7.1 further describes that the MPC design, welding, testing and inspection requirements meet the guidance of ISG-18 [7.1.2] such that leakage from the Confinement Boundary is non-credible. Section 7.2 addresses confinement for normal and off-normal conditions, and concludes that since the MPC confinement vessel remains intact, and the design bases temperatures and pressure are not exceeded, leakage from the MPC Confinement Boundary is not credible. Confinement for accident conditions is addressed in Section 7.3, which concludes that there is no mechanistic failure mode that could result in a breach of the Confinement Boundary, and escape of radioactive materials to the environment.

Since fuel rod cladding is not considered in the design criteria for the confinement of radioactive material under normal, off-normal, or accident conditions of storage, no specific analysis or test results are required to demonstrate cladding integrity.

SUPPLEMENTAL DATA

3.6.1 Calculation Packages

In addition to the calculations presented in Chapter 3, supporting calculation packages have been prepared to document other information pertinent to the analyses. Supporting calculation packages back up the summary results reported in the FSAR. The Calculation Packages are referenced in the body of the FSAR and are maintained as proprietary documents in Holtec's Configuration Control system.

3.6.2 Computer Programs

Two computer programs, all with a well established history of usage in the nuclear industry, have been utilized to perform structural and mechanical analyses documented in this FSAR. These codes are ANSYS and LS-DYNA. A third computer program, Visual Nastran, is also described below even though it is not explicitly used in this FSAR. It may, however, be used to perform the seismic stability evaluation of HI-STORM FW casks for a specific ISFSI site where NUREG/CR-6865 is not applicable (see Subsection 3.4.4.1.2).

i. ANSYS Mechanical

ANSYS is the original (and commonly used) name for ANSYS Mechanical general-purpose finite element analysis software. ANSYS Mechanical is the version of ANSYS commonly used for structural applications. It is a self contained analysis tool incorporating pre-processing (geometry creation, meshing), solver, and post processing modules in a unified graphical user interface. ANSYS Mechanical is a general purpose finite element modeling package for numerically solving a wide variety of mechanical problems. These problems include: static/dynamic structural analysis (both linear and non-linear), heat transfer and fluid problems, as well as acoustic and electro-magnetic problems.

ANSYS Mechanical has been independently QA validated by Holtec International and used for structural analysis of casks, fuel racks, pressure vessels, and a wide variety of SSCs, for over twenty years.

ii. LS-DYNA

LS-DYNA is a general purpose finite element code for analyzing the large deformation static and dynamic response of structures including structures coupled to fluids. The main solution methodology is based on explicit time integration and is therefore well suited for the examination of the response to shock loading. A contact-impact algorithm allows difficult contact problems to be easily treated. Spatial discretization is achieved by the use of four node tetrahedron and eight node solid elements, two node beam elements, three and four node shell elements, eight node solid shell

elements, truss elements, membrane elements, discrete elements, and rigid bodies. A variety of element formulations are available for each element type. Adaptive re-meshing is available for shell elements. LS-DYNA currently contains approximately one hundred constitutive models and ten equations-of-state to cover a wide range of material behavior.

In this safety analysis report, LS-DYNA is used to analyze all loading conditions that involve short-time dynamic effects.

LS-DYNA is maintained in a QA-validated status in Holtec's Configuration Control system.

iii. Visual Nastran

Visual Nastran [3.6.1] is used for rigid body motion simulation of the cask components, where a simplified analysis is appropriate. VisualNastran is a kinematics simulation code that includes large orientation change capability, simulation of impacts, and representation of contact and friction behavior. Visual Nastran Desktop (VN) performs time history dynamic analysis of freestanding structures using the acceleration time-histories in the three orthogonal directions as the input. It provides a complete articulation of the dynamic response of the rigid body, including sliding, precession, and tipping (and combinations thereof). Visual Nastran is maintained in a QA-validated status by Holtec International.

All three computer codes have been benchmarked and QA-validated to establish their veracity.

The compliance matrix below provides the necessary information to document their validation status, and the measures employed pursuant to ISG-21 and Holtec's QA program, to ensure error-free solutions.

ISG-21 and QA Compliance Matrix for Computer Codes				
	Item	ANSYS	LS-DYNA	Visual Nastran
1.	Benchmark and QA-validation are documented in Holtec Report No.(s) (Proprietary Reports)	HI-2012627	HI-961519	HI-2022896
2.	Computer Program Type (Public or Private Domain)	Public Domain	Public Domain	Public Domain
3.	Does Holtec maintain a system evaluating error notices if any are issued by the Code provider to evaluate their effect on the safety analyses carried out using the Code, including Part 21 notification? (Yes/No)	Yes	Yes	Yes
4.	Is the use of the Code restricted to personnel qualified under the Company's personnel qualification program? (Yes/No)	Yes	Yes	Yes
5.	Has benchmarking been performed against sample problems with known independently obtained numerical solutions (Yes/No)	Yes	Yes	Yes
6.	Have element types used in the safety analyses herein also employed in the benchmarking effort? (Yes/No)	Yes	Yes	N/A
7.	Are the element types used in this FSAR also used in other Holtec dockets that support other CoCs? (Yes/No)	Yes	Yes	N/A
8.	Is each update of the Code vetted for backwards consistency with prior updates? (Yes/No)	Yes	Yes	Yes
9.	Is the use of the Code limited to the range of parameters specified in the User Manual provided by the Code Developer? (Yes/No)	Yes	Yes	Yes
10.	Are the element aspect ratios, where applicable, used in the simulation model within the limit recommended by the Code Developer or Holtec's successful experience in other safety analyses? (Yes/No)	Yes	Yes	N/A
11.	Are element sizes used in the simulation models consistent with past successful analyses in safety significant applications? (Yes/No)	Yes	Yes	N/A
12.	Was every computer run in this chapter free of an error warning (i.e., in hidden warnings in the Code that indicate a possible error in the solution? (Yes/No)	Yes	Yes	N/A
13.	If the answer to the above is No, then is the annotated warning discussed in the discussion of the result in this report?	N/A	N/A	N/A

3.7 COMPLIANCE WITH THE STRUCTURAL REQUIREMENTS IN PART 72

Supporting information to provide reasonable assurance with respect to the adequacy of the HI-STORM FW system to store spent nuclear fuel in accordance with the stipulations of 10CFR72 is presented throughout this FSAR. The following statements are applicable to an affirmative structural safety evaluation:

- The design and structural analysis of the HI-STORM FW system is in compliance with the provisions of Chapter 3 of NUREG-1536 as applicable.

- The HI-STORM FW structures, systems, and components (SSC) that are important to safety (ITS) are identified in the licensing drawings in Section 1.5. The licensing drawings present the HI-STORM FW SSCs in adequate detail and the explanatory narratives in Sections 3.1 and 3.4 provide sufficient textual details to allow an independent evaluation of their structural effectiveness.

- The requirements of 10CFR72.24 with regard to information pertinent to structural evaluation is provided in Chapters 2, 3, and 12.

- Technical Specifications pertaining to the structures of the HI-STORM FW system have been provided in Chapter 13 herein pursuant to the requirements of 10CFR72.26.

- A series of analyses to demonstrate compliance with the requirements of 10CFR72.122(b) and (c), and 10CFR72.24(c)(3) have been performed which show that SSCs in the HI-STORM FW system designated as ITS possess an adequate margin of safety with respect to all load combinations applicable to normal, off-normal, accident, and natural phenomenon events. In particular, the following information is provided:

  i. Load combinations for the fuel basket, enclosure vessel, and the HI-STORM FW/HI-TRAC VW overpacks for normal, off-normal, accident, and natural phenomenon events are provided in Subsection 3.1.2.2.

  ii. Stress limits applicable to the Code materials are found in Section 3.3.

  iii. The stress and displacement response of the fuel basket, the enclosure vessel, and the HI-STORM FW/HI-TRAC VW overpacks for all applicable loads have been computed by analysis and reported in Subsections 3.4.3 and 3.4.4. Descriptions of stress analysis models are presented in Subsection 3.1.3.

- The structural design and fabrication details of the fuel baskets whose safety function

in the HI-STORM FW system is to maintain nuclear criticality safety, are provided in the drawings in Section 1.5. The structural factors of safety, summarized in Section 3.4 for all credible load combinations under normal, off-normal, accident, and natural phenomenon events demonstrate that the acceptance criteria are satisfied in all cases. In particular, the maximum lateral deflection in the fuel basket panels under accident events has been determined to be within the limit used in the criticality analysis (see Subsection 3.4.4.1.4). Thus, the requirement of 10CFR72.124(a), with respect to structural margins of safety for SSCs important to nuclear criticality safety are fully satisfied.

- Structural margins of safety during handling, packaging, and transfer operations, under the provisions of 10CFR Part 72.236(b), imply that the lifting and handling devices be engineered to comply with the stipulations of ANSI N14.6, NUREG-0612. The requirements of the governing standards for handling operations are summarized in Subsection 3.4.3 herein. Factors of safety for all ITS components under lifting and handling operations are summarized in tables in Section 3.4, which show that adequate structural margins exist in all cases.

- Consistent with the provisions of 10CFR72.236(i), the Confinement Boundary for the HI-STORM FW system has been engineered to maintain confinement of radioactive materials under normal, off-normal, and postulated accident conditions. This assertion of confinement integrity is made on the strength of the following information provided in this FSAR.

  i. The MPC Enclosure Vessel which constitutes the Confinement Boundary is designed and fabricated in accordance with Section III, Subsection NB (Class 1 nuclear components) of the ASME Code to the maximum extent practicable.

  ii. The primary lid of the MPC Enclosure Vessel is welded using a strength groove weld and is subjected to multiple liquid penetrant examinations and pressure testing to establish a maximum confidence in weld joint integrity.

  iii. The closure system of the MPC Enclosure Vessel consists of *two* independent isolation barriers.

  iv. The Confinement Boundary is constructed from stainless steel alloys with a proven history of material integrity under the environmental conditions of an ISFSI.

  v. The load combinations for normal, off-normal, accident, and natural phenomena events have been compiled and applied on the MPC Enclosure Vessel (Confinement Boundary). The results, summarized in Section 3.4, show that the factor of safety (with respect to the appropriate limits) is

greater than one in all cases. Design Basis natural phenomena events such as tornado-borne missiles (large, intermediate, or small) have also been analyzed to evaluate their potential for reaching and breaching the Confinement Boundary. Analyses presented in Section 3.4 and supplemented by Appendices 3.A and 3.B show that the integrity of the Confinement Boundary is preserved under all design basis projectile impact scenarios.

- The information on structural design included in this FSAR complies with the requirements of 10CFR72.120 and 10CFR72.122.

- The structural design features in the HI-STORM FW system are in compliance with the specific requirements of 10CFR72.236(e), (f), (g), (h), (i), (j), (k), and (m).

3.8 REFERENCES

[3.1.1] NUREG-0612, "Control of Heavy Loads at Nuclear Power Plants," United States Nuclear Regulatory Commission.

[3.1.2] ANSI N14.6-1993, "American National Standard for Special Lifting Devices for Shipping Containers Weighing 10000 Pounds (4500 kg) or More for Nuclear Materials," American National Standards Institute, Inc.

[3.1.3] D. Burgreen, "Design Methods for Power Plant Structures", Arcturus Publishers, 1975.

[3.1.4] HI-STORM 100 FSAR, Holtec Report No. HI-2002444, Revision 7 [USNRC Docket 72-1014].

[3.1.5] NUREG/CR-1815, "Recommendations for Protecting Against Failure by Brittle Fracture in Ferritic Steel Shipping Containers Up to Four Inches Thick"

[3.1.6] Aerospace Structural Metals Handbook, Manson.

[3.1.7] SHAKE2000, A Computer Program for the 1-D Analysis of Geotechnical Earthquake Engineering Problems, G.A. Ordonez, Dec. 2000.

[3.1.8] LS-DYNA, Version 971, Livermore Software Technology, 2006.

[3.1.9] "Construction of True-Stress-True-Strain Curves for LS-DYNA Simulations," Holtec Proprietary Position Paper DS-307, Revision 2.*

[3.1.10] HI-STAR 180 SAR, Holtec Report No. HI-2073681, Revision 3 [USNRC Docket 71-9325].

[3.3.1] ASME Boiler & Pressure Vessel Code, Section II, Part D, 2007.

[3.3.2] HI-STAR 60 SAR, Holtec Report No. HI-2073710, Revision 2 [USNRC Docket 71-9336].

[3.3.3] Holtec Proprietary Report HI-2043215, "Sourcebook for Metamic Performance Assessment", Revision 2.

* Supporting document submitted with the HI-STORM FW License Application (Docket 72-1032).

[3.3.4] Holtec Proprietary Report HI-2043162, "Spent Fuel Storage Expansion at Diablo Canyon Power Plant for Pacific Gas and Electric Co.", Revision 1 (USNRC Docket Nos. 50-275 and 50-323).

[3.3.5] American Concrete Institute, ACI-318-05.

[3.3.6] American Concrete Institute, "Code Requirements for Nuclear Safety Related Structures" (ACI-349-85) and Commentary (ACI-349R-85).

[3.3.7] J.H. Evans, "Structural Analysis of Shipping Casks, Volume 8, Experimental Study of Stress-Strain Properties of Lead Under Specified Impact Conditions", ORNL/TM-1312, Vol. 8, ORNL, Oak Ridge, TN, August, 1970.

[3.4.1] ANSYS 11.0, ANSYS, Inc., 2007.

[3.4.2] ASME Boiler & Pressure Vessel Code, Section III, Subsection NF, 2007.

[3.4.3] ASME Boiler & Pressure Vessel Code, Section III, Appendices, 2007.

[3.4.4] ASME Boiler & Pressure Vessel Code, Section III, Subsection NB, 2007.

[3.4.5] Witte, M., et al., "Evaluation of Low-Velocity Impacts Tests of Solid Steel Billet onto Concrete Pads, and Application to Generic ISFSI Storage Cask for Tipover and Side Drop", Lawrence Livermore National Laboratory, UCRL-ID-126295, Livermore, California, March 1997.

[3.4.6] Doug Ammerman and Gordon Bjorkman, "Strain-Based Acceptance Criteria for Section III of the ASME Boiler and Pressure Vessel Code", Proceedings of the 15th International Symposium on the Packaging and Transportation of Radioactive Materials, PATRAM 2007, October 21-26, 2007, Miami, Florida, USA.

[3.4.7] NUREG/CR-6865, "Parametric Evaluation of Seismic Behavior of Freestanding Spent Fuel Dry Storage Systems," 2005.

[3.4.8] NUREG-0800, "Standard Review Plan for the Review of Safety Analysis Reports for Nuclear Power Plants," Section No. 3.7.1, 1989.

[3.4.9] Bechtel Topical Report BC-TOP-9A, "Design of Structures for Missile Impact", Revision 2 (September 1974).

[3.4.10] 10CFR71, Waste Confidence Decision Review, USNRC, September 11, 1990.

[3.4.11] Holtec Proprietary Report HI-2094353, "Analysis of the Non-Mechanistic Tipover Event of the Loaded HI-STORM FW Storage Cask", Latest Revision.

[3.4.12] Oberg, E. et. al., Machinery's Handbook, Industrial Press Inc., 27th Edition.

[3.4.13] Holtec Proprietary Report HI-2094418, "Structural Calculation Package for HI-STORM FW System", Latest Revision.

[3.4.14] EPRI NP-440, Full Scale Tornado Missile Impact Tests, 1977.

[3.4.15] Holtec Proprietary Report HI-2094392, "Tornado Missile Analysis for HI-STORM FW System", Latest Revision.

[3.4.16] Young, W., Roark's Formulas for Stress & Strain, McGraw Hill Book Company, 6th Edition.

[3.4.17] Interim Staff Guidance - 15, "Materials Evaluation", Revision 0.

[3.4.18] Timoshenko, S., Strength of Materials (Part II), Third Edition, 1958.

[3.4.19] "Mechanical Testing and Evaluation", ASM Handbook, Volume 8, 2000.

[3.4.20] Adkins, H.E., Koeppel, B.J., Tang, D.T., "Spent Nuclear Fuel Structural Response When Subject to an End Drop Impact Accident," Proceedings ASME/JSME Pressure Vessels and Piping Conference, PVP-Vol. 483, American Society of Mechanical Engineers, New York, New York, 2004.

[3.4.21] Chun, R., Witte, M., Schwartz, M., "Dynamic Impact Effects on Spent Fuel Assemblies", Lawrence Livermore National Laboratory, Report UCID-21246, 1987.

[3.4.22] Rust, J.H., Nuclear Power Plant Engineering, Haralson Publishing Company, 1979.

[3.4.23] NUREG/CR-1864, "A Pilot Probabilistic Risk Assessment of a Dry Cask Storage System at a Nuclear Power Plant", USNRC, Washington D.C., 2007.

[3.4.24] EPRI TR-103949, "Temperature Limit Determination for the Inert Dry Storage of Spent Nuclear Fuel", May 1994.

[3.6.1] Visual Nastran 2004, MSC Software, 2004.

APPENDIX 3.A - RESPONSE OF HI-STORM FW AND HI-TRAC VW TO TORNADO WIND LOAD AND LARGE MISSILE IMPACT

Withheld in Accordance with 10 CFR 2.390

APPENDIX 3.B - MISSILE PENETRATION ANALYSES FOR HI-STORM FW AND HI-TRAC VW

Withheld in Accordance with 10 CFR 2.390

APPENDIX 3.C - CODE CASE N-284-2 STABILITY CALCULATIONS FOR MPC SHELL

Withheld in Accordance with 10 CFR 2.390

CHAPTER 4* THERMAL EVALUATION

4.0 OVERVIEW

The HI-STORM FW system is designed for long-term storage of spent nuclear fuel (SNF) in a vertical orientation. The design envisages an array of HI-STORM FW systems laid out in a rectilinear pattern stored on a concrete ISFSI pad in an open environment. In this chapter, compliance of HI-STORM FW system's thermal performance to 10CFR72 requirements for outdoor storage at an ISFSI using 3-D thermal simulation models is established. The analyses consider passive rejection of decay heat from the stored SNF assemblies to the environment under normal, off-normal, and accident conditions of storage. Finally, the thermal margins of safety for long-term storage of both moderate burnup (up to 45,000 MWD/MTU) and high burnup spent nuclear fuel (greater than 45,000 MWD/MTU) in the HI-STORM FW system are quantified. Safe thermal performance during on-site loading, unloading and transfer operations, collectively referred to as "short-term operations" utilizing the HI-TRAC VW transfer cask is also evaluated.

The HI-STORM FW thermal evaluation follows the guidelines of NUREG-1536 [4.4.1] and ISG-11 [4.1.4]. These guidelines provide specific limits on the permissible maximum cladding temperature in the stored commercial spent fuel (CSF)† and other Confinement Boundary components, and on the maximum permissible pressure in the confinement space under certain operating scenarios. Specifically, the requirements are:

1. The fuel cladding temperature must meet the temperature limit appropriate to its burnup level and condition of storage or handling set forth in Table 4.3.1.
2. The maximum internal pressure of the MPC should remain within its design pressures for normal, off-normal, and accident conditions set forth in Table 2.2.1.
3. The temperatures of the cask materials shall remain below their allowable limits set forth in Table 2.2.3 under all scenarios.

As demonstrated in this chapter, the HI-STORM FW system is designed to comply with all of the criteria listed above. Sections 4.1 through 4.3 describe thermal analyses and input data that are common to all conditions of storage, handling and on-site transfer operations. All thermal analyses to evaluate normal conditions of storage in a HI-STORM FW storage module are described in Section 4.4. All thermal analyses to evaluate normal handling and on-site transfer in a HI-TRAC VW transfer cask are described in Section 4.5. All thermal analyses to evaluate off-normal and accident conditions are described in Section 4.6. This SAR chapter is in full compliance with ISG-11 and with NUREG-1536 guidelines, subject to the exceptions and clarifications discussed in Chapter 1, Table 1.0.3.

---

* This chapter has been prepared in the format and section organization set forth in Regulatory Guide 3.61. However, the material content of this chapter also fulfills the requirements of NUREG-1536. Pagination and numbering of sections, figures, and tables are consistent with the convention set down in Chapter 1, Section 1.0, herein. All terms-of-art used in this chapter are consistent with the terminology of the Glossary. Finally, all evaluations and results presented in this Chapter are supported by calculation packages cited herein (References [4.1.9] and [4.1.10]).

† Defined as nuclear fuel that is used to produce energy in a commercial nuclear reactor (See Glossary).

As explained in Section 1.2, the storage of SNF in the fuel baskets in the HI-STORM FW system is configured for a three-region storage system. Figures 1.2.1 and 1.2.2 provide the information on the location of the regions and Tables 1.2.3 and 1.2.4 provide the permissible specific heat load (heat load per fuel assembly) in each region for the PWR and BWR MPCs, respectively. The Specific Heat Load (SHL) values in each region are guided by the following considerations of ALARA and preservation of fuel integrity in long-term storage.

- Region I: Located in the core region of the basket is permitted to store fuel with medium specific heat load.
- Region II: This is the intermediate region flanked by the core region (Region I) from the inside and the peripheral region (Region III) on the outside. This region has the maximum SHL in the basket.
- Region III: Located in the peripheral region of the basket, this region has the smallest SHL. Because a low SHL means a low radiation dose emitted by the fuel, the low heat emitting fuel around the periphery of the basket serves to block the radiation from the Region II fuel, thus reducing the total quantity of radiation emanating from the MPC in the lateral direction.

Thus, the 3-region arrangement serves to minimize the peak fuel cladding temperature in the MPC as well as the radiation dose from the MPC. By limiting the SHL in the core region of the basket, core temperature gradients in the radial direction are minimized, thus minimizing thermal stresses in the fuel and fuel basket. The salutary consequences of this regionalized loading arrangement become evident from the computed peak cladding temperatures in this chapter, which show a large margin to the ISG-11 limit discussed earlier.

4.1 DISCUSSION

The aboveground HI-STORM FW system consists of a sealed MPC situated inside a vertically-oriented, ventilated storage overpack. Air inlet and outlet ducts that allow for air cooling of the stored MPC are located at the bottom and top, respectively, of the cylindrical overpack (see Figure 4.1.1). The SNF assemblies reside inside the MPC, which is sealed with a welded lid to form the Confinement Boundary. The MPC contains a Metamic-HT egg-crate fuel basket structure with square-shaped compartments of appropriate dimensions to allow insertion of the fuel assemblies prior to welding of the MPC lid and closure ring. The MPC is backfilled with helium to the design-basis pressures (Table 4.4.8). This provides a stable, inert environment for long-term storage of the SNF. Heat is rejected from the SNF in the HI-STORM FW system to the environment by passive heat transport mechanisms only.

The helium backfill gas plays an important role in the MPC's thermal performance. The helium fills all the spaces between solid components and provides an improved conduction medium (compared to air) for dissipating decay heat in the MPC. Within the MPC the pressurized helium environment sustains a closed loop thermosiphon action, removing SNF heat by an upward flow of helium through the storage cells. This MPC internal convection heat dissipation mechanism is illustrated in Figure 4.1.2. On the outside of the MPC a ducted overpack construction with a vertical annulus facilitates an upward flow of air by buoyancy forces. The annulus ventilation flow cools the hot MPC surfaces and safely transports heat to the outside environment. The annulus ventilation cooling mechanism is illustrated in Figure 4.1.1. To ensure that the helium gas is retained and is not diluted by lower conductivity air, the MPC Confinement Boundary is designed as an all-seal-welded pressure vessel with redundant closures. It is demonstrated in Section 12.1 that the failure of one field-welded pressure boundary seal will not result in a breach of the pressure boundary. The helium gas is therefore assumed to be retained in an undiluted state, and is credited in the thermal analyses.

An important thermal design criterion imposed on the HI-STORM FW system is to limit the maximum fuel cladding temperature as well as the fuel basket temperature to within design basis limits for long-term storage of design basis SNF assemblies. An equally important requirement is to minimize temperature gradients in the MPC so as to minimize thermal stresses. In order to meet these design objectives, the MPC baskets are designed to possess certain distinctive characteristics, as summarized below.

The MPC design minimizes resistance to heat transfer within the basket and basket periphery regions. This is ensured by an uninterrupted panel-to-panel connectivity realized in the egg-crate basket structure. The MPC design incorporates top and bottom plenums with interconnected downcomer paths formed by the annulus gap in the aluminum shims. The top plenum is formed by the gap between the bottom of the MPC lid and the top of the honeycomb fuel basket. The bottom plenum is formed by flow holes near the base of all cell walls. The MPC basket is designed to minimize structural discontinuities (i.e., gaps) which introduce added thermal resistances to heat flow. Consequently, temperature gradients are minimized in the design, which results in lower thermal stresses within the basket. Low thermal stresses are also ensured by an MPC design that permits unrestrained axial and radial growth of the basket. The possibility of stresses due to restraint on basket periphery thermal growth is eliminated by providing adequate basket-to-canister shell gaps

to allow for basket thermal growth during all operational modes.

The most important contributor to minimizing thermal stresses and maximizing heat transmission within the fuel basket is its material of construction (Metamic-HT) which has approximately ten times the thermal conductivity of the stainless steel material used in the stainless steel baskets in the HI-STORM 100 System [4.1.8]. The Metamic-HT plates in the HI-STORM FW MPCs are also considerably thicker than their counterparts in the stainless baskets, resulting in an additional enhancement in conduction heat transfer.

The MPCs regionalized fuel storage scenarios are defined in Figures 1.2.1 and 1.2.2 in Chapter 1 and design maximum decay heat loads for storage of zircaloy clad fuel are listed in Tables 1.2.3 and 1.2.4. The axial heat distribution in each fuel assembly is conservatively assumed to be non-uniformly distributed with peaking in the active fuel mid-height region (see axial burnup profiles in Figures 2.1.3 and 2.1.4. Table 4.1.1 summarizes the principal operating parameters of the HI-STORM FW system.

The fuel cladding temperature limits that the HI-STORM FW system is required to meet are discussed in Section 4.3 and given in Table 2.2.3. Additionally, when the MPCs are deployed for storing High Burnup Fuel (HBF) further restrictions during certain fuel loading operations (vacuum drying) are set forth herein to preclude fuel temperatures from exceeding the normal temperature limits. To ensure explicit compliance, a specific term "short-term operations" is defined in Chapter 2 to cover all fuel loading activities. ISG-11 fuel cladding temperature limits are applied for short-term operations.

The HI-STORM FW system (i.e., HI-STORM FW overpack, HI-TRAC VW transfer cask and MPC) is evaluated under normal storage (HI-STORM FW overpack), during off-normal and accident events and during short-term operations in a HI-TRAC VW. Results of HI-STORM FW thermal analysis during normal (long-term) storage are obtained and reported in Section 4.4. Results of HI-TRAC VW short-term operations (fuel loading, on-site transfer and vacuum drying) are reported in Section 4.5. Results of off-normal and accident events are reported in Section 4.6.

Table 4.1.1 HI-STORM FW OPERATING CONDITION PARAMETERS	
Condition	**Value**
MPC Decay Heat, max.	Tables 1.2.3 and 1.2.4
MPC Operating Pressure	7 atm (absolute)
Normal Ambient Temperature	Table 2.2.2
Helium Backfill Pressure	Table 4.4.8

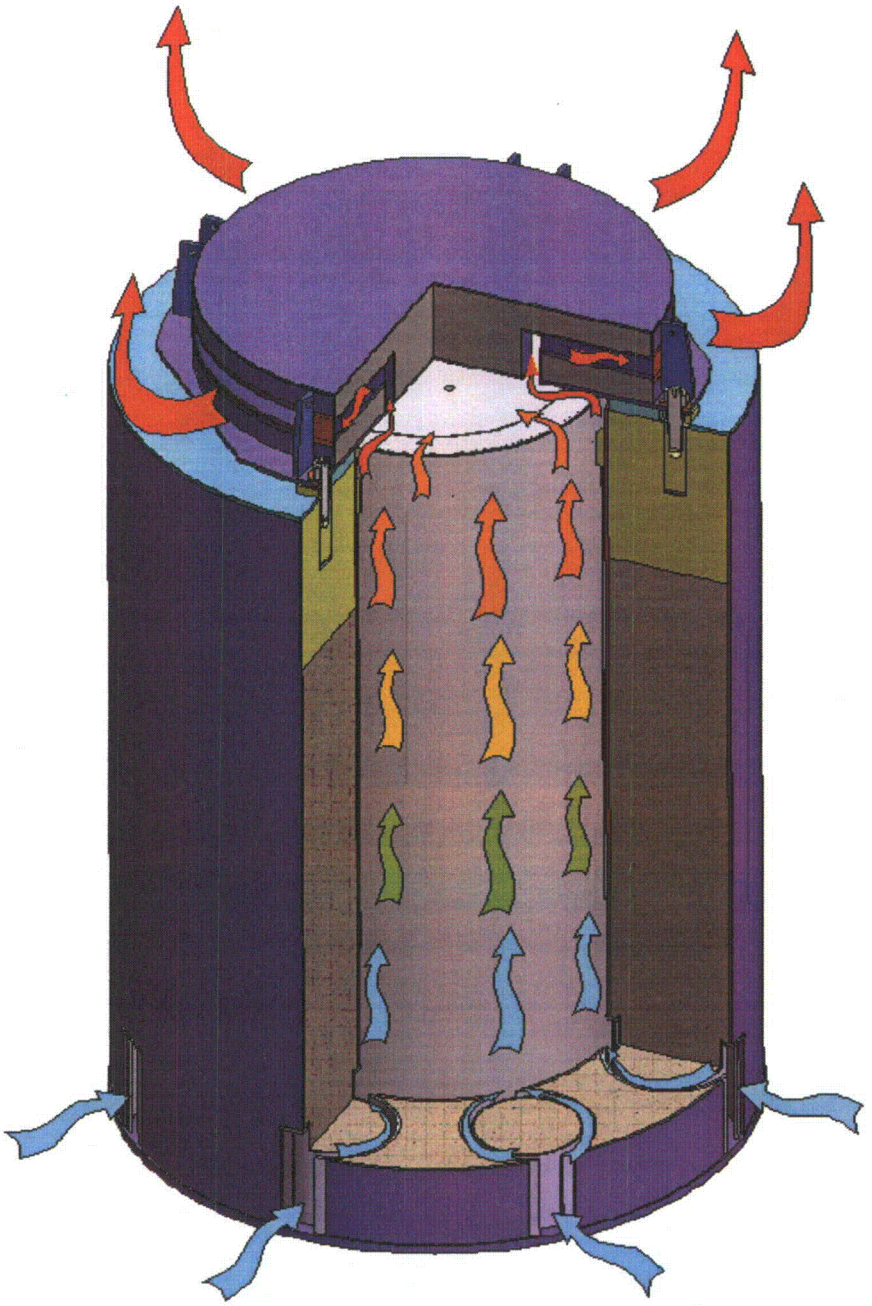

Figure 4.1.1: Ventilation Flow in the HI-STORM FW System

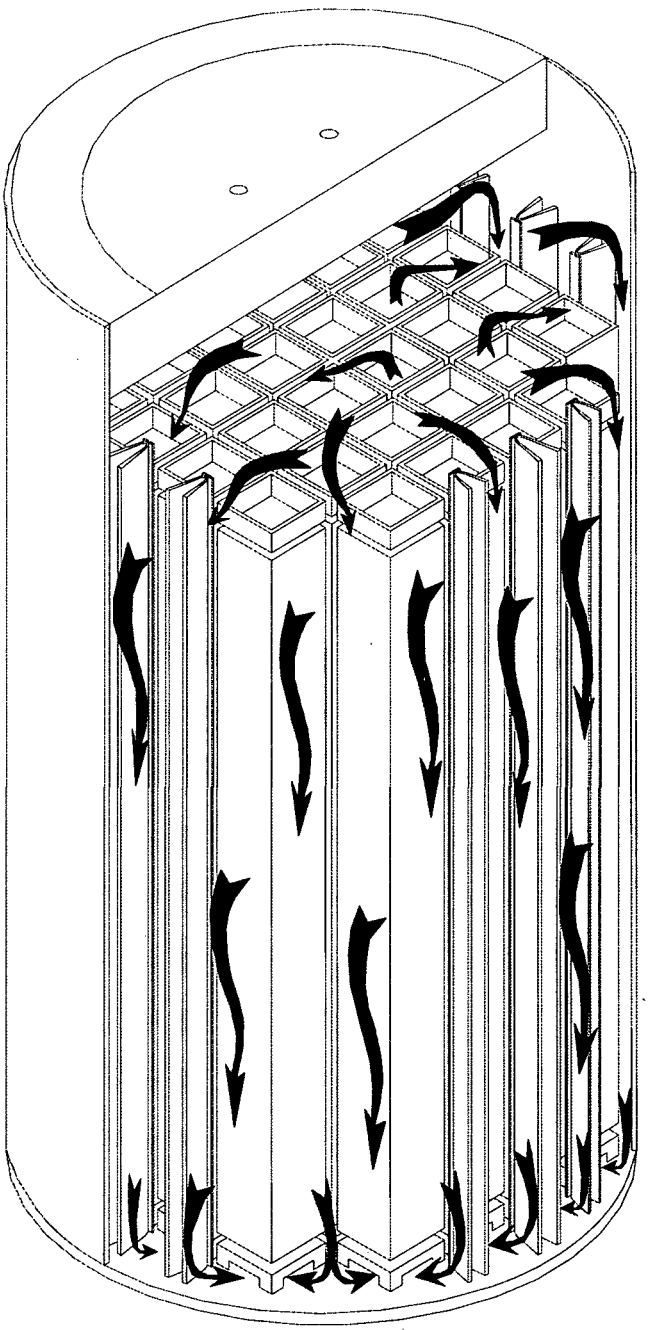

Figure 4.1.2: MPC Internal Helium Circulation

4.2 SUMMARY OF THERMAL PROPERTIES OF MATERIALS

The thermo-physical properties listed in the tables in this section are identical to those used in the HI-STORM 100 FSAR [4.1.8], except for Metamic-HT and aluminum shims. Materials present in the MPCs include Alloy X*, Metamic-HT, aluminum, and helium. Materials present in the HI-STORM FW storage overpack include carbon steels and concrete. Materials present in the HI-TRAC VW transfer cask include carbon steel, lead, air, and demineralized water. In Table 4.2.1, a summary of references used to obtain cask material properties for performing all thermal analyses is presented.

Individual thermal conductivities of the alloys that comprise the Alloy X materials and the bounding Alloy X thermal conductivity are reported in Appendix 1.A of this report. Tables 4.2.2 and 4.2.3 provide numerical thermal conductivity data of materials at several representative temperatures.

Surface emissivity data for key materials of construction are provided in Table 4.2.4. The emissivity properties of painted external surfaces are generally excellent. Kern [4.2.5] reports an emissivity range of 0.8 to 0.98 for a wide variety of paints. In the HI-STORM FW thermal analysis, an emissivity of 0.85† is applied to painted surfaces. The solar absorbtivity, α_s of paints are generally low. The NASA technical publication [4.2.20] reports α_s in the range of 0.03 to 0.54. For a robustly bounding analysis α_s equal to 0.85 is applied to all exposed overpack surfaces.

In Table 4.2.5, the heat capacity and density of the MPC, overpack and CSF materials are presented. These properties are used in performing transient (i.e., hypothetical fire accident condition) analyses. The temperature-dependent values of the viscosities of helium and air are provided in Table 4.2.6.

The heat transfer coefficient for exposed surfaces is calculated by accounting for both natural convection and thermal radiation heat transfer. The natural convection coefficient depends upon the product of Grashof (Gr) and Prandtl (Pr) numbers. Following the approach developed by Jakob and Hawkins [4.2.9], the product Gr×Pr is expressed as $L^3\Delta TZ$, where L is height of the overpack, ΔT is overpack surface temperature differential and Z is a parameter based on air properties, which are known functions of temperature, evaluated at the average film temperature. The temperature dependent values of Z are provided in Table 4.2.7.

---

* Alloy X is defined in Appendix 1.A to designate a group of stainless steel alloys permitted for use in the HI-STORM FW system. In this chapter the terms Alloy X and stainless steel are used interchangeably.

† This is conservative with respect to prior cask industry practice, which has historically utilized higher emissivities [4.2.16].

Table 4.2.1

SUMMARY OF HI-STORM FW SYSTEM MATERIALS
THERMAL PROPERTY REFERENCES

Material	Emissivity	Conductivity	Density	Heat Capacity
Helium	N/A	Handbook [4.2.2]	Ideal Gas Law	Handbook [4.2.2]
Air	N/A	Handbook [4.2.2]	Ideal Gas Law	Handbook [4.2.2]
Zircaloy	[4.2.3], [4.2.17], [4.2.18], [4.2.7]	NUREG [4.2.17]	Rust [4.2.4]	Rust [4.2.4]
UO_2	Note 1	NUREG [4.2.17]	Rust [4.2.4]	Rust [4.2.4]
Stainless Steel (machined forgings)[Note 2]	Kern [4.2.5]	ASME [4.2.8]	Marks' [4.2.1]	Marks' [4.2.1]
Stainless Steel Plates[Note 3]	ORNL [4.2.11], [4.2.12]	ASME [4.2.8]	Marks' [4.2.1]	Marks' [4.2.1]
Carbon Steel	Kern [4.2.5]	ASME [4.2.8]	Marks' [4.2.1]	Marks' [4.2.1]
Concrete	Note 1	Marks' [4.2.1]	Appendix 1.D of HI-STORM 100 FSAR [4.1.8]	Handbook [4.2.2]
Lead	Note 1	Handbook [4.2.2]	Handbook [4.2.2]	Handbook [4.2.2]
Water	Note 1	ASME [4.2.10]	ASME [4.2.10]	ASME [4.2.10]
Metamic-HT	Test Data [Appendix 1.B]	Test Data [4.2.6]	Test Data [4.2.6]	Test Data [4.2.6]
Aluminum	Test Data [Appendix 1.B]	ASM [4.2.19]	ASM [4.2.19]	ASM [4.2.19]

Note 1: Emissivity not reported as radiation heat dissipation from these surfaces is conservatively neglected.

Note 2: Used in the MPC lid.

Note 3: Used in the MPC shell and baseplate.

Table 4.2.2

SUMMARY OF HI-STORM FW SYSTEM MATERIALS
THERMAL CONDUCTIVITY DATA

Material	At 200°F (Btu/ft-hr-°F)	At 450°F (Btu/ft-hr-°F)	At 700°F (Btu/ft-hr-°F)	At 1000°F (Btu/ft-hr-°F)
Helium	0.0976	0.1289	0.1575	0.1890
Air*	0.0173	0.0225	0.0272	0.0336
Alloy X	8.4	9.8	11.0	12.4
Carbon Steel	24.4	23.9	22.4	20.0
Concrete**	1.05	1.05	1.05	1.05
Lead	19.4	17.9	16.9	N/A
Water	0.392	0.368	N/A	N/A
Metamic-HT	Table 1.B.2			
Aluminum**	69.3	69.3	69.3	69.3

* At lower temperatures, Air conductivity is between 0.0139 Btu/ft-hr-°F at 32°F and 0.0176 Btu/ft-hr-°F at 212°F.

** Conservatively assumed to be constant for the entire range of temperatures.

Table 4.2.3*

SUMMARY OF FUEL ELEMENT COMPONENTS
THERMAL CONDUCTIVITY DATA

Zircaloy Cladding		**Fuel (UO_2)**	
Temperature (°F)	Conductivity (Btu/ft-hr-°F)	Temperature (°F)	Conductivity (Btu/ft-hr-°F)
392	8.28	100	3.48
572	8.76	448	3.48
752	9.60	570	3.24
932	10.44	793	2.28

* See Table 4.2.1 for cited references.

Table 4.2.4

SUMMARY OF MATERIALS SURFACE EMISSIVITY DATA*

Material	**Emissivity**
Zircaloy	0.80
Painted surfaces	0.85
Stainless steel (machined forgings)	0.36
Stainless Steel Plates	0.587**
Carbon Steel	0.66
Metamic-HT***	See Appendix 1.B, Table 1.B.2
Aluminum***	See Appendix 1.B, Table 1.B.2

* See Table 4.2.1 for cited references.

** Lower bound value from the cited references in Table 4.2.1.

*** Metamic-HT and Aluminum shim surfaces are hard anodized to yield high emissivities. Surface emissivity of hard anodized surfaces is reported in Appendix 1.B.

Table 4.2.5

DENSITY AND HEAT CAPACITY PROPERTIES SUMMARY*

Material	Density (lbm/ft^3)	Heat Capacity (Btu/lbm-°F)
Helium	(Ideal Gas Law)	1.24
Air	(Ideal Gas Law)	0.24
Zircaloy	409	0.0728
Fuel (UO_2)	684	0.056
Carbon steel	489	0.1
Stainless steel	501	0.12
Concrete	140**	0.156
Lead	710	0.031
Water	62.4	0.999
Metamic-HT	Table 1.B.2	Table 1.B.2
Aluminum	177.3	0.207

* See Table 4.2.1 for cited references.

** Conservatively understated value.

Table 4.2.6

GASES VISCOSITY* VARIATION WITH TEMPERATURE

Temperature (°F)	Helium Viscosity (Micropoise)	Temperature (°F)	Air Viscosity (Micropoise)
167.4	220.5	32.0	172.0
200.3	228.2	70.5	182.4
297.4	250.6	260.3	229.4
346.9	261.8	338.4	246.3
463.0	288.7	567.1	293.0
537.8	299.8	701.6	316.7
737.6	338.8	1078.2	377.6
921.2	373.0	-	-
1126.4	409.3	-	-

* Obtained from Rohsenow and Hartnett [4.2.2].

Table 4.2.7

VARIATION OF NATURAL CONVECTION PROPERTIES PARAMETER "Z" FOR AIR WITH TEMPERATURE

Temperature (°F)	Z ($ft^{-3}°F^{-1}$)*
40	2.1×10^{6}
140	9.0×10^{5}
240	4.6×10^{5}
340	2.6×10^{5}
440	1.5×10^{5}

* Obtained from Jakob and Hawkins [4.2.9]

4.3 SPECIFICATIONS FOR COMPONENTS

HI-STORM FW system materials and components designated as "Important to Safety" (i.e., required to be maintained within their safe operating temperature ranges to ensure their intended function) are summarized in Tables 2.2.3. The thermal bases supporting the temperature limits are provided in Table 4.3.1. Long-term integrity of SNF is ensured by the HI-STORM FW system thermal evaluation which demonstrates that fuel cladding temperatures are maintained below design basis limits. The neutron absorber material used in MPC baskets for criticality control (Metamic-HT) is stable in excess of 1000°F*. Accordingly 1000°F is conservatively adopted as the short-term temperature limit for neutron absorber materials. The overpack concrete, the primary function of which is shielding, will maintain its structural, thermal and shielding properties provided that American Concrete Institute (ACI) guidance on temperature limits (see Appendix 1.D in reference [4.1.8]) is followed.

Compliance to 10CFR72 requires, in part, identification and evaluation of short-term, off-normal and severe hypothetical accident conditions. The inherent mechanical characteristics of cask materials and components ensure that no significant functional degradation is possible due to exposure to short-term temperature excursions outside the normal long-term temperature limits. For evaluation of HI-STORM FW system thermal performance, material temperature limits under normal, short-term operations, and off-normal and accident conditions are provided in Table 2.2.3. Fuel temperature limits mandated by ISG-11 [4.1.4] are adopted for evaluation of cladding integrity under normal, short term operations, off-normal and accident conditions. These limits are applicable to all fuel types, burnup levels and cladding materials approved by the NRC for power generation.

* B_4C is a refractory material that is unaffected by high temperature (on the order of 1000°F) and aluminum is solid at temperatures in excess of 1000°F.

Table 4.3.1

TEMPERATURE LIMITS OF CRITICAL COMPONENTS, °F

Fuel Cladding (Note 1)		
Condition	MBF	HBF
Normal storage	Table 2.2.3	Table 2.2.3
Short-term operations	Table 2.2.3	Table 2.2.3
Off-normal and Accident conditions	Table 2.2.3	Table 2.2.3
Metamic-HT (Note 2)		
Normal storage	Table 2.2.3	
Short term operations, Off-Normal and Accident conditions	Table 2.2.3	
Aluminum Shims (Note 3)		
Normal storage	Table 2.2.3	
Short term operations, Off-normal and Accident conditions	Table 2.2.3	
HI-TRAC VW Jacket		
Short term operations and off-normal conditions	Table 2.2.3 (Note 4)	
Accident condition	NA (Note 5)	

Notes:

1. Temperature limits per ISG-11, Rev. 3 [4.1.4].
2. The B_4C component in Metamic-HT is a refractory material that is unaffected by high temperature (on the order of 1000°F) and the aluminum component is solid at temperatures in excess of 1000°F.
3. To preclude melting the temperature limits are set well below the melting temperature of Aluminum Alloys.
4. Temperature limit is defined by the saturation temperature of water at water jacket design pressure specified in Table 2.2.1.
5. The jacket water is assumed to be lost under accident conditions.

4.4 THERMAL EVALUATION FOR NORMAL CONDITIONS OF STORAGE

The HI-STORM FW System (i.e., HI-STORM FW overpack and MPC) and HI-TRAC VW transfer cask thermal evaluation is performed in accordance with the guidelines of NUREG-1536 [4.4.1] and ISG-11 [4.1.4]. To ensure a high level of confidence in the thermal evaluation, 3-dimensional models of the MPC, HI-STORM FW overpack and HI-TRAC VW transfer cask are constructed to evaluate fuel integrity under normal (long-term storage), off-normal and accident conditions and in the HI-TRAC VW transfer cask under short-term operation and hypothetical accidents. The principal features of the thermal models are described in this section for HI-STORM FW and Section 4.5 for HI-TRAC VW. Thermal analyses results for the long-term storage scenarios are obtained and reported in this section.

4.4.1 Overview of the Thermal Model

As illustrated in the drawings in Section 1.5, the basket is a matrix of interconnected square compartments designed to hold the fuel assemblies in a vertical position under long term storage conditions. The basket is a honeycomb structure of Metamic-HT plates that are slotted and arrayed in an orthogonal configuration to form an integral basket structure. The Metamic-HT neutron absorber plates contain 10% (min.) Boron Carbide in an aluminum matrix reinforced with nanoparticles of alumina to provide criticality control, while maximizing heat conduction capabilities (see Appendix 1.B).

Thermal analysis of the HI-STORM FW System is performed for limiting heat load scenarios defined in Chapter 1 for regionalized storage (Figures 1.2.1 and 1.2.2). Each fuel assembly is *assumed to be generating heat at the maximum permissible rate (Tables 1.2.3 and 1.2.4)*. While the assumption of limiting heat generation in each storage cell imputes a certain symmetry to the cask thermal problem, it grossly overstates the total heat duty of the system in most cases because it is unlikely that any basket would be loaded with fuel emitting heat at their limiting values in *each* storage cell. Thus, the thermal model for the HI-STORM FW system is inherently conservative for real life applications. Other noteworthy features of the thermal analyses are:

i. While the rate of heat conduction through metals is a relatively weak function of temperature, radiation heat exchange increases rapidly as the fourth power of absolute temperature.

ii. Heat generation in the MPC is axially non-uniform due to non-uniform axial burnup profiles in the fuel assemblies.

iii. Inasmuch as the transfer of heat occurs from inside the basket region to the outside, the temperature field in the MPC is spatially distributed with the lowest values reached at the periphery of the basket.

As noted in Chapter 1 and in Section 3.2, the height of the PWR MPC cavity can vary within a rather large range to accommodate spent nuclear fuel of different lengths. The heat load limits in Table 1.2.3 (PWR MPC) and Table 1.2.4 (BWR MPC) for regionalized storage are, however, fixed regardless of the fuel (and hence MPC cavity) length. Because it is not a'priori obvious whether the shortest or the longest fuel case will govern, thermal analyses are performed for the lowerbound, upperbound and reference-height MPCs.

4.4.1.1 Description of the 3-D Thermal Model

i. Overview

The HI-STORM FW System is equipped with two MPC designs, MPC-37 and MPC-89 engineered to store 37 and 89 PWR and BWR fuel assemblies respectively. The interior of the MPC is a 3-D array of square shaped cells inside an irregularly shaped basket outline confined inside the cylindrical space of the MPC cavity. To ensure an adequate representation of these features, a 3-D geometric model of the MPC is constructed using the FLUENT CFD code pre-processor [4.1.2]. Because the fuel basket is made of a single isotropic material (Metamic-HT), the 3-D thermal model requires no idealizations of the fuel basket structure. However, since it is impractical to model every fuel rod in every stored fuel assembly explicitly, the cross-section bounded by the inside of the storage cell (inside of the fuel channel in the case of BWR MPCs), which surrounds the assemblage of fuel rods and the interstitial helium gas (also called the "rodded region"), is replaced with an "equivalent" square homogeneous section characterized by an effective thermal conductivity. Homogenization of the cell cross-section is discussed under item (ii) below. For thermal-hydraulic simulation, each fuel assembly in its storage cell is represented by an equivalent porous medium. For BWR fuel, the presence of the fuel channel divides the storage cell space into two distinct axial flow regions, namely, the in-channel (rodded) region and the square prismatic annulus region (in the case of PWR fuel this modeling complication does not exist). The methodology to represent the spent fuel storage space as a homogeneous region with equivalent conductivities is identical to that used in the HI-STORM 100 Docket No. 72-1014 [4.1.8].

ii. Details of the 3-D Model

The HI-STORM FW fuel basket is modeled in the same manner as the model described in the HI-STAR 180 SAR (NRC Docket No. 71-9325) [4.1.11]. Modeling details are provided in the following:

Fuel Basket 3D Model

The MPC-37 and MPC-89 fuel baskets are essentially an array of square cells within an irregularly shaped basket outline. The fuel basket is confined inside a cylindrical cavity of the MPC shell. Between the fuel basket-to-shell spaces, thick Aluminum basket shims are installed to facilitate heat dissipation. To ensure an adequate representation of the fuel basket a geometrically accurate 3D

model of the array of square cells and Metamic-HT plates is constructed using the FLUENT pre-processor. Other than the representation of fuel assemblies inside the storage cell spaces as porous region with effective thermal-hydraulic properties as described in the next paragraph, the 3D model includes an explicit articulation of other canister parts... The basket shims are explicitly modeled in the peripheral spaces. The fuel basket is surrounded by the MPC shell and outfitted with a solid welded lid above and a baseplate below. All of these physical details are explicitly articulated in a quarter-symmetric 3D thermal model of the HI-STORM FW.

Fuel Region Effective Planar Conductivity

In the HI-STORM FW thermal modeling, the cross section bounded by the inside of a PWR storage cell and the channeled area of a BWR storage cell is replaced with an "equivalent" square section characterized by an effective thermal conductivity in the planar and axial directions. Figure 4.4.1 pictorially illustrates this concept. The two conductivities are unequal because while in the planar direction heat dissipation is interrupted by inter-rod gaps; in the axial direction heat is dissipated through a continuous medium (fuel cladding). The equivalent planar conductivity of the storage cell space is obtained using a 2D conduction-radiation model of the bounding PWR and BWR fuel storage scenarios defined in the table below. The fuel geometry, consisting of an array of fuel rods with helium gaps between them residing in a storage cell, is constructed using the ANSYS code [4.1.1] and lowerbound conductivities under the assumed condition of stagnant helium (no-helium-flow-condition) are obtained. In the axial direction, an area-weighted average of the cladding and helium conductivities is computed. Axial heat conduction in the fuel pellets is conservatively ignored.

The effective fuel conductivity is computed under three bounding fuel storage configurations for PWR fueled MPC-37 and one bounding scenario for BWR fueled MPC-89. The fuel storage configurations are defined below:

Storage Scenario	MPC	Fuel
PWR: Short Fuel	Minimum Height MPC-37	14x14 Ft. Calhoun
PWR: Standard Fuel	Reference Height MPC-37	W-17x17
PWR: XL Fuel	Maximum Height MPC-37	AP1000
BWR	MPC-89	GE-10x10

The fuel region effective conductivity is defined as the calculated equivalent conductivity of the fuel storage cell due to the combined effect of conduction and radiation heat transfer in the manner of the approach used in the HI-STORM 100 system (Docket No. 72-1014). Because radiation is proportional to the fourth power of absolute temperature, the effective conductivity is a strong function of temperature. The ANSYS finite element model is used to characterize fuel resistance at several representative storage cell temperatures and the effective thermal conductivity as a function of temperature obtained for all storage configurations defined above and tabulated in Table 4.4.1.

Heat Rejection from External Surfaces

The exposed surfaces of the HI-STORM FW dissipate heat by radiation and external natural convection heat transfer. Radiation is modeled using classical equations for radiation heat transfer (Rohsenow & Hartnett [4.2.2]). Jakob and Hawkins [4.2.9] recommend the following correlations for natural convection heat transfer to air from heated vertical and horizontal surfaces:

Turbulent range:

$$h = 0.19(\Delta T)^{1/3} \text{ (Vertical, } GrPr > 10^9)$$

$$h = 0.18(\Delta T)^{1/3} \text{ (Horizontal Cylinder, } GrPr > 10^9)$$

(in conventional U.S. units)

Laminar range:

$$h = 0.29\left(\frac{\Delta T}{L}\right)^{1/4} \text{ (Vertical, } GrPr < 10^9)$$

$$h = 0.27\left(\frac{\Delta T}{D}\right)^{1/4} \text{ (Horizontal Cylinder, } GrPr < 10^9)$$

(in conventional U.S. Units)

where ΔT is the temperature differential between the cask's exterior surface and ambient air and GrPr is the product of Grashof and Prandtl numbers. During storage conditions, the cask cylinder and top surfaces are cooled by natural convection. The corresponding length scales L for these surfaces are the cask diameter and length, respectively. As described in Section 4.2, Gr×Pr can be expressed as $L^3\Delta TZ$, where Z (from Table 4.2.7) is at least 2.6×10^5 at a conservatively high surface temperature of 340°F. Thus the turbulent condition is always satisfied assuming a lowerbound L (8 ft) and a small ΔT (~10°F).

Determination of Solar Heat Input

The intensity of solar radiation incident on exposed surfaces depends on a number of time varying parameters. The solar heat flux strongly depends upon the time of the day as well as on latitude and day of the year. Also, the presence of clouds and other atmospheric conditions (dust, haze, etc.) can significantly attenuate solar intensity levels. In the interest of conservatism, the effects of dust, haze, angle of incidence, latitude, etc. that act to reduce insolation, are neglected.

The insolation energy absorbed by the HI-STORM FW is the product of incident insolation and surface absorbtivity. To model insolation heating a reasonably bounding absorbtivity equal to 0.85 is incorporated in the thermal models. The HI-STORM FW thermal analysis is based on 12-hour daytime insolation specified in Article 71.71(c) (1) of the Transport Regulations [4.6.1]. During long-term storage, the HI-STORM FW Overpack is cyclically subjected to solar heating during the

12-hour daytime period followed by cooling during the 12-hour nighttime. Due to the large mass of metal and the size of the cask, the dynamic time lag exceeds the 12-hour heating period. Accordingly, the HI-STORM FW model includes insolation on exposed surfaces averaged over a 24-hour time period.

HI-STORM FW Annulus

The HI-STORM FW is engineered with internal flow passages to facilitate heat dissipation by ventilation action. During fuel storage ambient air is drawn from intake ducts by buoyancy forces generated by the heated column of air in the HI-STORM FW annulus. The upward moving air extracts heat from the MPC external surfaces by convection heat transfer. As great bulk of the heat is removed by the annulus air, the adequacy of the grid deployed to model annulus heat transfer must be confirmed prior to performing design basis calculations. To this end a grid sensitivity study is conducted in Subsection 4.4.1.6 to define the converged grid discretization of the annulus region. The converged grid is deployed to evaluate the thermal state of the HI-STORM FW system under normal, off-normal and accident conditions of storage.

iii. Principal Attributes of the 3D Model

The 3-D model implemented to analyze the HI-STORM FW system is entirely based on the HI-STORM 100 thermal model except that the radiation effect is simulated by the more precise "DO" model (in lieu of the DTRM model used in HI-STORM 100) in FLUENT in the manner of HI-STAR 180 in docket 71-9325. This model has the following key attributes:

a) The fuel storage spaces are modeled as porous media having effective thermal-hydraulic properties.

b) In the case of BWR MPC-89, the fuel bundle and the small surrounding spaces inside the fuel "channel" are replaced by an equivalent porous media having the flow impedance properties computed using a conservatively articulated 3-D CFD model [4.4.2]. The space between the BWR fuel channel and the storage cell is represented as an open flow annulus. The fuel channel is also explicitly modeled. The channeled space within is also referred to as the "rodded region" that is modeled as a porous medium. The fuel assembly is assumed to be positioned coaxially with respect to its storage cell. The MPC-89 storage cell occupied with channeled BWR fuel is shown in Figure 4.4.4.

   In the case of the PWR CSF, the porous medium extends to the entire cross-section of the storage cell. As described in [4.4.2], the CFD models for both the BWR and PWR storage geometries are constructed for the Design Basis fuel defined in Table 2.1.4. The model contains comprehensive details of the fuel which includes grid straps, BWR water rods and PWR guide and instrument tubes (assumed to be plugged for conservatism).

c) The effective conductivities of the MPC storage spaces are computed for bounding fuel storage configurations defined in Paragraph 4.4.1.1(ii). The in-plane thermal conductivities are obtained using ANSYS [4.1.1] finite element models of an array of fuel rods enclosed by a square box. Radiation heat transfer from solid surfaces (cladding and box walls) is enabled in these models. Using these models the effective conduction-radiation conductivities are obtained and reported in Table 4.4.1. For heat transfer in the axial direction an area weighted mean of cladding and helium conductivities are computed (see Table 4.4.1). Axial conduction heat transfer in the fuel pellets and radiation heat dissipation in the axial direction are conservatively ignored. Thus, the thermal conductivity of the rodded region, like the porous media simulation for helium flow, is represented by a 3-D continuum having effective planar and axial conductivities.

d) The internals of the MPC, including the basket cross-section, aluminum shims, bottom flow holes, top plenum, and circumferentially irregular downcomer formed by the annulus gap in the aluminum shims are modeled explicitly. For simplicity, the flow holes are modeled as rectangular openings with an understated flow area.

e) The inlet and outlet vents in the HI-STORM FW overpack are modeled explicitly to incorporate any effects of non-axisymmetry of inlet air passages on the system's thermal performance.

f) The air flow in the HI-STORM FW/MPC annulus is simulated by the k-ω turbulence model with the transitional option enabled. The adequacy of this turbulence model is confirmed in the Holtec benchmarking report [4.1.6]. The annulus grid size is selected to ensure a converged solution.(See Section 4.4.1.6).

g) A limited number of fuel assemblies (upto 12 in MPC-37 and upto 16 in MPC-89) classified as damaged fuel are permitted to be stored in the MPC inside Damaged Fuel Containers (DFCs). A DFC can be stored in the outer peripheral locations of both MPC-37 and MPC-89 as shown in Figures 2.1.1 and 2.1.2, respectively. DFC emplaced fuel assemblies have a higher resistance to helium flow because of the debris screens. However, DFC fuel storage does not affect temperature of hot fuel stored in the core of the basket because DFC storage is limited by Technical Specifications for placement in the peripheral storage locations away from hot fuel. For this reason the thermal modeling of the fuel basket under the assumption of all storage spaces populated with intact fuel is justified.

h) As shown in HI-STORM FW drawings in Section 1.5 the HI-STORM FW overpack is equipped with a heat shield to protect the inner shell and concrete from radiation

heating by the emplaced MPC. The heat shield, inner and outer shells and concrete are explicitly modeled.

i) To maximize lateral resistance to heat dissipation in the fuel basket, 0.4 mm full length inter- panel gaps are conservatively assumed to exist at all intersections. This approach is identical to that used in the thermal analysis of the HI-STAR 180 Package in Docket 71-9325. The shims installed in the MPC peripheral spaces (See MPC-37 and MPC-89 drawings in Section 1.5) are explicitly modeled. For conservatism bounding as-built gaps (3 mm basket-to-shims and 3 mm shims-to-shell) are assumed to exist and incorporated in the thermal models.

j) The thermal models incorporate all modes of heat transfer (conduction, convection and radiation) in a conservative manner.

k) The Discrete Ordinates (DO) model, previously utilized in the HI-STAR 180 docket (Docket 71-9325), is deployed to compute radiation heat transfer.

l) Laminar flow conditions are applied in the MPC internal spaces to obtain a lowerbound rate of heat dissipation.

The 3-D model described above is illustrated in the cross-section for the MPC-89 and MPC-37 in Figures 4.4.2 and 4.4.3, respectively. A closeup of the fuel cell spaces which explicitly include the channel-to-cell gap in the 3-D model applicable to BWR fueled basket (MPC-89) is shown in Figure 4.4.4. The principal 3-D modeling conservatisms are listed below:

1) The storage cell spaces are loaded with high flow resistance design basis fuel assemblies (See Table 2.1.4).
2) Each storage cell is generating heat at its limiting value under the regionalized storage scenarios defined in Chapter 2, Section 2.1.
3) Axial dissipation of heat by conduction in the fuel pellets is neglected.
4) Dissipation of heat from the fuel rods by radiation in the axial direction is neglected.
5) The fuel assembly channel length for BWR fuel is overstated.
6) The most severe environmental factors for long-term normal storage - ambient temperature of 80°F and 10CFR71 insolation levels - were coincidentally imposed on the system.
7) Reasonably bounding solar absorbtivity of HI-STORM FW overpack external surfaces is applied to the thermal models.
8) To understate MPC internal convection heat transfer, the helium pressure is understated.
9) No credit is taken for contact between fuel assemblies and the MPC basket wall or between the MPC basket and the basket supports.
10) Heat dissipation by fuel basket peripheral supports is neglected.

11) Lowerbound fuel basket emissivity function defined in the Metamic-HT Sourcebook [4.2.6] is adopted in the thermal analysis.
12) Lowerbound stainless steel emissivity obtained from cited references (See Table 4.2.1) are applied to MPC shell.
13) The k-ω model used for simulating the HI-STORM FW annulus flow yields uniformly conservative results [4.1.6].
14) Fuel assembly length is conservatively modeled equal to the height of the fuel basket.

The effect of crud resistance on fuel cladding surfaces has been evaluated and found to be negligible [4.1.8]. The evaluation assumes a thick crud layer (130 μm) with a bounding low conductivity (conductivity of helium). The crud resistance increases the clad temperature by a very small amount (~0.1°F) [4.1.8]. Accordingly this effect is neglected in the thermal evaluations.

4.4.1.2 Fuel Assembly 3-Zone Flow Resistance Model*

The HI-STORM FW System is evaluated for storage of representative PWR and BWR fuel assemblies determined by a separate analysis, to provide maximum resistance to the axial flow of helium. These are (i) PWR fuel: W17x17 and (ii) BWR fuel: GE10x10. During fuel storage helium enters the MPC fuel cells from the bottom plenum and flows upwards through the open spaces in the fuel storage cells and exits in the top plenum. Because of the low flow velocities the helium flow in the fuel storage cells and MPC spaces is in the laminar regime ($Re < 100$). The bottom and top plenums are essentially open spaces engineered in the fuel basket ends to facilitate helium circulation. In the case of BWR fuel storage, a channel enveloping the fuel bundle divides the flow in two parallel paths. One flow path is through the in-channel or rodded region of the storage cell and the other flow path is in the square annulus area outside the channel. In the global thermal modeling of the HI-STORM FW System the following approach is adopted:

(i) In BWR fueled MPCs, an explicit channel-to-cell gap is modeled.
(ii) The fuel assembly enclosed in a square envelope (fuel channel for BWR fuel or fuel storage cell for PWR fuel) is replaced by porous media with equivalent flow resistance.

The above modeling approach is illustrated in Figure 4.4.4.

In the FLUENT program, porous media flow resistance is modeled as follows:

$$\Delta P/L = D\mu V \qquad \text{(Eq. 1)}$$

* This Sub- section duplicates the methodology used in the HI-STORM FSAR, Rev. 7, supporting CoC Amendment # 5 in Docket 72-1014 [4.1.8].

where $\Delta P/L$ is the hydraulic pressure loss per unit length, D is the flow resistance coefficient, μ is the fluid viscosity and V is the superficial fluid velocity. In the HI-STORM FW thermal models the fuel storage cell length between the bottom and top plenums* is replaced by porous media. As discussed below the porous media length is partitioned in three zones with discrete flow resistances.

To characterize the flow resistance of fuel assemblies inside square envelopes (fuel channel for BWR fuel or fuel storage cell for PWR fuel) 3D models of W-17x17 and GE-10x10 fuel assemblies are constructed using the FLUENT CFD program. These models are embedded with several pessimistic assumptions to overstate flow resistance. These are:

(a) Water rods (BWR fuel) and guide tubes (PWR fuel) are assumed to be blocked
(b) Fuel rods assumed to be full length
(c) Channel length (BWR fuel) overstated
(d) Bounding grid thickness used
(e) Bottom fittings resistance overstated
(f) Bottom nozzle lateral flow holes (BWR fuel) assumed to be blocked

The flow resistance coefficients computed from the 3D flow models [4.4.2] are adopted herein.

4.4.1.3 Bounding Flow Resistance Data

Holtec report [4.4.2] has identified W17x17 OFA and GE 12/14 10x10 fuel assemblies as the design basis fuel for computing the flow resistance coefficients required to compute the in-cell flow of helium in PWR storage cells and of in-channel flow of channeled BWR assemblies placed in a BWR storage cell (See Figure 4.4.4). These resistance coefficients form the basis for the thermal-hydraulic analyses in Docket 72-1014 in the CoC amendments 5. These resistance coefficients are appropriate and conservative for HI-STORM FW analysis because of the following reasons:

i. The coefficients define the upperbound pressure drop per unit length of fueled space (Eq. 1 in Section 4.4.1.2).
ii. The storage cell opening in the MPC-37 (PWR fuel) is equal to or greater than the cell openings of the PWR MPCs (such as MPC-32) licensed in the HI-STORM 100 System in Docket 72-1014 [4.1.8]. In the case of BWR fuel storage the channeled fuel located inside the storage cell is modeled explicitly as shown in Figure 4.4.4. The bounding flow resistance coefficients obtained from the cited reference above is applied to the channeled space porous media.
iii. The length of porous media incorporated in the HI-STORM FW FLUENT models meets or exceeds the fuel assembly length of the longest fuel listed in this SAR.

* These are the flow hole openings at the lower end of the fuel basket and a top axial gap to facilitate helium circulation. The flow holes are explicitly included in the 3D thermal models with an understated flow area.

Thus the flow resistance defined in the manner above is significantly conservative for modeling the Ft. Calhoun 14x14 fuel placed in the limiting minimum height MPC-37 (See Table 4.4.2). In the following, explicit calculations for the case of MPC-37 are performed to quantify the conservatism introduced by using the "bounding" resistance data in the FLUENT analysis.

4.4.1.4 Evaluation of Flow Resistance in Enlarged Cell MPCs

The flow resistance factors used in the porous media model are bounding for all fuel types and MPC baskets. This was accomplished for the PWR fueled MPC-37 by placing the most resistive Westinghouse 17x17 fuel assembly in the smaller cell opening MPC-32 approved under the HI-STORM 100 Docket 72-1014, CoC Amendment No. 5 and computing the flow resistance factors. In the case of BWR fueled MPC-89 the most resistive GE-10x10 fuel assembly in the channeled configuration is explicitly modeled in the MPC-89 fuel storage spaces as shown in Figure 4.4.4. The channeled space occupied by the GE-10x10 fuel assembly is modeled as a porous region with effective flow resistance properties computed by deploying an independent 3D FLUENT model of the array of fuel rods and grid spacers.

In the PWR fuel resistance modeling case physical reasoning suggests that the flow resistance of a fuel assembly placed in the larger MPC-37 storage cell will be less than that computed using the (smaller) counterpart cells cavities in the MPC-32. However to provide numerical substantiation FLUENT calculations are performed for the case of W-17x17 fuel placed inside the MPC-32 cell opening of 8.79" and the enlarged MPC-37 cell opening of 8.94". The FLUENT results for the cell pressure drops under the baseline (MPC-32) and enlarged cell opening (MPC-37) scenarios are shown plotted in Figure 4-4-7. The plot shows that, as expected, the larger cell cross section case (MPC-37) yields a smaller pressure loss. Therefore, the MPC-37 flow resistance is bounded by the MPC-32 flow resistance used in the FLUENT simulations in the SAR. This evaluation is significant because the MPC-37 basket is determined as the limiting MPC and therefore the licensing basis HI-STORM FW temperatures by use of higher-than-actual resistance are overstated.

4.4.1.5 Screening Calculations to Ascertain Limiting Storage Scenario

To define the thermally most limiting HI-STORM FW storage scenario the following cases are evaluated under the design maximum heat load defined in Tables 1.2.3 and 1.2.4:

(i) MPC-89
(ii) Minimum height MPC-37
(iii) Reference height MPC-37
(iv) Maximum height MPC-37

To evaluate the above scenarios, 3D FLUENT screening models of the HI-STORM FW cask are constructed, Peak Cladding Temperatures (PCT) computed and tabulated in Table 4.4.2. The results of the calculations yield the following:

(a) Fuel storage in MPC-37 produces a higher peak cladding temperature than that in MPC-89
(b) Fuel storage in the minimum height MPC-37 is limiting (produces the highest peak cladding temperature).

To bound the HI-STORM FW storage temperatures the limiting scenario ascertained above is adopted for evaluation of all normal, off-normal and accident conditions.

4.4.1.6 Grid Sensitivity Studies

The discretization of the MPC and the HI-STORM/MPC annulus region must be sufficiently dense to insure a converged solution. Because the flow field in the annulus is in the transition and turbulent regimes, the grid size and layout are critical to insuring a converged solution. In the MPC internal space, however, the flow is uniformly laminar (no laminar boundary layer to turbulent zone transition effects) and therefore, the grid size is relatively unimportant. The sensitivity study was accordingly performed on the annulus region outside the MPC and the grid size in the axial direction within the MPC. All sensitivity analyses were carried out for the case of 47.05 kW design maximum heat load for the (limiting) MPC-37 canister.

a. The HI-STORM FW annulus grid sensitivity results are tabulated below.

Run No	Number of Radial Cells	y^+	PCT (°C)	Permissible Limit (°C)	Clad Temperature Margin (°C)
1	6	21	353	400	47
2	10	5	357	400	43
3	11	4	364	400	36
4	12	3	376	400	24
5	17	0.7	375	400	25
Note 1: The y^+ reported in the third column above is a measure of grid adequacy provided by the FLUENT code. Values of $y^+ \sim 1$ indicate an adequate level of mesh refinement is reached to resolve the viscosity affected region near the wall. Note 2: The annulus grid is refined in two ways, namely, by increasing the number of radial cells and also by clustering the cells near the MPC and overpack innershell walls.					

As can be seen from the above table, the thermal solution is quite sensitive to the grid density in the annulus region. The above results show that Run No 5 is reasonably converged. To provide further assurance of convergence, the sensitivity results are evaluated in accordance with the ASME Journal procedure for control of numerical accuracy [4.4.3]. Towards this end the Grid Convergence Index (GCI), which is a measure of the solution uncertainty, is computed. The GCI for the finest grid (i.e. 17 radial cells) computes to be 1.3×10^{-5}% which provides further assurance of grid convergence.

Having obtained grid convergence in the annulus region, the Run No 5 grid is adopted for further grid sensitivity studies below.

b. The results of axial grid refinement in the fueled region are summarized below.

Grid Refinement	Number of Axial Cells	PCT (°C)	Permissible Limit (°C)	Clad Temperature Margin (°C)
Baseline run (Run No 5 adopted from above)	84[Note 1]	375	400	25
Refined Grid	101	376	400	24
Note 1: As explained below the baseline grid is adopted for thermal evaluation of the HI-STORM FW.				

The above results show that the solution is essentially unchanged by further grid refinement in the axial direction. This result is in keeping with the fact that the flow field in the MPC internal space is uniformly laminar. Based on the above results, Run No 5 grid layout is adopted for the thermal analysis of the HI-STORM FW.

4.4.2 Effect of Neighboring Casks

HI-STORM FW casks are typically stored on an ISFSI pad in regularly spaced arrays (See Section 1.4, Figures 1.4.1 and 1.4.2). Relative to an isolated HI-STORM FW the heat dissipation from a HI-STORM FW cask placed in an array is somewhat disadvantaged. However, as the analysis in this Sub-section shows, the effect of the neighboring casks on the peak cladding temperature in the "surrounded" cask is insignificant.

(i) Effect of Insolation

The HI-STORM FW casks are subject to insolation heating during daytime hours. Presence of surrounding casks has the salutary effect of partially blocking insolation flux. This effect, results in lower temperatures and in the interest of conservatism is ignored in the analysis.

(ii) Effect of Radiation Blocking

The presence of surrounding casks has the effect of partially blocking radiation heat dissipation from the Overpack cylindrical surfaces. Its effect is evaluated in Sub-section 4.4.2.1.

(iii) Effect of Flow Area Reduction

The presence of surrounding casks have the effect of reducing the access flow area around the casks from an essentially unbounded space around it to certain lateral flow passages defined by the spacing between casks (See Figures 1.4.1 and 1.4.2). A reduction in flow area for ventilated casks is not

acceptable if the access area falls below the critical flow area in the ventilation flow passages. The HI-STORM FW critical flow area is reached in the narrow annular passage. The lateral flow passages access flow area defined by the product of minimum gap between casks and cask height is computed below. The calculation uses the lowerbound 180 inch cask pitch defined in Table 1.4.1.

Annulus Area (A_{min}):
MPC OD: 75.5 in
Overpack ID: 81 in
A_{min}: 676.0 in^2

Lateral Access Area (A_o):
Cask Pitch: 180 in
Overpack OD: 139 in
Overpack Body Height: 187.25 in
Min. cask spacing: 180 – 139 = 41 in
A_o: 7677.2 in^2

The above numerical exercise shows that $A_o >> A_{min}$ and therefore there is an adequate access area surrounding the interior casks for the ventilation air to feed the inlet ducts..

4.4.2.1 Analytical Evaluation of the Effect of Surrounding Casks

In a rectilinear array of HI-STORM FW casks the unit situated in the center of the grid is evidently hydraulically most disadvantaged, because of potential interference to air intake from surrounding casks. Furthermore, the presence of surrounding casks has the effect of partially blocking radiation heat dissipation from the centrally located cask. This situation is illustrated in Figure 4.4.5. To simulate these effects in a conservative manner, a hypothetical square cavity defined by the tributary area A_o of cask shown in Figure 4.4.5 is erected around the centrally located HI-STORM FW. The hypothetical square cavity has the following attributes:

1. The hypothetical square cavity (with the subject HI-STORM FW situated co-axially in it) is constructed for the15 ft minimum cask pitch defined in Section 1.4.1.
2. The cavity walls are impervious to air. In this manner as shown in Figure 4.4.6 lateral access to ambient air is choked.
3. The cavity walls are defined as reflecting surfaces from the inside and insulated from the outside. In this manner lateral dissipation of heat by radiation is blocked.
4. The hypothetical square cavity is open at the top as shown in Figure 4.4.6 to allow ambient air access for ventilation cooling in a conservative manner.

The principal results of the hypothetical square cavity thermal model are tabulated below and compared with the baseline thermal results tabulated in Section 4.4.4.

Model	Peak Clad Temperature (°F)	Margin-to-Limit (°F)
Single Cask Model	707	45
Hypothetical Square Cavity Thermal Model	705*	47

The results show that the presence of surrounding casks has essentially no effect on the fuel cladding temperatures (the difference in the results is within the range of numerical round-off). These results are in line with prior thermal evaluations of the effect of surrounding casks in the NRC approved HI-STORM 100 System in Docket 72-1014.

4.4.3 Test Model

The HI-STORM FW thermal analysis is performed on the FLUENT [4.1.2] Computational Fluid Dynamics (CFD) program. To ensure a high degree of confidence in the HI-STORM FW thermal evaluations, the FLUENT code has been benchmarked using data from tests conducted with casks loaded with irradiated SNF ([4.1.3],[4.1.7]). The benchmark work is archived in QA validated Holtec reports ([4.1.5],[4.1.6]).These evaluations show that the FLUENT solutions are conservative in all cases. In view of these considerations, additional experimental verification of the thermal design is not necessary. FLUENT has also been used in all Holtec International Part 71 and Part 72 dockets since 1996.

4.4.4 Maximum and Minimum Temperatures

4.4.4.1 Maximum Temperatures

The 3-D model from the previous subsection is used to determine temperature distributions under long-term normal storage conditions for both MPC-89 and MPC-37. Tables 4.4.2, 4.4.3 and 4.4.5 provide key thermal and pressure results from the FLUENT simulations, respectively. The peak fuel cladding result in these tables is actually overstated by the fact that the 3-D FLUENT cask model incorporates the effective conductivity of the fuel assembly sub-model. Therefore the FLUENT models report the peak temperature *in the fuel storage cells.* Thus, as the fuel assembly models include the fuel pellets, the FLUENT calculated peak temperatures are actually peak pellet centerline temperatures which bound the peak cladding temperatures with a modest margin.

The following observations can be derived by inspecting the temperature field obtained from the thermal models:

* The lower computed temperature is an artifact of the use of overstated inlet and outlet loss coefficients in the single cask model. The result supports the conclusion that surrounding casks have essentially no effect on the Peak Cladding Temperatures.

- The fuel cladding temperatures are below the regulatory limit (ISG-11 [4.1.4]) under all regionalized storage scenarios defined in Chapter 1 (Figures 1.2.1 and 1.2.2).

- The maximum temperature of the basket structural material is within its design limit.

- The maximum temperatures of the MPC pressure boundary materials are below their design limits.

- The maximum temperatures of concrete are within the guidance of the governing ACI Code (see Table 2.2.3).

The above observations lead us to conclude that the temperature field in the HI-STORM FW System with a loaded MPC containing heat emitting SNF complies with all regulatory temperature limits (Table 2.2.3). In other words, the thermal environment in the HI-STORM FW System is in compliance with Chapter 2 Design Criteria.

4.4.4.2 Minimum Temperatures

In Table 2.2.2 of this report, the minimum ambient temperature condition for the HI-STORM FW storage overpack and MPC is specified to be -40°F. If, conservatively, a zero decay heat load with no solar input is applied to the stored fuel assemblies, then every component of the system at steady state would be at a temperature of -40°F. Low service temperature (-40°F) evaluation of the HI-STORM FW is provided in Chapter 3. All HI-STORM FW storage overpack and MPC materials of construction will satisfactorily perform their intended function in the storage mode under this minimum temperature condition.

4.4.4.3 Effect of Elevation

The reduced ambient pressure at site elevations significantly above the sea level will act to reduce the ventilation air mass flow, resulting in a net elevation of the peak cladding temperature. However, the ambient temperature (i.e., temperature of the feed air entering the overpack) also drops with the increase in elevation. Because the peak cladding temperature also depends on the feed air temperature (the effect is one-for-one within a small range, i.e., 1°F drop in the feed air temperature results in ~1°F drop in the peak cladding temperature), the adverse ambient pressure effect of increased elevation is partially offset by the ambient air temperature decrease. The table below illustrates the variation of air pressure and corresponding ambient temperature as a function of elevation.

Elevation (ft)	Pressure (psia)	Ambient Temperature Reduction versus Sea Level
Sea Level (0)	14.70	0°F

2000	13.66	7.1°F
4000	12.69	14.3°F

A survey of the elevation of nuclear plants in the U.S. shows that nuclear plants are situated near about sea level or elevated slightly (~1000 ft). The effect of the elevation on peak fuel cladding temperatures is evaluated by performing calculations for a HI-STORM FW system situated at an elevation of 1500 feet. At this elevation the ambient temperature would decrease by approximately 5°F (See Table above). The peak cladding temperatures are calculated under the reduced ambient temperature and pressure at 1500 feet elevation for the limiting regionalized storage scenario evaluated in Table 4.4.2. The results are presented in Table 4.4.9.

These results show that the PCT, including the effects of site elevation, continues to be well below the regulatory cladding temperature limit of 752°F. In light of the above evaluation, it is not necessary to place ISFSI elevation constraints for HI-STORM FW deployment at elevations up to 1500 feet. If, however, an ISFSI is sited at an elevation greater than 1500 feet, the effect of altitude on the PCT shall be quantified as part of the 10 CFR 72.212 evaluation for the site using the site ambient conditions.

4.4.5 Maximum Internal Pressure

4.4.5.1 MPC Helium Backfill Pressure

The quantity of helium emplaced in the MPC cavity shall be sufficient to produce an operating pressure of 7 atmospheres (absolute) during normal storage conditions defined in Table 4.1.1. Thermal analyses performed on the different MPC designs indicate that this operating pressure requires a certain minimum helium backfill pressure (P_b) specified at a reference temperature (70°F). The minimum backfill pressure for each MPC type is provided in Table 4.4.7. A theoretical upper limit on the helium backfill pressure also exists and is defined by the design pressure of the MPC vessel (Table 2.2.1). The upper limit of P_b is also reported in Table 4.4.7. To bound the minimum and maximum backfill pressures listed in Table 4.4.7 with a margin, a helium backfill specification is set forth in Table 4.4.8.

To provide additional helium backfill range for less than design basis heat load canisters a Sub-Design-Basis (SDB) heat load scenario is defined wherein each fuel storage location is assumed to be generating heat at 80% of the Design Basis fuel assembly heats defined in Tables 1.2.3 and 1.2.4 and the MPC sufficiently backfilled to yield 6 atmospheres absolute pressure. The storage cell and MPC heat load limits under the SDB scenario are specified in Table 4.4.11. Calculations show that the maximum cladding temperature under the SDB scenario meet the ISG-11 temperature limits. The helium backfill pressure limits supporting this scenario are defined in Table 4.4.10. These backfill limits maybe optionally adopted by a cask user if the decay heats of the loaded fuel assemblies meet the SDB decay heat limits stipulated above.

Two methods are available for ensuring that the appropriate quantity of helium has been placed in an MPC:

i. By pressure measurement
ii. By measurement of helium backfill volume (in standard cubic feet)

The direct pressure measurement approach is more convenient if the FHD method of MPC drying is used. In this case, a certain quantity of helium is already in the MPC. Because the helium is mixed inside the MPC during the FHD operation, the temperature and pressure of the helium gas at the MPC's exit provides a reliable means to compute the inventory of helium. A shortfall or excess of helium is adjusted by a calculated raising or lowering of the MPC pressure such that the reference MPC backfill pressure is within the range specified in Table 4.4.8 or Table 4.4.10 (as applicable).

When vacuum drying is used as the method for MPC drying, then it is more convenient to fill the MPC by introducing a known quantity of helium (in standard cubic feet) by measuring the quantity of helium introduced using a calibrated mass flow meter or other measuring apparatus. The required quantity of helium is computed by the product of net free volume and helium specific volume at the reference temperature (70°F) and a target pressure that lies in the mid-range of the Table 4.4.8 pressures.

The net free volume of the MPC is obtained by subtracting B from A, where

A = MPC cavity volume in the absence of contents (fuel and non-fuel hardware) computed from nominal design dimensions

B = Total volume of the contents (fuel including DFCs, if used) based on nominal design dimensions

Using commercially available mass flow totalizers or other appropriate measuring devices, an MPC cavity is filled with the computed quantity of helium.

4.4.5.2 MPC Pressure Calculations

The MPC is initially filled with dry helium after fuel loading and drying prior to installing the MPC closure ring. During normal storage, the gas temperature within the MPC rises to its maximum operating basis temperature. The gas pressure inside the MPC will also increase with rising temperature. The pressure rise is determined using the ideal gas law. The MPC gas pressure is also subject to substantial pressure rise under hypothetical rupture of fuel rods and large gas inventory non-fuel hardware (PWR BPRAs). To minimize MPC gas pressures the number of BPRA containing fuel assemblies must be limited to 30.

Table 4.4.4 presents a summary of the MPC free volumes determined for the fixed height MPC-89 and lowerbound height MPC-37 fuel storage scenarios. The MPC maximum gas pressure is computed for a postulated release of fission product gases from fuel rods into this free space. For these scenarios, the amounts of each of the release gas constituents in the MPC cavity are summed and the resulting total pressures determined from the ideal gas law. A concomitant effect of rod ruptures is the increased pressure and molecular weight of the cavity gases with enhanced rate of heat dissipation by internal helium convection and lower cavity temperatures. As these effects are substantial under large rod ruptures the 100% rod rupture accident is evaluated with due credit for increased heat dissipation under increased pressure and molecular weight of the cavity gases. Based on fission gases release fractions (NUREG 1536 criteria [4.4.1]), rods' net free volume and initial fill gas pressure, maximum gas pressures with 1% (normal), 10% (off-normal) and 100% (accident condition) rod rupture are given in Table 4.4.5. The maximum computed gas pressures reported in Table 4.4.5 are all below the MPC internal design pressures for normal, off-normal and accident conditions specified in Table 2.2.1.

Evaluation of Non-Fuel Hardware

The inclusion of PWR non-fuel hardware (BPRA control elements and thimble plugs) to the PWR basket influences the MPC internal pressure through two distinct effects. The presence of non-fuel hardware increases the effective basket conductivity, thus enhancing heat dissipation and lowering fuel temperatures as well as the temperature of the gas filling the space between fuel rods. The gas volume displaced by the mass of non-fuel hardware lowers the cavity free volume. These two effects, namely, temperature lowering and free volume reduction, have opposing influence on the MPC cavity pressure. The first effect lowers gas pressure while the second effect raises it. In the HI-STORM FW thermal analysis, the computed temperature field (with non-fuel hardware excluded) has been determined to provide a conservatively bounding temperature field for the PWR baskets. The MPC cavity free space is computed based on conservatively computed volume displacement by fuel with non-fuel hardware included. This approach ensures conservative bounding pressures.

During in-core irradiation of BPRAs, neutron capture by the B-10 isotope in the neutron absorbing material produces helium. Two different forms of the neutron absorbing material are used in BPRAs: Borosilicate glass and B_4C in a refractory solid matrix (Al_2O_3). Borosilicate glass (primarily a constituent of Westinghouse BPRAs) is used in the shape of hollow pyrex glass tubes sealed within steel rods and supported on the inside by a thin-walled steel liner. To accommodate helium diffusion from the glass rod into the rod internal space, a relatively high void volume (~40%) is engineered in this type of rod design. The rod internal pressure is thus designed to remain below reactor operation conditions (2,300 psia and approximately 600°F coolant temperature). The B_4C- Al_2O_3 neutron absorber material is principally used in B&W and CE fuel BPRA designs. The relatively low temperatures of the poison material in BPRA rods (relative to fuel pellets) favor the entrapment of helium atoms in the solid matrix.

Several BPRA designs are used in PWR fuel. They differ in the number, diameter, and length of poison rods. The older Westinghouse fuel (W-14x14 and W-15x15) has used 6, 12, 16, and 20 rods per assembly BPRAs and the later (W-17x17) fuel uses up to 24 rods per BPRA. The BPRA rods in the older fuel are much larger than the later fuel and, therefore, the B-10 isotope inventory in the 20-rod BPRAs bounds the newer W-17x17 fuel. Based on bounding BPRA rods internal pressure, a large hypothetical quantity of helium (7.2 g-moles/BPRA) is assumed to be available for release into the MPC cavity from each BPRA containing fuel assembly. For a bounding evaluation the maximum permissible number of BPRA containing fuel assemblies (see discussion at the beginning of this Section) are assumed to be loaded. The MPC cavity pressures (including helium from BPRAs) are summarized in Table 4.4.5 for the bounding MPC-37 (shortest MPC height and design heat load) and MPC-89 (design heat load) storage scenarios.

4.4.6 Engineered Clearances to Eliminate Thermal Interferences

Thermal stress in a structural component is the resultant sum of two factors, namely: (i) restraint of free end expansion and (ii) non-uniform temperature distribution. To minimize thermal stresses in load bearing members, the HI-STORM FW system is engineered with adequate gaps to permit free thermal expansion of the fuel basket and MPC in axial and radial directions. In this subsection, differential thermal expansion calculations are performed to demonstrate that engineered gaps in the HI-STORM FW System are adequate to accommodate thermal expansion of the fuel basket and MPC.

The HI-STORM FW System is engineered with gaps for the fuel basket and MPC to expand thermally without restraint of free end expansion. The following gaps are evaluated:

a. Fuel Basket-to-MPC Radial Gap
b. Fuel Basket-to-MPC Axial Gap
c. MPC-to-Overpack Radial Gap
d. MPC-to-Overpack Axial Gap

The FLUENT thermal model provides the 3-D temperature field in the HI-STORM FW system from which the changes in the above gaps are directly computed. Table 4.4.6 provides the initial minimum gaps and their corresponding value during long-term storage conditions. Significant margins against restraint to free-end expansion are available in the design.

4.4.7 Evaluation of System Performance for Normal Conditions of Storage

The HI-STORM FW System thermal analysis is based on a detailed 3-D heat transfer model that conservatively accounts for all modes of heat transfer in the MPC and overpack. The thermal model incorporates conservative assumptions that render the results for long-term storage to be conservative.

Temperature distribution results obtained from this thermal model show that the maximum fuel cladding temperature limits are met with adequate margins. Expected margins during normal storage will be much greater due to the conservative assumptions incorporated in the analysis. As justified next the long-term impact of elevated temperatures reached in the HI-STORM FW system is minimal. The maximum MPC basket temperatures are below the recommended limits for susceptibility to stress, corrosion and creep-induced degradation. A complete evaluation of all material failure modes and causative mechanisms has been performed in Chapter 8 which shows that all selected materials for use in the HI-STORM FW system will render their intended function for the service life of the system. Furthermore, stresses induced due to the associated temperature gradients are modestly low (See Structural Evaluation Chapter 3).

Table 4.4.1

EFFECTIVE FUEL PROPERTIES UNDER BOUNDING FUEL STORAGE CONFIGURATIONS[Note 1]

	Conductivity (Btu/hr-ft-°F)			
	PWR: Short Fuel		**PWR: Standard Fuel**	
Temperature (°F)	Planar	Axial	Planar	Axial
200	0.247	0.813	0.231	0.759
450	0.443	0.903	0.387	0.845
700	0.730	1.016	0.601	0.951
	PWR: XL Fuel		**BWR Fuel**	
	Planar	Axial	Planar	Axial
200	0.239	0.787	0.283	0.897
450	0.393	0.875	0.426	0.988
700	0.599	0.984	0.607	1.104

Thermal Inertia Properties		
	Density (lb/ft^3)	Heat Capacity (Btu/lb-°F)[Note 2]
PWR: Short Fuel	165.8	0.056
PWR: Standard Fuel	176.2	0.056
PWR: XL Fuel	187.5	0.056
BWR Fuel	255.6	0.056

Note 1: Bounding fuel storage configurations defined in 4.4.1.1(ii).

Note 2: The lowerbound heat capacity of principal fuel assembly construction materials tabulated in Table 4.2.5 (UO_2 heat capacity) is conservatively adopted.

Note 3: The fuel properties tabulated herein are used in screening calculations to define the limiting scenario for fuel storage (See Table 4.4.2).

Table 4.4.2

RESULTS OF SCREENING CALCULATIONS UNDER NORMAL STORAGE CONDITIONS

Storage Scenario	Peak Cladding Temperature, °C (°F)
MPC-37	
Minimum Height*	**353 (667)**
Reference Height	342 (648)
Maximum Height	316 (601)
MPC-89	333 (631)

Notes:

(1) The highest temperature highlighted above is reached under the case of minimum height MPC-37 designed to store the short height Ft. Calhoun 14x14 fuel. This scenario is adopted in Chapter 4 for the licensing basis evaluation of fuel storage in the HI-STORM FW system.

(2) All the screening calculations were performed using a baseline mesh.

* Bounding scenario adopted in this Chapter for all thermal evaluations.

Table 4.4.3

MAXIMUM TEMPERATURES IN THE LIMITING HI-STORM FW STORAGE SCENARIO UNDER LONG-TERM NORMAL STORAGE*

Component	Temperature, °C (°F)
Fuel Cladding	375 (707)
MPC Basket	361 (682)
Basket Periphery	297 (567)
Aluminum Basket Shims	276 (529)
MPC Shell	246 (475)
MPC Lid[Note 1]	243 (469)
Overpack Inner Shell	128 (262)
Overpack Outer Shell	60 (140)
Overpack Body Concrete[Note 1]	88 (190)
Overpack Lid Concrete[Note 1]	113 (235)
Area Averaged Air outlet†	104 (219)

Note 1: Maximum section average temperature is reported.

* The temperatures reported in this table (all for shortest fuel scenario of MPC-37) are below the design temperatures specified in Table 2.2.3, Chapter 2.

† Reported herein for the option of temperature measurement surveillance of outlet ducts air temperature as set forth in the Technical Specifications.

Table 4.4.4

MINIMUM MPC FREE VOLUMES

Item	Lowerbound Height MPC-37 (ft^3)	MPC-89 (ft^3)
Net Free Volume*	211.89	210.12

**Net free volumes are obtained by subtracting basket, fuel, aluminum shims, spacers, basket supports and DFCs metal volume from the MPC cavity volume.*

Table 4.4.5

SUMMARY OF MPC INTERNAL PRESSURES UNDER LONG-TERM STORAGE*

Condition	MPC-37 (psig)	MPC-89*** (psig)
Initial backfill** (at 70°F)	45.5	45.5
Normal:		
intact rods	98.0	98.0
1% rods rupture	99.1	98.6
Off-Normal (10% rods rupture)	109.1	103.9
Accident (100% rods rupture)	195.5	156.3

* Per NUREG-1536, pressure analyses with ruptured fuel rods (including BPRA rods for PWR fuel) is performed with release of 100% of the ruptured fuel rod fill gas and 30% of the significant radioactive gaseous fission products.

** Conservatively assumed at the Tech. Spec. maximum value (see Table 4.4.8).

*** Conservatively the MPC-37 cavity average temperature is adopted for pressure calculations.

Table 4.4.6

SUMMARY OF HI-STORM FW DIFFERENTIAL THERMAL EXPANSIONS

Gap Description	Cold Gap U (in)	Differential Expansion δ_i (in)	Is Free Expansion Criterion Satisfied (i.e., $U > \delta_i$)
Fuel Basket-to-MPC Radial Gap	0.125	0.112	Yes
Fuel Basket-to-MPC Axial Gap	1.5	0.421	Yes
MPC-to-Overpack Radial Gap	5.5	0.128	Yes
MPC-to-Overpack Minimum Axial Gap	3.5	0.372	Yes

Table 4.4.7

THEORETICAL LIMITS* OF MPC HELIUM BACKFILL PRESSURE**

MPC	Minimum Backfill Pressure (psig)	Maximum Backfill Pressure (psig)
MPC-37	40.3	46.6
MPC-89***	40.3	46.6

* The helium backfill pressures are set forth in the Technical Specifications with a margin (see Table 4.4.8).

** The pressures tabulated herein are at 70°F reference gas temperature.

*** Conservatively the MPC-37 cavity average temperature is adopted for pressure calculations.

Table 4.4.8 MPC HELIUM BACKFILL PRESSURE SPECIFICATIONS		
MPC	**Item**	**Specification**
MPC-37	Minimum Pressure	42.5 psig @ 70°F Reference Temperature
	Maximum Pressure	45.5 psig @ 70°F Reference Temperature
MPC-89*	Minimum Pressure	42.5 psig @ 70°F Reference Temperature
	Maximum Pressure	45.5 psig @ 70°F Reference Temperature
* Conservatively the MPC-37 cavity average temperature is adopted for pressure calculations.		

Table 4.4.9 MAXIMUM HI-STORM FW TEMPERATURES AT ELEVATED SITES*	
Component	**Temperature, °C (°F)**
Fuel Cladding	374 (705)
MPC Basket	360 (680)
Aluminum Basket Shims	275 (527)
MPC Shell	246 (475)
MPC Lid[Note 1]	242 (468)
Overpack Inner Shell	126 (259)
Overpack Body Concrete[Note 1]	86 (187)
Overpack Lid Concrete[Note 1]	112 (234)
Note 1: Maximum section average temperature is reported.	

* The temperatures reported in this table (all for the bounding scenario defined in Table 4.4.2) are below the design temperatures specified in Table 2.2.3, Chapter 2.

Table 4.4.10 MPC HELIUM BACKFILL PRESSURE LIMITS UNDER THE SUB-DESIGN-BASIS HEAT LOAD SCENARIO[Note 1]		
MPC	**Item**	**Specification**
MPC-37	Minimum Pressure	42.0 psig @ 70°F Reference Temperature
	Maximum Pressure	50.0 psig @ 70°F Reference Temperature
MPC-89	Minimum Pressure	42.0 psig @ 70°F Reference Temperature
	Maximum Pressure	50.0 psig @ 70°F Reference Temperature
Note 1: The Sub-Design-Basis heat load scenario is defined in Section 4.4.5.1.		

Table 4.4.11 SUB-DESIGN BASIS HEAT LOAD LIMITS	
MPC-37	
Region 1 Cells	0.904 kW/assy
Region 2 Cells	1.424 kW/assy
Region 3 Cells	0.776 kW/assy
Total	37.6 kW
MPC-89	
Region 1 Cells	0.352 kW/assy
Region 2 Cells	0.496 kW/assy
Region 3 Cells	0.352 kW/assy
Total	37.1 kW
Note: The MPC-37 and MPC-89 storage cell regions are defined in Figures 1.2.1 and 1.2.2 respectively.	

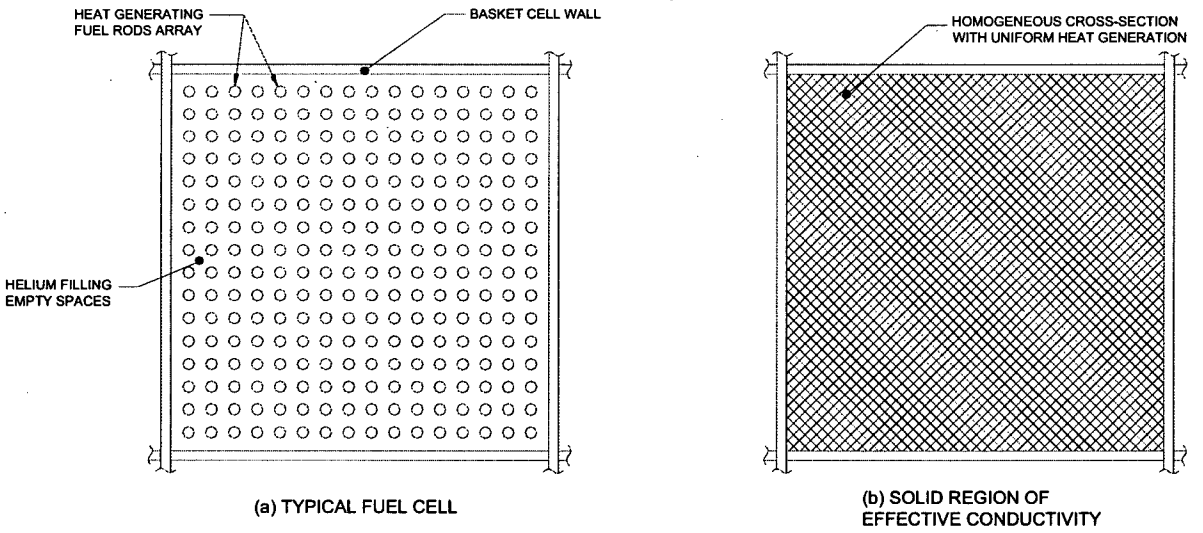

Figure 4.4.1: Homogenization of the Storage Cell Cross-Section

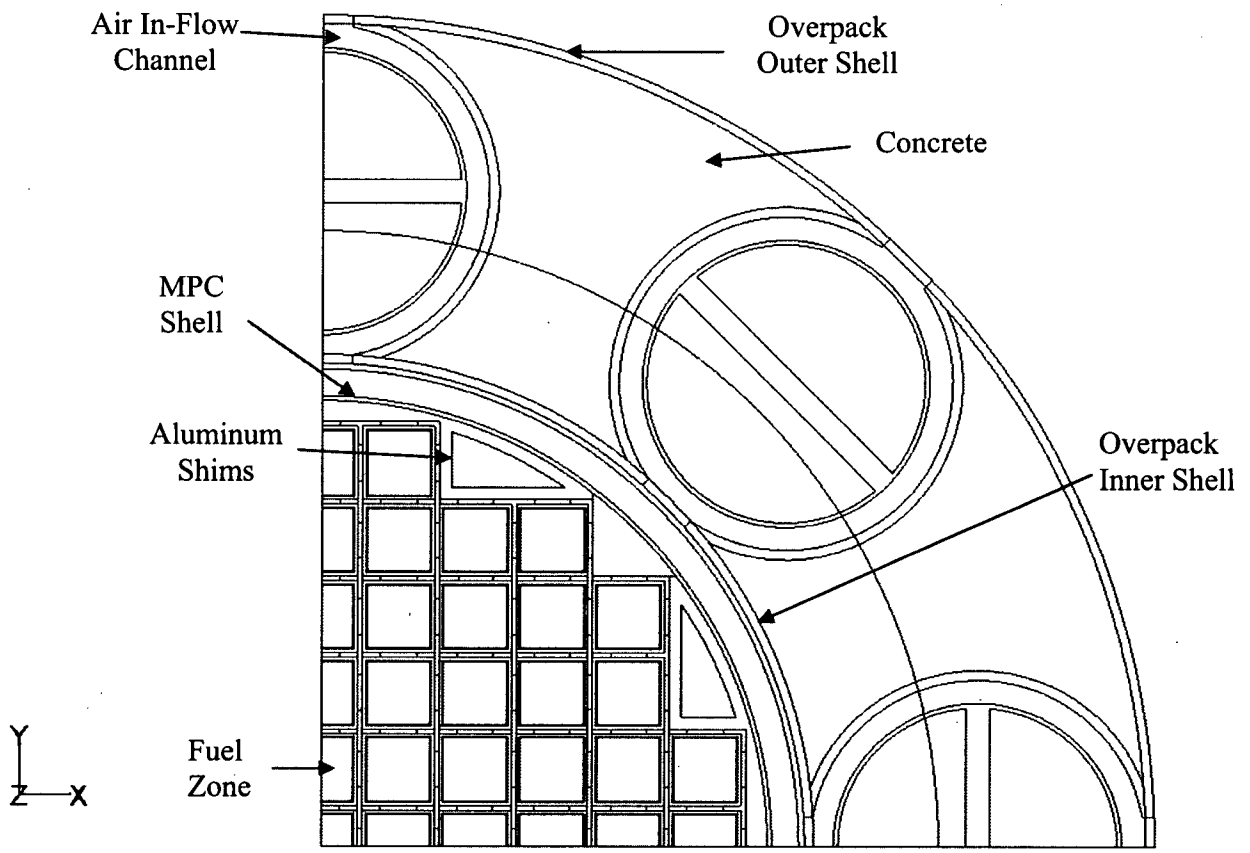

Figure 4.4.2: Planar View of HI-STORM FW MPC-89 Quarter Symmetric 3-D Model

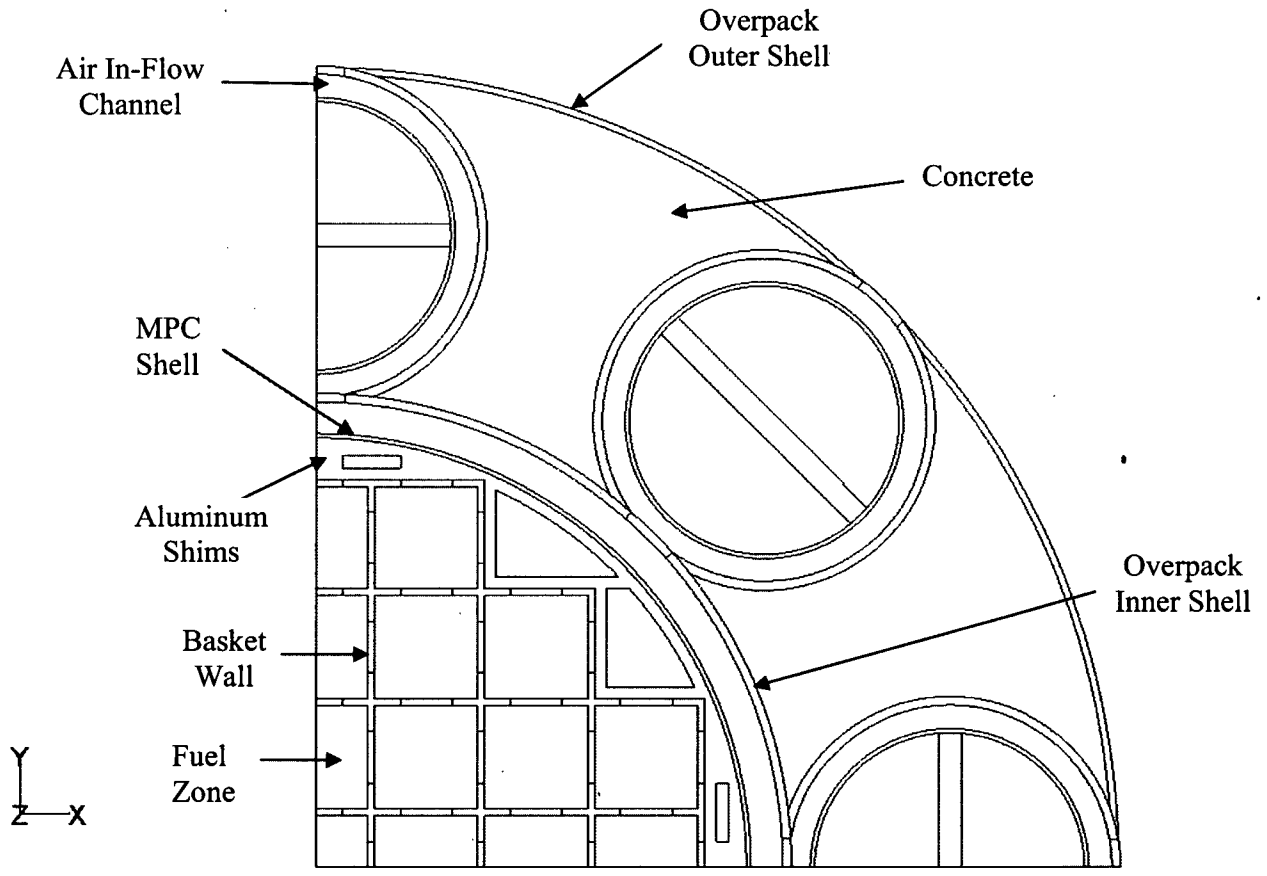

Figure 4.4.3: Planar View of HI-STORM FW MPC-37 Quarter Symmetric 3-D Model

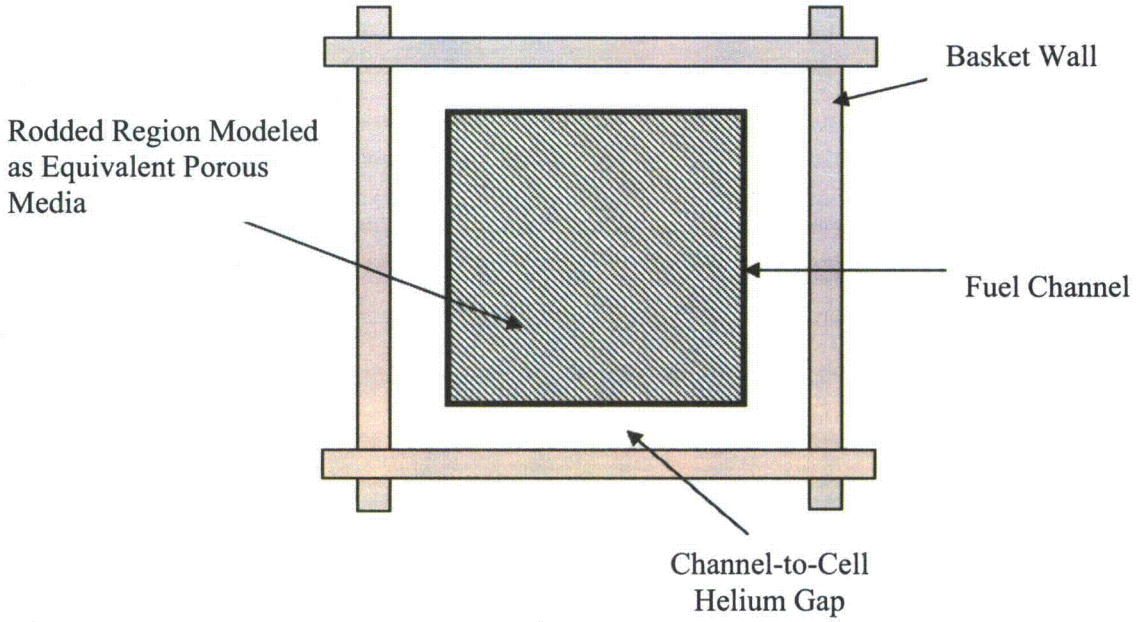

Figure 4.4.4: Closeup View of the MPC-89 Channeled Fuel Spaces

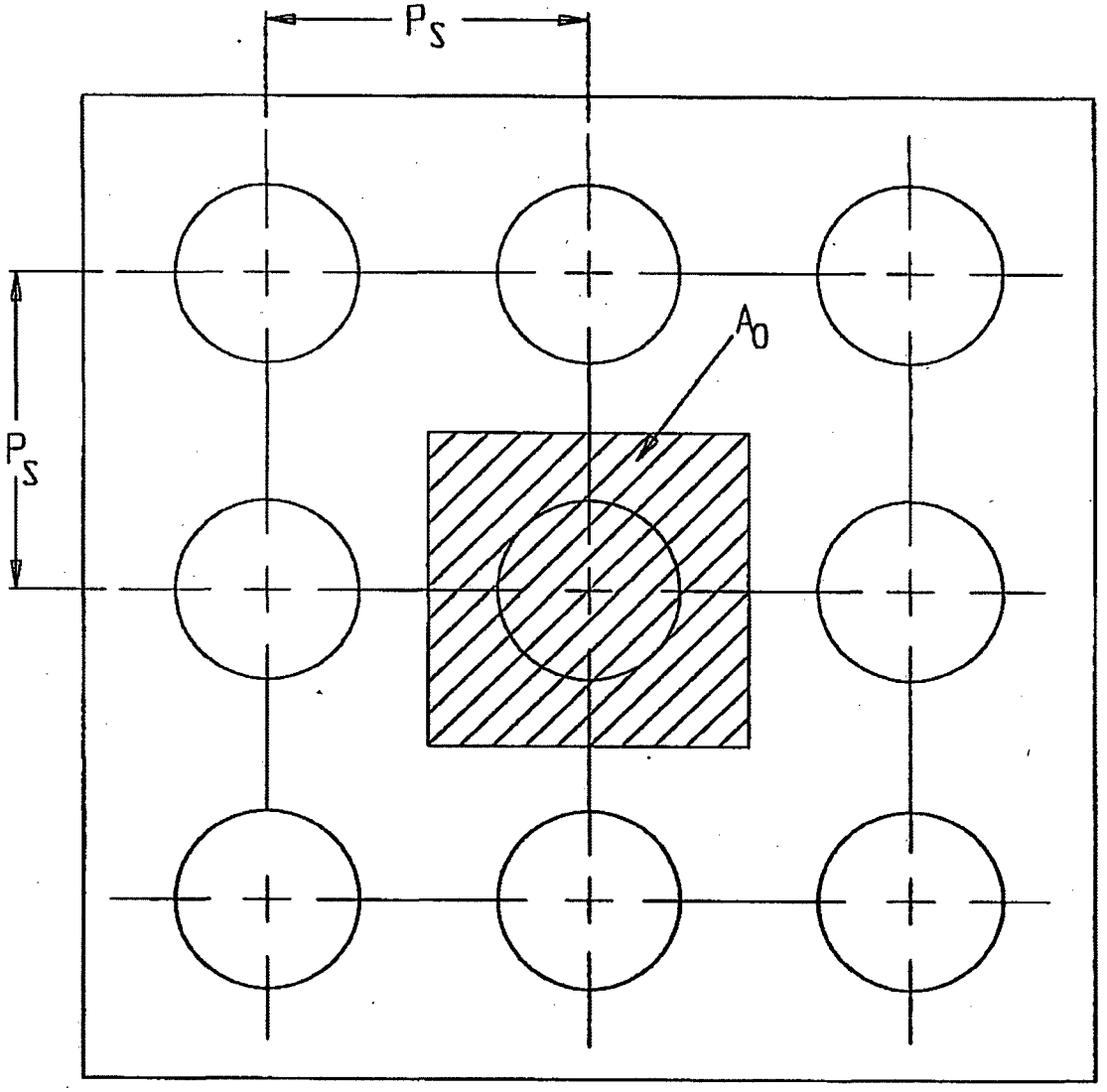

Legend:
P_s: Cask pitch
A_o: Tributary area

Figure 4.4.5: Illustration of a Centrally Located Cask in a Cask Array

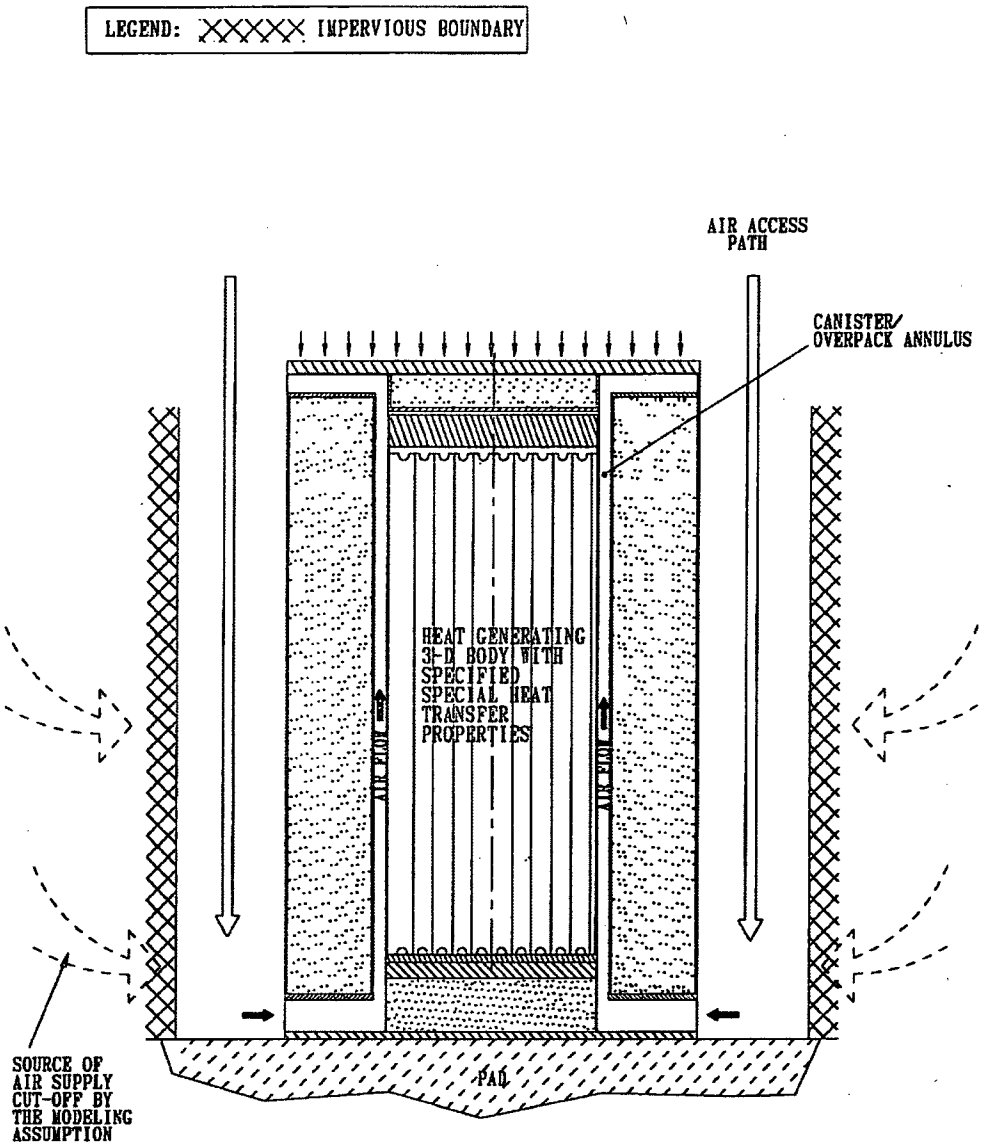

Figure 4.4.6: Illustration of the Hypothetical Square Cavity Thermal Model

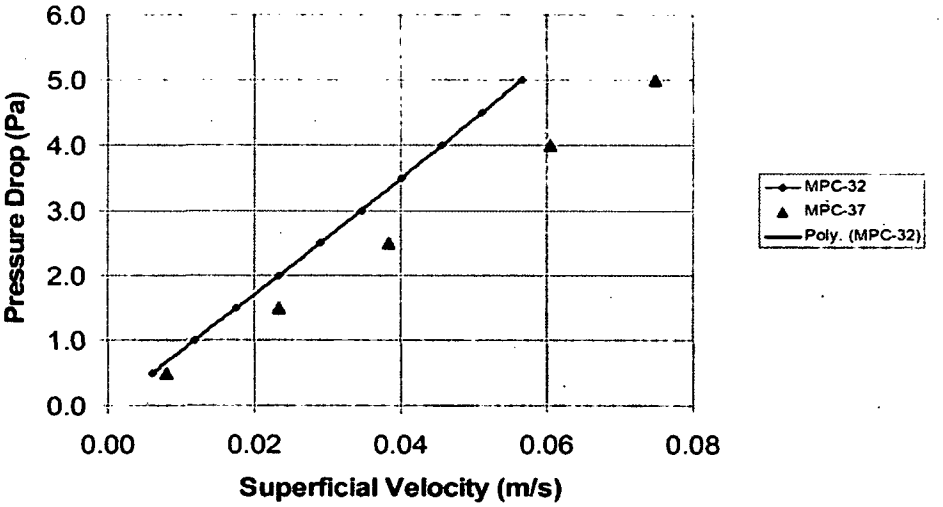

Figure 4.4.7: Storage Cell Pressure Drop as a Function of In-Cell Helium Velocity

4.5 THERMAL EVALUATION OF SHORT-TERM OPERATIONS

4.5.1 Thermally Limiting Evolutions During Short-Term Operations

Prior to placement in a HI-STORM FW overpack, an MPC must be loaded with fuel, outfitted with closures, dewatered, dried, backfilled with helium and transported to the HI-STORM FW module. In the unlikely event that the fuel needs to be returned to the spent fuel pool, these steps must be performed in reverse. Finally, if required, transfer of a loaded MPC between HI-STORM FW overpacks or between a HI-STAR transport overpack and a HI-STORM FW storage overpack must be carried out in a safe manner. All of the above operations, henceforth referred to as "short-term operations", are short duration events that would likely occur no more than once or twice for an individual MPC.

Chapter 9 provides a description of the typical loading steps involved in moving nuclear fuel from the spent fuel pool to dry storage in the HI-STORM FW system. The transition from a wet to a dry environment, to comply with ISG-11, Rev. 3, must occur without exceeding the short-term operation temperature limits (see Table 4.3.1).

The loading steps that present the limiting thermal condition during short term operations for the fuel are those when either one or both of the following conditions exist:

i. The MPC's fuel storage space is evacuated of fluids resulting in a significant decease in internal heat transmission rates. This condition obtains if the vacuum drying method for removing moisture from the canister is employed.

ii. The removal of heat from the external surfaces of the MPC is impeded because of the air gap between the canister and HI-TRAC VW. This condition exists, for example, when the loaded MPC is being moved inside HI-TRAC VW for staging and transfer of the MPC to the HI-STORM FW overpack.

In this section, the thermally limiting scenarios during short-term operations are identified and analyzed.

Because onsite transport of the MPC occurs with the HI-TRAC VW in the vertical orientation, the thermosiphon action within the MPC is preserved at all times. The only (rare) departure from a purely vertical orientation occurs if a tilting of the HI-TRAC VW is needed to clear an obstruction such as a low egress bay door opening at a plant. In such a case the operational imperative for HI-TRAC VW tilting must be ascertained and the permissible duration of non-vertical configuration must be established on a site-specific basis and compliance with the thermal limits of ISG-11 [4.1.4] must be demonstrated as a part of the site-specific safety evaluation under 10CFR72.212.

4.5.2 HI-TRAC VW Thermal Model

4.5.2.1 On-Site Transfer

The HI-TRAC VW transfer cask is used to load and unload the HI-STORM FW concrete storage overpack, including onsite transport of the MPCs from the loading facility to an ISFSI pad. Within a loaded HI-TRAC VW, heat generated in the MPC is transported from the contained fuel assemblies to the MPC shell through the fuel basket and the basket-to-shell gaps via conduction and thermal radiation. From the outer surface of the MPC to the ambient atmosphere, heat is transported within across multiple concentric layers, representing the air gap, the HI-TRAC VW inner shell, the lead shielding, the HI-TRAC VW outer shell, the water jacket space and the jacket shell. From the surface of the HI-TRAC VW's enclosure shell heat is rejected to the atmosphere by natural convection and radiation.

A small diametral gap exists between the outer surface of the MPC and the inner surface of the HI-TRAC VW overpack which may be filled with water during an operational state to serve as a heat sink and radiation absorber. The water jacket, which provides neutron shielding for the HI-TRAC VW overpack, surrounds the outer cylindrical steel wall of the HI-TRAC VW body. Heat is transported through the water jacket by a combination of conduction through steel ribs and convection heat transfer in the water spaces. The bottom face of the HI-TRAC VW is in contact with a supporting surface which is a thermal heat sink. This face is conservatively modeled as an insulated surface. The HI-TRAC VW is an open top construction which is modeled as an opening to allow air exchange with the ambient.

The HI-TRAC VW Transfer Cask thermal analysis is based on a detailed heat transfer model that conservatively accounts for all modes of heat transfer in the MPC and HI-TRAC VW. The thermal model incorporates several conservative features listed below:

i. Severe levels of environmental factors - bounding ambient temperature, 32.2°C (90°F), and constant solar flux - were coincidentally imposed on the thermal design. A bounding solar absorbtivity of 0.85 is applied to all exposed surfaces.

ii. The HI-TRAC VW Transfer Cask-to-MPC annular gap is analyzed based on the nominal design dimensions. No credit is considered for the gap reduction that would occur as a result of differential thermal expansion with design basis fuel at hot conditions. The MPC is considered to be concentrically aligned with the cask cavity and the annulus is filled with air. This scenario maximizes thermal resistance.

iii. The HI-TRAC VW baseplate is in thermally communicative contact with supporting surfaces. For conservatism an insulated boundary condition is applied to the baseplate.

iv. The HI-TRAC VW fluid columns (namely air in the annulus and water in the water jacket) are allowed to move. In other words natural convection heat transfer by annulus air and water is credited in the analysis.

v. To maximize lateral resistance to heat dissipation in the fuel basket conservatively postulated 0.4 mm full length panel gaps are assumed at all intersections. This approach is similar to the approach in the approved HI-STAR 180 Package in Docket 71-9325. The shims installed in the MPC peripheral spaces (See MPC-37 and MPC-89 drawings in Section 1.5) are explicitly modeled. For conservatism reasonably bounding gaps (2.5 mm basket-to-shims and 2.5 mm shims-to-shell) are incorporated in the thermal models.

The grid deployed in the HI-TRAC VW thermal model is confirmed to be grid independent through mesh sensitivity studies. The studies refined the radial mesh in HI-TRAC VW annulus and water jacket regions. The thermal solutions obtained show that the temperatures are essentially unchanged.

To evaluate on-site transfer operations a HI-TRAC VW thermal model is constructed under the limiting scenario of fuel storage in the minimum height MPC-37 (See Section 4.4.1.5) at design maximum heat load specified in Chapter 1, Section 1.2. The model adopts the MPC thermal modeling methodology described in Section 4.4 and the properties of design basis 14x14 Ft. Calhoun fuel defined in Table 4.4.1 under the limiting fuel storage scenario cited above. Results of on-site transfer analyses are provided in Subsection 4.5.4.3.

4.5.2.2 Vacuum Drying

The initial loading of SNF in the MPC requires that the water within the MPC be drained and replaced with helium. For MPCs containing moderate burnup fuel assemblies only, this operation may be carried out using the conventional vacuum drying approach upto design basis heat load. In this method, removal of moisture from the MPC cavity is accomplished by evacuating the MPC after completion of MPC draining operation. Vacuum drying of MPCs containing high burnup fuel assemblies is permitted up to threshold heat loads defined in Table 4.5.1. High burnup fuel drying in MPCs generating greater than threshold heat load is performed by a forced flow helium drying process as discussed in Section 4.5.4.

Prior to the start of the MPC draining operation, both the HI-TRAC VW annulus and the MPC are full of water. The presence of water in the MPC ensures that the fuel cladding temperatures are lower than design basis limits by large margins. As the heat generating active fuel length is uncovered during the draining operation, the fuel and basket mass will undergo a gradual heat up from the initially cold conditions when the heated surfaces were submerged under water. To minimize fuel temperatures during vacuum drying operations the HI-TRAC VW annulus must be water filled. The necessary operational steps required to ensure this requirement are set forth in Chapter 9.

A 3-D FLUENT thermal model of the MPC is constructed in the same manner as described in Section 4.4. The principal input to this model is the effective conductivity of fuel under vacuum drying operations. To bound the vacuum drying operations the effective conductivity of fuel is computed assuming the MPC is filled with water vapor at a very low pressure (1 torr). The methodology for computing the effective conductivity is given in Section 4.4.1 and effective properties of design basis fuel under vacuum conditions tabulated in Table 4.5.8. To ensure a conservative evaluation the thermal model is incorporated with the following assumptions:

i. Bounding steady-state condition is reached with the MPC decay heat load set equal to the design heat load (Tables 1.2.3 and 1.2.4) for MPCs fueled with Moderate Burnup Fuel and threshold heat load defined in Table 4.5.1 for MPCs fueled with one or more High Burnup fuel assemblies.

ii. The external surface of the MPC shell is postulated to be at the boiling temperature of water 100°C (212°F).

iii. The bottom surface of the MPC is insulated.

iv. MPC internal convection heat transfer is suppressed.

Results of vacuum condition analyses are provided in Subsection 4.5.4.1.

4.5.3 Maximum Time Limit During Wet Transfer Operations

Fuel loading operations are typically conducted with the HI-TRAC VW and its contents (water filled MPC) submerged in pool water. Under these conditions, the HI-TRAC VW is essentially at the pool water temperature. When the HI-TRAC VW transfer cask and the loaded MPC under water-flooded conditions is removed from the pool, the water, fuel, MPC and HI-TRAC VW metal absorb the decay heat emitted by the fuel assemblies. This results in a slow temperature rise of the HI-TRAC VW with time, starting from an initial (pool water) temperature. The rate of temperature rise is limited by the thermal inertia of the HI-TRAC VW system.

In accordance with NUREG-1536, water inside the MPC cavity during wet transfer operations is not permitted to boil. This requirement is met by imposing time limits for fuel to remain submerged in water after a loaded HI-TRAC VW cask is removed from the pool. The time limits are conservatively computed under an assumed adiabatic temperature rise of the cask with design heat load and understated thermal inertia of the cask defined in Table 4.5.3. The computed time limits are tabulated in Table 4.5.4.

As set forth in the HI-STORM FW operating procedures, in the unlikely event that the maximum allowable time provided in Table 4.5.3 is found to be insufficient to complete all wet transfer operations, a forced water circulation shall be initiated and maintained to remove the decay heat from the MPC cavity. In this case, relatively cooler water will enter via MPC lid ports and heated water will exit from the vent port. The minimum water flow rate required to maintain the MPC

cavity water temperature below boiling with an adequate subcooling margin is determined as follows:

$$M_W = \frac{Q}{C_{pW}(T_{max} - T_{in})}$$

where:

M_W = minimum water flow rate (lb/hr)
C_{pw} = water heat capacity (Btu/lb-°F)
T_{max} = suitably limiting temperature below boiling (°F)
T_{in} = water supply temperature to MPC

4.5.4 Analysis of Limiting Thermal States During Short-Term Operations

4.5.4.1 Vacuum Drying

The vacuum drying option is evaluated for the two limiting scenarios defined in Section 4.5.2.2 to address Moderate Burnup Fuel under design basis heat load and High Burnup Fuel under threshold heat load defined in Table 4.5.1. The principle objective of the analysis is to ensure compliance with ISG-11 temperature limits. For this purpose 3-D FLUENT thermal models of the MPC-37 and MPC-89 canisters are constructed as described in Section 4.5.2.2 and bounding steady state temperatures computed. The results are tabulated in Tables 4.5.6 and 4.5.7. The results show that the cladding temperatures comply with the ISG-11 limits for moderate and high burnup fuel in Table 4.3.1 by robust margins.

4.5.4.2 Forced Helium Dehydration

To reduce moisture to trace levels in the MPC using a Forced Helium Dehydration (FHD) system, a conventional, closed loop dehumidification system consisting of a condenser, a demoisturizer, a compressor, and a pre-heater is utilized to extract moisture from the MPC cavity through repeated displacement of its contained helium, accompanied by vigorous flow turbulation. Demoisturization to the3 torr vapor pressure criteria required by NUREG 1536 is assured by verifying that the helium temperature exiting the demoisturizer is maintained at or below the psychrometric threshold of 21°F for a minimum of 30 minutes. Appendix 2.B of [4.1.8] provides a detailed discussion of the design criteria and operation of the FHD system.

The FHD system provides concurrent fuel cooling during the moisture removal process through forced convective heat transfer. The attendant forced convection-aided heat transfer occurring during operation of the FHD system ensures that the fuel cladding temperature will remain below the applicable peak cladding temperature limit in Table 2.2.3. Because the FHD operation induces a state of forced convection heat transfer in the MPC, (in contrast to the quiescent mode of natural convection in long term storage), it is readily concluded that the peak fuel cladding temperature under the latter condition will be greater than that during the FHD operation phase. In the event that

the FHD system malfunctions, the forced convection state will degenerate to natural convection, which corresponds to the conditions of normal onsite transfer. As a result, if the FHD machine fails then the peak fuel cladding temperatures will approximate the value reached during normal onsite transfer, discussed below.

4.5.4.3 Normal On-site Transfer

An MPC-37 situated inside a HI-TRAC VW is evaluated under the design heat load defined in Section 1.2. The MPC-37 is evaluated because it yields the highest fuel and cask temperatures (See Table 4.4.2). This scenario is analyzed using the same 3D FLUENT model of the MPC-37 articulated in Section 4.4 for normal storage with due recognition of it situated in the HI-TRAC VW transfer cask. The HI-TRAC VW model discussed in Section 4.5.2 is adopted to construct a global model of an MPC-37 situated inside the HI-TRAC VW and dissipating heat by natural convection and radiation to ambient air.

While the duration of onsite transport is generally short to preclude the MPC and HI-TRAC VW from reaching a steady-state, a conservative approach is adopted herein by assuming steady state maximum temperatures are reached. The principle objectives of the HI-TRAC VW analyses are to demonstrate:

i) Cladding integrity
ii) Confinement integrity
iii) Neutron shield integrity

The appropriate criteria are provided in Tables 2.2.1 (pressure limits) and 2.2.3 (temperature limits).

The results of thermal analyses tabulated in Table 4.5.2 show that the cladding temperatures are below the ISG-11 temperature limits of High and Moderate Burnup Fuel (Table 4.3.1). Actual margins during HI-TRAC VW operations will be much larger due to the many conservative assumptions incorporated in the analysis.

The water in the water jacket surrounding the HI-TRAC VW body provides necessary neutron shielding. During normal handling and onsite transfer operations this shielding water is contained within the water jacket at elevated internal pressure. The water jacket is equipped with two pressure relief devices set to an adequately high pressure to prevent boiling. Under HI-TRAC VW operations, the bulk temperature of water remains below the temperature limit specified in Table 2.2.3. Accordingly, water is in the liquid state and the neutron shielding function is maintained. The cladding, neutron shield and HI-TRAC VW component temperatures are provided in Table 4.5.2. The confinement boundary integrity is evaluated in the Section 4.5.6.

4.5.5 Cask Cooldown and Reflood Analysis During Fuel Unloading Operation

NUREG-1536 requires an evaluation of cask cooldown and reflood procedures to support fuel unloading from a dry condition. Past industry experience generally supports cooldown of cask internals and fuel from hot storage conditions by direct water quenching. Direct MPC cooldown is effectuated by introducing water through the lid drain line. From the drain line, water enters the MPC cavity near the MPC baseplate. Steam produced during the direct quenching process will be vented from the MPC cavity through the lid vent port. To maximize venting capacity, both vent port RVOA connections must remain open for the duration of the fuel unloading operations. As direct water quenching of hot fuel results in steam generation, it is necessary to limit the rate of water addition to avoid MPC overpressurization. For example, steam flow calculations using bounding assumptions (100% steam production and MPC at design pressure) show that the MPC is adequately protected under a reflood rate of 3715 lb/hr. Limiting the water reflood rate to this amount or less would prevent exceeding the MPC design pressure.

4.5.6 Maximum Internal Pressure (Load Case NB in Table 2.2.7)

After fuel loading and vacuum drying, but prior to installing the MPC closure ring, the MPC is initially filled with helium. During handling and on-site transfer operations in the HI-TRAC VW transfer cask, the gas temperature will correspond to the thermal conditions within the MPC analyzed in Section 4.5.4.3. Based on this analysis the MPC internal pressure is computed under the assumption of maximum helium backfill specified in Table 4.4.8 and confirmed to comply with the short term operations pressure limit in Table 2.2.1. The results are tabulated in Table 4.5.5.

Table 4.5.1 THRESHOLD HEAT LOADS UNDER VACUUM DRYING OF HIGH BURNUP FUEL		
Storage Zone[Note 1]	**MPC-37 (kW)**	**MPC-89 (kW)**
Region 1	0.8	0.35
Region 2	0.97	0.35
Region 3	0.97	0.44
MPC Heat Load	34.36	34.75
Note 1: Storage zones are defined in Figures 1.2.1 and 1.2.2.		

Table 4.5.2

HI-TRAC VW TRANSFER CASK STEADY STATE MAXIMUM TEMPERATURES[Note 1]

Component	Temperature, °C (°F)
Fuel Cladding	388 (730)
MPC Basket	375 (707)
Basket Periphery	305 (581)
Aluminum Basket Shims	283 (541)
MPC Shell	254 (489)
MPC Lid[Note 2]	244 (471)
HI-TRAC VW Inner Shell	144 (291)
HI-TRAC VW Radial Lead Gamma Shield	143 (289)
Water Jacket Bulk Water	134 (273)

Note 1: The temperatures tabulated herein are updated to reflect the changes in helium backfill pressures in Table 4.4.8.
Note 2: Maximum section average temperature is reported.

Table 4.5.3

HI-TRAC VW TRANSFER CASK LOWERBOUND WEIGHTS AND THERMAL INERTIAS

Component	Weight (lbs)	Heat Capacity (Btu/lb-°F)	Thermal Inertia (Btu/°F)
Lead	45627	0.031	1414
Carbon Steel	43270	0.1	4327
Stainless Steel	19561	0.12	2347
Aluminum	6734	0.207	1394
Metamic-HT	7349	0.22	1617
Fuel	46250	0.056	2590
MPC Cavity Water	6611	0.999	6604
Total	175402	-	20294

Table 4.5.4

MAXIMUM ALLOWABLE TIME FOR WET TRANSFER OPERATIONS

Initial temperature °F	Time Duration (hr)
100	14.2
110	12.9
120	11.6
130	10.4
140	9.1
150	7.8

Table 4.5.5

MPC CONFINEMENT BOUNDARY PRESSURE UNDER ON-SITE TRANSPORT

Condition	Pressure (psig)
Initial backfill pressure (at 70°F) (Tech. Spec. maximum in Table 4.4.8)	45.5
Maximum pressure	101.9

Table 4.5.6

MAXIMUM TEMPERATURES OF MPC-37 DURING VACUUM DRYING CONDITIONS

Component	Temperatures @DB Heat Load[Note 1] °C (°F)	Temperatures @ Threshold Heat Load[Note 2] °C (°F)
Fuel Cladding	480 (896)	384 (723)
MPC Basket	464 (867)	367 (693)
Basket Periphery	357 (675)	288 (550)
Aluminum Basket Shims	278 (532)	232 (450)
MPC Shell	156 (313)	142 (288)
MPC Lid[Note 3]	107 (225)	100 (212)

Note 1: Addresses vacuum drying of Moderate Burnup Fuel under Design Basis heat load defined in Section 1.2.
Note 2: Addresses vacuum drying of High Burnup Fuel under threshold heat load (Table 4.5.1).
Note 3: Maximum section temperature reported.

Table 4.5.7

MAXIMUM TEMPERATURES OF MPC-89 DURING VACUUM DRYING CONDITIONS

Component	Temperatures @DB Heat Load[Note 1] °C (°F)	Temperatures @ Threshold Heat Load[Note 2] °C (°F)
Fuel Cladding	464 (867)	376 (709)
MPC Basket	449 (840)	359 (678)
Basket Periphery	348 (658)	286 (547)
Aluminum Basket Shims	275 (527)	232 (450)
MPC Shell	158 (316)	144 (291)
MPC Lid[Note 3]	127 (261)	110 (230)

Note 1: Addresses vacuum drying of Moderate Burnup Fuel under Design Basis heat load defined in Section 1.2.
Note 2: Addresses vacuum drying of High Burnup Fuel under threshold heat load (Table 4.5.1).
Note 3: Maximum section temperature reported.

Table 4.5.8

EFFECTIVE CONDUCTIVITY OF DESIGN BASIS FUEL[Note 1] UNDER VACUUM DRYING OPERATIONS
(Btu/hr-ft-°F)

Temperature (°F)	Planar	Axial
200	0.111	0.737
450	0.273	0.805
700	0.538	0.900
1000	0.977	1.040

Note 1: Ft. Calhoun 14x14 fuel is defined as the design basis fuel under the limiting condition of fuel storage in the minimum height MPC-37 (See Table 4.4.2).

4.6 OFF-NORMAL AND ACCIDENT EVENTS

4.6.1 Off-Normal Events

4.6.1.1 Off-Normal Pressure (Load Case NB in Table 2.2.7)

This event is defined as a combination of (a) maximum helium backfill pressure (Table 4.4.8), (b) 10% fuel rods rupture, (c) limiting fuel storage configuration and (d) off-normal ambient temperature. The principal objective of the analysis is to demonstrate that the MPC off-normal design pressure (Table 2.2.1) is not exceeded. The MPC off-normal pressures are reported in Table 4.6.7. The result is below the off-normal design pressure (Table 2.2.1).

4.6.1.2 Off-Normal Environmental Temperature

This event is defined by a time averaged ambient temperature of 100°F for a 3-day period (Table 2.2.2). The results of this event (maximum temperatures and pressures) are provided in Table 4.6.1 and 4.6.7. The results are below the off-normal condition temperature and pressure limits (Tables 2.2.3 and 2.2.1).

4.6.1.3 Partial Blockage of Air Inlets

The HI-STORM FW system is designed with debris screens installed on the inlet and outlet openings. These screens ensure the air passages are protected from entry and blockage by foreign objects. As required by the design criteria presented in Chapter 2, it is postulated that the HI-STORM FW air inlet vents are 50% blocked. The resulting decrease in flow area increases the flow resistance of the inlet ducts. The effect of the increased flow resistance on fuel temperature is analyzed for the normal ambient temperature (Table 2.2.2) and a limiting fuel storage configuration. The computed temperatures are reported in Table 4.6.1 and the corresponding MPC internal pressure in Table 4.6.7. The results are confirmed to be below the temperature limits (Table 2.2.3) and pressure limit (Table 2.2.1) for off-normal conditions.

4.6.1.4 FHD Malfunction

This event is defined in Subsection 12.1.5 as stoppage of the FHD machine following loss of power or active component trip. The principal effect of this event is stoppage of helium circulation through the MPC and transitioning of heat dissipation in the MPC from forced convection to natural circulation cooling. To bound this event an array of adverse conditions are assumed to have developed coincidentally, as noted below:

a. Steady state maximum temperatures have been reached.
b. Design maximum heat load in the limiting MPC-37 is assumed .
c. Air (not water) is in the HI-TRAC FW annulus.

d. The helium pressure in the MPC is at the minimum possible value of 20 psig.

Under the FHD malfunction condition the principal requirement to ensure the off-normal cladding temperature limits mandated by ISG-11, Rev. 3 (see Table 2.2.3) must be demonstrated. For this purpose an array of adverse conditions are defined above and the Peak Cladding Temperature (PCT) computed using the 3D FLUENT model of the transfer cask articulated in Section 4.5. The PCT computes as 433°C which is significantly below the 570°C off-normal temperature limit.

4.6.2 Accident Events

4.6.2.1 Fire Accident (Load Case AB in Table 2.2.13)

Although the probability of a fire accident affecting a HI-STORM FW system during storage operations is low due to the lack of combustible materials at an ISFSI, a conservative fire event has been assumed and analyzed. The only credible concern is a fire from an on-site transport vehicle fuel tank. Under a postulated fuel tank fire, the outer layers of HI-TRAC VW or HI-STORM FW overpacks are heated for the duration of fire by the incident thermal radiation and forced convection heat fluxes. The amount of fuel in the on-site transporter is limited to a volume of 50 gallons. The data necessary to define the fire event is provided in Table 2.2.8.

(a) HI-STORM FW Fire

The fuel tank fire is conservatively assumed to surround the HI-STORM FW overpack. Accordingly, all exposed overpack surfaces are heated by radiation and convection heat transfer from the fire. Based on NUREG-1536 and 10 CFR 71 guidelines [4.6.1], the following fire parameters are assumed:

1. The average emissivity coefficient must be at least 0.9. During the entire duration of the fire, the painted outer surfaces of the overpack are assumed to remain intact, with an emissivity of 0.85. It is conservative to assume that the flame emissivity is 1.0, the limiting maximum value corresponding to a perfect blackbody emitter. With a flame emissivity conservatively assumed to be 1.0 and a painted surface emissivity of 0.85, the effective emissivity coefficient is 0.85. Because the minimum required value of 0.9 is greater than the actual value of 0.85, use of an average emissivity coefficient of 0.9 is conservative.

2. The average flame temperature must be at least 1475°F (802°C). Open pool fires typically involve the entrainment of large amounts of air, resulting in lower average flame temperatures. Additionally, the same temperature is applied to all exposed cask surfaces, which is very conservative considering the size of the HI-STORM FW cask. It is therefore conservative to use the 1475°F (802°C) temperature.

3. The fuel source must extend horizontally at least 1 m (40 in), but may not extend more than

3 m (10 ft), beyond the external surface of the cask. Use of the minimum ring width of 1 meter yields a deeper pool for a fixed quantity of combustible fuel, thereby conservatively maximizing the fire duration (specified in Table 2.2.8).

4. The convection coefficient must be that value which may be demonstrated to exist if the cask were exposed to the fire specified. Based upon results of large pool fire thermal measurements [4.6.2], a conservative forced convection heat transfer coefficient of 4.5 Btu/(hr×ft^2×°F) is applied to exposed overpack surfaces during the short-duration fire.

Based on the 50 gallon fuel volume, the overpack outer diameter and the 1 m fuel ring width [4.6.1], the fuel ring surrounding the overpack covers 154.1 ft^2 and has a depth of 0.52 inch. From this depth and the fuel consumption rate of 0.15 in/min, the calculated fire duration is provided in Table 2.2.8. The fuel consumption rate of 0.15 in/min is a lowerbound value from a Sandia National Laboratories report [4.6.2]. Use of a lowerbound fuel consumption rate conservatively maximizes the duration of the fire.

To evaluate the impact of fire heating of the HI-STORM FW overpack, a thermal model of the overpack cylinder was constructed using FLUENT. A transient study is conducted for the duration of fire and post-fire of sufficient duration to reach maximum temperatures. The bounding steady state HI-STORM FW normal storage temperatures (shortest fuel scenario in MPC-37, see Table 4.4.3) are adopted as the initial condition for the fire accident (fire and post-fire) evaluation. The transient study was conducted for a sufficiently long period to allow temperatures in the overpack to reach their maximum values and begin to recede.

Due to the severity of the fire condition radiative heat flux, heat flux from incident solar radiation is negligible and is not included. Furthermore, the smoke plume from the fire would block most of the solar radiation.

The thermal transient response of the storage overpack is determined using FLUENT. Time-histories for points in the storage overpack are monitored for the duration of the fire and the subsequent post-fire equilibrium phase.

Heat input to the HI-STORM FW overpack while it is subjected to the fire is from a combination of incident radiation and convective heat flux to all external surfaces. This can be expressed by the following equation:

$$q_F = h_{fc}(T_A - T_S) + \sigma\varepsilon[(T_A + C)^4 - (T_S + C)^4]$$

where:

q_F =Surface Heat Input Flux (Btu/ft^2-hr)
h_{fc} = Forced Convection Heat Transfer Coefficient (4.5 Btu/ft^2-hr-°F)
σ = Stefan-Boltzmann Constant
T_A = Fire Temperature (1475°F)
C= Conversion Constant (460 (°F to °R))

T_S = Surface Temperature (°F)
ε = Average Emissivity (0.90 per 10 CFR 71.73)

The forced convection heat transfer coefficient is based on the results of large pool fire thermal measurements [4.6.2].

After the fire event, the ambient temperature is restored and the storage overpack cools down (post-fire temperature relaxation). Heat loss from the outer surfaces of the storage overpack is determined by the following equation:

$$q_S = h_S (T_S - T_A) + \sigma\varepsilon [(T_S + C)^4 - (T_A + C)^4]$$

where:

q_S =Surface Heat Loss Flux (W/m^2 (Btu/ft^2-hr))
h_S = Natural Convection Heat Transfer Coefficient (Btu/ft^2-hr-°F)
T_S = Surface Temperature (°F))
T_A = Ambient Temperature (°F)
σ = Stefan-Boltzmann Constant
ε = Surface Emissivity
C= Conversion Constant (460 (°F to °R))

In the post-fire temperature relaxation phase, h_s is obtained using literature correlations for natural convection heat transfer from heated surfaces [4.2.9]. Solar insolation was included during post-fire event. An emissivity of bare carbon steel (see Table 4.2.4) is used for all the cask outer surfaces during post-fire analysis.

The results of the fire and post-fire events are reported in Table 4.6.2. These results demonstrate that the fire accident event has a minor affect on the fuel cladding temperature. Localized regions of concrete upto 1 inch depth are exposed to temperatures in excess of accident temperature limit. The bulk concrete temperature remains below the short-term temperature limit. The temperatures of the basket and components of MPC and HI-STORM FW overpack (see Table 4.6.2) are within the allowable temperature limits.

Table 4.6.2 shows a slight increase in fuel temperature following the fire event. Thus the impact on the MPC internal helium pressure is correspondingly small. Based on a conservative analysis of the HI-STORM FW system response to a hypothetical fire event, it is concluded that the fire event does not adversely affect the temperature of the MPC or contained fuel. Thus, the ability of the HI-STORM FW system to maintain the spent nuclear fuel within design temperature limits during and after fire is assured.

(b) HI-TRAC VW Fire

In this subsection the fuel cladding and MPC pressure boundary integrity under an exposure to a short duration fire event is demonstrated. The HI-TRAC VW is initially (before fire) assumed to be loaded to design basis decay heat and has reached steady-state maximum temperatures. The analysis assumes a fire from a 50 gallon transporter fuel tank spill. The fuel spill, as discussed in Subsection 4.6.2.1(a) is assumed to surround the HI-TRAC VW in a 1 m wide ring. The fire parameters are same as that assumed for the HI-STORM FW fire discussed in this preceding subsection. In this analysis, the HI-TRAC VW and its contents are conservatively postulated to undergo a transient heat-up as a lumped mass from the decay heat and heat input from the fire.

Based on the specified 50 gallon fuel volume, HI-TRAC VW cylinder diameter (7.9 ft) and the 1 m fuel ring width, the fuel ring area is 115.2 ft^2 and has a depth of 0.696 in. From this depth and the fuel consumption rate of 0.15 in/min, the fire duration τ_f is calculated to be 4.64 minutes (279 seconds). The fuel consumption rate of 0.15 in/min is a lowerbound value from Sandia Report [4.6.1]. Use of a lowerbound fuel consumption rate conservatively maximizes the duration of the fire.

From the HI-TRAC VW fire analysis, a bounding rate of temperature rise 2.722°F per minute is determined. Therefore, the total temperature rise is computed as the product of the rate of temperature rise and τ_f is 12.6°F. Because the cladding temperature at the start of fire is substantially below the accident temperature limit, the fuel cladding temperature limit during HI-TRAC VW fire is not exceeded. To confirm that the MPC pressure remains below the design accident pressure (Table 2.2.1) the MPC pressure resulting from fire temperature rise is computed using the Ideal Gas Law. The result (see Table 4.6.7) is below the pressure limit (see Table 2.2.1).

4.6.2.2 Jacket Water Loss

In this subsection, the fuel cladding and MPC boundary integrity is evaluated under a postulated (non-mechanistic) loss of water from the HI-TRAC VW water jacket. For a bounding analysis, all water compartments are assumed to lose their water and be replaced with air. The HI-TRAC VW is assumed to have the maximum thermal payload (design heat load) and assumed to have reached steady state (maximum) temperatures. Under these assumed set of adverse conditions, the maximum temperatures are computed and reported in Table 4.6.3. The results of jacket water loss evaluation confirm that the cladding, MPC and HI-TRAC VW component temperatures are below the limits prescribed in Chapter 2 (Table 2.2.3). The co-incident MPC pressure is also computed and compared with the MPC accident design pressure (Table 2.2.1). The result (Table 4.6.7) shows a positive margin of safety.

4.6.2.3 Extreme Environmental Temperatures

To evaluate the effect of extreme weather conditions, an extreme ambient temperature (Table 2.2.2) is postulated to persist for a 3-day period. For a conservatively bounding evaluation the extreme temperature is assumed to last for a sufficient duration to allow the HI-STORM FW system to reach steady state conditions. Because of the large mass of the HI-STORM FW system, with its corresponding large thermal inertia and the limited duration for the extreme temperature, this assumption is conservative. Starting from a baseline condition evaluated in Section 4.4 (normal ambient temperature and limiting fuel storage configuration) the temperatures of the HI-STORM FW system are conservatively assumed to rise by the difference between the extreme and normal ambient temperatures (45°F). The HI-STORM FW extreme ambient temperatures computed in this manner are reported in Table 4.6.4. The co-incident MPC pressure is also computed (Table 4.6.7) and compared with the accident design pressure (Table 2.2.1), which shows a positive safety margin. The result is confirmed to be below the accident limit.

4.6.2.4 100% Blockage of Air Inlets

This event is defined as a complete blockage of all eight bottom inlets for a significant duration (32 hours). The immediate consequence of a complete blockage of the air inlets is that the normal circulation of air for cooling the MPC is stopped. An amount of heat will continue to be removed by localized air circulation patterns in the overpack annulus and outlet ducts, and the MPC will continue to radiate heat to the relatively cooler storage overpack. As the temperatures of the MPC and its contents rise, the rate of heat rejection will increase correspondingly. Under this condition, the temperatures of the overpack, the MPC and the stored fuel assemblies will rise as a function of time.

As a result of the considerable inertia of the storage overpack, a significant temperature rise is possible if the inlets are substantially blocked for extended durations. This accident condition is, however, a short duration event that is identified and corrected through scheduled periodic surveillance. Nevertheless, this event is conservatively analyzed assuming a substantial duration of blockage. The HI-STORM FW thermal model is the same 3-Dimensional model constructed for normal storage conditions (see Section 4.4) except for the bottom inlet ducts, which are assumed to be impervious to air. Using this model, a transient thermal solution of the HI-STORM FW system starting from normal storage conditions is obtained. The results of the blocked ducts transient analysis are presented in Table 4.6.5 and compared against the accident temperature limits (Table 2.2.3). The co-incident MPC pressure (Table 4.6.7) is also computed and compared with the accident design pressure (Table 2.2.1). All computed results are well below their respective limits.

4.6.2.5 Burial Under Debris (Load Case AG in Table 2.2.13)

Burial of the HI-STORM FW system under debris is not a credible accident. During storage at the ISFSI there are no structures that loom over the casks whose collapse could completely bury the

casks in debris. Minimum regulatory distances from the ISFSI to the nearest ISFSI security fence precludes the close proximity of substantial amount of vegetation. There is no credible mechanism for the HI-STORM FW system to become completely buried under debris. However, for conservatism, the scenario of complete burial under debris is considered.

For this purpose, an exceedingly conservative analysis that considers the debris to act as a perfect insulator is considered. Under this scenario, the contents of the HI-STORM FW system will undergo a transient heat up under adiabatic conditions. The minimum available time ($\Delta\tau$) for the fuel cladding to reach the accident limit depends on the following: (i) thermal inertia of the cask, (ii) the cask initial conditions, (iii) the spent nuclear fuel decay heat generation and (iv) the margin between the initial cladding temperature and the accident temperature limit. To obtain a lowerbound on $\Delta\tau$, the HI-STORM FW overpack thermal inertia (item i) is understated, the cask initial temperature (item ii) is maximized, decay heat overstated (item iii) and the cladding temperature margin (item iv) is understated. A set of conservatively postulated input parameters for items (i) through (iv) are summarized in Table 4.6.6. Using these parameters $\Delta\tau$ is computed as follows:

$$\Delta\tau = \frac{m \times c_p \times \Delta T}{Q}$$

where:

$\Delta\tau$ = minimum available burial time (hr)
m = Mass of HI-STORM FW System (lb)
c_p = Specific heat capacity (Btu/lb-°F)
ΔT = Permissible temperature rise (°F)
Q = Decay heat load (Btu/hr)

Substituting the parameters in Table 4.6.6, the minimum available burial time is computed as 85.1 hours. The co-incident MPC pressure (see Table 4.6.7) is also computed and compared with the accident design pressure (Table 2.2.1). These results indicate that HI-STORM FW has a substantial thermal sink capacity to withstand complete burial-under-debris events.

4.6.2.6 Evaluation of Smart Flood (Load Case AD in Table 2.2.13)

A number of design measures are taken in the HI-STORM FW system to limit the fuel cladding temperature rise under a most adverse flood event (i.e., one that is just high enough to block the inlet duct). An unlikely adverse flood accident is assumed to occur with flood water upto the inlet height and is termed as 'smart flood'. The inlet duct is narrow and tall so that blocking the inlet ducts completely would require that flood waters wet the bottom region of the MPC creating a heat sink.

The inlet duct is configured to block radiation efficiently even if the radiation emanating from the MPC is level (coplanar) with the duct penetration. The MPC stands on the base plate, which is welded to the inner and outer shell of the overpack. Thus, if the flood water rises high enough to

block air flow through the bottom ducts, the lower region of the MPC will be submerged in the water. Although heat transport through air circulation is cut off in this scenario, the reduction is substantially offset by flood water cooling.

The MPCs are equipped with the thermosiphon capability, which brings the heat emitted by the fuel to the bottom region of the MPC as the circulating helium flows along the downcomer space around the basket. This places the heated helium in close thermal communication with the flood water, further enhancing convective cooling via the flood water.

The most adverse flood condition exists when the flood waters are high enough to block the inlet ducts but no higher. In this scenario, the MPC surface has minimum submergence in water and the ventilation air is completely blocked. In fact, as the flood water begins to accumulate on the ISFSI pad, the air passage size in the inlet vents is progressively reduced. Therefore, the rate of floodwater rise with time is necessary to analyze the thermal-hydraulic problem. For the reference design basis flood (DBF) analysis in this FSAR, the flood waters are assumed to rise instantaneously to the height to block the inlet vents and stay at that elevation for 32 hours. The consequences of the DBF event is bounded by the 100% blocked ducts events evaluated in Section 4.6.2.4. If the duration of the flood blockage exceeds the DBF blockage duration then a site specific evaluation shall be performed in accordance with the methodology presented in this Chapter and evaluated for compliance with Subsection 2.2.3 criteria.

Table 4.6.1

OFF-NORMAL CONDITION MAXIMUM HI-STORM FW TEMPERATURES

Component	**Off-Normal Ambient Temperature °C (°F)**	**Partial Inlets Duct Blockage °C (°F)**
Fuel Cladding	386 (727)	385 (725)
MPC Basket	372 (702)	371 (700)
Aluminum Basket Shims	287 (549)	285 (545)
MPC Shell	257 (495)	257 (495)
MPC Lid*	254 (489)	252 (486)
Overpack Inner Shell	139 (282)	141 (286)
Overpack Outer Shell	71 (160)	62 (144)
Overpack Body Concrete*	99 (210)	95 (203)
Overpack Lid Concrete*	124 (255)	122 (252)

Table 4.6.2

HI-STORM FW FIRE AND POST-FIRE ACCIDENT ANALYSIS RESULTS

Component	Initial Condition °C (°F)	End of Fire Condition °C (°F)	Post-Fire Cooldown °C (°F)
Fuel Cladding	375 (707)	375 (707)	377 (711)
MPC Basket	361 (682)	361 (682)	363 (685)
Basket Periphery	297 (567)	297 (567)	299 (570)
Aluminum Basket Shims	276 (529)	276 (529)	278 (532)
MPC Shell	246 (475)	251 (484)	251 (484)
MPC Lid[Note 1]	243 (469)	245 (473)	245 (473)
Overpack Inner Shell	128 (262)	140 (284)	140 (284)
Overpack Outer Shell	60 (140)	340 (644) [Note 3]	340 (644) [Note 3]
Overpack Body Concrete[Note 1]	88 (190)	100 (212)	100 (212)
Overpack Lid Concrete[Note 1]	113 (235)	125 (257)	125 (257)

Note 1: Maximum section average temperature is reported.
Note 2: The temperatures tabulated herein are obtained by adding a conservatively postulated temperature increment to a baseline mesh thermal solution that suitably bounds the effects of grid sensitivity evaluated in Para 4.4.1.6 of Subsection 4.4.1.
Note 3: Surface average temperature is reported.

Table 4.6.3 HI-TRAC VW JACKET WATER LOSS MAXIMUM TEMPERATURES	
Component	**Temperature °C (°F)**
Fuel Cladding	432 (810)
MPC Basket	416 (781)
Basket Periphery	342 (648)
Aluminum Basket Shims	314 (597)
MPC Shell	290 (554)
MPC Lid*	263 (505)
HI-TRAC VW Inner Shell	205 (401)
HI-TRAC VW Radial Lead Gamma Shield	204 (399)

* Maximum section average temperature is reported.

Table 4.6.4 EXTREME ENVIRONMENTAL CONDITION MAXIMUM HI-STORM FW TEMPERATURES	
Component	**Temperature* °C (°F)**
Fuel Cladding	400 (752)
MPC Basket	386 (727)
Basket Periphery	322 (612)
Aluminum Basket Shims	301 (574)
MPC Shell	271 (520)
MPC Lid[Note 1]	268 (514)
Overpack Inner Shell	153 (307)
Overpack Outer Shell	85 (185)
Overpack Body Concrete[Note 1]	113 (235)
Overpack Lid Concrete[Note 1]	138 (280)
Average Air Outlet	129 (264)
Note 1: Maximum section average temperature is reported.	

* Obtained by adding the difference between extreme ambient and normal temperature difference (25°C (45°F)) to normal condition temperatures reported in Table 4.4.3.

Table 4.6.5

RESULTS OF HI-STORM FW 32-HOURS BLOCKED INLET DUCTS THERMAL ANALYSIS

Component*	**Initial Condition °C (°F)**	**Final Condition °C (°F)**
Fuel Cladding	375 (707)	484 (903)
MPC Basket	361 (682)	468 (874)
Basket Periphery	297 (567)	404 (759)
Aluminum Basket Shims	276 (529)	380 (716)
MPC Shell	246 (475)	358 (676)
MPC Lid[Note 1]	243 (469)	313 (595)
Overpack Inner Shell	128 (262)	247 (477)
Overpack Outer Shell	60 (140)	105 (221)
Overpack Body Concrete[Note 1]	88 (190)	130 (266)
Overpack Lid Concrete[Note 1]	113 (235)	165 (329)

Note 1: Maximum section average temperature is reported.
Note 2: The temperatures tabulated herein are obtained by adding a conservatively postulated temperature increment to a baseline mesh thermal solution that suitably bounds the effects of grid sensitivity evaluated in Para 4.4.1.6 of Subsection 4.4.1.

* For a bounding evaluation, temperatures are computed at the lowerbound helium backfill pressure defined in Table 4.4.8. Temperatures of limiting components reported.

Table 4.6.6 SUMMARY OF INPUTS FOR BURIAL UNDER DEBRIS ANALYSIS	
Thermal Inertia Inputs*:	
M (Lowerbound HI-STORM FW Weight)	215000 kg
Cp (Carbon steel heat capacity)†	419 J/kg-°C
Clad initial temperature[Note 1]	390°C
Q (Decay heat)	47.05 kW
ΔT (clad temperature margin)‡	160°C
Note 1: Initial temperature conservatively postulated to bound the maximum cladding temperature.	

* Thermal inertia of fuel is conservatively neglected.

† Used carbon steel's specific heat since it has the lowest heat capacity among the principal materials employed in MPC and overpack construction (carbon steel, stainless steel, Metamic-HT and concrete).

‡ The clad temperature margin is conservatively understated in this table.

Table 4.6.7 OFF-NORMAL AND ACCIDENT CONDITION MAXIMUM MPC PRESSURES	
Condition	**Pressure (psig)**
Off-Normal Conditions	
Off-Normal Pressure*	111.6
Partial Blockage of Inlet Ducts	99.9
Accident Conditions	
HI-TRAC VW fire accident	103.3
Extreme Ambient Temperature	103.1
100% Blockage of Air Inlets	116.4
Burial Under Debris	130.8
HI-TRAC VW Jacket Water Loss	109.5

* The off-normal pressure event defined in Section 4.6.1.1 bounds the off-normal ambient temperature event (Section 4.6.1.2)

4.7 REGULATORY COMPLIANCE

4.7.1 Normal Conditions of Storage

NUREG-1536 [4.4.1] and ISG-11 [4.1.4] define several thermal acceptance criteria that must be applied to evaluations of normal conditions of storage. These items are addressed in Sections 4.1 through 4.4. Each of the pertinent criteria and the conclusion of the evaluations are summarized here.

As required by ISG-11 [4.1.4], the fuel cladding temperature at the beginning of dry cask storage is maintained below the anticipated damage-threshold temperatures for normal conditions for the licensed life of the HI-STORM FW System. Maximum clad temperatures for long-term storage conditions are reported in Section 4.4.

As required by NUREG-1536 (4.0,IV,3), the maximum internal pressure of the cask remains within its design pressure for normal conditions, assuming rupture of 1 percent of the fuel rods. Assumptions for pressure calculations include release of 100 percent of the fill gas and 30 percent of the significant radioactive gases in the fuel rods. Maximum internal pressures are reported in Section 4.4 and shown to remain below the normal design pressures specified in Table 2.2.1.

As required by NUREG-1536 (4.0,IV,4), all cask and fuel materials are maintained within their minimum and maximum temperature for normal and off-normal conditions in order to enable components to perform their intended safety functions. Maximum and minimum temperatures for long-term storage conditions are reported in Section 4.4 which are shown to be well below their respective Design temperature limits summarized in Table 2.2.3.

As required by NUREG-1536 (4.0,IV,5), the cask system ensures a very low probability of cladding breach during long-term storage. For long-term normal conditions, the maximum CSF cladding temperature is shown to be below the ISG-11 [4.1.4] limit of 400°C (752°F).

As required by NUREG-1536 (4.0,IV,7), the cask system is passively cooled. All heat rejection mechanisms described in this chapter, including conduction, natural convection, and thermal radiation, are completely passive.

As required by NUREG-1536 (4.0,IV,8), the thermal performance of the cask is within the allowable design criteria specified in SAR Chapters 2 and 3 for normal conditions. All thermal results reported in Section 4.4 are within the design criteria under all normal conditions of storage.

4.7.2 Short-Term Operations

Evaluation of short-term operations is presented in Section 4.5 wherein complete compliance with the provisions of ISG-11 [4.1.4] is demonstrated. In particular, the ISG-11 requirement to ensure that maximum cladding temperatures under all fuel loading and short-term operations be below 400°C (752°F) for high burnup fuel and below 570°C (1058°F) for moderate burnup fuel (Table 4.3.1) is demonstrated.

Further, as required by NUREG-1536 (4.0,IV, 4), all cask and fuel materials are maintained within their minimum and maximum temperature for all short-term operations in order to enable components to perform their intended safety functions.

As required by NUREG-1536 (4.0,IV,8), the thermal performance of the cask is within the allowable design criteria specified in SAR Chapters 2 and 3 for all short-term operations.

4.7.3 Off-Normal and Accident Conditions

As required by NUREG-1536 (4.0,IV,3), the maximum internal pressure of the cask is evaluated in Section 4.6 and shown to remain within its off-normal and accident design pressure, assuming rupture of 10 percent and 100 percent of the fuel rods, respectively. Assumptions for pressure calculations include release of 100 percent of the fill gas and 30 percent of the significant radioactive gases in the fuel rods.

4.8 REFERENCES

[4.1.1] ANSYS Finite Element Modeling Package, Swanson Analysis Systems, Inc., Houston, PA, 1993.

[4.1.2] FLUENT Computational Fluid Dynamics Software, Fluent, Inc., Centerra Resource Park, 10 Cavendish Court, Lebanon, NH 03766.

[4.1.3] "The TN-24P PWR Spent-Fuel Storage Cask: Testing and Analyses," EPRI NP-5128, (April 1987).

[4.1.4] "Cladding Considerations for the Transportation and Storage of Spent Fuel," Interim Staff Guidance – 11, Revision 3, USNRC, Washington, DC.

[4.1.5] "Topical Report on the HI-STAR/HI-STORM Thermal Model and its Benchmarking with Full-Size Cask Test Data," Holtec Report HI-992252, Revision 1, Holtec International, Marlton, NJ, 08053.

[4.1.6] "Identifying the Appropriate Convection Correlation in FLUENT for Ventilation Air Flow in the HI-STORM System", Revision 1, Holtec Report HI-2043258, Holtec International, Marlton, NJ, 08053.

[4.1.7] "Performance Testing and Analyses of the VSC-17 Ventilated Concrete Cask", EPRI TR-100305, (May 1992).

[4.1.8] "Holtec International Final Safety Analysis Report for the HI-STORM 100 Cask System", Holtec Report No. 2002444, Revision 7, NRC Docket No. 72-1014.

[4.1.9] "Thermal Evaluation of HI-STORM FW", Holtec Report HI-2094400, Revision 0.

[4.1.10] "Effective Thermal Properties of PWR Fuel in MPC-37", Holtec Report HI-2094356, Revision 0.

[4.1.11] "Safety Analysis Report on the HI-STAR 180 Package", Holtec Report HI-2073681, Latest Revision.

[4.2.1] Baumeister, T., Avallone, E.A. and Baumeister III, T., "Marks' Standard Handbook for Mechanical Engineers," 8th Edition, McGraw Hill Book Company, (1978).

[4.2.2] Rohsenow, W.M. and Hartnett, J.P., "Handbook of Heat Transfer," McGraw Hill Book Company, New York, (1973).

[4.2.3] Creer et al., "The TN-24P Spent Fuel Storage Cask: Testing and Analyses," EPRI NP-5128, PNL-6054, UC-85, (April 1987).

[4.2.4] Rust, J.H., "Nuclear Power Plant Engineering," Haralson Publishing Company, (1979).

[4.2.5] Kern, D.Q., "Process Heat Transfer," McGraw Hill Kogakusha, (1950).

[4.2.6] "Metamic-HT Qualification Sourcebook", Holtec Report HI-2084122, Latest Revision.

[4.2.7] "Spent Nuclear Fuel Effective Thermal Conductivity Report," US DOE Report BBA000000-01717-5705-00010 REV 0, (July 11, 1996).

[4.2.8] ASME Boiler and Pressure Vessel Code, Section II, Part D, (1995).

[4.2.9] Jakob, M. and Hawkins, G.A., "Elements of Heat Transfer," John Wiley & Sons, New York, (1957).

[4.2.10] ASME Steam Tables, 3rd Edition (1977).

[4.2.11] "Nuclear Systems Materials Handbook, Vol. 1, Design Data", ORNL TID 26666.

[4.2.12] "Scoping Design Analyses for Optimized Shipping Casks Containing 1-, 2-, 3-, 5-, 7-, or 10-Year-Old PWR Spent Fuel", ORNL/CSD/TM-149 TTC-0316, (1983).

[4.2.13] Not used.

[4.2.14] Not used.

[4.2.15] Not used.

[4.2.16] USNRC Docket no 72-1027, TN-68 FSAR & Docket no 72-1021 TN-32 FSAR.

[4.2.17] Hagrman, Reymann and Mason, "MATPRO-Version 11 (Revision 2) A Handbook of Materials Properties for Use in the Analysis of Light Water Reactor Fuel Rod Behavior," NUREG/CR-0497, Tree 1280, Rev. 2, EG&G Idaho, August 1981.

[4.2.18] "Effective Thermal Conductivity and Edge Conductance Model for a Spent-Fuel Assembly," R. D. Manteufel & N. E. Todreas, Nuclear Technology, 105, 421- 440, (March 1994).

[4.2.19] Aluminum Alloy 2219 Material Data Sheet, ASM Aerospace Specification Metals, Inc., Pompano Beach, FL.

[4.2.20] "Spacecraft Thermal Control Coatings References", NASA Publication NASA/TP-2005-212792, December 2005.

[4.4.1] NUREG-1536, "Standard Review Plan for Dry Cask Storage Systems," USNRC, (January 1997).

[4.4.2] "Pressure Loss Charactersistics for In-Cell Flow of Helium in PWR and BWR Storage Cells", Holtec Report HI-2043285, Revision 6, Holtec International, Marlton, NJ, 08053.

[4.4.3] "Procedure for Estimating and Reporting of Uncertainty due to Discretization in CFD Applications", I.B. Celik, U. Ghia, P.J. Roache and C.J. Freitas (Journal of Fluids Engineering Editorial Policy on the Control of Numerical Accuracy).

[4.6.1] United States Code of Federal Regulations, Title 10, Part 71.

[4.6.2] Gregory, J.J. et. al., "Thermal Measurements in a Series of Large Pool Fires", SAND85-1096, Sandia National Laboratories, (August 1987).